

SYMMETRY AND STRUCTURE OF BICRYSTALS

Thesis submitted in accordance with the requirements  
of the University of Liverpool for the degree of  
Doctor in Philosophy by:

Demosthenes S. Vlachavas

Department of Metallurgy  
and Materials Science

November 1980

Ἀφιερῶται στοὺς γονεῖς μου  
ἢ ὑποστήριξη καὶ κατανόηση τῶν  
ὁποίων μου ἐπέτρεψαν νὰ ὀλοκλη-  
ρώσω αὐτὴ τὴν ἐργασία

\*\*\* \*\* \*\* \*\* \*\*

To my parents without whose  
support and understanding this thesis  
could not have been written

## Acknowledgements

The work described in this thesis was carried out by the author in the Department of Metallurgy and Materials Science of the University of Liverpool between October 1977 and August 1980 under the supervision of Dr. R.C. Pond. No part of this thesis has been submitted for a degree at this, or any other, University. The work of others has been freely drawn upon and duly acknowledged in the text, and an alphabetic list of references is included at the end of the thesis.

The author wishes to express his most sincere thanks to Dr. R.C. Pond for his constant advice and encouragement throughout the course of this work and his painstaking help in preparing the manuscript.

Thanks are also due to Professors D. Hull and B.L. Eyre for providing the facilities for research in the Department of Metallurgy and Materials Science.

My thanks, too, are to Mr. R. Devenish for many informative discussions, for an early insight into the mysteries of experimental electron microscopy as well as for his willing and expert technical assistance particularly during the specimen preparation stage.

To others, who have provided advice and assistance during this work, I would like to express my sincere thanks. I am particularly grateful to:

Dr. A.G. Cullis of the Royal Signal and Radar Establishment for kindly supplying the silicon bulk used for the experimental work.

Dr. P. Rez for providing the STACKFAULT computer program outlined in chapter 10.

Dr M. Romero, Mr. V. Korotchenko and Mr. J. Manson for their valuable guidance in preparing this thesis.

Mr. J. Gillies for his expert photographic work.

Finally, my thanks to my family as well as Dr. J. Tsoukalas for their constant support and encouragement during the three years in which this project was being carried out.



## Abstract

Recent developments in the theory of grain boundaries have been largely concerned with the development of sophisticated geometrical methods for describing the structure of (primarily) large-angle boundaries. This is necessary since the atomic structure and properties of a grain boundary depend, in general, on a large number of parameters. In the simplest case of a planar boundary nine parameters are required to characterize the boundary. The relative orientation of the crystals and the interface can be specified by 6 parameters while three are required to define the location of the boundary.

It is, therefore, evident that the investigation of the atomic structure and properties of a grain boundary is, generally, more complicated than that of a single crystal. It is the aim of this thesis to point out an approach facilitating this task. The proposed approach is based on symmetry considerations of grain boundaries. Such considerations can be employed for simplifying calculations of tensor analysis or quantum mechanics. However, in order to do this a comprehensive framework of symmetry classes is required.

In chapters 1 and 2 of this thesis the proposed approach and symmetry theory are outlined. The crystallographic model of a grain boundary is then developed in chapter 3. The discussion in this chapter indicates that the structure of a bicrystal requires a description not only of the arrangement of the atoms, but also of the inter-relation of the two crystals. The most complete description of the bicrystal symmetry can be given on the basis of the theory of two-coloured symmetry within the framework of the Shubnikov groups.

According to the crystallographic model the symmetry of a bicrystal can be obtained by superimposing the geometrical figures representing the symmetry groups of the two adjacent crystals. This is examined in detail in chapter 4 where a group-theoretical method is derived for determining the symmetry resulting by the superposition of two point groups. The method is subsequently used (chapter 5) for the determination of the permissible symmetry groups of interfaces.

In the next two chapters the variation of the bicrystal symmetry with relative displacement of the adjacent crystals and the location of the interface is investigated. The extension of the symmetry considerations to interphase boundaries and to other planar crystal defects is examined in chapter 8. In the same chapter the application of symmetry to the study of atomic structure and properties of interfaces is examined.

The final part of the thesis is concerned with the experimental investigation of the structure of twins in silicon using a special imaging technique in the transmission electron microscope. This technique allows rigid-body translations at twin boundaries to be revealed as stacking-fault-like fringes. Thus, the structure of the  $\Sigma=3$ , coherent and incoherent, twins is determined.

ERRATA

## D. VLACHAVAS "Symmetry and structure of bicrystals"

Page	Line*	Instead of...	Read...
3	-1	a interface	an interface
5	5	remaining	remainder
5	13	aparent	apparent
5	-10	mentional	mentioned
9	-7	unterstood	understood
10	1	economical	economically
10	3	primarily	primary
10	-11	intergrated	integrated
10	-6	since can	since they can
11	5	aparent	apparent
15	1	comperatively	comparatively
15	6	cocept	concept
16	10	adding	adding
20	-11	remaining	remainder
20	-4	sides	sites
20	-3	sides	sites
24	6	deviation	derivation
25	2	varing	varying
26	14	non-paraller	non-parallel
26	-6	these	These
27	-6	confirmed	confined
28	-10	treaded	treated

\* Negative numbers indicate counting from the bottom of the page

## D. VLACHAVAS "Symmetry and structure of bicrystals"

Page	Line	Instead of...	Read...
29	-12	deviation	derivation
32	5	extented	extended
32	-4	equilateral	equilateral
33	5	A	An
37	-11	mainly	namely
40	5	consequently	consecutively
41	-7	(a)the	(a)they
43	7	consisted	consistent
45	14	should	should be
47	6	these	those
49	-5	perpenticular	perpendicular
49	-1	C2/m'	cm'
50	-2	extent	extend
52	-11	rod	band
65	6	$S_{=0}$ an	$S_{=0}$ be an
72	-11	can further	can be further
72	-9	can applied	can be applied
74	3	dichromatic	dichromatic
74	2	versus	versa
75	5	versus	versa
75	13	displament	displacement
76	-2	versus	versa
80	6	present to	present in
85	1	matter	manner
85	-2	discontinum	discontinuum

## D. VLACHAVAS "Symmetry and structure of bicrystals"

Page	Line	Instead of...	Read...
88	-4	arbitrarilly	arbitrarily
89	2	arbitrarilly	arbitrarily
90	4	choise	choice
91	9	for the	for a
91	11	of f	f
93	-6	unterstood	understood
94	12	to the	with the
95	-3	permits to	permits one to
96	-4	distiguishing	distinguishing
96	-3	abritrary	arbitrary
97	2	facilites	facilitates
98	-2	fundamental	fundamental
99	13	unterstood	understood
102	-12	imposses continuation	imposes continuity
102	-8	imposed	imposed
102	-3	crusial	crucial
105	-2	superimposed	superimposed
108	-13	measurent	measurement
108	-13	choise	choice
109	9	do	did
109	14	occuping	occupying
110	11	singificantly	significantly
116	16	comparitably	comparitively
117	-8	rear	near

## D. VLACHAVAS "Symmetry and structure of bicrystals"

Page	Line	Instead of...	Read...
120	10	DCS	DSC
124	10	bombartment	bombardment
126	2	stradding	straddling
126	2	succeful	successful
128	15	dolten	dotted
129	-4	evidences are	evidence is
130	13	accouracy	accuracy
132	11	frince	fringe
133	8	been	being
137	-4	extention	extension
139	-5	/12	/6
154	9	order	order for
155	-9	such so	such that
155	-6	such so	such that
157	13	order	order for
160	8	denote	denoted
162	-5	matter	manner
163	10	deviation	derivation
167	9	deviation	derivation
177	4	reduce	reduction
179	8	transport	transpose
180	-3	convenge showly	converge slowly
189	14	insulated	situated
190	-4	algorith	algorithm

## D. VLACHAVAS "Symmetry and structure of bicrystals"

Page	Line	Instead of...	Read...
192	5	it	is
192	-10	slides	slices
192	-2	slides	slices
193	-13	sticked	stuck
199	7	flesible	feasible

Table 9.3.1, line 9, instead of "dampts" read "damps"

Figure 5.4.4, line 3 in caption, instead of "fillen" read "filled"

## CONTENTS

	<u>Page</u>
<u>CHAPTER 1</u>	
INTRODUCTION	
1.1 Objectives of the theoretical part . . . . .	1
1.1.1 Earlier work on interfacial sym- metry . . . . .	2
1.1.2 The present approach . . . . .	3
1.2 Outline of grain boundary models . . . . .	6
1.3 Objectives of the experimental part . . . . .	9
<u>CHAPTER 2</u>	
SYMMETRY OF OBJECTS	
2.1 Classical symmetry . . . . .	12
2.2 Antisymmetry . . . . .	15
2.2.1 Introduction of antisymmetry . . . . .	15
2.2.2 Groups of antisymmetry of finite objects . . . . .	16
2.2.3 Groups of antisymmetry of infinite figures . . . . .	17
<u>CHAPTER 3</u>	
CRYSTALLOGRAPHIC TREATMENT OF INTERFACES	
3.1 A model of bicrystals . . . . .	19
3.1.1 The ideal bicrystal . . . . .	19
3.1.2 Dichromatic complex . . . . .	20
3.1.3 Dichromatic pattern . . . . .	20
3.1.4 Degrees of freedom of an interface . . . . .	21
3.1.5 Manufacture of an ideal bicrystal . . . . .	22
3.2 Crystallographic definitions for interfaces . . . . .	23
3.2.1 Dichromatic point groups . . . . .	23
3.2.2 Bicrystal point groups . . . . .	24
3.3 Crystallographic framework . . . . .	25
3.3.1 Antisymmetry classes of interfacial symmetry . . . . .	25
3.3.2 Classes of dichromatic complexes . . . . .	26
3.3.3 Symmetry classes of bicrystals . . . . .	28
<u>CHAPTER 4</u>	
SUPERPOSITION OF SYMMETRIES	
4.1 The principle of composite systems . . . . .	31
4.1.1 The geometrical interpretation of the Neumann-Curie principle . . . . .	32
4.1.2 Kinds of symmetry operations created by superposition of point groups . . . . .	33
4.2 Group-theoretical formulation of the super- position of symmetries . . . . .	34
4.2.1 Ordinary symmetry operations . . . . .	35
4.2.2 Colour-reversing symmetry operations . . . . .	36
4.2.3 Group-theoretical expression of the dichromatic point groups . . . . .	38



4.3 Point groups obtained by the superposition of two identical point groups . . . . .	40
4.3.1 The procedure . . . . .	40
4.3.2 Rules . . . . .	41
4.3.3 Non-crystallographic dichromatic point groups . . . . .	42

CHAPTER 5

SYMMETRY GROUPS OF DICHROMATIC COMPLEXES AND BICRYSTALS

5.1 Permissible symmetry groups for dichromatic complexes . . . . .	44
5.2 Examples of symmetry classification of dichromatic complexes . . . . .	46
5.2.1 Non-crystallographic dichromatic point group . . . . .	46
5.2.2 CSL dichromatic symmetry groups in cubic and hexagonal crystal systems	48
5.2.3 Twinning in pyrite . . . . .	49
5.3 Permissible symmetry groups of bicrystals . . . . .	50
5.3.1 Centrosymmetric and centroantisymmetric bicrystal groups . . . . .	50
5.3.2 Restriction of the other symmetry operations . . . . .	51
5.3.3 Symmetry classes of bicrystals . . . . .	52
5.3.4 Spatial symmetry groups of bicrystals	53
5.4 Examples of symmetry classification of bicrystals . . . . .	55
5.4.1 Twinning in the hexagonal system . . . . .	55
5.4.2 Twinning in the orthorhombic system	56
5.4.3 Twinning in the tetragonal system . . . . .	58
5.4.4 Twinning in the monoclinic system . . . . .	58

CHAPTER 6

VARIATION OF SYMMETRY WITH RELATIVE DISPLACEMENT

6.1 Point symmetry variation . . . . .	61
6.1.1 Subgroup relations in the point symmetry variation . . . . .	62
6.1.2 Conservation of colour-reversing symmetry operations . . . . .	63
6.1.3 Conservation of ordinary symmetry operations . . . . .	64
6.1.4 Conservation of (ordinary or colour-reversing) symmetry elements . . . . .	65
6.2 Example of point symmetry variation . . . . .	67
6.2.1 Conservation of symmetry elements . . . . .	68
6.2.2 Conservation of sets of symmetry operations . . . . .	69
6.2.3 Equivalent composites . . . . .	70
6.3 Variation of the spatial symmetry . . . . .	71
6.3.1 Displacements conserving a periodic composite . . . . .	72
6.3.2 Displacement vector set for dichromatic complexes and bicrystals . . . . .	73
6.3.3 General and special displacements . . . . .	74
6.3.4 Determination of the spatial groups for general displacements . . . . .	75
6.3.5 Determination of the spatial groups for special displacements . . . . .	76

	6.4 Example of spatial symmetry variation . . .	77
<u>CHAPTER 7</u>	GENERAL RELATIONS OF DICHROMATIC SYMMETRY AND BICRYSTAL SYMMETRY	
	7.1 Bicrystal symmetry for a given misorientation	82
	7.1.1 Determination of the point symmetry	83
	7.1.2 Sectional-plane method . . . . .	85
	7.2 Characteristic features of bicrystals . . .	87
	7.2.1 Rigid and non-rigid interfaces . . .	87
	7.2.2 Parity-related interfaces . . . . .	89
	7.3 Group-theoretical considerations concerning equivalent dichromatic complexes and energetically degenerated bicrystals . . .	90
	7.3.1 Originating configurations and variant sets . . . . .	90
	7.3.2 Group-theoretical approach . . . . .	91
	7.3.3 Symmetry degenerated configurations	93
<u>CHAPTER 8</u>	CONCLUDING REMARKS CONCERNING THE INTERFACIAL SYMMETRY	
	8.1 Crystallography of grain boundaries . . .	95
	8.1.1 Symmetry considerations of planar defects in superlattices . . . . .	97
	8.2 Crystallography of interphase boundaries . .	101
	8.2.1 Point symmetry of interphase boundaries . . . . .	101
	8.2.2 Spatial symmetry of interphase boundaries . . . . .	103
	8.2.3 Examples of interphase symmetry . .	104
	8.3 Discussion . . . . .	106
<u>CHAPTER 9</u>	ELECTRON MICROSCOPY OF GRAIN BOUNDARIES	
	9.1 Determination of the geometrical parameters	114
	9.1.1 The determination of the misorientation matrix . . . . .	115
	9.1.2 Determination of the boundary plane	117
	9.2 Method for measuring the rigid-body translation across a grain boundary . . .	119
	9.2.1 The principle of the method . . . . .	120
	9.2.2 Limitation of the method . . . . .	121
	9.2.3 The sensitivity of the technique . .	123
<u>CHAPTER 10</u>	TWIN BOUNDARIES IN SILICON	
	10.1 The $\Sigma=3$ , $\{111\}$ twin . . . . .	124
	10.1.1 Determination of the interfacial crystallography . . . . .	125
	10.1.2 Determination of the rigid-body displacement . . . . .	126
	10.1.3 The structure of the coherent twin in silicon . . . . .	127

10.2	The {211} incoherent twin . . . . .	130
10.2.1	Determination of the interfacial crystallography . . . . .	130
10.2.2	Determination of the rigid-body displacement . . . . .	131
10.2.3	The structure of the {211} incoherent twin . . . . .	133
10.3	The use of polycrystalline silicon for solar cells . . . . .	134
10.3.1	Electrical characteristics of solar cells . . . . .	135
10.3.2	Discussion of the electrical properties of twins in silicon . . . . .	136
<u>APPENDIX 1</u>	Nomenclature of symmetry groups, elements and operations . . . . .	138
<u>APPENDIX 2</u>	The 'dimensional' description of symmetry groups	142
<u>APPENDIX 3</u>	Two-sided, two-coloured rosette groups . . . . .	144
<u>APPENDIX 4</u>	Two-sided, two-coloured band groups . . . . .	146
<u>APPENDIX 5</u>	Graphical representation of point groups superposition . . . . .	149
<u>APPENDIX 6</u>	The proof of theorems 4.2.1 and 4.2.2 . . . . .	151
<u>APPENDIX 7</u>	The proof of theorems 4.2.3 and 4.2.4 . . . . .	153
	A7.1 The doubled symmetry case . . . . .	153
	A7.2 The single symmetry case . . . . .	157
<u>APPENDIX 8</u>	Examples of point symmetry superposition . . . . .	160
	A8.1 Superposition in monoclinic hemihedral holoaxial class . . . . .	160
	A8.2 Superposition in hexagonal tetartohedral class . . . . .	162
	A8.3 Superposition in tetragonal antihemihedral class . . . . .	162
<u>APPENDIX 9</u>	Points groups containing 8- or 12-fold rotation (or rotoinversion) axes . . . . .	164
<u>APPENDIX 10</u>	Rod groups containing 8- and 12-fold rotation (or rotoinversion) axes . . . . .	167
<u>APPENDIX 11</u>	Subgroups of spatial symmetry groups . . . . .	170
	A11.1 Subgroups of one-coloured spatial groups . . . . .	171
	A11.2 Subgroups of two-coloured spatial groups . . . . .	171

<u>APPENDIX 12</u>	Accurate determination of the beam direction in electron diffraction patterns . . . . .	174
	A12.1 Description of the method . . . . .	175
	A12.2 Application of the method . . . . .	176
<u>APPENDIX 13</u>	The accurate determination of the misorientation matrix . . . . .	179
	A13.1 The least-squares method for the calculation of the misorientation matrix . . . . .	181
	A13.2 The solution of the constrained least-squares minimization equations	184
	A13.3 Error propagation in the calculation of the misorientation matrix . . . . .	187
<u>APPENDIX 14</u>	A package of computer programs for the fast solution of electron diffraction spot/Kikuchi line patterns . . . . .	189
	A14.1 Description of the procedure . . . . .	189
	A14.2 Program INDEX for the indexing of electron diffraction spot/ Kikuchi line patterns . . . . .	190
<u>APPENDIX 15</u>	Preparation methods of silicon samples for transmission electron microscopy . . . . .	192
	A15.1 Samples from bulk material . . . . .	192
	A15.2 Transmission electron microscopy sample preparation . . . . .	193
<u>APPENDIX 16</u>	Covalent bonding in diamond-structure-type materials . . . . .	197
<u>APPENDIX 17</u>	Additional electron diffraction information for silicon . . . . .	199
	A17.1 Silicon structure data . . . . .	199
	A17.2 Extinction distances of silicon . . . . .	199
	A17.3 Anomalous absorption coefficients for silicon . . . . .	200
	A17.4 Determination of the crystal deviation from the Bragg reflecting position . . . . .	201
References . . . . .		202

(The tables and figures are contained in the text and appear on an unnumbered page directly following the page on which they are first mentioned. Footnotes are also contained in the text and appear in the end of the section in which they are mentioned)

## Chapter 1

### INTRODUCTION

#### 1.1 Objectives of the theoretical part

Grain boundaries play an important role in controlling physical properties of polycrystalline solids. On account of this, the structure of grain boundaries has been studied extensively in recent years (Chadwick & Smith, 1976). Most of the work carried out has been based on sophisticated experimental procedures as well as making use of powerful tools of modern physics to investigate the structure and/or the properties of interfaces. The present work is intended to supplement rather than compete with the physically based literature. The approach is phenomenological and the questions which are asked are: how are different causes/effects inter-related; and, what mathematical similarities are there in the formulation and manipulation of different grain-boundary properties?

The relationship between cause and effect can be studied on the basis of Neumann's (1885) principle. This principle states that 'the symmetry elements of any (macroscopic) physical property of a crystal must include all the symmetry elements of the point group of the crystal'. This implies that any given physical property may possess a higher symmetry than that possessed by the crystal. What is mandatory is that it can not be of a lower symmetry than that of the crystal.

Neumann's principle has been extensively used for the study of single crystals. But its validity is more general; recently Pond & Bollmann (1979) pointed out that Neumann's principle holds equally well for bicrystals. An immediate implication is that the symmetry of the class to which a particular bicrystal belongs determines the type and extent of anisotropy exhibited by a given bicrystal in regard to the (macroscopic) physical properties.

A given symmetry has the same effect on different physical properties represented by the same tensor irrespectively of their physical nature. In a bicrystal belonging to a particular class all physical properties represented by a tensor of the same kind and rank possess the same scheme of non-vanishing coefficients. Once the effect of various symmetries on the tensors of different ranks and types is worked out, all that is necessary to determine the effect of symmetry on a particular physical property is to establish the kind and rank of the tensor by which it is represented. The usefulness and convenience of such a broad classification and general treatment are thus apparent. In order to use tensor calculus, however, a comprehensive crystallographic framework is required. This is the aim of the theoretical part of this thesis.

#### 1.1.1 Earlier work on interfacial symmetry

The symmetry of bicrystals <sup>1\*</sup> has been studied by employing concepts from two-coloured symmetry (Mokievskii & Shafranovskii, 1957; Curien & Le Corre, 1958; Curien & Donnay, 1959), the theory of representations (Indenbom, 1960), the theory of two-sided infinite plane groups (Holser, 1958a) and the general study of crystal shapes (Mokievskii, Shafranovskii & Afanas'ev, 1965; Shafranovskii & Pis'mennyi, 1961; Shafranovskii, 1960; Mokievskii, 1968). The last three approaches, although using different concepts, are based on the same principle. The derivation of the symmetry classes is based on successive consideration of the crystal faces of simple form and the combination of them. However, this approach does not give the symmetry group of the bicrystal but only the symmetry of the interface; the atomic configuration along

---

\* all footnotes are contained in the text and appear directly following the section on which they are mentioned.

side the boundary plane is neglected.

Curien & Le Corre (1958), on the other hand, have proposed that in twinning by merohedry or by reticular merohedry<sup>2</sup> the symbolism of 'black-white' Shubnikov groups can be used to designate the various twin laws (see also Mokievskii, Shafranovskii, Vovk & Afanas'ev, 1966). Thus every twin law gives the geometrical relationship between two crystals, a 'black' one and a 'white' one. It corresponds, therefore, to a colour-reversing symmetry operation (see section 3.3). Although generalized extensions of this approach have been proposed (Curien & Donnay, 1959; Takeda, Donnay & Appleman, 1967) its use has been restricted to twins only.

It was only recently that the symmetry of a general grain boundary was considered by Pond & Bollmann (1979). They proposed, independently, the employment of the two-coloured symmetry classes for the classification of a general bicrystal. Moreover, they showed that a complete crystallographic framework can be established for the classification of the interfacial symmetry. Such a framework is determined in this thesis.

### 1.1.2 The present approach

The study of the interfacial symmetry is necessarily based on the already established theory of symmetry (see e.g. Weyl, 1952; Neuman, 1956; Coxeter, 1969). The latter provides schemes for the classification of the symmetry of any object; the various schemes are discussed in chapter 2. In order to establish which of these schemes are consistent with the interfacial symmetry a geometrical model is required. Such a model as well as the associated crystallographic concepts are developed in chapter 3.

An important concept introduced in connection with the geometrical modelling of an interface is the 'dichromatic complex'. This is the

configuration of two interpenetrating lattice-complexes, i.e. sets of points describing the space symmetry of the adjacent crystals<sup>3</sup>. The dichromatic complex, although a purely mathematical concept, permits:

- (a) a comprehensive description of the interfacial symmetry in terms of the component crystals, and,
- (b) it can be used for the determination of the various interfacial symmetries created by two given crystals in a given misorientation.

Having established the geometrical model attention is focused on the symmetry groups which are consistent with the geometry of either the dichromatic complex or the bicrystal. The point groups of the former can be established by bearing in mind that they correspond to symmetries created by the superposition of the point symmetries of the associated lattice-complexes. Thus, the determination of the point groups is carried out by employing the group-theoretical method given in chapter 4. This method enables the point symmetry created by the superposition of two point groups to be studied in terms of the misorientation of the two components. The application of this method shows that the point groups of the dichromatic complexes are isomorphic to the antisymmetry point groups and a list of all permissible point groups is given in section 4.3. Furthermore, the method permits the determination of the point groups of the dichromatic patterns<sup>4</sup>.

The conclusions reached in chapters 3 and 4 are subsequently used for the determination of the symmetry classes of dichromatic complexes and bicrystals. Tables covering all the possible cases as well as examples of particular cases are given in chapter 5. These tables are derived by assuming that the components of the dichromatic complex or bicrystal have a common origin. Pond & Bollmann (1979) have shown,



however, that the symmetry of dichromatic patterns or bicrystals can be changed if their components are displaced relative to each other. This is discussed in chapter 6 where an analytical procedure is developed for the systematic study of such variations of the symmetry.

The remaining of the theoretical part deals with the symmetry of bicrystals created for a given dichromatic complex. Thus, it is shown in chapter 7 that both the point and/or the translational bicrystal symmetry can be determined in a systematic way. Also, it is proved that group-theoretical considerations can be used in a comprehensive manner for predicting some interesting features of the interfacial symmetry. The most important of these is the occurrence of bicrystals with symmetry related structures (Pond & Bollmann, 1979). The implication of such cases is apparent (see e.g. Pond, 1977) and indicates that considerations of the interfacial symmetry may yield a model of grain boundary structure. This is of considerable importance on the grounds that all the current grain boundary structural models are basically of geometrical nature as is discussed in the next section.

- - -

- Footnotes
- 1: In effect, the treatment in the mentioned papers refer to twin related crystals, a rather special case of bicrystals.
  - 2: Twinning by 'merohedry' or by 'reticular merohedry' are terms introduced by Friedel (1926) but since his work is in French the English-speaking reader may find easier to refer to Cahn (1954) for a contemporary account of the development of the ideas involved.
  - 3: For a detailed definition of the lattice-complex

and dichromatic complex see section 3.1.

- 4: A dichromatic pattern has been defined by Pond & Bollmann (1979) as the configuration of two interpenetrating lattices.

## 1.2 Outline of grain boundary models

The development of grain boundary theories (i.e. models tending to explain the structure and/or the properties of grain boundaries) was necessarily parallel to advances in the understanding of the crystalline state. Thus, it was not until the crystalline nature of metals was accepted that the first grain boundary theory was put forward (Ewing & Rosenhain, 1901; Rosenhain, 1925; see also King & Chalmers, 1949 for a review). The main disadvantage of the Rosenhain's 'amorphous cement' model was that it necessitated a thick grain boundary layer (see e.g. Desch, 1912; Ke, 1947; McLean, 1957).

Gough (1928) then suggested that a defined atomic arrangement at the grain boundary layer should provide a means of accommodating the change in orientation between the two crystals. This was extended by Hargreaves & Hills (1929) who formulated Gough's idea into the first theory of grain boundary structure related to the crystal lattice geometry ('transition-lattice' model). Burgers (1940) and Bragg (1940) subsequently described the boundary in terms of an array of dislocation lines accommodating the misorientation between the two crystals. Their proposals were confirmed by the observations of Lomer & Nye (1952) and Vogel, Pfann, Corey & Thomas (1953).

Around the same time several theories (Mott, 1948; Kê, 1949; Smoluchowski, 1953; Friedel, Cullity & Crussard, 1953) were put forward but none was completely successful. Each was put forward to explain particular properties and, while having some quantitative success with

properties which it was put forward to explain, did not explain other properties. Thus, the majority of recent theories have been based on the suggestions of Bragg (1940) and Burgers (1940). The development of this model for low-angle boundaries was due to Frank (1950) who presented a formulae relating the angular misorientation of the two crystals to the Burgers vectors and spacings of dislocations required to produce that misorientation. Read & Shockley (1950) used Frank's formula for the calculation of the energy of low-angle boundaries and their results showed good agreement with experimental results (Dunn, Daniels & Bolton, 1950).

Brandon, Ralph, Ranganathan & Wald (1964) and Brandon (1966) combined the dislocation array idea with the coincidence-site lattice (CSL) model of Friedel (1926) and Ellis & Treuting (1951)<sup>1</sup> in order to describe the structure of high-angle boundaries. Experimental evidence (see e.g. Kronberg & Wilson, 1949) indicated that the CSL model provides a reasonable explanation of certain interfaces. However, more systematic experiments by Aust & Rutter (1959) and Aust, Ferran & Cizeron (1963) showed that not all the boundaries had the exact CSL misorientation, but that angular deviations up to  $\pm 5^\circ$  from exact coincidence could be observed. It became, therefore, necessary to find a more general mathematical framework for expressing the concept of coincidence, and generalizing the ideas to include all possible misorientations. One way in which this problem may be approached has been developed by Bollmann (1970) and is the O-lattice theory.

Bollmann's model generalized the concept of coincidence to consider not just coincidence of lattice sites between crystals, but coincidence of equivalent points within two misorientated crystals. The O-lattice model enables a grain boundary dislocation structure to be

constructed for any boundary (see e.g. Warrington & Bollmann, 1972; Christian, 1975; Smith & Pond, 1976) and also enables the possible Burgers vectors of grain boundary dislocations to be obtained (Grimmer, Bollmann & Warrington, 1974). However, the optimum structure as predicted by the O-lattice is calculated from a purely geometrical consideration of the crystals making up the interface, and takes no account of the possibility of different interatomic interactions occurring in different materials with the same lattice type.

Relatively recently a number of papers<sup>2</sup> were published concerned with computer simulation of the structure (and properties) of grain boundaries in an attempt to account for the influence of the interatomic interactions. These calculations show, to a greater or lesser extent, that coincidence boundaries display minima in the energy vs. misorientation curve.

Another feature obtained by preliminary computer simulation of grain boundary structures was revealed about 1967-1970 by Chalmers and co-workers whose work developed an alternative concept of coincidence. On the basis of these calculations, and subsequent work (see e.g. Pond, Smith & Clark, 1974; Pond, 1975, 1976; Pond, Smith & Vitek, 1976), a new model of the structure of coincidence-related boundaries was proposed, in which the maintenance of a periodic structure in the interface is central, rather than the occupation of coincidence sites. It is still true, however, that coincidence misorientations produce lower energy interfaces than random ones, the misorientation being unaffected by the presence of a translation. Thus, it was proposed that the periodicity of boundaries between crystals in a CSL orientation remains of fundamental importance in defining the nature of grain boundary dislocations and the location of minima in the energy of grain boundary.

- - -

Footnotes 1: The identity between the two approaches was pointed

out by Whitwhan, Mouflard & Lacombe (1951).

2: See Hasson and co-workers (1970-1972c); Weins and co-workers (1969-1972b); Dahl and co-workers (1970-1972b); Pond and co-workers (1976, 1979); Smith et al. (1977); Pond & Vitek (1977); Bristowe & Crocker (1975), and, Geary & Bacon (1976).

### 1.3 Objectives of the experimental work

The aim of the experimental part of this thesis was to use transmission electron microscopy for analysing the structure of grain boundaries formed by CSL related crystals. This involved the determination of rigid-body translations at grain boundaries by using an imaging mode which allows them to be revealed as stacking-fault like fringes. This technique has been used for investigating the structure of twin boundaries in aluminium (Pond & Smith, 1974), stainless steel (Pond, Smith & Clark, 1974) and copper (Pond & Smith, 1976). There are several reasons, such as easy specimen preparation, relatively simple structure, comparison with computer simulated grain boundary structure, which have contributed, at least in the initial stage, towards the application of the method to metals.

In this thesis, because of its technological importance, the material chosen was silicon. The significance of the grain boundary structure studies in this material can be understood by the following considerations. During the last years there has been an impact on terrestrial use of solar cells. These are photovoltaic devices designed to convert sunlight into electric power. The advantages of solar cells lie in their ability to provide significant quantities of electrical energy from an inexhaustible resource without the problems of pollution or physical danger. However, the technology for photovoltaic conversion must

be further developed to make it economical viable for terrestrial applications. The efforts in photovoltaic research are mainly concentrated on polycrystalline silicon cells. The primary goal is the development and fabrication of low cost silicon base materials.

One of the key factors controlling the cost of terrestrial silicon solar cell production is the process of growing silicon sheet. It is well recognized by now (Hovel, 1975; Palz, 1979) that the cost of silicon sheet has to be substantially reduced to meet the requirements of low-cost photovoltaic arrays. The current process of producing silicon sheet is entirely based on the conventional Czochralski ingot growth and wafering as practiced by the semiconductor industry. The order of magnitude reduction in cost required by low-cost silicon sheet can not be met by this current technology (Koliwan, Daud & Liu, 1979). Clearly, alternative sheet growth processes are needed.

The prospects for significant cost reduction seem very good, particularly with the ribbon or polycrystalline silicon growth processes. The silicon obtained by these growth methods differs from that produced for semiconductor intergrated circuit applications. The low-cost silicon sheet is structurally and chemically less perfect; these imperfections are the direct result of the growth processes. Such imperfections may influence the electrical and/or mechanical properties of the material with immediate consequences in the solar cell performance. Grain boundary effects are probably the most important since can short circuit the junction or barrier, and often recombination velocities in the boundary are very high. The first contributes a low resistance and the second yields a low quantum efficiency. Potential barriers often exist at grain boundaries and these can add to the series resistance if the grains do not extend through the film.

The above considerations indicate the great importance of the study of the grain boundary structure in silicon. Most of the sheet methods produce a polycrystalline sheet where the majority of the boundaries are twins (Helmreich & Seiter, 1979; Johan et al. 1979). Thus, the significance of knowing the structure of the twins is aparent. These considerations indicate the background in which the experimental work of this thesis lies. In chapter 10 the structure of the coherent and the  $\Sigma=3$ ,  $\{211\}$  twins is determined. The obtained structure is interpreted in terms of atomic bonding as well as in connection to results obtained by measurements of the electrical properties of appropriate specimens reported by other workers.

## Chapter 2

### SYMMETRY OF OBJECTS

#### 2.1 Classical symmetry<sup>1</sup>

Symmetry groups are sets of geometrical transformations (symmetry operations) which operating on an object leave it in a condition indistinguishable from its original condition. The classical theory of symmetry was originally developed in the publications of Fedorov (1891) and Schönflies (1891). Subsequently, numerous works (see e.g. Bravais, 1866; Niggli, 1919; Speiser, 1924) have been carried out leading to the establishment of a complete framework for the symmetry theory. This framework serves to classify any 1-, 2- or 3-dimensional object since any given object can possess one and only one combination of symmetry operations. These ideas were soon applied in fields such as geometrical crystallography, physical theory of crystal structures, the dynamical theory of crystal lattice and the theory of electron structure.

The conventional treatment for deriving the various symmetry classes is to consider initially the point groups (in 1-, 2- or 3-dimensions) and then to combine these symmetry operations with the appropriate translational symmetry. The symmetry of the obtained configuration of single points can be described by considering the concept of 'lattice-complex' (Gitterkomplex) introduced by Niggli (1919, 1924). A lattice-complex is the totality of all points which can be derived from a given point,  $xyz$ , by the employment of all the point symmetry operations of a given spatial group<sup>2</sup>. The translation group is then applied to this point configuration so that an identical lattice is generated for all points equivalent to  $xyz$ <sup>3</sup>.

A lattice-complex is, by definition, different from a lattice which is a periodic array of (mathematical) points specifying the translational



(but not the point) symmetry of the crystal. Thus, to each lattice-complex corresponds a lattice (which can be found if the translational group of the particular spatial group is considered); but the inverse is not always true. The lattice-complex and the lattice can be identical<sup>4</sup> only for the cases where the particular spatial symmetry group belongs to the holosymmetric class of the crystal system.

The classification scheme of the theory of symmetry is based on the following principles. Firstly, the dimensions of the space 'in' which the object is considered restrict the kind of symmetry operations being consistent with the geometry of the object. For example, a one-dimensional object can not have any symmetry operation besides the transformations which leave the one-dimensional space invariant. Secondly, owing to the particular features of the object, particular geometric elements (point, line, plane, cell or some combination of them) are required to remain invariant under all operations<sup>5</sup> of the symmetry groups in a class; the well-known distinction between point and space groups is an example.

The two principles mentioned above constitute the basis for a comprehensive classification of symmetry classes, namely, the 'dimensional' description of symmetry groups (Neronova & Belov, 1961; Holser, 1961). This is an expression of the dimensions of space remaining invariant for each symmetry class. This is examined in appendix 2, whereas the classification of (classical) symmetry groups according to their dimensional description is given in table 2.1.1.

It is perhaps appropriate to give the full definitions of some of the classes appearing in table 2.1.1. The class of rod groups,  $G_{3,1}^1$ , for example, is associated with figures without singular points and planes but with a singular translation axis. On the other hand, the

TABLE 2.1.1

Dimensional description of (classical) symmetry classes for  
1-, 2- and 3-dimensional systems

Invariance	Symbol	No. of groups	Comments
0	$G_0^1$	1	(1)
0,1	$G_{1,0}^1$	2	1-dimensional point groups (2)
0,1,2	$G_{2,1,0}^1$	5	(2)
0,1,2,3	$G_{3,2,1,0}^1$	16	strip groups (3)
0,1,3 } (4) 0,2,3 }	$\left\{ \begin{array}{l} G_{3,1,0}^1 \\ G_{3,2,0}^1 \end{array} \right.$	31	two-sided, one-coloured rosette groups (5)
0,2	$G_{2,0}^1$	10	2-dimensional point groups (6)
0,3	$G_{3,0}^1$	32	3-dimensional point groups (7)
1	$G_1^1$	2	1-dimensional space groups (7)
1,2	$G_{2,1}^1$	7	line groups in 2-dimensions (7)
1,2,3	$G_{3,2,1}^1$	31	two-sided, one-coloured band groups (8)
1,3	$G_{3,1}^1$	75	rod groups (line groups in 3-dimensions) (9)
2	$G_2^1$	17	2-dimensional space groups (7)
2,3	$G_{3,2}^1$	80	layer groups (10)
3	$G_3^1$		space groups (Fedorov groups) (7)

(1) Neronova & Belov (1961); Niggli (1959)

(2) Niggli (1959)

(3) Nowacki (1960); Holser (1960)

TABLE 2.1.1-continued

- (4) the equivalence of classes 0,1,3 and 0,2,3 is discussed by Holser (1961)
- (5) Alexander & Herrmann (1929); Weber (1929); Hermann (1929a); Heesch (1929)
- (6) Niggli (1959); Mackay (1957)
- (7) International Tables of X-ray Crystallography (1969)
- (8) Speiser (1924); Belov (1956)
- (9) Hermann (1929a); see also in International Tables of X-ray Crystallography (1969)
- (10) Hermann (1929a); Alexander & Herrmann (1929); Weber (1929)

symmetry of figures without singular points but with a singular plane (on which two non-parallel translation axes are present) is described by the layer class  $G_{3,2}^1$ .

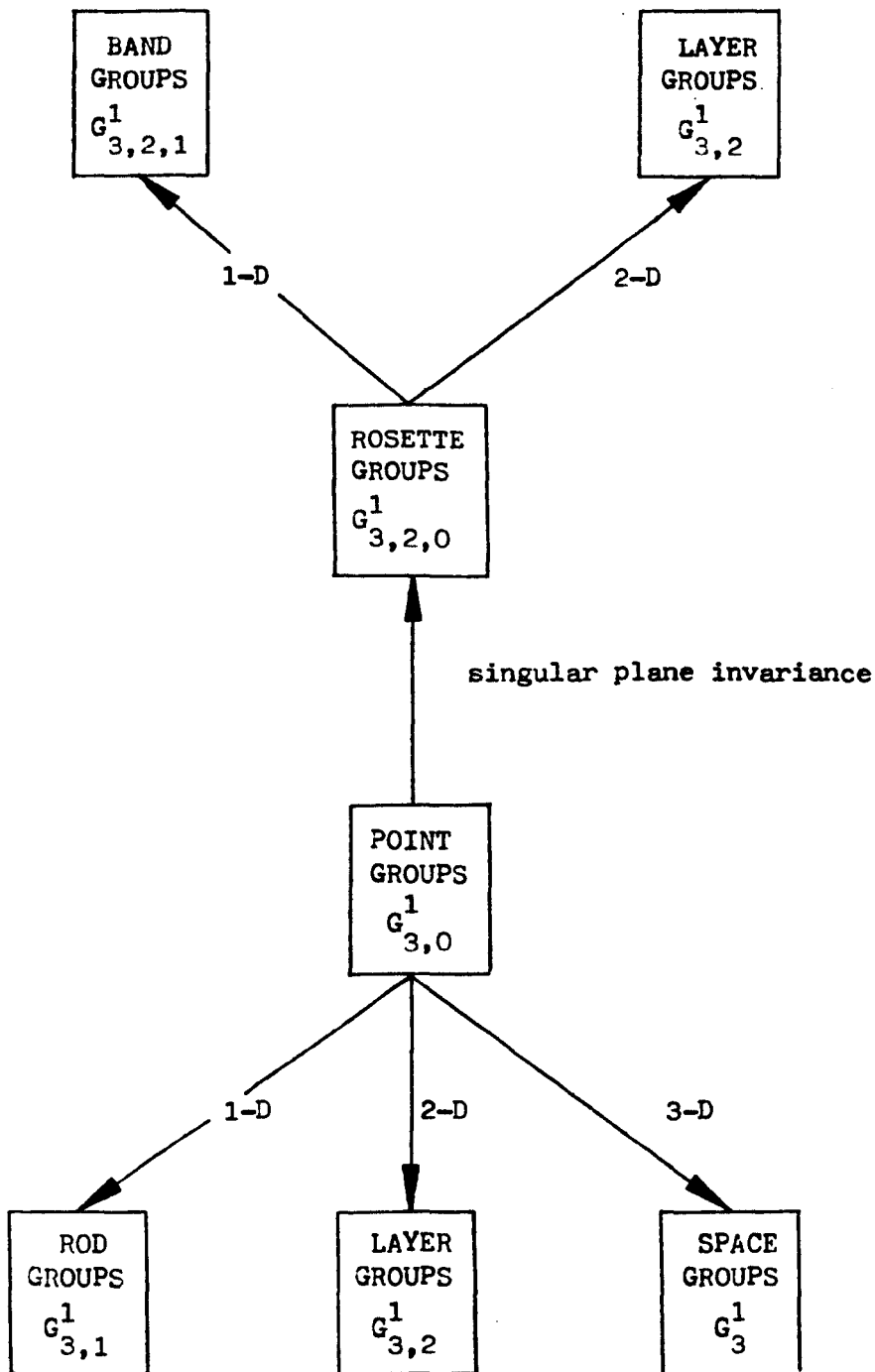
The classes  $G_{3,2,0}^1$  and  $G_{3,2,1}^1$  (together with the  $G_{3,2}^1$ ) are special cases of symmetry consistent with objects containing a singular plane. The former class corresponds to rosettes, i.e. to figures with a singular point and a singular plane. The other class mentioned above is the class of bands where a singular translation axis is considered in addition to the singular point and singular plane. It is of interest to notice that the class  $G_{3,2,1}^1$  bears the same relationship to  $G_{3,2,0}^1$  as the class  $G_{3,1}^1$  to  $G_{3,0}^1$ . This can be seen in figure 2.1.1 which indicates the relationships between the symmetry classes mentioned above.

- - -

- Footnotes
- 1: The nomenclature used in this thesis for denoting symmetry groups, elements and operations is outlined in appendix 1.
  - 2: The term 'spatial symmetry groups' denotes symmetry groups where 1-, 2- or 3-dimensional translation symmetry is included in addition to point symmetry. Spatial symmetry groups should be distinguished from space symmetry groups since the latter involve combinations of point symmetry operations with 3-dimensional translation symmetry.
  - 3: Obviously, it is possible to work in the converse sense and operate first with the translation group and then with all symmetry operations apart from those of the translational group.
  - 4: Provided that an appropriate 'starding' point is considered for the lattice-complex.
  - 5: This includes translations as well as operations of rotation and reflection.

Figure 2.1.1

Schematic representation of the relationships among some symmetry groups.



## 2.2 Antisymmetry

Comparatively recently generalizations of symmetry have been developed. The most straightforward of these generalizations is the concept of antisymmetry (or two-coloured or Shubnikov symmetry) groups. This concept is now briefly examined.

### 2.2.1 Introduction of antisymmetry

The concept of two-coloured symmetry is based on the ideas developed by Heesch (1930) and Shubnikov (1945, 1951). They worked out a theory of symmetry groups in which an operation interchanging black and white colours is considered in addition to the usual geometrical operations. In this respect, antisymmetry is the correspondence of faces, points or other crystallographic objects having some property denoted by a colour or sign, to other faces, points or objects symmetrically related in position, but having the same property with the opposite colour or sign.

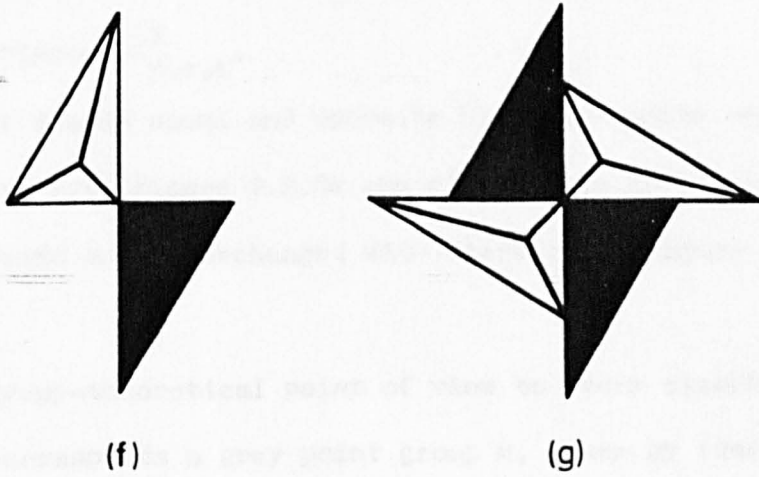
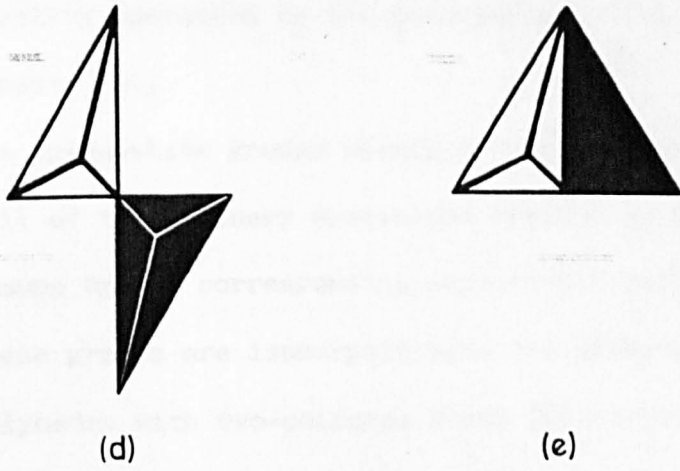
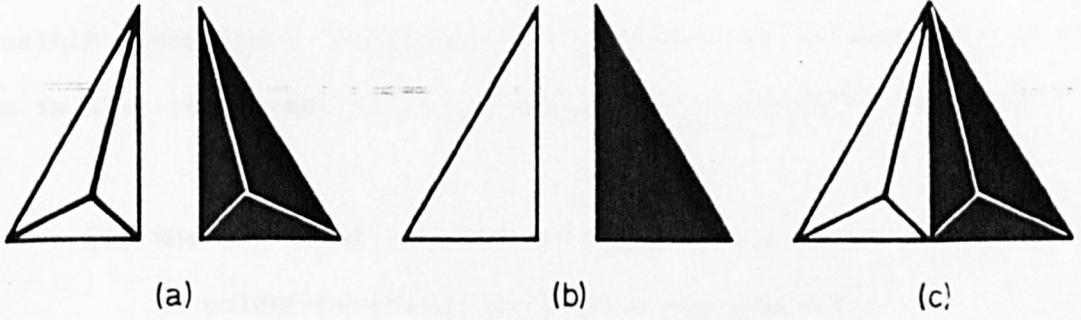
Operations of antisymmetry transfer the object to a symmetrically related position and change its colour or sign. These are called colour-reversing operations (or antioperations) in contrast to the ordinary symmetry operations of the classical crystallography<sup>1</sup>. Thus, the antiidentity operation, for example, corresponds to the operation of changing the colour while keeping the object in its original position. Operations of reflection in a plane and colour-exchange or of inversion in an arbitrary point and colour-exchange (successively performed) will be termed colour-reversing reflection (antireflection) or colour-reversing inversion (antiinversion) respectively.

Some of the antisymmetry operations are schematically represented in figure 2.2.1 with reference to (geometrical) transformations of oblique tetrahedra coloured either black or white. The tetrahedra can

Figure 2.2.1

Schematic representation of some antioperations are shown by using oblique tetrahedra which may point either upwards (a) or downwards (b). The antioperations shown are: colour-reversing mirror plane (c), two-fold colour-reversing rotation axis placed perpendicular to the plane of the diagram (d), two-fold colour-reversing rotation axis in the plane of the diagram (e), colour-reversing centre of symmetry (f), and a four-fold roto-inversion colour-reversing axis (g).





point either upwards (figure 2.2.1a) or downwards (figure 2.2.1b).

### 2.2.2 Groups of antisymmetry of finite objects

The consideration of colour exchanging operations in addition to the classical symmetry operations implies an increase in the number of permissible operations. Consequently, the number of antisymmetry point groups is also increased; it is appropriate to classify these groups into:

- (1) the classical (or one-coloured) groups, i.e. groups where no colour-reversing operations are present,
- (2) the grey (or neutral) groups obtained by adding the anti-identity operation to the generators of the classical groups, and,
- (3) the black-white groups obtained by replacing some (but not all) of the ordinary operations present in the classical groups by the corresponding colour-reversing operations. These groups are isomorphic with the symmetry groups of polyhedra with two-coloured faces (Shubnikov, 1951).

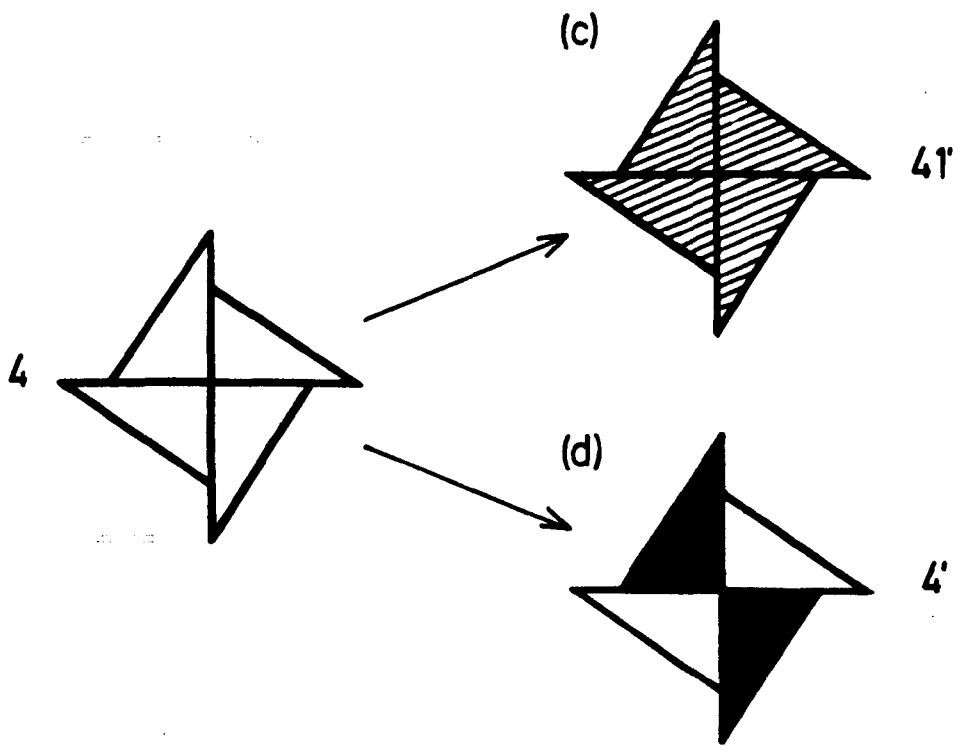
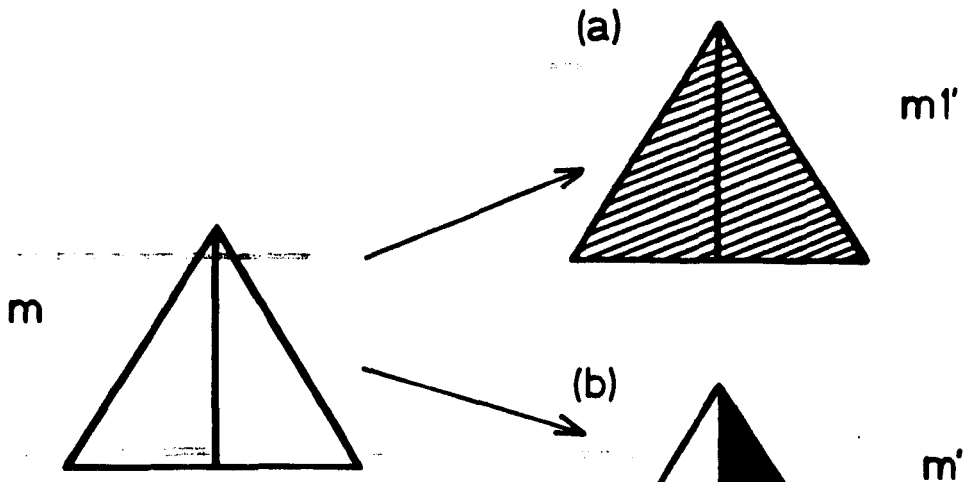
The term 'two-coloured' groups is used in this thesis to denote the set of all (classical, grey and black-white) groups with a given dimensional description  $G_{r,s,t}^2$ .

In the grey groups equal and opposite black and white objects are exactly superposed (see figure 2.2.2a and c), whereas in the black-white groups white objects are interchanged with black ones (figure 2.2.2b and d).

From the group-theoretical point of view to every classical point group<sup>2</sup>  $G$  there corresponds a grey point group  $M$ , given by (see Koptsik, 1966; Bertaut, 1968; Boyle, 1969; Krishnamurti & Gopalakrishnamurti, 1969; Schelkens, 1970; Sumberg et al. 1972):

Figure 2.2.2

Examples of transformation of classical (one-coloured) point groups into grey (a,c) or black-white (b,d) point groups.



$$M = G + \underline{C}G \quad (2.2.1)$$

where  $\underline{C}$  is the operation of antiidentity and the summation is to be understood in the Galois (1897) sense, i.e. as a juxtaposition of elements.

Black-white groups, on the other hand, are defined by:

$$M(H) = H + \underline{C}(G-H) \quad (2.2.2)$$

where  $H$  is a halving subgroup of  $G$ , and  $G-H$  means the set of elements of  $G$  that do not belong to  $H$ . A halving subgroup is defined as a subgroup of index 2 (i.e. it has half as many elements as  $G$ ) and is, therefore, an invariant subgroup (Higman, 1955).

The two-coloured point groups,  $G_{3,0}^2$ , often called Heesch groups, were first derived by Heesch (1930) and later by Shubnikov (1951). In 1960 to 1965 two-coloured groups keeping as special (invariant) elements certain points, lines or planes (i.e. subgroups of  $G_{3,0}^2$ ) were derived. To the known 158 Heesch groups were added the two-dimensional, two-coloured point groups,  $G_{2,0}^2$  (Nowacki, 1960; Palistrant, 1965), the  $G_{2,1,0}^2$  (Palistrant, 1965) and the  $G_{3,2,1,0}^2$  (Shubnikov, 1962a-c) groups. The dimensional description of the two-coloured classes of symmetry groups is given in table 2.2.1.

### 2.2.3 Groups of antisymmetry of infinite figures

By passing from finite to infinite figures the possibility of translational symmetry must be considered in addition to the point symmetry operations. The combination of translations and colour exchange implies the occurrence of colour-reversing translations (or antitranslations). An immediate consequence is that the number of lattices (i.e. the number of non-equivalent ways of arranging black and white points in the space) increases.

The derivation of the two-coloured lattices is based on the fundamental property of the colour translation; two consecutive colour

TABLE 2.2.1

Dimensional description of two-coloured symmetry classes for  
1-, 2- and 3-dimensional systems

Invariance	Symbol	No. of groups	Comments
0	$G_0^2$	2	(1)
0,1	$G_{1,0}^2$	5	two-coloured, 1-dimensional point groups
0,1,2	$G_{2,1,0}^2$		(2)
0,1,2,3	$G_{3,2,1,0}^2$		two-coloured strip groups (3)
0,1,3 } (4)	$\left\{ \begin{array}{l} G_{3,1,0}^2 \\ G_{3,2,0}^2 \end{array} \right.$	125	two-sided, two-coloured rosette groups (5)
0,2,3 }			
0,2	$G_{2,0}^2$		two-coloured, 2-dimensional point groups (6)
0,3	$G_{3,0}^2$	122	two-coloured, 3-dimensional point (Heesch) groups (7)
1	$G_1^2$	7	two-coloured, 1-dimensional space groups (1)
1,2	$G_{2,1}^2$		two-coloured line groups in 2-dimensions (8)
1,2,3	$G_{3,2,1}^2$	179	two-sided, two-coloured band groups (9)
1,3	$G_{3,1}^2$	394	two-sided, two-coloured rod groups (10)
2	$G_2^2$	80	two-coloured pattern groups (11)

TABLE 2.2.1-continued

Invariance	Symbol	No. of groups	Comments
2,3	$G_{3,2}^2$	530	two-sided, two-coloured layer groups (12)
3	$G_3^2$	1651	two-coloured space groups in 3-dimensions (Shubnikov groups) (13)

- (1) Neronova & Belov (1961)
- (2) Palistrant (1965)
- (3) Shubnikov (1962a,b)
- (4) the equivalence is discussed by Holser (1961)
- (5) see appendix 3
- (6) Nowacki (1960); Palistrant (1965)
- (7) Heesch (1929); Shubnikov (1951); Koptsik (1966)
- (8) Belov (1956)
- (9) see appendix 4
- (10) Neronova & Belov (1961); Galyarskii & Zamorzaev (1965);  
Shubnikov (1959)
- (11) Heesch (1929); Cochran (1952); see also Shubnikov &  
Koptsik (1974)
- (12) Neronova & Belov (1961); Palistrant & Zamorzaev (1963)
- (13) Heesch (1929); Zamorzaev (1953, 1957, 1962); Belov,  
Neronova & Smirnova (1955, 1957); Koptsik (1966)

translations in one direction are equivalent to one uncoloured translation in the same direction. The two-coloured lattices are classified into:

- (1) the classical, and,
- (2) the black-white (or antitranslation) lattices.

Belov, Neronova & Smirnova (1955) shown that in three dimensions there are 36 two-coloured Bravais lattices including the 14 classical but excluding a further 14 grey lattices.

The 1651 two-coloured space groups,  $G_3^2$ , were first derived by Zamorzaev (1953, 1962) and it was he who introduced the term 'Shubnikov groups'. The remaining classes of two-coloured symmetry groups were derived between 1929 and 1963; references for these groups are given in table 2.2.1.

- - -

- Footnotes 1: Subsequently, the terms 'element of symmetry' or 'symmetry operation' will be understood to include elements or operations of antisymmetry respectively (unless specifically is stated to be otherwise).
- 2:  $G$  is not necessarily one of the 32 classical point groups, but it can be any one-coloured point group (Koptsik, 1966; Boyle, 1969).



## Chapter 3

### CRYSTALLOGRAPHIC TREATMENT OF INTERFACES

#### 3.1 A model of bicrystals

An interface is considered to be the surface separating two (semi-infinite) crystals differing in chemical composition and/or the orientation of their respective lattices. The geometrical relationships existing between the two crystals define the interfacial symmetry. This can be expressed by referring to the 'ideal bicrystal'.

##### 3.1.1 The ideal bicrystal

An ideal bicrystal is defined as the assembly of two semi-infinite crystals (differing in chemical composition and/or the orientation of their lattices) separated by a geometrical plane, the interface. One of the two semi-infinite crystals is designated 'white' and the other 'black'; this designation is, however, quite arbitrary and there is no difference between a white and a black point except that they belong to different crystals.

The term 'ideal bicrystal' (or simply bicrystal) is used in this work to denote a strictly mathematical configuration<sup>1</sup>. This definition implies that:

- (1) the interface is considered to be a unique plane in the bicrystal as it represents a surface of a two-dimensional mathematical discontinuity which may be associated with a sharp change in physical properties, and,
- (2) an ideal bicrystal extends to infinity.

For symmetry considerations it is often advantageous to disregard the atomic structure of the adjacent crystals. The interface is, then, considered as the unique plane separating the black and white semi-infinite lattice-complexes<sup>2</sup> (see section 2.1 for the definition of a lattice-complex).

### 3.1.2 Dichromatic complex

Furthermore, in some cases, depending on what is studied, the requirement of the unique plane can be relaxed. This is equivalent to allowing the black and white lattice-complexes to interpenetrate each other. The configuration so obtained consists of two differently orientated and/or different lattice-complexes and is called a 'dichromatic complex'. The introduction of this concept involves a significant simplification as far as the symmetry studies of bicrystals are concerned since their symmetry can be studied in direct relation to the symmetry of the component structure(s). Moreover, in this case the symmetry of a bicrystal corresponds directly to the correlative part of the dichromatic complex symmetry, i.e. a section of the spatial group taken at the interface position (this is examined in section 7.1).

### 3.1.3 Dichromatic pattern

It must be mentioned that the term 'dichromatic complex' is to be distinguished from the concept of the 'dichromatic pattern' introduced by Pond & Bollmann (1979). They defined the dichromatic pattern as consisting of two interpenetrating<sup>3</sup> lattices. In the remaining of the thesis the term dichromatic complex is considered to include the dichromatic pattern concept as well, unless it is specifically stated to be otherwise.

The dichromatic pattern provides a comprehensive skeleton for the construction of an ideal bicrystal. This is because, once the boundary plane is fixed in the dichromatic pattern the appropriate bases may be filled at the sides of the white lattice on the one side of the boundary and at the sides of the black lattice on the other side. As soon as the interface is realized the remainder of the lattices lose their meaning.

The difference between dichromatic patterns and dichromatic

complexes is illustrated in figure 3.1.1. This shows (figure 3.1.1a) the dichromatic complex formed between two diamond-structure-type lattice-complexes (they are related by the CSL rotation  $[001]/36.9^\circ$ ). In this particular case the associated dichromatic pattern is formed by two f.c.c. lattices (figure 3.1.1b) in the same misorientation relationship.

The above example indicates an alternative procedure for obtaining the dichromatic complex. Thus, it is obtained by locating appropriate sets of points to each lattice position of the dichromatic pattern (in the correct orientation). It is, therefore, clear that the dichromatic complex has the same periodicity as the associated dichromatic pattern.

#### 3.1.4 Degrees of freedom of an interface

The relative position of the two crystals across an interface is fully described, without any particular reference to an interfacial structure model, by determining:

- (1) the misorientation relationship<sup>4</sup>,
- (2) the relative translational position of the two crystals, and,
- (3) the orientation of the interface plane.

The white lattice-complex is considered fixed in space and is used as reference. Any misorientation present is considered<sup>5</sup> to arise from the appropriate movement and/or rotation of the black lattice-complex. Following Seitz (1936)<sup>6</sup> the symbol  $\{R'/\underline{t}\} = \{([hkl]/\theta)'/\underline{t}\}$  is introduced for describing the relative position and misorientation of the two components. The  $R' = ([hkl]/\theta)'$  means that a lattice-complex originally coincident with the white lattice-complex and with the same colour is rotated by an angle  $\theta$  about  $[hkl]$  (using the coordinate system of the white lattice-complex) and subsequently undergoes colour reversal from white to black<sup>7</sup> and a shift characterized by a vector  $\underline{t}$  (which is

Figure 3.1.1

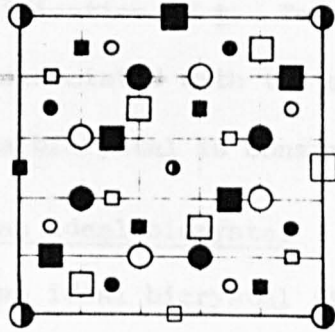
Schematic representation showing the difference between a dichromatic complex and a dichromatic pattern:

- (a) (001) projection of a dichromatic complex formed by two lattice-complexes of the diamond-structure type in  $[001]/36.9^\circ$  misorientation
- (b) (001) projection of a dichromatic pattern formed by two f.c.c. lattices in  $[001]/36.9^\circ$  misorientation

Key: Open symbols: positions of the white lattice/lattice-complex  
Filled symbols: positions of the black lattice/lattice-complex  
Large circles: in the plane of the paper  
Small circles:  $+a/2$  out of the paper  
Large squares:  $+a/4$  out of the paper  
Small squares:  $+3a/4$  out of the paper

The displacement of the black lattice-sites from the neutral lattice-sites (indicated by dots).

For dislocations constructed by a given lattice-complex all geometrical degrees of freedom are required for specifying the orientation relationship between the black and white components. These degrees of freedom are associated with the specification of the axis,  $l$ , and angle,  $\theta$ , of rotation; the other three degrees are

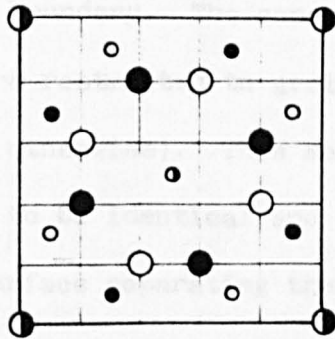


(a)

- (1) to obtain the lattice-sites pattern,
- (2) to specify the orientation of the boundary plane, and,
- (3) to locate the appropriate lattice-sites at the

sites of the white lattice on the one side of the boundary and at the sites of the black lattice on the other.

The above model was derived by bearing in mind a general



(b)

orientation of the lattice-sites pattern, and, on the lattice-sites on the one side of the crystals, atomic relaxation or stress moments are considered. This immediately yields that symmetry changes

the displacement of the black lattice-complex away from the neutral origin position).

For dichromatic complexes constructed by a given lattice-complex six geometrical degrees of freedom are required for specifying the misorientation relationship between the black and white components. Three degrees of freedom are associated with the specification of the axis,  $[hkl]$ , and angle,  $\theta$ , of rotation; the other three degrees are required for the specification of  $\underline{t}$ . Two additional degrees of geometrical freedom are associated with the specification of the interface plane,  $u=[pqr]$ , when a bicrystal is constructed.

### 3.1.5 Manufacture of an ideal bicrystal

To manufacture an ideal bicrystal it is, therefore, necessary (Pond & Bollmann, 1979):

- (1) to obtain the appropriate dichromatic pattern,
- (2) to specify the orientation of the boundary plane, and,
- (3) to locate the appropriate bases (atomic motifs) at the sites of the white lattice on the one side of the boundary and at the sites of the black lattice on the other.

The above developed model was derived by bearing in mind a general (grain or interphase) boundary. The considerations in the remaining of this work, however, are restricted to grain boundaries (unless specifically is stated to be otherwise). This means that the two lattice-complexes are considered to be identical and the grain boundary is considered as the planar surface separating them. Interphase boundaries will be considered separately in section 8.2.

- - -

Footnotes 1: This means that imperfections such as dislocations on the interface or in either of the crystals, atomic relaxation or stress movements are not considered. This immediately yields that symmetry changes

introduced by such deviations from the normal configuration are not included in the considerations of this thesis.

- 2: It is hoped that the advantages of this formulation will become apparent in due course.
- 3: The fact that a lattice is, by definition, infinite does not necessarily involve that the two lattices are interpenetrating, since they can be considered to be 'in' different metric spaces.
- 4: The misalignment between the two components of a bicrystal (or a dichromatic complex) will be called its misorientation relationship (or simply misorientation).
- 5: This treatment refers, obviously, to grain boundaries only; for the case of interphase boundaries a similar procedure can be devised (see section 8.2).
- 6: The original paper is written in German; for an English translation see Cracknell (1968).
- 7: Obviously, it is possible to work in the converse sense and operate first the colour reversal and then the rotation  $[hk.l]/\theta$ .

### 3.2 Crystallographic definitions for interfaces

Dichromatic complexes and bicrystals are 'objects' in the sense of the theory of symmetry. This means that they possess spatial and/or point symmetry. The function of this section is to deduce the symmetry terminology relevant to the study of interfaces.

#### 3.2.1 Dichromatic point groups

A dichromatic point group<sup>1</sup> is a group in the mathematical sense containing symmetry operations (being consistent with each other and with the dichromatic complex geometry) which leave one point of the dichromatic complex unmoved.

The dichromatic point groups can be established in a way similar to that used in classical crystallography for deriving the 32 point groups. This procedure is based on the determination of the set of

symmetry operations being consistent with the dichromatic complex geometry. This imposes limitations upon the permissible symmetry elements. The point groups are then determined by considering combinations amongst the symmetry elements so obtained.

Alternatively, the dichromatic point groups can be determined directly in a far more elegant and comprehensive way. The deviation method is based on the fact that a dichromatic complex is, by definition, the configuration of two interpenetrating lattice-complexes (section 3.1). Accordingly, the dichromatic point symmetry is expressed by the point group obtained by the superposition of two identical point groups (in the appropriate misorientation). In this respect the dichromatic point groups can be determined by applying the group-theoretical method which is developed in chapter 4.

### 3.2.2 Bicrystal point groups

A bicrystal point group is a group in the mathematical sense containing symmetry operations (being consistent with each other and with the bicrystal geometry) which leave one point of the bicrystal unmoved.

The bicrystal point groups can be determined by either establishing the permissible symmetry operations and then investigating combinations between them or by considering the relationship between dichromatic complexes and bicrystals. The former procedure is preferable since the existing crystallographic framework can be directly used for establishing the combinations of symmetry elements.

The alternative procedure is based on the considerations given in section 7.1 where it is shown that the bicrystal point groups are obtained by considering each one of the dichromatic point groups. For the particular point group a sectional plane (corresponding to the



interface plane) is employed and the resulting symmetry is investigated by varying the orientation of the sectional plane. This method, although not very useful for a general study of the bicrystal point groups, can be used for determining the groups associated to a particular dichromatic complex.

- - -

Footnote 1: The term 'dichromatic point group' is not to be confused with the 'two-coloured group' term referred to in section 2.2 (note that Belov, Neronova & Smirnova (1955, 1957) used the term 'dichromatic groups' when referring to the antisymmetry groups).

### 3.3 Crystallographic framework

As Pond & Bollmann (1979) pointed out the symmetry of both the dichromatic complexes and bicrystals can be classified according to the established framework of the theory of symmetry (see chapter 2). This is examined here by using the dimensional description of symmetry classes. But before doing so, the significance of employing antisymmetry classes is briefly considered.

#### 3.3.1 Antisymmetry classes of interfacial symmetry

Dichromatic complexes and bicrystals were introduced as sets of white and black points. The designation of white and black is quite arbitrary and there is no difference between a white and a black point except that they belong to different lattice-complexes. As far as the symmetry is considered, the question arises of the possible symmetry types (groups) of the white/black point distribution.

Let  $\underline{C}$  be the transformation reversing the colours of points. The problem of determining the possible types of dichromatic complex or bicrystal symmetry is the construction of all possible groups containing

besides the usual (geometrical) transformations the symmetry operations obtained by combining the latter with the transformation  $\underline{C}$ . This problem has been extensively considered by Shubnikov and co-workers who have shown that these groups form the antisymmetry classes (see section 2.2).

### 3.3.2 Classes of dichromatic complexes

Dichromatic complexes are three-dimensional objects and, hence, their symmetry classes are considered 'in' the three-dimensional space. This means that all the symmetry classes of dichromatic complexes must have three-dimensional highest invariance, i.e. only classes with dimensional description  $G_{3,t}^2$  must be taken into account.

In order to establish further the symmetry classes of dichromatic complexes, the dimension of the lowest invariance, which each symmetry class must possess, has to be determined. This is, in fact, equivalent to establish the number,  $n$ , of non-parallel translational axes present in the dichromatic complex. In practical terms, the determination of the number  $n$  fixes the index  $t$  in the symbol  $G_{3,t}^2$ .

Pond & Bollmann (1979) have shown that dichromatic patterns can have translational symmetry in zero-, one-, two- or three-dimensions. The same holds for dichromatic complexes (see section 3.1). Non-periodic dichromatic complexes are obtained by rotations of the black lattice-complex about a singular point, the common origin. The symmetry class,  $G_{3,0}^2$ , of dichromatic complexes with singular points contains the two-coloured point groups (see table 2.2.1). these groups are often called Heesch groups and a complete list is given by Shubnikov & Koptsik (1974).

Dichromatic complexes containing a singular line and, hence, exhibiting one-dimensional periodicity are formed only when the rotation axis  $[hkl]$  is rational. On the other hand, dichromatic complexes with

two-dimensional translational symmetry contain a singular plane and occur only for non-cubic lattices (or where the component lattices have different lattice parameters or Bravais classes). The symmetry groups of dichromatic complexes with one- or two-dimensional translations while transforming the three-dimensional space into itself keep a singular line or plane respectively invariant. Thus, the symmetry classes for dichromatic complexes with one or two (non-parallel) translation axes are those of two-coloured rod groups,  $G_{3,1}^2$ , or layer groups,  $G_{3,2}^2$ , respectively. Complete lists of two-coloured, two-sided rod and layer groups have been published by Neronova & Belov (1961).

Finally, three-dimensional periodic dichromatic complexes arise from rotations  $[hkl]/\theta$  leading to coincidence site lattices. The symmetry of the dichromatic complexes with singular lattices correspond to the two-coloured class  $G_3^2$ , and, hence, these complexes are classified by using the two-coloured space groups. These groups are also called Shubnikov groups and a complete enumeration was published by Belov, Neronova & Smirnova (1955). This list, however, contains a number of misprints and errors. Corrections pointed out by Donnay, Belov, Neronova & Smirnova (1958) and a consistent table was published by Belov, Neronova & Smirnova (1957).

The discussion above has been tactically confirmed to crystallographic groups only. Attention is now directed briefly to non-crystallographic classes. As mentioned by Pond & Bollmann (1979) 8- and 12-fold axes can be created by appropriate rotations  $[hkl]/\theta^1$ . Therefore, 8- and 12-fold rotation or rotoinversion axes have to be considered in addition to crystallographic axes in the case of one-dimensional periodic dichromatic complexes (see section 4.3). Moreover, the associated non-crystallographic point groups are also included in the considera-

tions since they describe the point symmetry of dichromatic complexes with one-dimensional translational symmetry<sup>2</sup>.

### 3.3.3 Symmetry classes of bicrystals

Bicrystals are three-dimensional objects containing a singular plane, the interface. The presence of the singular plane introduces further restrictions as far as the symmetry classes of bicrystals are concerned since this plane must be invariant under any operation of the bicrystal symmetry group. Consequently, except for the three-dimensional highest invariance, the bicrystal classes must possess a two-dimensional invariance as well. Thus, the bicrystal classes have a dimensional description of the form  $G_{3,2,t}^2$ .

The singular plane of the bicrystal classes need not be polar<sup>3</sup>, i.e. the 'front' and 'back' sides of the plane need not be different. Examples of non-polar boundary planes are growth twins in Ge, Si or deformation twins observed in various metals. On the other hand, in the (110) twin in aragonite as illustrated by Bragg & Claringbull (1965) (see also section 5.4) the boundary plane is not the same on both sides; it contains a glide plane first noted by Donnay (1954).

The polar character of interface planes was first treaded theoretically for the case of twins by Schaacke (1938) at about the same time that the first case (Baveno twin in fieldspar) was recognized by Bragg (1937) (see also section 5.4). Therefore, it is necessary to consider symmetry groups known as two-sided groups (Shubnikov & Koptsik, 1974). The two-sided character of the groups involves that transformations making the two sides coincide with each another are permitted; and, hence, the two-sided groups include the polar as well as the non-polar plane classes.

The boundary plane might exhibit zero-, one-, or two-dimensional

translational symmetry (Pond & Bollmann, 1979). In the case of non-periodic bicrystals the symmetry group transforms both the three-dimensional space and the unique plane into themselves and at the same time keeps the singular point invariant. Thus, non-periodic bicrystals belong to the symmetry class  $G_{3,2,0}^2$  which is the two-sided, two-coloured rosette class. A complete list of the two-sided, two-coloured rosette groups is derived in appendix 3.

If one-dimensional periodicity is present on the interface the symmetry group must leave a singular line as well as the two- and three-dimensional spaces invariant. Consequently, bicrystals with one-dimensional periodicity are classified in terms of two-sided, two-coloured band groups,  $G_{3,2,1}^2$ . The complete list of these groups is derived in appendix 4. Finally, bicrystals with two-dimensional translational symmetry are described by the symmetry class of two-sided, two-coloured layers,  $G_{3,2}^2$  (Neronova & Belov, 1961).

In concluding it should be noticed that in this section the deviation of the symmetry classes for dichromatic complexes and bicrystals is based on the dimensional description of the various symmetry classes. However, not all the groups of the symmetry classes mentioned above are permissible for dichromatic complexes and bicrystals. This is because of the special features possessed by both dichromatic complexes and bicrystals. This is the subject of chapter 5.

- - -

- Footnotes
- 1: The formation of non-crystallographic symmetry elements is examined from the group-theoretical point of view in section 4.3.
  - 2: It should be noticed that non-periodic dichromatic complexes (i.e. complexes obtained by rotations of the black component about a non-rational direction)

can not possess an 8- or 12-fold axis.

- 3: A plane is called polar if its two surfaces are not (physically) equal to one another; in other terms, a polar plane has a 'front' and a 'back' side.

## Chapter 4

### SUPERPOSITION OF SYMMETRIES

#### Introduction

As was mentioned earlier the dichromatic point group can be determined by considering the superposition of two (classical) point groups in the correct misorientation. The symmetry created by such a superposition can be investigated by the group-theoretical method presented in this chapter.

The basis of the method is the geometrical interpretation of the Neumann-Curie principle outlined in section 4.1. The discussion in this section indicates the qualitative approach for studying the superposition of two point groups. The conclusions reached are subsequently used (section 4.2) for a formulation of the principle in terms of the group theory postulates.

The quantitative approach has been developed having in mind the particular connection with the dichromatic point groups. In view of this the group theoretical expressions yield a procedure enabling the study of the symmetry of the superposed point groups as a function of the misorientation relationship. Consequently, the method developed allows a systematic study of all the permissible dichromatic point groups. The method is applied in chapter 5 where tables containing all the permissible point groups for the dichromatic complexes are determined.

#### 4.1 The principle of composite systems

The aim of this section is to analyze the relationship between the point symmetries of a composite and its components. Such a relationship is governed by the 'principle of the superposition of the symmetry groups'

(Neumann, 1885; Curie, 1894, 1908) which states that the symmetry group of two (or more) objects, regarded as a whole, is the highest common subgroup or the lowest common supergroup of the symmetry groups of the components.

This principle extended to physical properties constitutes the fundamental concept in the field of physical applications of the symmetry theory. For the purposes of the present work, however, a simple geometrical interpretation of the principle is adequate.

#### 4.1.1 The geometrical interpretation of the Neumann-Curie principle

Consider the simple case of superposition of the symmetries of a cube (group  $m3m$ ) and a tetragonal prism (group  $4/mmm$ ), where their centres of gravity and four-fold axes coincide. In this particular example the composite symmetry will be either  $4/mmm$  (if the planes of symmetry of the two figures coincide) or  $4/m$ . This result can be expressed in the general way by stating that the combination of two (or more) geometrically different figures<sup>1</sup> into a composite will comprise only those symmetry elements which are common to all components. The symmetry group of the composite is in this case the common subgroup (including the trivial cases) of the symmetry groups of the components.

A composite with symmetry higher than that of the components can be formed if identical components are considered. In the case of a regular hexagon composed of equilateral triangles, for example, the symmetry of the whole ( $6mm$ ) is higher than the symmetry of the components ( $3m$ ). Thus, if the components are identical then the symmetry group of the composite may be a supergroup of the symmetry group of the components.



#### 4.1.2 Kinds of symmetry operations created by superposition of point groups

A necessary condition imposed by the Neumann-Curie principle is that the relative position of the components must be taken into account in order to determine the symmetry operations of the composite. A immediate consequence of this condition is illustrated by the following example.

Consider figure 4.1.1a which shows separately two components with symmetry 4 in mirror orientation. When they are superposed (figure 4.1.1b), so that they have the same origin, the 4-fold axes of the separate individuals coincide, and, hence, the composite has also a 4-fold axis. But when superposed, there is further symmetry in the composite: any part on the left, say, of one component is related to a similar point on the right of the other component by the symmetry operation which relates the two components. Therefore, the composite has the common symmetry of the individuals augmented by the operation of the mirror reflection.

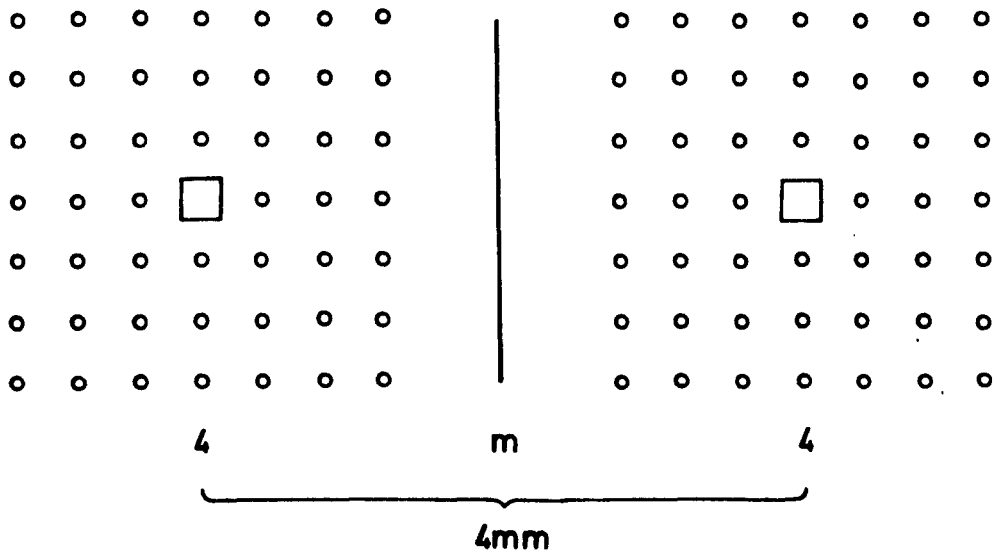
The above example indicates that it is possible for the composite to contain a symmetry element created not by the coincidence but by the appropriate orientation of symmetry elements of the components. Thus, the requirement to account for the relative position of the symmetry operation of the components leads to the above mentioned important aspect of the composite symmetry. This is of great importance in the case of dichromatic point groups.

Referring to dichromatic complexes rotation of the black lattice-complex relative to the white one creates a dichromatic complex with symmetry generally different to that of the white or black lattice-complex. This is because:

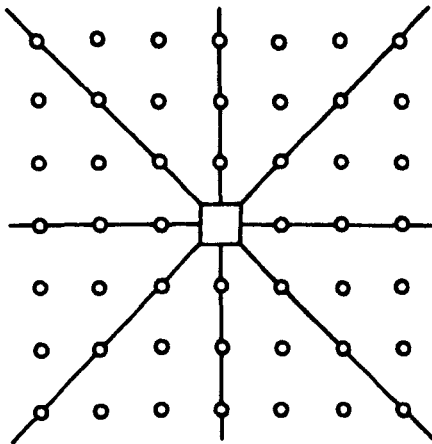
Figure 4.1.1

Superposition of two equivalent components. In (a) the components, each exhibiting symmetry 4, are shown in a mirror orientation. The composite obtained by their superposition (b) exhibits symmetry  $4mm$ .

(a)



(b)



- (a) symmetry elements parallel, after rotation, to one another, in both the white and black lattice-complexes, are conserved
- (b) symmetry elements of the lattice-complexes not parallel after rotation are suppressed; yet they can give rise to colour-reversing operations present in the dichromatic complex.

According to the above discussion it is straightforward to predict the symmetry of the dichromatic complex when the white and black lattice-complexes are given and the misorientation between them is known (see appendix 5). However, for a systematic study of the dichromatic classes an analytical method simplifies the task a great deal. This method allowing the study of the symmetry variation with the misorientation relationship and/or the component symmetry is particularly useful for components with high symmetry (for example cubic groups).

- - -

Footnote 1: Two figures are geometrically different if they can not be converted into one another by transformations of motion and/or similarity. They are also called non-equivalent objects.

#### 4.2 Group-theoretical formulation of the superposition of symmetries

In the previous section a qualitative approach of the Neumann-Curie principle was discussed. For the systematic study of the dichromatic point groups it is, however, necessary to have a quantitative expression and this is the subject of the present section.

The following notation is introduced. Let both the white and black lattice-complexes exhibit a symmetry described by a point group  $G_o$  of order  $r_w$  and elements  $\underline{g}_i$ . The group of the white and black lattice-complexes are designated  $G_w$  and  $G_b$  respectively and they have the same order and elements as  $G_o$ <sup>1</sup>. Operation of the symmetry transformations

$\underline{g}_i$  on a general point gives all the general points of the point group  $G_o$  (see appendix 5). Therefore, before rotation the general points expressed relative to the white system are given by  $\underline{g}_i \underline{x}$ , where  $\underline{x}$  is the position vector of the 'starting' point.

When the black lattice is rotated by  $[hkl]/\theta$ , two sets of points are present, namely, the sets of white and black points. Thus, the number of points is doubled and their positions (relative to the white coordinate system) are  $\underline{g}_i \underline{x}$  (white points) and  $\underline{Rg}_i \underline{x}$  (black points), where  $\underline{R}$  is the matrix describing the vector transformation of the black lattice-complex. Moreover, while the symmetry operations of  $G_w$  are  $\underline{g}_i$ , those of  $G_b$  are expressed relative to the white coordinate system by  $\underline{Rg}_i \underline{R}^{-1}$  (see e.g. Eisenhart, 1933).

#### 4.2.1 Ordinary symmetry operations

Any ordinary symmetry operation in the dichromatic point group relates two points of the same colour; this operation must relate pairs of white as well as black points. Moreover, this symmetry operation must be common in the white and black point groups, since none of the black and white configurations are altered but only their orientation is changed during the rotation. Therefore, the necessary and sufficient condition that an ordinary symmetry operation is present in the dichromatic point group is that identical elements of  $G_w$  and  $G_b$  are coincident<sup>3</sup>.

Consequently, the ordinary symmetry operations in the dichromatic point group are those elements of  $G_o$  which satisfy the relation:

$$\underline{g}_i = \underline{Rg}_j \underline{R}^{-1} \quad (4.2.1)$$

where  $\underline{g}_i$  and  $\underline{g}_j$  are expressed relative to the coordinate system of the white lattice-complex.

Now, let  $D_o$  be the set of elements of  $G_o$  for which relation (4.2.1)

holds. In appendix 6 the following theorem is proved:

**Theorem 4.2.1:** The ordinary symmetry operations of the dichromatic point group form a subgroup (including the trivial ones) of the point group of the white (and black) lattice-complex.

The elements of the subgroup  $D_0$  are denoted by  $h_{\underline{i}}$ . This theorem immediately yields (see appendix 6):

**Theorem 4.2.2:** The order of the dichromatic point group ( $r$ ) is equal to  $2/k$  times the order of the white point group ( $r_w$ ), where  $k$  is an integer.

A consequence of the last theorem is that only symmetry operations of order equal to or less than twice the order of the point group  $G_0$  can be present in a dichromatic point group. The equality, however, holds only when the dichromatic point group is a cyclic one (see e.g. Cornwell, 1969).

#### 4.2.2 Colour-reversing symmetry operations

Attention is now focused on the colour-reversing symmetry operations.

Theorem 4.2.1 propounds that the general points of the dichromatic point group are as follows:

white points:  $\{ h_{\underline{1}} w, h_{\underline{2}} w, \dots, h_{\underline{r_0}} w \}$

black points:  $\{ h_{\underline{1}} b, h_{\underline{2}} b, \dots, h_{\underline{r_0}} b \}$

where  $\underline{w}$  and  $\underline{b}$  are the white and black 'starting' points respectively, and  $h_{\underline{i}}$  ( $i=1,2,\dots,r_0$ ;  $r_0$  being the order of  $D_0$ ) are the elements of the group  $D_0$ .

The relation between  $\underline{w}$  and  $\underline{b}$  can be found if it is born in mind that the black points are obtained by a rotation of the white ones.

Thus,  $\underline{b} = \underline{Rg}_{\underline{k}} \underline{w}$ , where  $\underline{g}_{\underline{k}}$  is a symmetry operation of  $G_0$  ( $\underline{g}_{\underline{k}}$  could be an element of  $D_0$  or not). Therefore, the above sets can be written as:

white points:  $\{ \underline{h}_{\underline{1}} \underline{w}, \underline{h}_{\underline{2}} \underline{w}, \dots, \underline{h}_{\underline{r}} \underline{w} \}$

black points:  $\{ \underline{h}_{\underline{1}} \underline{Rg}_{\underline{k}} \underline{w}, \underline{h}_{\underline{2}} \underline{Rg}_{\underline{k}} \underline{w}, \dots, \underline{h}_{\underline{r}} \underline{Rg}_{\underline{k}} \underline{w} \}$

Any colour-reversing symmetry element of the dichromatic point group must relate a white and a black point of the above sets. Therefore, the colour-reversing operations are given by:

$$\underline{C}_{\underline{m}} = \underline{h}_{\underline{i}} \underline{g}_{\underline{k}}^{-1} \underline{R}^{-1} \underline{h}_{\underline{j}}^{-1} = \underline{h}_{\underline{i}} \underline{g}_{\underline{k}}^{-1} \underline{h}_{\underline{1}}^{-1} \underline{R}^{-1}$$

(in view of the fact that the relation (4.2.1) can be written as

$$\underline{h}_{\underline{1}}^{-1} \underline{R}^{-1} = \underline{R}^{-1} \underline{h}_{\underline{j}}^{-1}), \text{ or:}$$

$$\underline{C}_{\underline{m}} = \underline{h}_{\underline{i}} \underline{g}_{\underline{m}} \underline{h}_{\underline{n}} \underline{R}^{-1} \quad (4.2.2)$$

The set of the colour-reversing operations  $\underline{C}_{\underline{m}}$  is denoted by  $D_{\underline{c}}$ . The conditions under which the set of symmetry operations  $D = D_0 + D_{\underline{c}}$  forms a group are examined in appendix 7. For reasons that will be made clear immediately below two cases were considered in appendix 7, mainly, the 'doubled symmetry' and the 'single symmetry' cases.

In the former case the colour-reversing elements are given by  $\underline{C}_{\underline{a}} = \underline{h}_{\underline{b}} \underline{R}^{-1}$  and the proof given in appendix 7 immediately yields:

Theorem 4.2.3: A dichromatic point group of order  $2r_0$  is

formed by any rotation  $\underline{R}$  such that (a)  $\underline{Rg}_{\underline{1}} \underline{R}^{-1} = \underline{g}_{\underline{2}}$

for any two elements  $\underline{g}_{\underline{1}}, \underline{g}_{\underline{2}}$  of  $G_0$ , and,

(b)  $\underline{RR} = \underline{g}_{\underline{3}}$  ( $\underline{g}_{\underline{3}} \in G_0$ ).

Also, for any  $\underline{R}$  satisfying the above theorem it follows that:

Theorem 4.2.4: In the doubled symmetry case the ordinary elements of the dichromatic point group are

all the operations of the group  $G_0$ , whereas the colour-reversing symmetry operations are given by  $G R^{-1} = \{ \underline{g}_1 R^{-1}, \underline{g}_2 R^{-1}, \dots, \underline{g}_r R^{-1} \}$ .

For the single symmetry case, where the colour-reversing elements are given by a relation of the form  $\underline{c}_a = \underline{g}_b R^{-1}$  with  $\underline{g}_b \in \{ G_0 - D_0 \}$ <sup>5</sup> the fulfilment of the group postulates (see appendix 7) gives the following:

**Theorem 4.2.5:** In the single symmetry case a dichromatic point group is formed for any rotation  $\underline{R}$  which satisfies the relation  $\underline{g}_1 = \underline{R} \underline{g}_1 \underline{R}$  for all the elements of  $D_2$  (where  $D_2$  is a factor 2 supergroup of  $D_0$  and at the same time a subgroup of  $G_0$ ). The ordinary elements of the dichromatic point group are the elements of the group  $D_0$  and the colour-reversing operations are given by  $\underline{g}_k R^{-1}$  with  $\underline{g}_k \in \{ D_2 - D_0 \}$ <sup>6</sup>.

#### 4.2.3 Group-theoretical expression of the dichromatic point groups

If the rotation  $\underline{R}$  (obtained from either theorem 4.2.3 or 4.2.5) is equal to a symmetry operation of the white point group, i.e.  $\underline{R} = \underline{g}_i$ , then the relation  $\underline{R} \underline{g}_1 \underline{R}^{-1} = \underline{g}_2$  holds for all the elements of the white point group. Consequently, this case corresponds to complete coincidence of the white and black point groups and, hence, the dichromatic point group is a grey point group isomorphic to the white point group (see section 2.2). This is expressed as follows:

**Theorem 4.2.6:** Rotations  $\underline{R}$  being equal to a symmetry operation of the white point group yield a dichromatic complex with symmetry of the grey point group



$D = D_0 + 1'D_0$  (where  $1'$  is the antiidentity operation).

For other rotations obtained according to theorem 4.2.3 or 4.2.5 the dichromatic point group is isomorphic to a two-coloured point group (see below). Any other rotation yields a dichromatic point group being isomorphic to  $G_0$  or to the point group 1:

Theorem 4.2.7: For all the rotations  $R$  which satisfy theorem 4.2.3 or 4.2.5 and are not symmetry operations of  $G_0$  the dichromatic point group formed is given by  $D = D_0 + 1'(D_2 - D_0)$  where  $D_0$  is equal to  $G_0$  (doubled symmetry case) or a subgroup of  $G_0$  (single symmetry case).

For the doubled symmetry case the rotation  $R$  is determined from the equation  $\underline{RR} = \underline{g}_1$ . Therefore, it can easily be shown that:

Theorem 4.2.8: If the point group  $G_0$  contains a symmetry rotation  $\theta$  about a direction  $[hkl]$ , then the rotation  $\theta/2$  (and its symmetrical equivalent) about the direction  $[hkl]$  give rise to a dichromatic point group of order twice the order of  $G_0$ .

A special case of this theorem is the following rule given by Pond & Bollmann (1979): "colour-reversing rotation axes,  $U'$ , arise when two ordinary  $U/2$ -fold rotation axes are coincident and  $\theta$  is  $2\pi/U$ ".

Until now the rotation  $R$  has been assumed to be a proper rotation. However, this is the case for a (centrosymmetrical) lattice. If no centre of symmetry is present in the lattice-complex then improper rotations must be considered as well<sup>7</sup>. The rotation is, then, expressed as  $\underline{Ri}$ , where  $\underline{i}$  is the (ordinary) inversion operation and the colour-reversing

symmetry operations are given by  $h_{\underline{i}} R_{\underline{i}}^{-1}$  (double case) or  $g_{\underline{i}} R_{\underline{i}}^{-1}$  (single case).

- - -
- Footnotes
- 1: The elements of  $G_{\underline{o}}$  have the same orientation as those of  $G_{\underline{w}}$ .
  - 2:  $R_{\underline{i}}$  is to be considered as a rotation and a colour-reversing operation consequentially applied.
  - 3: This implies, of course, that the elements of  $G_{\underline{w}}$  and  $G_{\underline{o}}$  are expressed relative to the same coordinate system.
  - 4: The summation is to be understood in the Galois (1897) sense, i.e. as a juxtaposition of elements.
  - 5:  $\{G_{\underline{o}} - D_{\underline{o}}\}$  is the set of elements of  $G_{\underline{o}}$  which do not belong to  $D_{\underline{o}}$ .
  - 6:  $\{D_{\underline{2}} - D_{\underline{o}}\}$  denotes the set of elements of  $D_{\underline{2}}$  which do not belong to  $D_{\underline{o}}$ .
  - 7: This obviously refers to dichromatic complexes but not dichromatic patterns.

#### 4.3 Point groups obtained by the superposition of two identical point groups

The group theoretical considerations given in the previous section allow the determination of all possible dichromatic point groups obtained by the superposition of two identical point groups. The main function of this section is to outline the procedure for this determination.

##### 4.3.1 The procedure

For a given white group  $G_{\underline{w}}$  with elements  $g_{\underline{i}}$  ( $i=1,2,\dots,r_{\underline{w}}$ ) both the doubled and the single symmetry cases have to be considered. In the former case the conditions for forming a dichromatic point group are given by theorems 4.2.3 and 4.2.4. Consequently, for every element  $g_{\underline{i}}$  a rotation  $R_{\underline{i}}$  is determined by solving the equation

$$R_{\underline{i}} R_{\underline{i}} = \underline{g}_i$$

(in fact  $R_{\underline{i}}$  is obtained by applying theorem 4.2.8). However, not all of these rotations correspond to a dichromatic point group. This is because, according to theorem 4.2.3,  $R_{\underline{i}}$  must additionally leave the  $G_o$  invariant, i.e.  $R_{\underline{i}}$  must satisfy the equations  $R_{\underline{i}} \underline{g}_j R_{\underline{i}}^{-1} = \underline{g}_j$ ,  $j=1,2,\dots,r_w$  and  $i \neq j$ . The number of  $R_{\underline{i}}$ 's fulfilling the later requirement can be further reduced by rejecting rotations  $R_{\underline{i}}$  being equivalent to a symmetry operation of  $G_w$  (theorem 4.2.6). The remaining  $R_{\underline{i}}$ 's yield a dichromatic point group of order  $2r_w$  with colour-reversing elements (expressed relative to the white coordinate system) given by  $\underline{g}_j R_{\underline{i}}^{-1}$  or  $\underline{g}_j R_{\underline{i}}^{-1}$  for proper or improper rotations respectively.

For dichromatic point groups corresponding to the single symmetry case the subgroups  $D_o$  of the white group  $G_w$  must be determined. Moreover, for each subgroup,  $D_o$ , its invariant supergroups which at the same time are subgroups of  $G_w$  must be found. The tables given in International Tables of X-ray Crystallography (1969) or the figure A9.2 simplify the task for the determination of the subgroups  $D_o$  and their supergroups  $D_2$ .

For each supergroup  $D_2$  the solution satisfying simultaneously the equations  $\underline{R} \underline{g}_i \underline{R} = \underline{g}_i$  ( $i=1,2,\dots$ ) where  $\underline{g}_i$  are the elements of the set  $\{D_2 - D_o\}$  is determined. Rotations corresponding to a solution so obtained are rejected if: (a) they are equivalent to a symmetry operation of  $G_w$ , (b) they conserve the  $G_w$  (i.e. they leave the point group  $G_w$  invariant). The latter condition is obvious, since such a rotation corresponds to the doubled symmetry case and therefore it has been considered previously.

#### 4.3.2 Rules

The application of the above procedure is demonstrated in appendix 8 where particular cases are considered. The superposition of any two

identical point groups can be treated in a similar fashion. In this way table 4.3.1 giving the black-white<sup>1</sup> groups created by the superposition of white and black groups is derived. The point groups of the dichromatic patterns corresponding to the superposition of holosymmetric (black and white) symmetry groups are marked by an 'asterisk' in table 4.3.1.

A number of interesting conclusions can be obtained from table 4.3.1. These are expressed in the following rules:

Rule 4.3.1: In the cases of 2-, 4- and 6-fold ordinary rotational axes rotation about a direction perpendicular to these axes results in a 2-fold colour-reversing rotational axis (or to a colour-reversing mirror plane in the case of improper rotations) except for some special rotation angles (for which higher symmetry results due to the particular symmetry).

Rule 4.3.2: For all the primitive symmetry classes rotation  $\theta = n2\pi/u$  about a  $u/2$ -fold ordinary axis results in a colour-reversing rotation axis  $u'$  (or a  $\bar{u}'$  axis for improper rotations).

Rule 4.3.3: For a mirror plane any rotation  $\theta \neq 180^\circ$  along a direction on the plane results in a colour-reversing mirror plane (or, in the case of improper rotation, in a two-fold colour-reversing rotational axis), except for  $\theta = 180^\circ$  where a  $mm'2'$  symmetry is created.

#### 4.3.3 Non-crystallographic dichromatic point groups

Rule 4.3.2 implies that in the particular case of a 4- or 6-fold ordinary axis special rotations (i.e.  $\theta = n2\pi/u$ ,  $u=8$  or  $12$  respectively)

TABLE 4.3.1

Black-white point groups obtained by the superposition of two identical point groups (grey groups are not included)

White point group	Black-white point group
<b>(a) primitive symmetry classes</b>	
1	$\bar{1}'$ 2' m'
2	2/m' $\bar{4}'$ 4' 22'2' 2m'm' 2' m'
3	$\bar{3}'$ $\bar{6}'$ 6' 32' 3m'
4	4/m' $\bar{8}'$ 8' 42'2' 4m'm' 2' m'
6	6/m' $\underline{\bar{12}}'$ $\underline{12}'$ 62'2' 6m'm' 2' m'
<b>(b) planar symmetry classes</b>	
m	2'/m 2'mm' 2' m'
2mm	mmm' $\bar{4}'2'm$ 4'mm' 22'2' 2m'm' 2'mm' 2' m'
3m	$\bar{3}'m$ $\bar{6}'2'm$ 6'mm' 32' 3m' 2'mm'
4mm	4/m'mm $\bar{8}'2'm$ 8'mm' 42'2' 4m'm' 2'mm' 2' m'
6mm	6/m'mm $\underline{\bar{12}}'2'm$ $\underline{12}'mm'$ 62'2' 6m'm' 2'mm' 2' m'
<b>(c) axial symmetry classes</b>	
222	m'm'm' $\bar{4}'2m'$ 4'22' 22'2' 2m'm' 2' m'
32	$\bar{3}'m'$ $\bar{6}'2m'$ 6'22' $\bar{4}'$ 4' 32' 3m' 22'2' 2m'm' 2' m'
422	4/m'm'm' $\bar{8}'2m'$ 8'22' $\bar{4}'2m'$ 4'22' 42'2' 4m'm' 22'2' 2m'm' 2' m'
622	6/m'm'm' $\underline{\bar{12}}'2m'$ $\underline{12}'22'$ $\bar{4}'2m'$ 4'22' 62'2' 6m'm' 22'2' 2m'm' 2' m'
<b>(d) central symmetry classes</b>	
* $\bar{1}$	2'/m'
* 2/m	4'/m mm'm' 2'/m'
$\bar{3}$	6'/m' $\bar{3}m'$ 2'/m'
4/m	8'/m 4/mm'm' 2'/m'
6/m	$\underline{12}'/m$ 6/mm'm' 2'/m'

TABLE 4.3.1-continued

White point group	Black-white point group
<b>(e) planar-axial symmetry classes</b>	
* $mmm$	$4'/mmm'$ $mm'm'$ $2'/m'$
* $\bar{3}m$	$6'/m'mm'$ $4'/m$ $\bar{3}m'$ $mm'm'$ $2'/m'$
* $4/mmm$	$8'/mmm'$ $4'/mmm'$ $4/mmm'm'$ $mm'm'$ $2'/m'$
* $6/mmm$	$12'/mmm'$ $6'/mmm'$ $6/mmm'm'$ $mm'm'$ $2'/m'$
<b>(f) inversion-primitive symmetry classes</b>	
$\bar{4}$	$4'/m'$ $\bar{4}2'm'$ $2'$ $m'$
$\bar{6}$	$6'/m'$ $\bar{6}2'm'$ $2'$ $m'$
<b>(g) inversion-planar symmetry classes</b>	
$\bar{4}2m$	$4'/m'mm'$ $\bar{4}'2m'$ $4'22'$ $\bar{4}2'm'$ $2m'm'$ $2'mm'$ $22'2'$ $2'$ $m'$
$\bar{6}2m$	$6'/mmm'$ $\bar{4}2'm$ $4'mm'$ $\bar{6}2'm'$ $2m'm'$ $2'mm'$ $22'2'$ $2'$ $m'$
<b>(h) classes of 23; 432</b>	
23	$m'\bar{3}'$ $\bar{4}'3m'$ $4'32'$ $6'$ $\bar{6}'$ $32'$ $3m'$ $2'$ $m'$ $22'2'$ $2m'm'$
432	$m'\bar{3}'m'$ $6'22'$ $\bar{6}'2m'$ $\bar{4}'2m'$ $8'22'$ $\bar{8}'2m'$ $32'$ $42'2'$ $22'2'$ $3m'$ $4m'm'$ $2m'm'$ $2'$ $m'$
<b>(i) classes of <math>\bar{4}3m</math>; <math>m3</math>; <math>m3m</math></b>	
$\bar{4}3m$	$m'\bar{3}'m$ $\bar{6}'2'm$ $6'mm'$ $32'$ $3m'$ $\bar{4}2'm'$ $2'mm'$ $2'$ $m'$
$m3$	$m\bar{3}m'$ $6'/m'$ $\bar{3}m'$ $mm'm'$ $2'/m'$
* $m3m$	$6'/m'mm'$ $4'/mmm'$ $8'/mmm'$ $\bar{3}m'$ $4/mmm'm'$ $mm'm'$ $2'/m'$

create an 8'- or 12'-fold (or  $\bar{8}'$ - or  $\bar{12}'$ -fold) colour-reversing rotational axis respectively. The consideration of the non-crystallographic rotation or rotoinversion axes in dichromatic point groups is now investigated.

Referring to the conventional crystallography, restrictions on the order of a rotation axis are imposed by the simultaneous occurrence of repetition due to the rotational and 2- or 3-dimensional periodicity. These restrictions imply that nets and lattices can be consisted with the symmetry of 1-, 2-, 3-, 4- and 6-fold rotation and rotoinversion axes only.

In the case of one-dimensional periodic objects, however, non-crystallographic axes lying along the periodic direction are consistent with the symmetry of the object. Moreover, non-crystallographic symmetry is permissible for finite (i.e. non-periodic) objects.

According to the above discussion point groups containing 8- and 12-fold axes are permissible dichromatic point groups only in the case of dichromatic complexes with one-dimensional periodicity. Since no complete list of these groups is available in the literature, the enumeration of the 8- and 12-fold two-coloured point and rod groups is given in appendices 9 and 10 respectively.

- - -

Footnote 1: Grey groups created by the superposition are not included in this table.

## Chapter 5

### SYMMETRY GROUPS OF DICHROMATIC COMPLEXES AND BICRYSTALS

#### 5.1 Permissible symmetry groups for dichromatic complexes

As was mentioned in section 3.3 the symmetry of dichromatic complexes can be classified according to the classes of two-coloured point, rod, layer or space groups. However, the restrictions imposed on the permitted symmetry operations mean that a number of two-coloured groups must be excluded. For example, restrictions arise due to the fact that dichromatic complexes are formed by two lattice-complexes which are not in complete coincidence (see section 3.1). Thus, not all points in a dichromatic complex can be neutral and, consequently, dichromatic point groups can not be grey point groups.

As far as dichromatic patterns are concerned they are formed by two interpenetrating (identical) Bravais lattices. Thus, their point groups correspond to symmetries created by the superposition of holosymmetric point groups. Referring to table 4.3.1 (where the holosymmetric point groups are marked by an asterisk) it is clear that the permissible two-coloured point groups of dichromatic patterns are those shown in table 5.1.1.

The periodicity occurring in dichromatic complexes arises by the existence of a superlattice<sup>1</sup> being common for the two components (see e.g. Santoro, 1974). The occurrence of this common superlattice implies that antitranslations are not permissible, or stated alternatively, the black-white lattices are excluded<sup>2</sup>. In fact, this restriction is the only one imposed on the permissible spatial symmetry of dichromatic complexes. Consequently, the only spatial groups which have to be excluded



TABLE 5.1.1

Permissible two-coloured point groups of  
dichromatic patterns with grey origin

Crystal system of white lattice	White point group	Point group of dichromatic pattern
triclinic	$\bar{1}$	$\bar{1}'$ $2'$ $m'$
monoclinic	$2/m$	$4'/m$ $mm'm'$ $2'/m'$
orthorhombic	$mmm$	$4'/mmm'$ $mm'm'$ $2'/m'$
hexagonal	$6/mmm$	$12'/mmm'$ $6'/mmm'$ $6'/mm'm'$ $mm'm'$ $2'/m'$
trigonal (rhombohedral)	$\bar{3}m$	$6'/m'mm'$ $4'/m$ $\bar{3}m'$ $mm'm'$ $2'/m'$
tetragonal	$4/mmm$	$8'/mmm'$ $4'/mmm'$ $4'/mm'm'$ $mm'm'$ $2'/m'$
cubic	$m\bar{3}m$	$6'/m'mm'$ $4'/mmm'$ $8'/mmm'$ $\bar{3}m'$ $4'/mm'm'$ $mm'm'$ $2'/m'$

are those corresponding to either a black-white lattice or to a grey point group.

As far as the spatial symmetry of dichromatic patterns is concerned, it can be determined by bearing in mind that the possible point groups are those in table 5.1.1. The spatial groups are then enumerated by selecting the spatial groups which are isomorphous with the point groups in this table. Thus, the tables of two-coloured rod and layer groups published by Neronova & Belov (1961) are considered<sup>3</sup> and the lists of the permissible groups for dichromatic patterns with one- and two-dimensional periodicity are established (tables 5.1.2 and 5.1.3 respectively). Similarly, the table of the two-coloured space groups given by Belov, Neronova & Smirnova (1957)<sup>4</sup> is used for determining the permissible dichromatic space groups (table 5.1.4).

It should be emphasized, however, that the given tables correspond to dichromatic patterns where the origin is a neutral point. If this is not the case the number of symmetry classes of dichromatic patterns is greater (see chapter 6) but the listing of the spatial groups for such cases is a very large task (an example serving to indicate the manner of derivation is presented in chapter 6).

- - -

Footnotes 1: The term 'superlattice' used here indicates a lattice obtained from the original lattice by means of a transformation matrix having integral elements and determinant larger than unity (Santoro & Mighell, 1972). In some publications (see e.g. Bucksch, 1971, 1972) the superlattice, as defined here, is called 'sublattice'.

2: Because of this the term 'black-white spatial group' is used, hereafter, to denote black-white symmetry groups with classical lattices.

TABLE 5.1.2

Permissible two-coloured rod groups of  
dichromatic patterns with grey origin

Number	Rod group	Number	Rod group
1	$\rho 1$	11	$\rho m'm'm$
2	$\rho 112'$	12	$\rho 4'/mmn'$
3	$\rho 2'11$	13	$\rho 4/mm'm'$
4	$\rho \bar{1}'$	14	$\rho 6/mm'm'$
5	$\rho 11m'$	15	$\rho 6'/mmn'$
6	$\rho m'11$	16	$\rho 6'/m'mm'$
7	$\rho 112'/m'$	17	$\rho \bar{3}m'$
8	$\rho 2'/m'11$	18	$\rho 8'/mmn'$
9	$\rho 4'/m$	19	$\rho \underline{12}'/mmn'$
10	$\rho mm'm'$		

TABLE 5.1.3

Permissible two-coloured layer groups of  
dichromatic patterns with grey origin

Number	Layer group	Number	Layer group
1	$p1$	14	$cm'm'm$
2	$p\bar{1}'$	15	$cmm'm'$
3	$p112'$	16	$p4'/m$
4	$p12'1$	17	$p4'/mnm'm$
5	$c12'1$	18	$p4'/mnm'm'$
6	$p11m'$	19	$p4/mnm'm$
7	$p1m'1$	20	$p\bar{3}1m'$
8	$c1m'1$	21	$p\bar{3}m'1$
9	$p112'/m'$	22	$p6'/mm'm$
10	$p12'/m'1$	23	$p6'/mnm'm'$
11	$c12'/m'1$	24	$p6'/m'm'm$
12	$pm'm'm$	25	$p6/mnm'm'$
13	$pmm'm'$	26	$p6'/m'mnm'$

TABLE 5.1.4

Permissible two-coloured space groups of  
dichromatic patterns with grey origin

Number	Space group	Number	Space group
1	P1	16	I4'/m
2	P1'	17	P4'/mm'm
3	P2'	18	P4'/mmm'
4	C2'	19	P4/mm'm'
5	Pm'	20	I4'/mm'm
6	Cm'	21	I4'/mmm'
7	P2'/m'	22	I4/mm'm'
8	C2'/m'	23	P31m'
9	Pm'm'm	24	P3m'1
10	Cm'm'm	25	R3m'
11	Cmm'm'	26	P6'/mm'm
12	Fm'm'm	27	P6'/mmm'
13	Im'mm'	28	P6'/m'm'm
14	Im'm'm	29	P6'/m'mm'
15	P4'/m	30	P6/mm'm'

- 3: In the case of rod groups, however, the groups containing 8- or 12-fold rotation axes must also be considered (see appendix 10).
- 4: This table contains the two-coloured space groups first enumerated by Zamorzaev (1953). The 1957 table, however, lists the space groups with nomenclature and arrangement concordant with the notation layed out in International Tables of X-ray Crystallography (1969). Also, the latter table contains the corrections to the list published by Belov, Nero-  
nova & Smirnova (1955) pointed out by Donnay et al. (1958). The only other difference in the two lists is that in the 1957 table the two-coloured space groups are classified according to the isomorphous Fedorov groups.

## 5.2 Examples of symmetry classification of dichromatic complexes

The primary aim of this section is to refer to particular dichromatic complexes and to demonstrate certain aspects of their symmetry. In the first example the possibility of a non-crystallographic point groups is illustrated. Then, attention is given to coincidence-site lattices formed by cubic or hexagonal ( $c/a=1.6311$ ) lattices. Finally, the (110) twin in pyrite is referred to as an example of dichromatic pattern with  $\Sigma=1$ .

### 5.2.1 Non-crystallographic dichromatic point group

As was already mentioned (section 4.3) a non-crystallographic group is created only if the white point group contains a 4- or 6-fold axis and the rotation axis is along this direction.

To demonstrate this, let the white and black lattices be simple cubic (symmetry group  $Pm3m$ ). The dichromatic pattern shown in figure

5.2.1 is obtained by a rotation  $[001]/45^\circ$  of the black lattice. The point symmetry of this pattern is determined by employing the analytical method given in chapter 4.

The white point group contains 48 symmetry operations which are given in table A1.3. The ordinary symmetry elements of the dichromatic point group are these elements of the white point group which satisfy the relation (see section 4.2):

$$\underline{\underline{R}} \underline{\underline{g}}_i \underline{\underline{R}}^{-1} = \underline{\underline{g}}_i$$

where

$$\underline{\underline{R}} = \begin{pmatrix} \cos(45^\circ) & \cos(45^\circ) & 0 \\ \cos(135^\circ) & \cos(45^\circ) & 0 \\ 0 & 0 & 1 \end{pmatrix}$$

The above relation is employed for each one of the elements of the point group  $m3m$  and the results are listed in table 5.2.1. According to this table, only 16 elements of the white group are also elements of the dichromatic point group. These elements form the group  $D_0 = 4/mmm$  which is, of course, a subgroup of the white group (theorem 4.2.1). The order of the group  $D_0$  is 16 and according to theorem 4.2.2 the order of the dichromatic point group must be equal to 32. In other words, the dichromatic point group must be one of the invariant supergroups of  $D_0$ ; reference to figure A9.2 shows that the dichromatic point group is the black-white group  $8'/mm'm'$ .

This is easily verified if it is recalled that the dichromatic point group  $D$  is given by  $D = D_0 + RD_0$ . Thus, the colour-reversing symmetry operations are given by  $\underline{\underline{R}} \underline{\underline{g}}_i$ , where  $\underline{\underline{g}}_i$  are the elements of  $D_0$ ; these operations are also listed in table 5.2.1. Comparing the elements of the dichromatic point group to those given in table A9.1a it is evident that the former is isomorphous to the group  $8'/mm'm'$ .

Figure 5.2.1

Projection along [001] of a dichromatic pattern formed by simple cubic lattices with misorientation  $[001]/45^\circ$ . The white lattice is indicated by open circles while the black one by filled circles. The dichromatic pattern exhibits  $8'/mm'm$  symmetry.



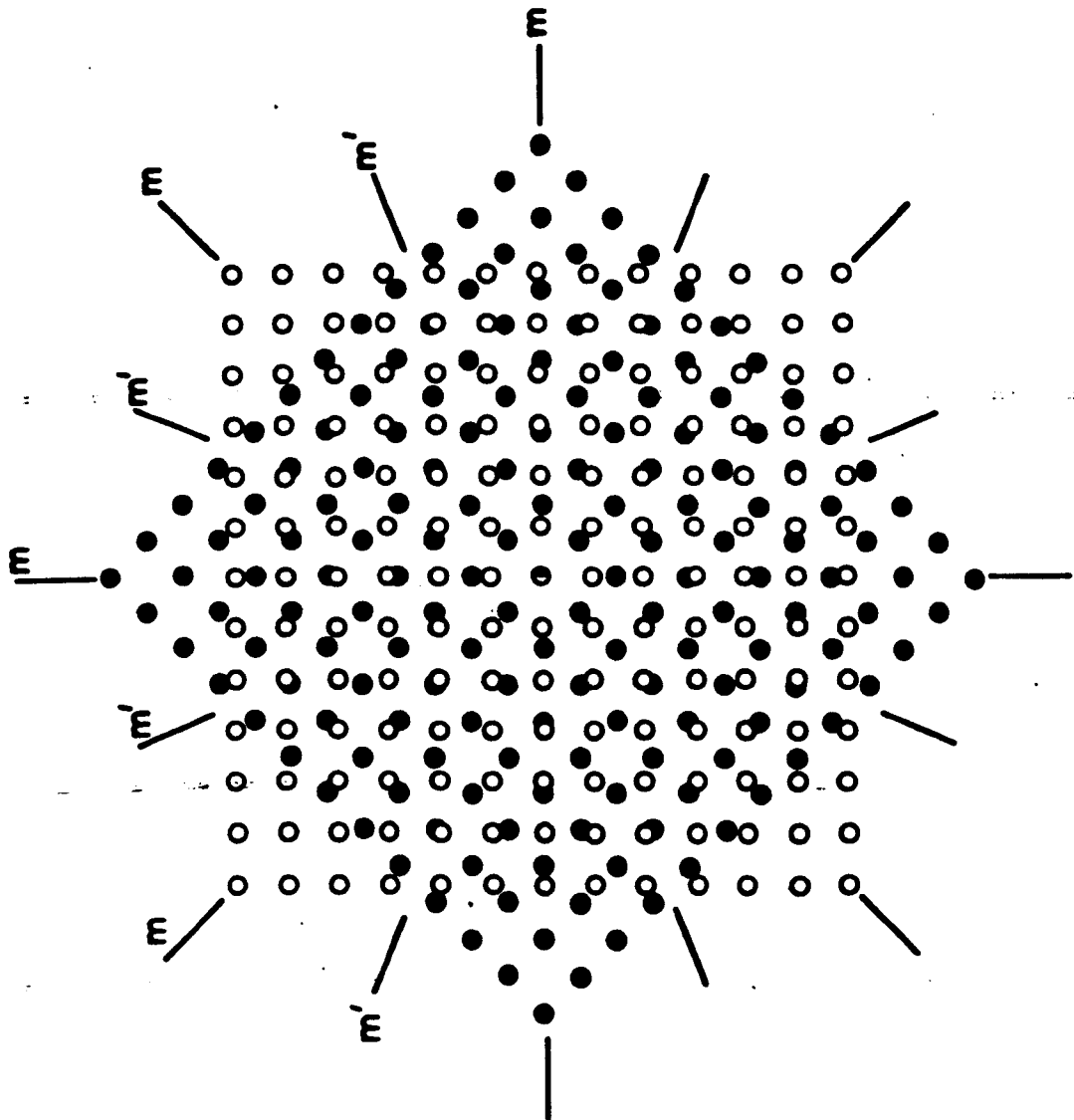


**TABLE 5.2.1**

Determination of the dichromatic point group formed by the superposition of two cubic lattices (point group  $m\bar{3}m$ ) with misorientation  $[001]/45^\circ$

$\underline{g}_i$	$\underline{Rg}_iR^{-1}$	$\underline{g}_iR^{-1}$	$\underline{g}_i$	$\underline{Rg}_iR^{-1}$	$\underline{g}_iR^{-1}$	$\underline{g}_i$	$\underline{Rg}_iR^{-1}$	$\underline{g}_iR^{-1}$	$\underline{g}_i$	$\underline{Rg}_iR^{-1}$	$\underline{g}_iR^{-1}$
1	1	$8^1_z$	$2^1_\theta$			i	i	$8^1_z$	$s_\theta$		
$3^1_\gamma$			$2^1_\kappa$			$6^1_\gamma$			$s_\kappa$		
$3^2_\gamma$			$2^1_\lambda$			$6^5_\gamma$			$s_\lambda$		
$3^1_\delta$			$4^1_z$	$4^1_z$	$8^3_z$	$6^1_\delta$			$4^1_x$		
$3^2_\delta$			$4^3_z$	$4^3_z$	$8^7_z$	$6^5_\delta$			$4^3_x$		
$3^1_\epsilon$			$4^1_x$			$6^1_\epsilon$			$4^1_y$		
$3^2_\epsilon$			$4^3_x$			$6^5_\epsilon$			$4^3_y$		
$3^1_\tau$			$4^1_y$			$6^1_\tau$			$4^1_z$	$4^1_z$	$8^7_z$
$3^2_\tau$			$4^3_y$			$6^5_\tau$			$4^3_z$	$4^3_z$	$8^3_z$
$2^1_\rho$	$2^1_x$	$2^1_\nu$	$2^1_x$	$2^1_\rho$	$2^1_\tau$	$s_\rho$	$s_x$	$s'_\nu$	$s_x$	$s_\rho$	$s'_\tau$
$2^1_\rho$	$2^1_y$	$2^1_\rho$	$2^1_y$	$2^1_\rho$	$2^1_\epsilon$	$s_\rho$	$s_y$	$s'_\rho$	$s_y$	$s_\rho$	$s'_\epsilon$
$2^1_\gamma$			$2^1_z$	$2^1_z$	$8^5_z$	$s_\gamma$			$s_z$	$s_z$	$8^5_z$

In order to determine the spatial symmetry group of the dichromatic pattern in figure 5.2.1 its periodicity must also be established. The pattern contains coincidence sites along the [001] (i.e. the rotation axis) and this is the only periodicity axis. Thus, the spatial symmetry of the pattern is described by the rod group  $\rho 8'/mm'm'$ .

### 5.2.2 CSL dichromatic symmetry groups in cubic and hexagonal crystal systems

Dichromatic patterns with three-dimensional translational symmetry are associated with CSL misorientation relationships. These rotations have been extensively studied for cubic materials (see e.g. Warrington & Bufalini, 1971).

Figure 5.2.2 shows the projections along [hkl] of some CSL based dichromatic patterns between cubic lattices; the [hkl] direction is a symmetry axis of the lattice. For each pattern the main symmetry elements are indicated in the figure but colour-reversing mirror glide planes, etc. generated in centred CSL cells have been omitted for clarity. For each of these patterns the space group is also shown in the figure.

In systems other than the cubic a CSL is only possible if axial ratios and interaxial angles happen to have particular values (Donnay & Donnay, 1954). Warrington (1975) considered the possibility of CSL formation in the hexagonal system for the ideal ratio  $c/a = \sqrt{8/3}$  and published a list of axis/angle pairs leading to CSL.

Figure 5.2.3 is a schematic representation of such CSL cells obtained by rotations along the [00.1] axis. Open and filled circles represent, as usual, the sites of the white and black lattice respectively. The main symmetry elements as well as the three-dimensional space group are indicated in the figure.

Figure 5.2.2

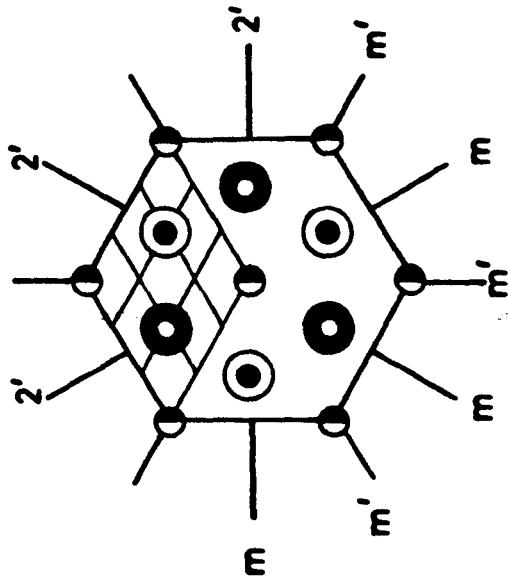
Projections along  $[hkl]$  of CSL dichromatic patterns formed by face-centred or body-centred cubic lattices. The component lattices,  $[hkl]/\theta$  and  $\Sigma$  are as follows:

- (a) fcc/fcc,  $[111]/60^\circ$ ,  $\Sigma=3$  (\*)
- (b) bcc/bcc,  $[111]/60^\circ$ ,  $\Sigma=3$
- (c) fcc/fcc,  $[001]/36.9^\circ$ ,  $\Sigma=5$  (\*)
- (d) bcc/bcc,  $[001]/36.9^\circ$ ,  $\Sigma=5$
- (e) fcc/fcc,  $[011]/38.9^\circ$ ,  $\Sigma=9$  (\*)
- (f) bcc/bcc,  $[011]/38.9^\circ$ ,  $\Sigma=9$
- (g) fcc/fcc,  $[011]/50.47^\circ$ ,  $\Sigma=11$  (\*)
- (h) bcc/bcc,  $[011]/50.47^\circ$ ,  $\Sigma=11$

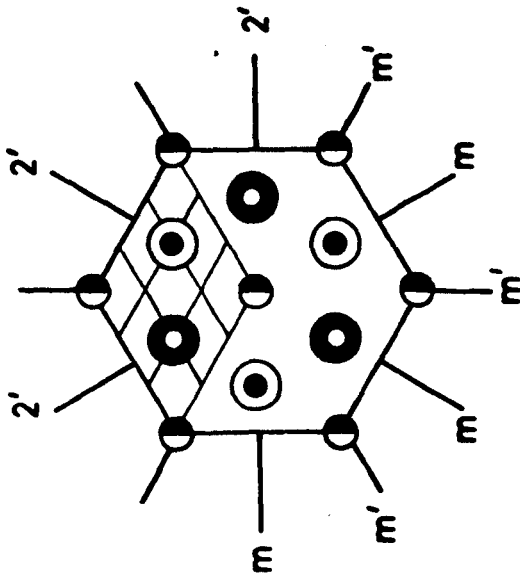
The size of symbols represents the ...ABABA... stacking along  $[001]$  and  $[011]$  and ...ABCABCAB... along  $[111]$ . Open and filled circles indicate the white and black lattices respectively.

(\* after Pond & Bollmann, 1979)

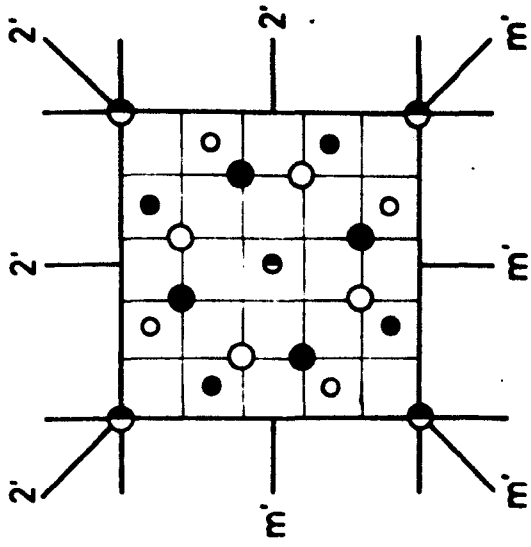
(b)  $\Sigma=3, P6'/m'm'm'$



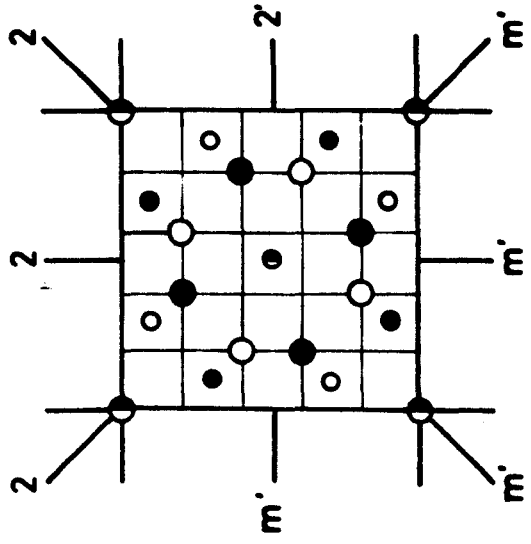
(a)  $\Sigma=3, P6'/m'm'm'$



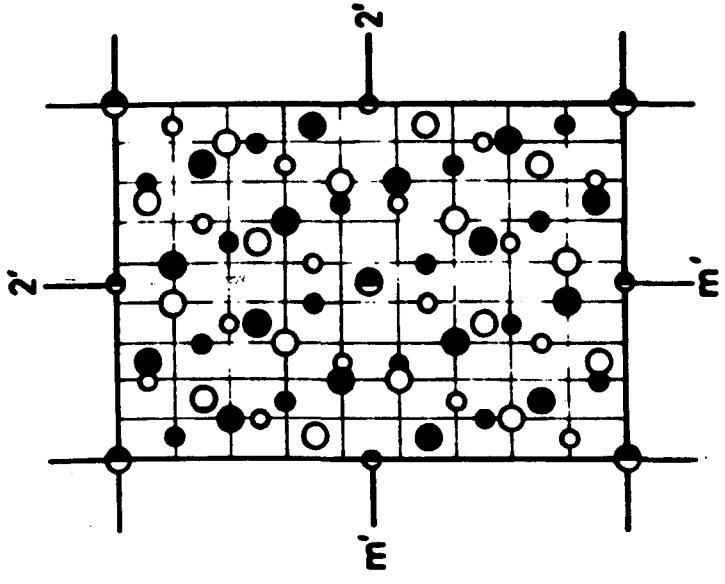
(c)  $\Sigma=5, 14/m\bar{m}m'$



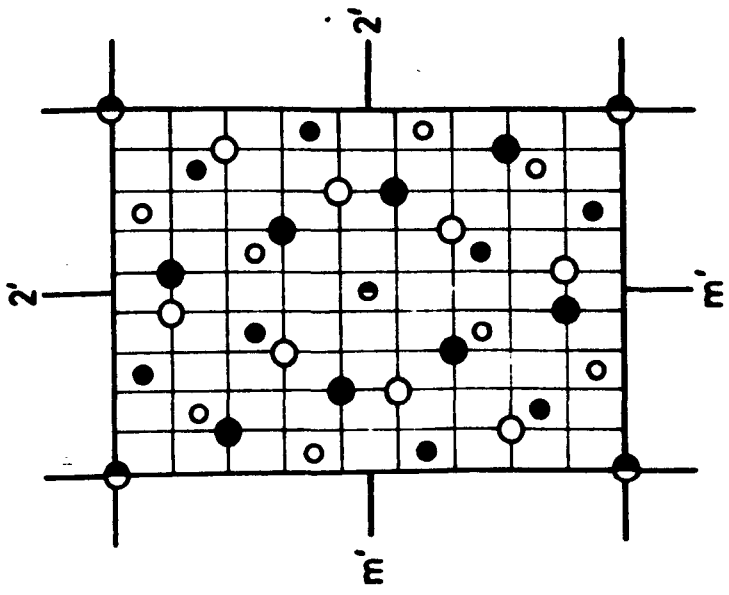
(d)  $\Sigma=5, 14/m\bar{m}m'$



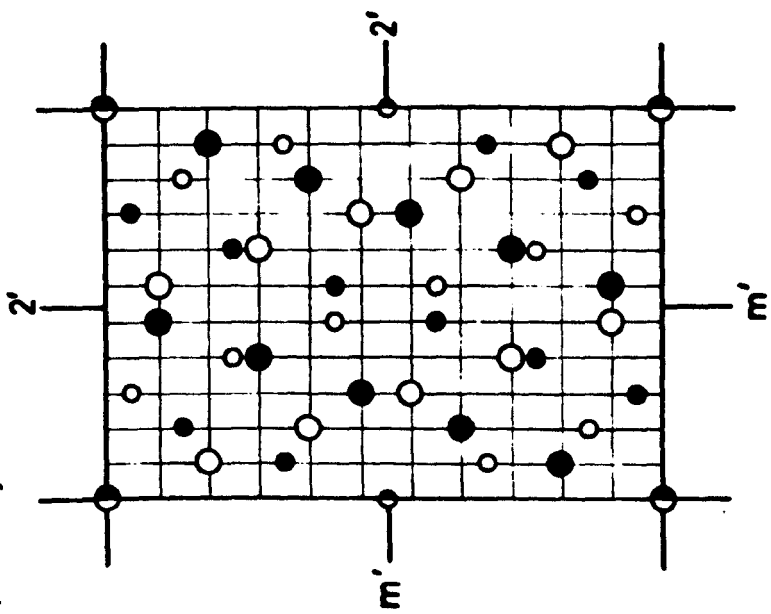
(f)  $\Sigma=9, Fm\bar{m}'m'$



(e)  $\Sigma=9, Im\bar{m}'m'$



(h)  $\Sigma=11, Cm m' m'$



(g)  $\Sigma=11, Cm m' m'$

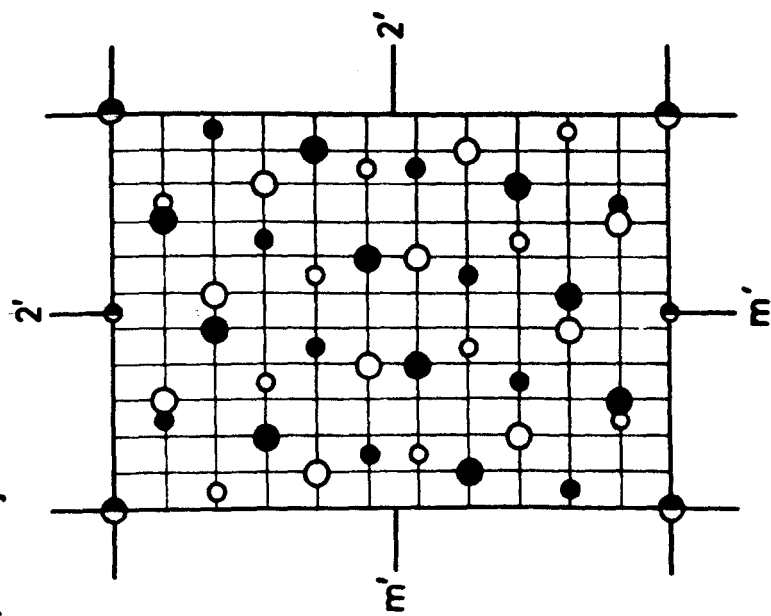




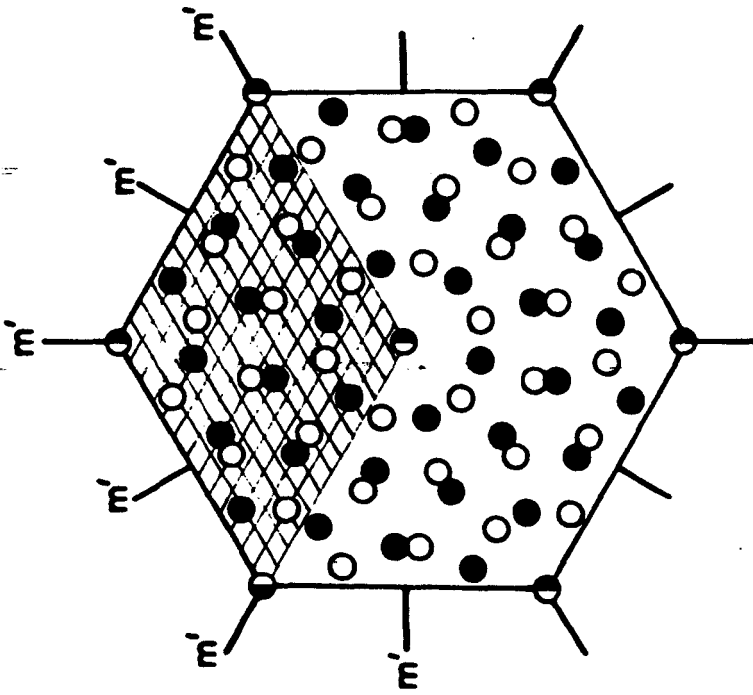
Figure 5.2.3

Projections along  $[00.1]$  of CSL dichromatic patterns formed by hexagonal lattices ( $c/a=1.633$ ). The white and black lattices are represented by open and filled circles:

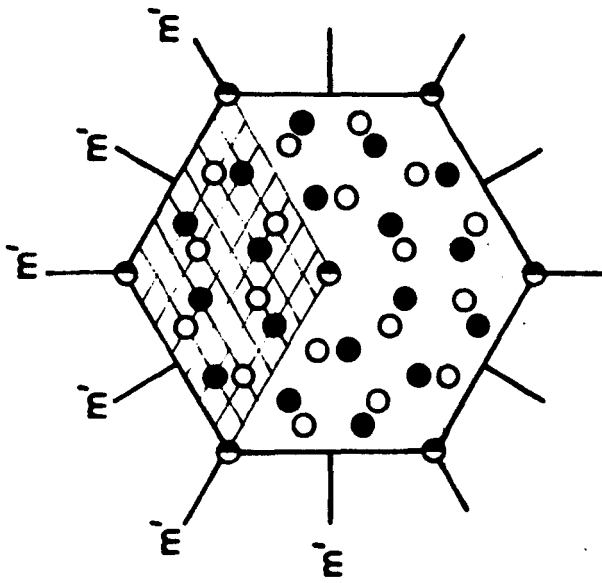
(a)  $[00.1]/21.79^\circ$ ,  $\Sigma=7$

(b)  $[00.1]/27.8^\circ$ ,  $\Sigma=13$

(b)  $\Sigma=13, P6/m\overline{m}m'$



(a)  $\Sigma=7, P6/m\overline{m}m'$



### 5.2.3 Twinning in pyrite

Twinned crystals of pyrite ( $\text{FeS}_2$ ) are typical examples of twinning by merohedry. The unit cell of  $\text{FeS}_2$  is cubic; its structure can be compared with the NaCl structure if it is supposed that Fe replaces Na and a  $\text{S}_2$  group replaces Cl (figure 5.2.4). The dumb-bell shaped  $\text{S}_2$  groups are so orientated that each of the eight small cubes into which the unit cube is divided has only one group pointing towards its centre.

Pyrite is cubic but belongs to the class  $m\bar{3}$  while its lattice which always possess the highest symmetry possible for the corresponding crystal system, has the symmetry  $m\bar{3}m$ . The lattice, therefore, possess a plane of symmetry parallel to (110), but the structure does not. Pyrite is often found twinned with respect to a (110) symmetry plane. Figure 5.2.5 shows the atomic configuration of the (110) twin in pyrite; this can be described by a reflection on the (110) plane.

Figure 5.2.6 shows the dichromatic complex corresponding to the (110) twin in pyrite; it is obtained by a reflection in (110). In this figure the atom positions are shown as either open or filled symbols depending on whether they belong to the white or black lattice-complex. The space group of the dichromatic complex in figure 5.2.6 is  $C2'/m'$  where the colour-reversing mirror plane is normal to the  $[110]$  axis of the white lattice complex.

By choosing the twin plane perpendicular to  $[110]_w$  and locating the appropriate atoms at the positions of the black lattice-complex on one side of the twin plane and of the white lattice-complex on the other side the configuration of figure 5.2.5 is obtained. The symmetry of the bicrystal is described by the two-coloured layer group  $C2/m'$ .

Figure 5.2.4

The structure of pyrite,  $\text{FeS}_2$ . The distance between the two sulphur atoms is  $2.10\text{\AA}$ ; however, their nearness has been over-emphasized in the figure in order to make the correspondence with the NaCl structure more obvious

(after Bragg & Claringbull, 1965)

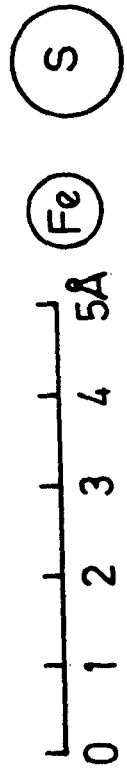
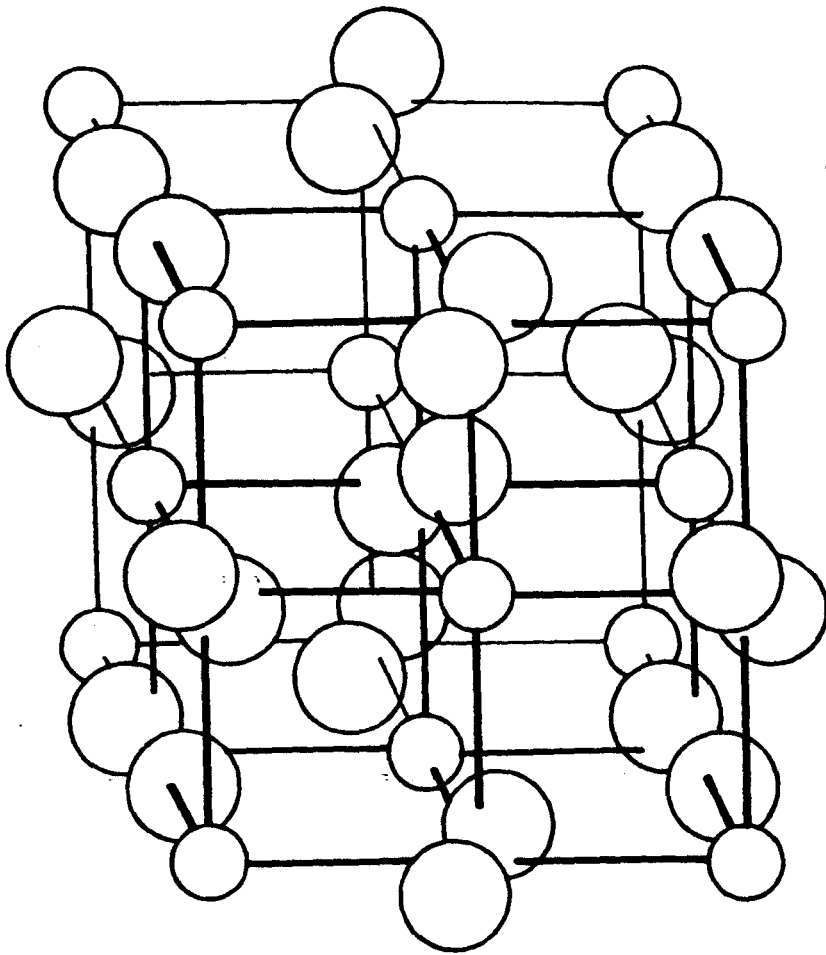


Figure 5.2.5

Structure of a (110) twin in pyrite projected on (001)

(after Cahn, 1954)

Key: Open symbols: positions of the white lattice-  
-complex  
Filled symbols: positions of the black lattice-  
-complex  
Large circles: Fe atoms in the plane of the paper  
Small circles: Fe atoms  $\pm a/2$  out of the paper  
Large squares: S atoms  $x$  out of the paper  
Small squares: S atoms  $1-x$  out of the paper  
Large triangles: S atoms  $1/2-x$  out of the paper  
Small triangles: S atoms  $1/2+x$  out of the paper

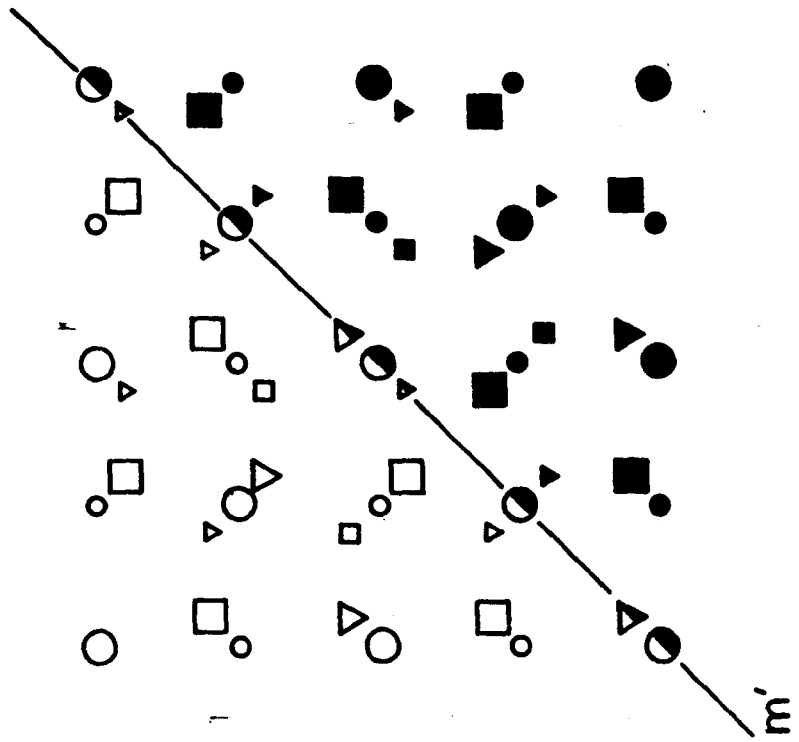
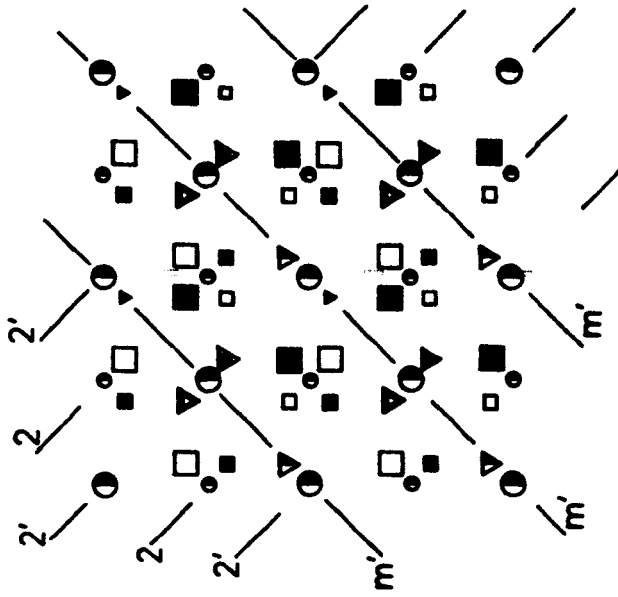
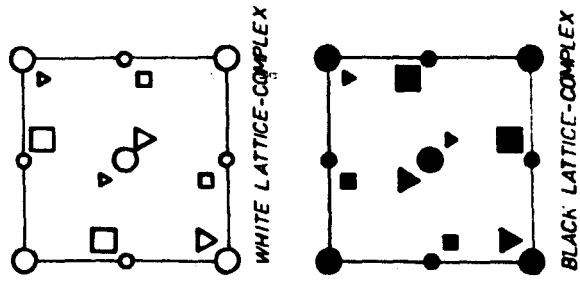


Figure 5.2.6

Dichromatic complex corresponding to the (110) twin in pyrite  
projected on (001)

Key: Open symbols: positions of the white lattice-  
-complex  
Filled symbols: positions of the black lattice-  
-complex  
Large circles: Fe atoms in the plane of the paper  
Small circles: Fe atoms  $\pm a/2$  out of the paper  
Large squares: S atoms  $x$  out of the paper  
Small squares: S atoms  $1-x$  out of the paper  
Large triangles: S atoms  $1/2-x$  out of the paper  
Small triangles: S atoms  $1/2+x$  out of the paper





### 5.3 Permissible symmetry groups of bicrystals

As in the case of dichromatic complexes, the misorientation between the two bicrystal components implies that grey point groups are not permissible. A bicrystal, however, possesses an additional feature, the interface. Any permissible symmetry elements must transform this plane into itself and moreover it must not interchange the two sides. This is carried out by considering each one of the possible symmetry operations.

#### 5.3.1 Centrosymmetric and centroantisymmetric bicrystal groups

Let the side of the unique plane towards the white crystal be called the white side and the opposite side be the black side. Any permissible symmetry element transform the unique plane into itself and also it must not interchange the black and white sides.

This implies that no ordinary centre of symmetry is consistent with a bicrystal class. The presence of an ordinary symmetry centre involves that both the sides of the unique plane must be neutral (i.e. white and black coloured at the same time). Therefore, centrosymmetrical<sup>1</sup> rosette groups are not permissible bicrystal groups.

Secondly, the possibility of centroantisymmetrical bicrystal groups is considered. At first sight it appears that the colour-reversing inversion centre is also not a permissible symmetry operation. The presence of a colour-reversing inversion centre on the boundary plane involves that the black lattice is identical to the white one and that the black lattice points assume positions which satisfy the white lattice (if the latter is considered to extent over the whole space). Thus, the colour-reversing inversion centre leaves the unique plane invariant and

at the same time does not interchange its two sides; additionally it implies that the white and black lattices are in complete coincidence.

In this case the two-dimensional discontinuity is conserved only when the structure of the grains is not centrosymmetrical and their mutual orientation corresponds to a colour-reversing inversion operation. This is possible, however, only when each component crystal has lower than holosymmetric symmetry (an example of centroantisymmetric bicrystal group is given in section 5.4).

### 5.3.2 Restrictions on the other point symmetry operations

In order to investigate the consistency of the rest of the point symmetry operations, it must be born in mind that symmetry operations of two kinds might be present in a bicrystal group, i.e. ordinary and colour-reversing operations.

The condition of colour invariance of the unique plane imposes restrictions on the orientation of both the ordinary and colour-reversing symmetry operations. This is because the white side of the unique plane is transformed into the black one only when the colour-reversing symmetry element is located 'in' the boundary plane. On the other hand, ordinary symmetry operations permitting a transformation of each side of the plane into itself must be perpendicular to the boundary plane. The only exceptions to the above rules are the cases of 3-, 4- and 6-fold colour-reversing rotoinversion axes<sup>2</sup> which must be orientated perpendicular to the plane. This is easily explained since these axes arise by the successive operation of a colour-reversing inversion and an ordinary proper rotation; the exception being the tetrad inversion axis  $\bar{4}$ .

As far as the order of the symmetry operations is concerned, this is determined by the presence of the unique plane through the restrictions

imposed on the operations by the nature of the associated symmetry groups as derived in section 3.3. Thus, three-, four- and six-fold axes serve as bicrystal symmetry operations equally well as two-fold axes. However, the three-, four- and six-fold axes may lie either perpendicular to the plane or within it. Mirror planes can also be orientated either parallel or perpendicular to the boundary plane. Accordingly the following restrictions are imposed on the kind and/or order of the symmetry operations present in a bicrystal. Three-, four- and six-fold rotation and rotoinversion axes must be ordinary and colour-reversing respectively and must be perpendicular to the boundary plane. Two-fold rotation axes and mirror planes can be either ordinary, in which case they are perpendicular to the boundary plane, or colour-reversing operations parallel to it.

Additional conditions are imposed on the combinations of the symmetry operations in a bicrystal group. It has been established (section 3.3) that the symmetry classes for bicrystals are the two-sided, two-coloured rosette, rod, and layer groups. It is evident from the construction of these groups that only certain relations are allowed between a pair (or among a set) of symmetry operations. For example, two-fold colour-reversing axes may lie at only  $90^\circ$  (or  $120^\circ$ ) to another. Furthermore, an ordinary and a colour-reversing element necessitate their product as a second colour-reversing element. The relations between a pair (or among a set) of symmetry operations in a bicrystal are governed by the theorems given by Loeb (1971).

### 5.3.3 Symmetry classes of bicrystals

Using the above conditions the permissible point groups for a bicrystal have been determined and are given in table 5.3.1. It would

**TABLE 5.3.1**

**Permissible bicrystal point groups**

Number	Bicrystal system	Bicrystal groups	
		Classical	Black-white
1	triclinic	1	
2			$\bar{1}'$
3	monoclinic	211	
4			$m'11$
5			$2/m'11$
6			$12'1$
7		1m1	
8			$12'/m1$
9	orthorhombic		$22'2'$
10		2mm	
11			$m'2'm$
12			$m'mm$
13	tetragonal	4	
14			$\bar{4}'$
15			$4/m'$
16			$42'2'$
17		4mm	
18			$\bar{4}'2'm$
19			$4/m'mm$
20	trigonal	3	
21			$\bar{3}'$
22			$32'$
23		3m	
24			$\bar{3}'m$
25	hexagonal	6	
26			$\bar{6}'$
27			$6/m'$
28			$62'2'$
29		6mm	
30			$\bar{6}'m2'$
31			$6/m'mm$

be of interest to notice that just one point group appears in this table for each of the 31 classes of rosettes. Thus, the point symmetry of bicrystals is classified according to the groups given in table 5.3.1 which can be regarded as the 31 bicrystal classes in an analogous manner to the 32 single crystal classes. Further inspection of table 5.3.1 indicates that the 31 bicrystal classes can be distributed amongst six 'bicrystal systems' which, in fact, are the systems for three-dimensional objects containing a singular point and a singular plane.

The characteristic symmetry for each of the six bicrystal systems is summarized in table 5.3.2 while figure 5.3.1 shows the stereographic representation of the 31 bicrystal classes. The following conventions are introduced for drawing these stereograms. The normal to the drawing plane is taken as the direction perpendicular to the interface. White and black points are considered above and below the page respectively; thus, solid circles and open squares are used to indicate the white and black point respectively.

#### 5.3.4 Spatial symmetry groups of bicrystals

The discussion above was restricted to the point symmetry only; bicrystals can, however, exhibit translational symmetry as well. The latter arises by the existence of a superlattice being common for the two bicrystal components (see e.g. Santoro & Mighell, 1972). A consequence of the presence of the common superlattice is that antitranslations are not permissible, or stated alternatively, the black-white lattices are excluded<sup>3</sup>. Consequently, the spatial groups of bicrystals are determined by combining (classical) translations with (two-coloured) point symmetry.

The determination of the spatial groups of bicrystals is based on table 5.3.1 where the permissible point groups are listed. The procedure

TABLE 5.3.2

CHARACTERISTIC SYMMETRY OF BICRYSTAL CLASSES

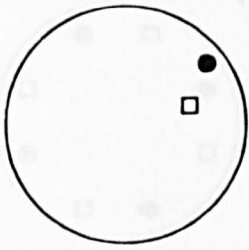
- TRICLINIC : 1-fold (ordinary identity or colour-reversing inversion) symmetry only
- MONOCLINIC : 2-fold ordinary or colour-reversing (rotation or rotoinversion) axis
- ORTHORHOMBIC: 2-fold ordinary and two 2-fold colour-reversing rotation axes or 2-fold colour-reversing and two 2-fold ordinary rotoinversion axes in three mutually perpendicular directions
- TETRAGONAL : 4-fold (ordinary rotation or colour-reversing rotoinversion) axis
- TRIGONAL : 3-fold (ordinary rotation or colour-reversing rotoinversion) axis
- HEXAGONAL : 6-fold (ordinary rotation or colour-reversing rotoinversion) axis

Figure 5.3.1

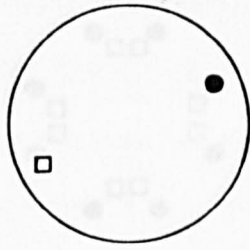
Stereograms of the bicrystal point groups. The normal to the page of the drawing is taken as the direction perpendicular to the interface. Solid circles and open squares represent points above and below the interface respectively.



bicrystal system



1



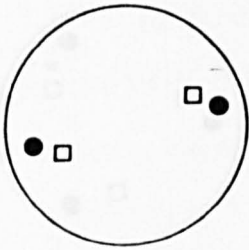
$\bar{1}$



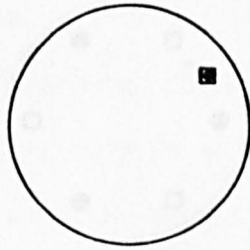
$2/m$

triclinic

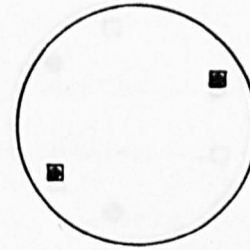
$\bar{1}$



211

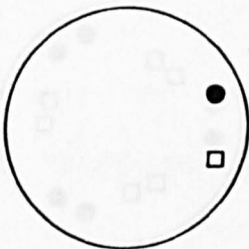


$m'\bar{1}1$



$2/m'\bar{1}1$

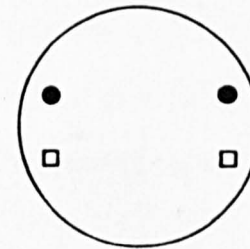
monoclinic



$12'\bar{1}$

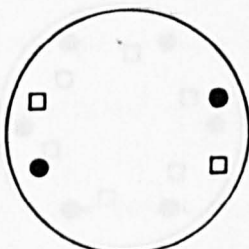


1m1

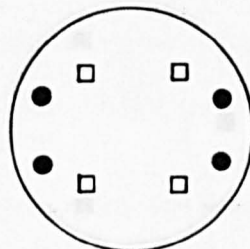


$12'/m1$

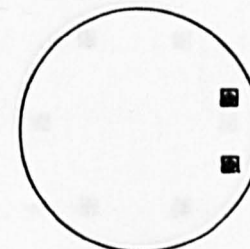
orthorhombic



$22'2'$



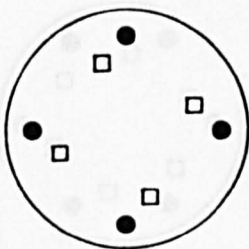
2mm



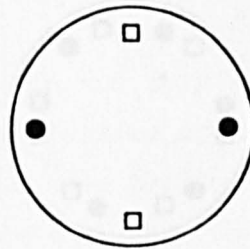
$m'2'm$



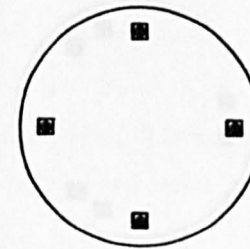
$m'mm$



4



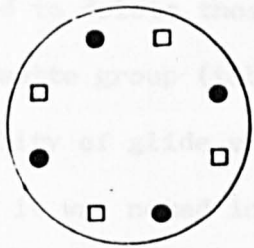
$\bar{4}$



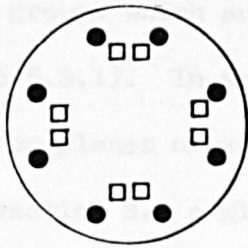
$4/m'$

tetragonal

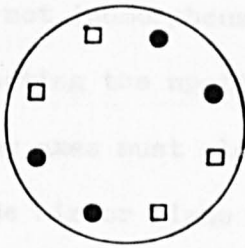
(continued on next page)



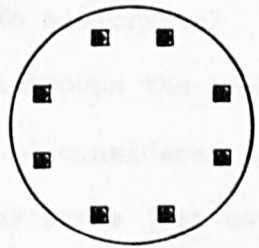
$42'2'$



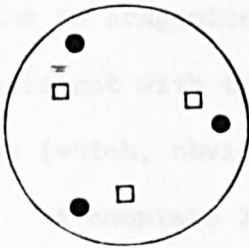
$4mm$



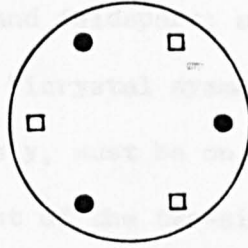
$\bar{4}2'm$



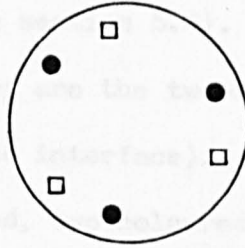
$4/m'mm$



$3$

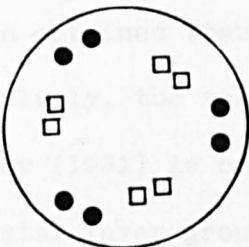


$\bar{3}'$

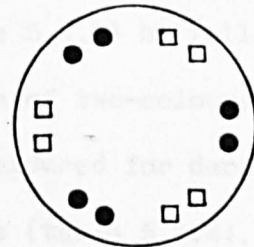


$32'$

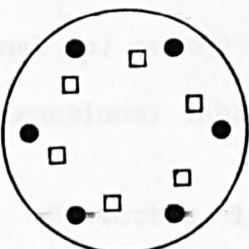
trigonal



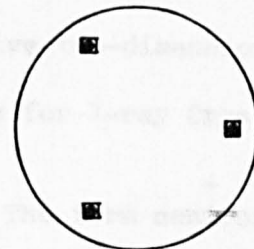
$3m$



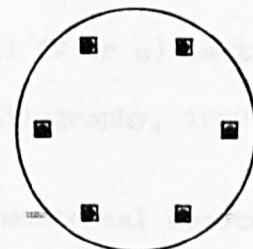
$\bar{3}'m$



$6$

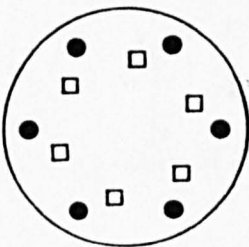


$\bar{6}'$

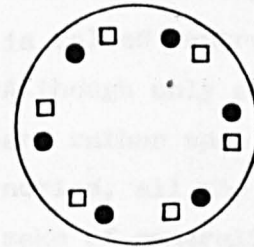


$6/m'$

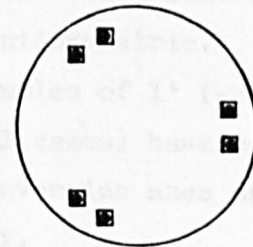
hexagonal



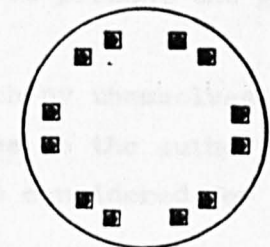
$6mm$



$\bar{6}2'2'$



$\bar{6}m2'$



$6/m'mm$

for establishing the spatial symmetry of bicrystals is, therefore, to consider the lists of the two-sided, two-coloured band or layer groups and to delete those groups which are not isomorphous to a bicrystal rosette group (table 5.3.1). In selecting the spatial groups the possibility of glide mirror planes or screw axes must also be considered. As it was noted in section 3.3 a glide mirror plane may serve just as well as a colour-reversing operation in bicrystals (this is the case for twins in aragonite and feldspars; see section 5.4). The only screw axes consistent with the bicrystal symmetry are the two-fold colour-reversing ones (which, obviously, must be on the interface).

A complete list of the two-sided, two-coloured band groups is given in appendix 4 (table A4.2). The permissible bicrystal band groups are then obtained (table 5.3.3) by following the procedure mentioned above. Similarly, the table of two-coloured layer groups given by Neronova & Belov (1961) is considered for deriving the list of the permissible bicrystal layer groups (table 5.3.4).

The periodicity of bicrystals is expressed by the one one-dimensional ( $\rho$ ) or the five two-dimensional (P or c) lattices (see e.g. International Tables for X-ray Crystallography, 1969).

- - -

- Footnotes 1: The term centrosymmetrical denotes a symmetry group containing an ordinary inversion centre. If a colour-reversing inversion centre is present the group is called centroantisymmetric.
- 2: Although only examples of 1' (which by themselves are rather special cases) have come to the author's notice, all the inversion axes are considered for the sake of generality.
- 3: Because of this, the term 'black-white spatial groups' is used, hereafter, to denote black-white symmetry groups with classical lattices.

TABLE 5.3.3

Permissible bicrystal band groups

Number	Bicrystal groups		Number	Bicrystal groups	
	Classical	Black-white		Classical	Black-white
1	$\rho 111$		16		$\rho 112'/m$
2		$\rho \bar{1}'11$	17		$\rho 112'/b$
3	$\rho 211$		18		$\rho 22'2'$
4		$\rho 12'1$	19		$\rho 22'_1 2'$
5		$\rho 12'_1 1$	20	$\rho 2mm$	
6		$\rho 112'$	21	$\rho 2mb$	
7		$\rho m'11$	22		$\rho m'2'm$
8		$\rho b'11$	23		$\rho b'2'b$
9	$\rho 1m1$		24		$\rho b'2'_1 m$
10	$\rho 11m$		25		$\rho m'2'_1 b$
11	$\rho 11b$		26		$\rho m'm2'$
12		$\rho 2/m'11$	27		$\rho b'm2'$
13		$\rho 2/b'11$	28		$\rho m'mm$
14		$\rho 12'/m1$	29		$\rho b'mm$
15		$\rho 12'_1/m1$	30		$\rho m'mb$
			31		$\rho b'mb$

TABLE 5.3.4

Permissible bicrystal layer groups

Number	Bicrystal groups		Number	Bicrystal groups	
	Classical	Black-white		Classical	Black-white
1	p1		21		$p22'_1 2'$
2		$p\bar{1}'$	22		$c22' 2'$
3	p211		23	p2mm	
4		$p112'$	24		$pm'm2'$
5		$p112'_1$	25		$pc'm2'_1$
6		$c112'$	26		$pc'c2'$
7		$pm'11$	27		$pc'2'm$
8	p11m		28	p2mb	
9	p11c		29		$pm'c2'_1$
10		$pc'11$	30		$pc'2'_1 b$
11	c11m		31		$pn'c2'$
12		$p2/m'11$	32		$pn'm2'_1$
13		$p112'/m$	33	p2cb	
14		$p112'_1/m$	34	c2mm	
15		$c112'/m$	35		$cm'm2'$
16		$p2/c'11$	36		$cb'm2'$
17		$p112'/b$	37		$pm'mm$
18		$p112'_1/b$	38		$pc'cm$
19		$p22' 2'$	39		$pn'cb$
20		$p22'_1 2'_1$	40		$pm'mb$

TABLE 5.3.4-continued

Number	Bicrystal groups		Number	Bicrystal groups	
	Classical	Black-white		Classical	Black-white
41		pc'mm	61		p4/m'mm
42		pn'mb	62		p4/n'cm
43		pc'cb	63		p4/m'cm
44		pm'cb	64		p4/n'mm
45		pc'mb	65	p3	
46		pn'mm	66		$\bar{p}3'$
47		cm'mm	67		p312'
48		cb'mm	68		p32'1
49	p4		69	p3m1	
50		$\bar{p}4'$	70	p31m	
51		p4/m'	71		$\bar{p}3'1m$
52		p4/n'	72		$\bar{p}3'm1$
53		p42'2'	73	p6	
54		$p42'_12'$	74		$\bar{p}6'$
55	p4mm		75		p6/m'
56	p4cm		76		p62'2'
57		$\bar{p}4'2'm$	77	p6mm	
58		$\bar{p}4'2'_1m$	78		$\bar{p}6'm2'$
59		$\bar{p}4'm2'$	79		$\bar{p}6'2'm$
60		$\bar{p}4'c2'$	80		p6/m'mm

#### 5.4 Examples of symmetry classification of bicrystals

This section deals with bicrystals where the interface is a twin boundary. Only twins in non-isometric materials are discussed here. In these cases a (perfect) CSL is formed only for appropriate values of the axial ratios and the interaxial angles (Donnay & Donnay, 1954). But, there are cases where a coincidence-site net is formed.

##### 5.4.1 Twinning in the hexagonal system

Much experimental work has been carried out on the deformation twinning elements for the hexagonal metals (see e.g. Clark & Craing, 1953). A survey (Rapperport & Hartley, 1960) of the deformation modes in h.c.p. metals reveals that those with  $c/a > 1.633$  twin only on  $\{10\bar{1}2\}$  planes while those with  $c/a < 1.633$  on  $\{11\bar{2}1\}$  planes as well as on  $\{10\bar{1}2\}$  planes.

The low-temperature phase of zirconium is typical of the metals with  $c/a < 1.633$ . It has a close-packed hexagonal structure with  $a=3.223$  and  $c=5.123\text{\AA}$  ( $c/a=1.589$ ). Figure 5.4.1 shows the configuration resulting from  $(10\bar{1}2)$  twinning in zirconium according to Westlake (1961). This configuration results by purely geometrical considerations and no local relaxation of the atoms on or near to the boundary was taken into account. In this diagram the atom positions are shown as either open or filled symbols depending on whether they belong to the matrix or the twin. Circles are in the plane of the paper, whereas squares are  $a/2$  above or below the page. The two components are related by a rotation approximately  $85^\circ$  along the  $[\bar{1}2\bar{1}0]$  direction.

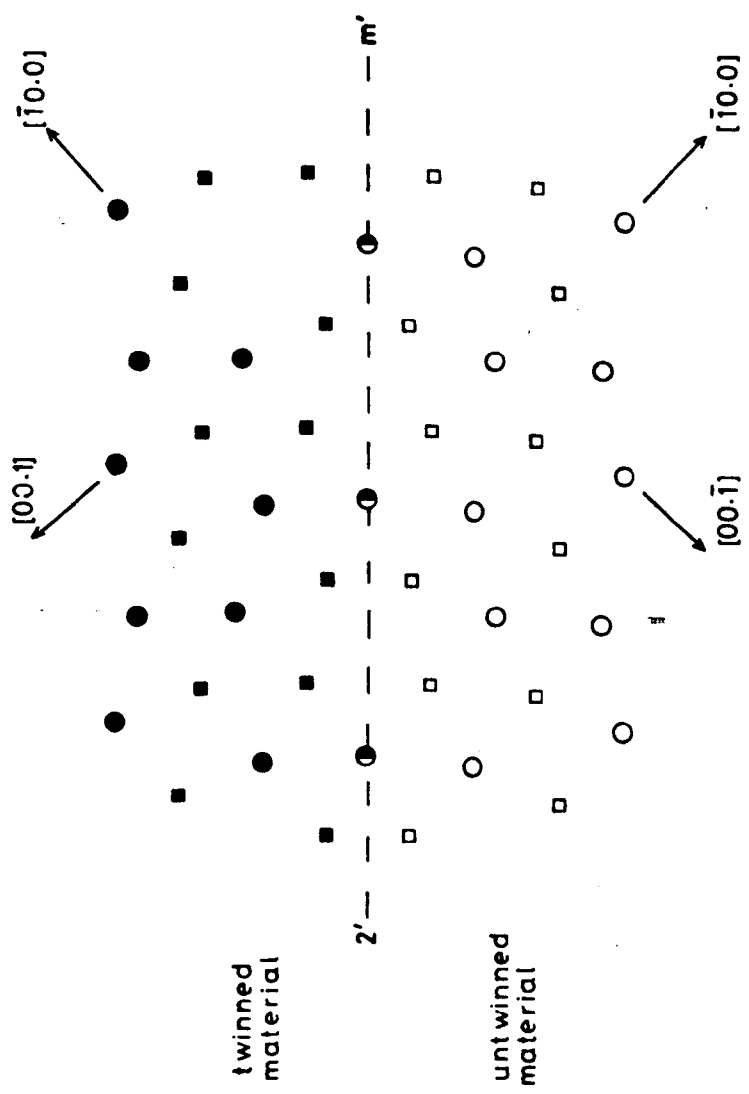
In the structure of zirconium the angle between the vectors  $[\bar{1}01\bar{1}]$  and  $[\bar{1}011]$  is equal to  $85.09^\circ$ . Consequently, a rotation  $[\bar{1}2\bar{1}0]/85.09^\circ$  leads to a coincidence net on the  $(10\bar{1}2)$ . The corresponding dichromatic

Figure 5.4.1

Twinning on  $(10\bar{1}2)$  planes in zirconium; projection on the  $(\bar{1}2\bar{1}0)$  plane. Circles and squares are atomic positions in the plane of the paper and  $\pm a/2$  out of the paper respectively.

(after Westlake, 1961)





complex shown in figure 5.4.2 exhibits, therefore, a two-dimensional periodicity.

The layer group of the dichromatic complex is  $pmm'2'$ . The ordinary mirror is parallel to the  $(\bar{1}2\bar{1}0)$  which is common to both the white and black lattices. The colour-reversing mirror plane and the 2-fold axis lie on  $(10\bar{1}2)_w$  and  $[\bar{1}011]_w$  respectively (the subscript denotes the coordinate system used for expressing the directions and planes).

In order to create the  $(10\bar{1}2)$  twin in zirconium the procedure outlined in section 3.1 is employed. Thus, by locating the composition plane of the twin parallel to the  $(10\bar{1}2)$  in such a way so it passes through the coincidence sites the configuration shown in figure 5.4.1 is obtained. The spatial symmetry of the bicrystal is described by the layer group  $pmm'2'$ .

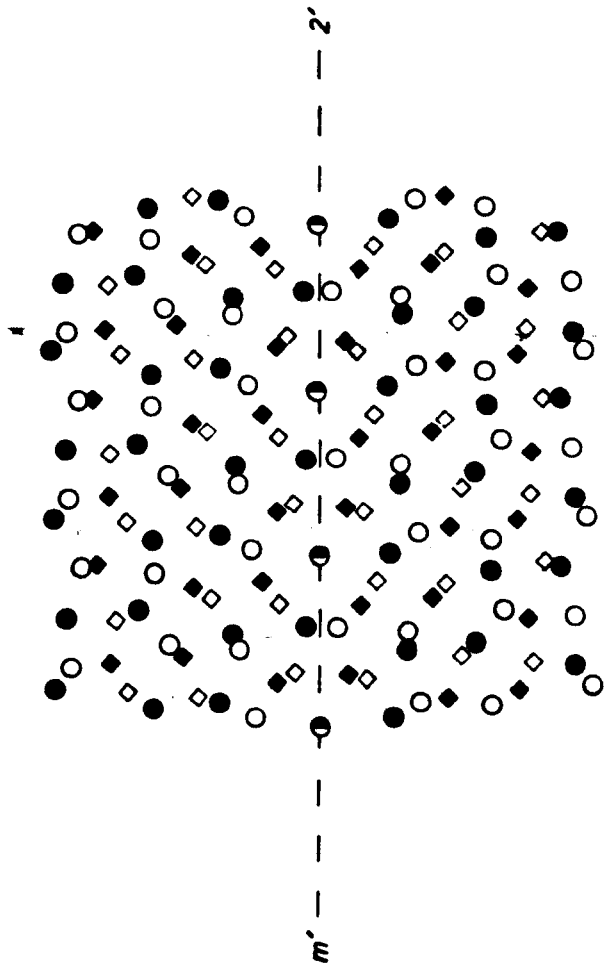
The structure of the  $(10\bar{1}2)$  twin in zirconium as shown in figure 5.4.1 corresponds to a high energy configuration because of the overlapping of atoms alongside the twin plane (i.e. atoms A and B). Rappaport & Hartley (1960) studied the deformation twins in zirconium, and they proposed that the motion of individual atoms leads to a lower energy configuration. According to them half the atoms in the twin plane assume compromising positions which do not satisfy the lattices of the twinned or the untwinned material. One can not, however, be certain of the motion of these atoms.

#### 5.4.2 Twinning in the orthorhombic system

Twin boundaries in  $\alpha$ -uranium can also be described in terms of a coincidence-site net. The twinning elements of uranium have been determined by Cahn (1953). Uranium belongs to the orthorhombic crystal class and it is found that twins of types I and II appear in addition to the

Figure 5.4.2

Dichromatic complex obtained by two lattice-complexes of the zirconium-structure type with misorientation  $[\bar{1}2\bar{1}0]/85.09^\circ$ . White and black points are represented, as usual, by open and full symbols. Circles are in the plane of the paper, whereas squares are  $\pm a/2$  out of the page.



coincidence  
site net

more usual compound twins. Cahn identified four families, of which two were of type I, one of type II and one compound (for definitions of type I and II or compound twins see, for example, Klassen-Neklyudova, 1964).

The structure of  $\alpha$ -uranium is illustrated in figure 5.4.3. From the lack of coincidence between the lattice points and the atomic positions, it would be expected that the atom movements are very irregular. This leads to doubt about the exact position of the twinning plane, and Cahn (1953) has settled its position subject to one of the following conditions: (a) the main adjustments of the atoms are minimized, (b) all atoms should move roughly the same distance (c) a proportion of the atoms should already be in coincidence points.

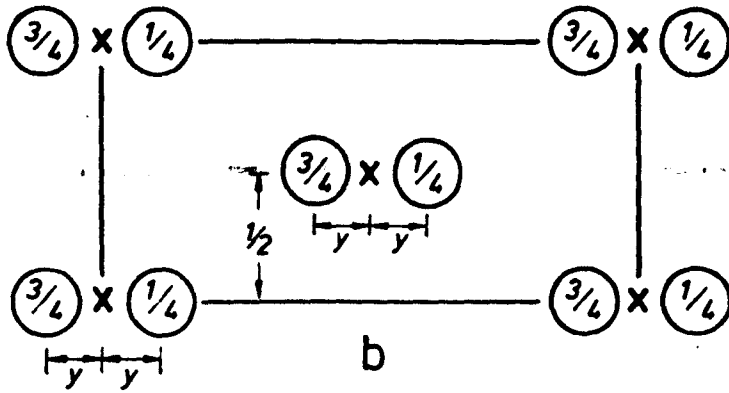
By imposing these conditions Cahn gave the structure of the (130) twin in  $\alpha$ -uranium; the (001) projection is shown in figure 5.4.4. The broken lines indicate the distortion of the region of contact according to Cahn.

Figure 5.4.4 shows that the black lattice-complex is rotated along (001) by an angle  $101^\circ$  approximately. Referring to the structure of  $\alpha$ -uranium a number of points can be found with an angular separation approximately equal to  $101^\circ$ . The angle between the points  $[250]$  and  $[2\bar{5}0]$  is equal to  $101.12^\circ$ . Therefore, the rotation  $[001]/101.12^\circ$  results in a coincidence site net on the  $(130)_w$  plane. Nearly coincidence sites are to be found by moving perpendicular to this plane. The (130) twin in  $\alpha$ -uranium corresponds, therefore, to a  $[001]/101.12^\circ$  rotation; the layer group of the bicrystal is  $cmm'2'$ .

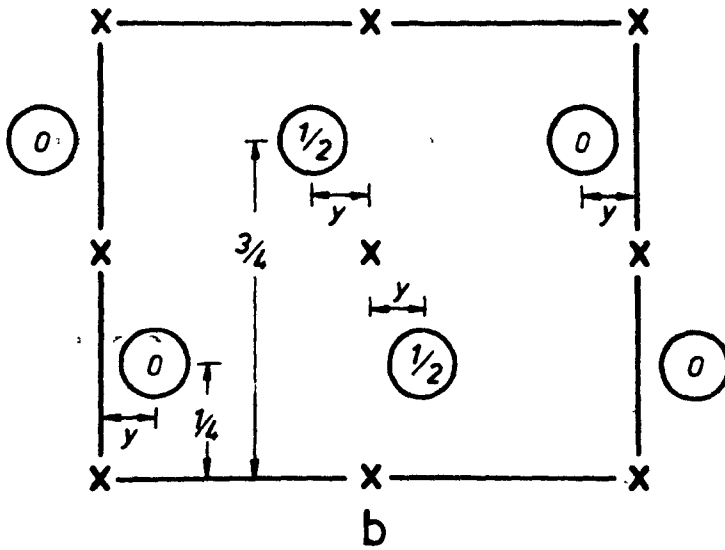
An second example of twinning in orthorhombic system refers to the aragonite. The structure of aragonite ( $\text{CaCO}_3$ ) is described by the

Figure 5.4.3

The structure of  $\alpha$ -uranium



a



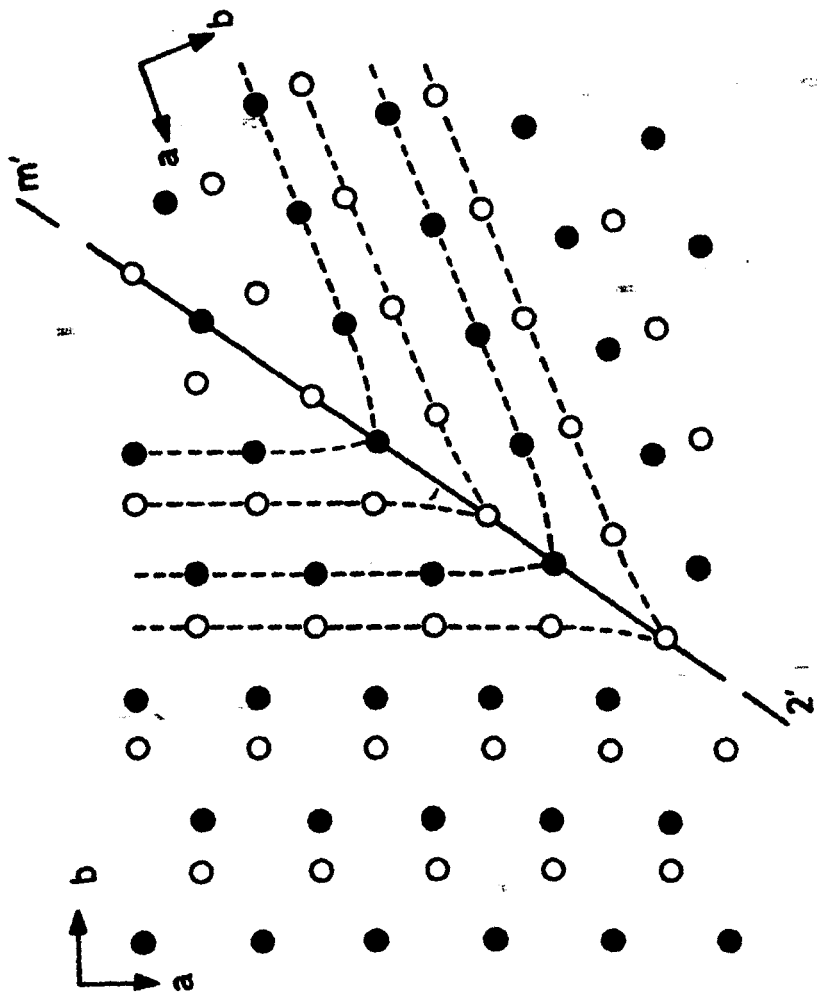
c

Figure 5.4.4

Twinning on  $(130)$  planes in  $\alpha$ -uranium; projection on  $(001)$ . The filled and open circles indicate atoms at  $c/4$  and  $3c/4$  respectively. The broken lines indicate the distortion at the region of contact.

(after Cahn, 1953)





orthorhombic space group  $Pm\bar{c}n$  ( $a=4.94$ ,  $b=7.94$ ,  $c=5.72\text{\AA}$ ) (Bragg, 1924) and the unit cell contains 4  $\text{CaCO}_3$  groups (figure 5.4.5). This structure is pseudo-hexagonal, with the  $c$  axis as the pseudo-hexagonal axis. The calcium atoms are arranged in a hexagonal array, but the arrangement of the  $\text{CO}_3$  groups lowers the symmetry to orthorhombic.

Single crystals of aragonite are rare; twinning about  $\{110\}$  is nearly always present. The atomic configuration of the  $(110)$  twin in aragonite is shown in figure 5.4.6. The two individuals of the twin are related by the colour-reversing glide plane which coincides with the twin plane.

#### 5.4.3 Twinning in the tetragonal system

The last example of twins in metals is the twinning of tin. The twin plane of white tin was first determined by Mügge (1917, 1927) and by Tanaka & Kamio (1931) as the  $(331)$  plane. Chalmers (1953), on the other hand, considered it as the  $(301)$  plane. A re-investigation by Clark, Craig & Chalmers (1950) has confirmed the latter indices, and also shown that the confusion arose from an improper choice of the unit cell in the earlier references.

The lattice of  $\beta$ -tin is body-centred tetragonal, with four atoms per unit cell at the points  $000$ ,  $\frac{1}{2}0\frac{1}{2}$ ,  $0\frac{1}{2}\frac{1}{2}$  and  $\frac{1}{2}\frac{1}{2}\frac{1}{2}$ , as shown in figure 5.4.7. The pattern of atomic positions alongside the twin boundary is shown in figure 5.4.8. Open and filled symbols represent the atomic positions in the matrix and twin respectively. Circles are atomic positions on the plane of the page and triangles are  $a/2$  above or below the page. The layer group of this configuration is  $cmm'2'$ .

#### 5.4.4 Twinning in the monoclinic system

The first example of twinning in the monoclinic system refers to the family of the feldspars. These minerals fall into two main groups,

Figure 5.4.5

The structure of aragonite,  $\text{CaCO}_3$ ; superimposed oxygen atoms have been made visible by symmetrical displacements. The heights of the atoms are measured above the face of the unit cell along the axis of projection in hundredths of the projected unit cell edge.

(after Bragg, 1924)

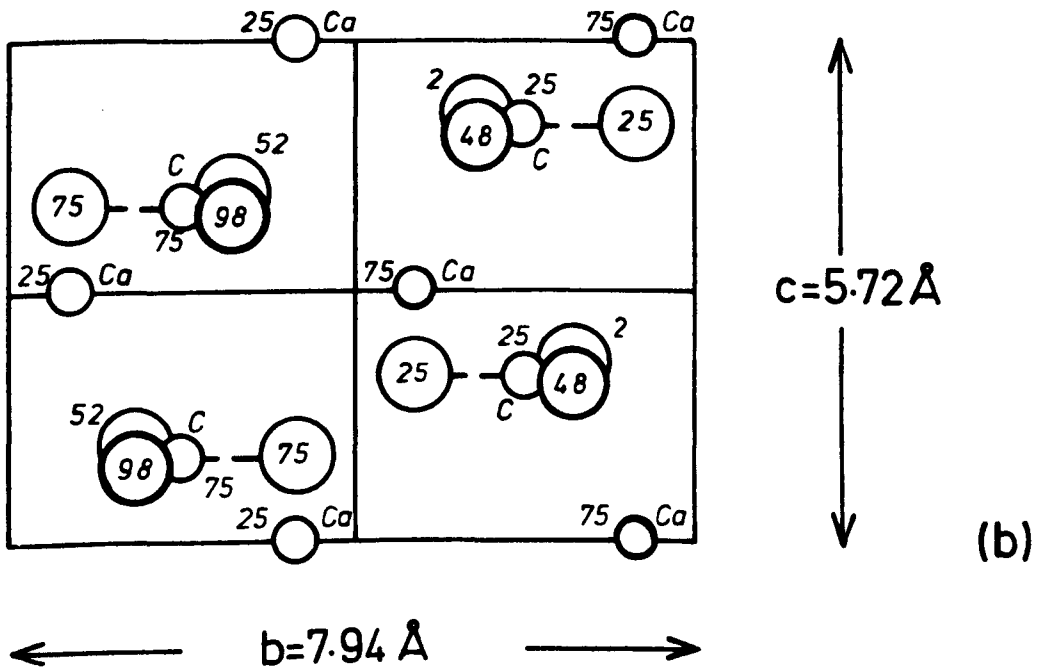
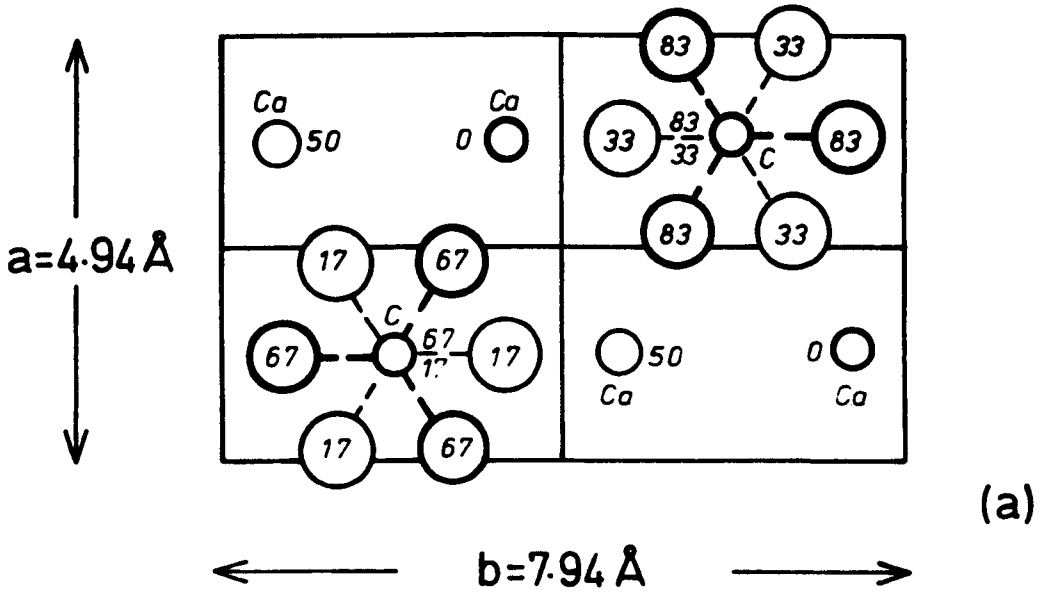


Figure 5.4.6

(110) twinning in aragonite; projection on (001) plane.

(after Bragg & Claringbull, 1965)

Key: Filled circles: Ca atoms in the plane of the page  
Open circles: Ca atoms at  $\pm 0.50c$  out of the page  
Crossed circles: C atoms at  $0.33c$  and  $0.83c$  or  
 $0.17c$  and  $0.67c$  out of the page  
Large filled squares: O atoms at  $0.17c$  out of the  
page  
Large open squares: O atoms at  $0.33c$  out of the page  
Small filled squares: O atoms at  $0.83c$  out of the  
page  
Small open squares: O atoms at  $0.67c$  out of the page

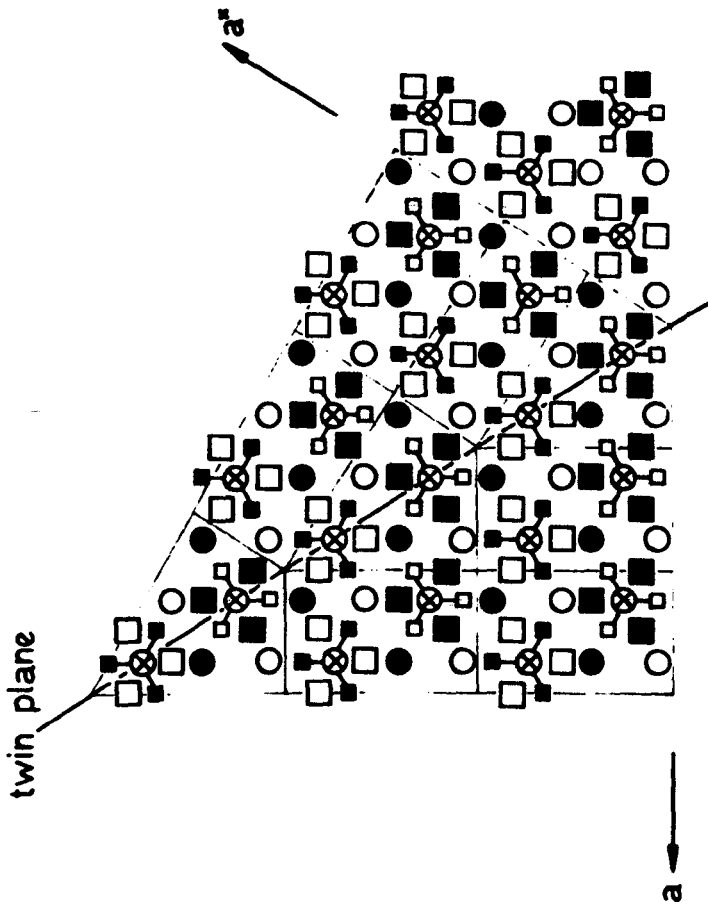


Figure 5.4.7

The structure of white tin

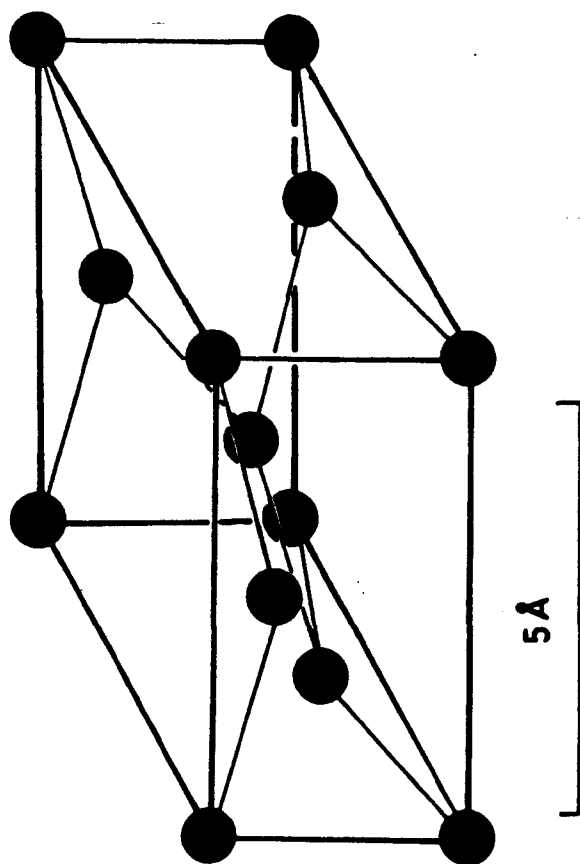
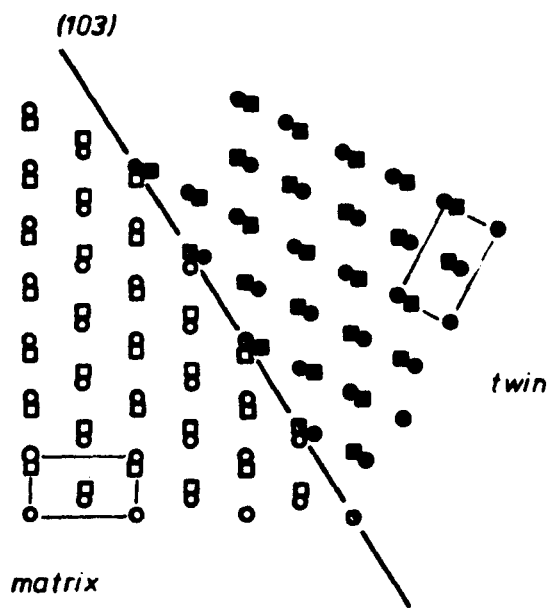




Figure 5.4.8

(103) twinning in  $\beta$ -tin, projected on (010) plane.

Key: Open symbols: positions of the white lattice-complex  
Filled symbols: positions of the black lattice-  
-complex  
Circles: positions on the plane of the paper  
Triangles:  $\pm b/2$  out of the page



one with monoclinic or very nearly monoclinic symmetry, the other definitely triclinic. One of the most remarkable features of the feldspars is the number of ways in which the crystals twin. The five common methods of twinning have simple and direct interpretations (Bragg & Claringbull, 1965). In this section, however, only the Baveno twin in orthoclase ( $\text{KAlSi}_3\text{O}_8$ ) is considered; orthoclase belongs to the monoclinic system with space group  $C2/m$  and unit cell constants  $a=8.562$ ,  $b=12.996$ ,  $c=7.193\text{\AA}$ ,  $\beta=116.01^\circ$  (Cole, Sörum & Kennard, 1949; Jones & Taylor, 1961).

The structure of the Baveno twin according to Bragg & Claringbull (1965) is shown in figure 5.4.9; the twin plane is (021). The two individuals (one in full line, the other in dotted line) have to be filled together after a relative displacement along the twin plane (021), which thus becomes a glide mirror plane. This is permissible for a growth twin but must cause severe stresses in the interface of a mechanical (deformation) twin.

The last example considered in this section is the twinning in serpierite,  $\text{Ca}(\text{Cu,Zn})_4(\text{OH})_6(\text{SO}_4)_2 \cdot 3\text{H}_2\text{O}$ . This material crystallizes in the monoclinic system with space group  $C2/c$ ,  $a=22.186$ ,  $b=6.250$ ,  $c=21.853\text{\AA}$ ,  $\beta=113.36^\circ$  and  $Z=8$  (Faraone, Sabelli & Zanazzi, 1967).

Figure 5.4.10 illustrates the arrangement of representative points in a serpierite twin according to Sabelli & Zanazzi (1968). The boundary, with the symmetry operations relating the two individuals of the twin, is outlined by a dashed line. At the boundary there is the formation of the two-fold screw axes parallel to  $[010]$  and inversion centres at  $\frac{1}{4}$  and  $\frac{3}{4}$ . These symmetry operations are colour-reversing ones, since they relate the two individuals of the twin.

Twinning in serpierite is an example of bicrystals where a colour-

Figure 5.4.9

Baveno twin; one individual is drawn in full line, the other dotted. The heights of the atoms are measured above the face of the unit cell along the axis of projection in hundredths of the projected unit cell edge.

(after Bragg & Claringbull, 1965)

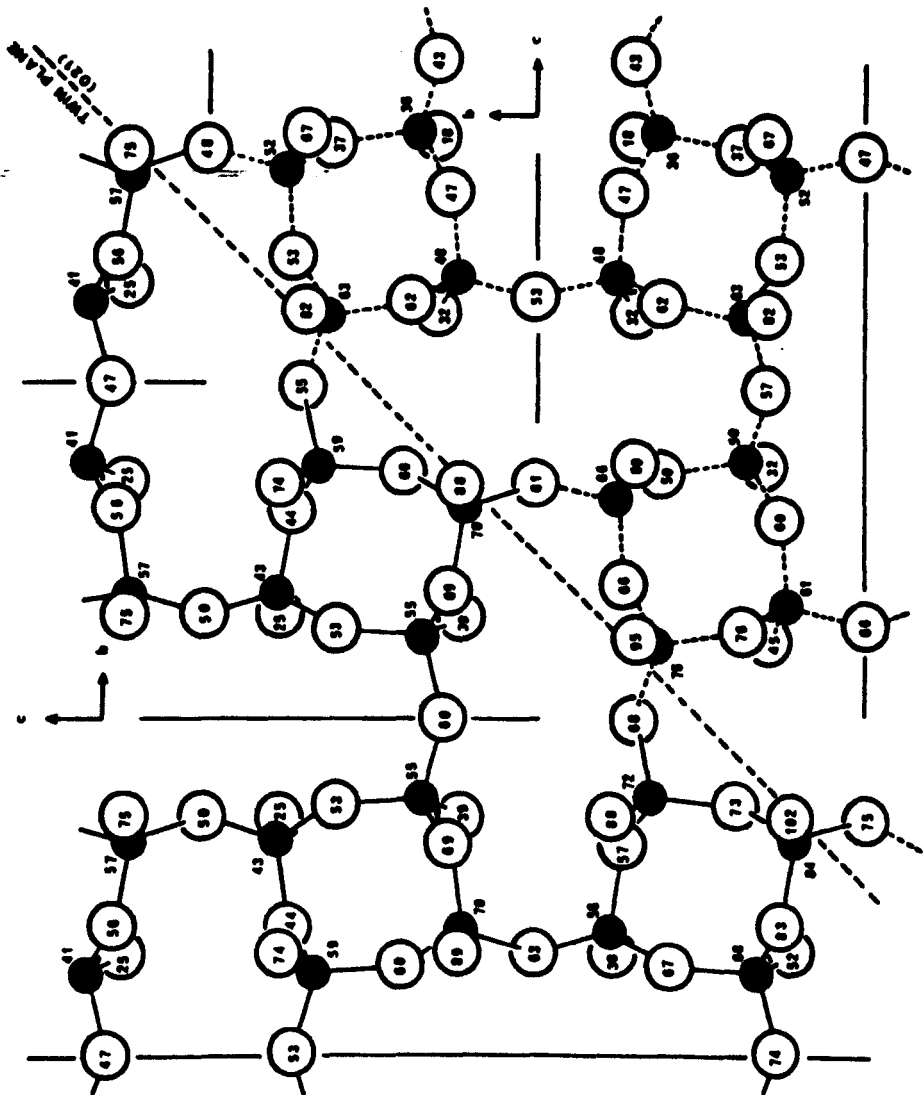
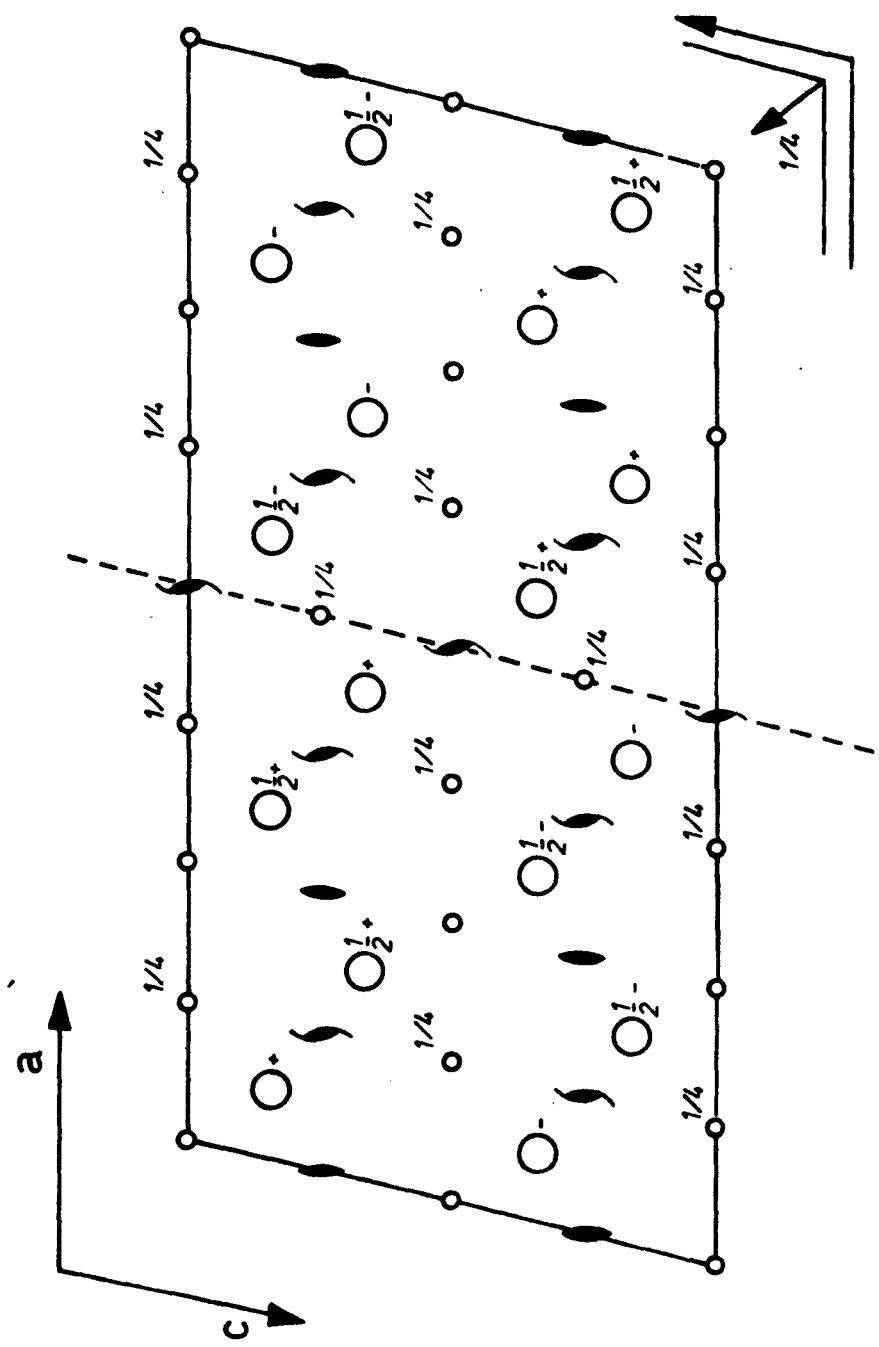


Figure 5.4.10

The arrangement of representative points in a serpierite twin. The boundary, with the twin symmetry operations, is outlined by a dashed line.

(after Sabelli & Zanazzi, 1968)



-reversing inversion centre or a colour-reversing two-fold screw axis is present on the boundary plane. The colour-reversing inversion centre implies that the lattice is continuous across the boundary. Indeed, the additional (colour-reversing) elements of the twin do not affect the symmetry of the lattice, being of the same kind as those still present in the structure, even if in positions not stated by the space group.



## Chapter 6

### VARIATION OF SYMMETRY WITH RELATIVE DISPLACEMENT

#### Introduction

The symmetry of dichromatic complexes or bicrystals depends on the misorientation and the relative position of their components. In the previous chapters the two components were assumed to have a common origin, and, hence the symmetry of dichromatic complexes and bicrystals was studied in relation to changes in the misorientation.

It remains, therefore, to consider symmetry variations due to relative displacements. Such variation is governed by general principles which are applied in the same way for both dichromatic complexes or bicrystals. Thus, in the cases where no distinction is required reference is made to a 'composite' which can equally well be a dichromatic complex or a bicrystal.

The study of the symmetry variation is carried out separately for finite and periodic composites. In section 6.1 the variation of the point symmetry is investigated and an analytical procedure is derived; the latter enables the determination of the conditions under which particular operations of symmetry are conserved. The application of this procedure is demonstrated for a particular example in section 6.2. Next, the case of periodic composites is considered and a method for determining the spatial symmetry variation is given in section 6.3. This method is used in the last section for studying the symmetry variation of a three-dimensional dichromatic pattern.

#### 6.1 Point symmetry variation

In order to study the point symmetry variation of a composite its white component will be considered fixed in space and any displacement

will result by the relative translation of the black component. If the latter is displaced away from its original position the geometrical relationships (i.e. the symmetry) between the two components changes. Some of the symmetry operations of the original composite might be destroyed after the displacement, while others are conserved<sup>1</sup>.

For example consider the composite in figure 6.1.1a obtained by the exact superposition of two (identical) components. The point symmetry of the components is  $4mm$ , and that of the composite  $4mm1'$  (grey point group). If the black component is, now, displaced by  $\underline{t}=(x,0,0)$ <sup>2</sup> the symmetry of the composite so obtained is reduced to  $m'm2'$  (figure 6.1.1b). This displacement conserves the symmetry operations  $1$ ,  $2_z^{1'}$ ,  $s_x'$ ,  $s_y'$  of the original composite but destroys all the remaining ones.

#### 6.1.1 Subgroup relations in the point symmetry variation

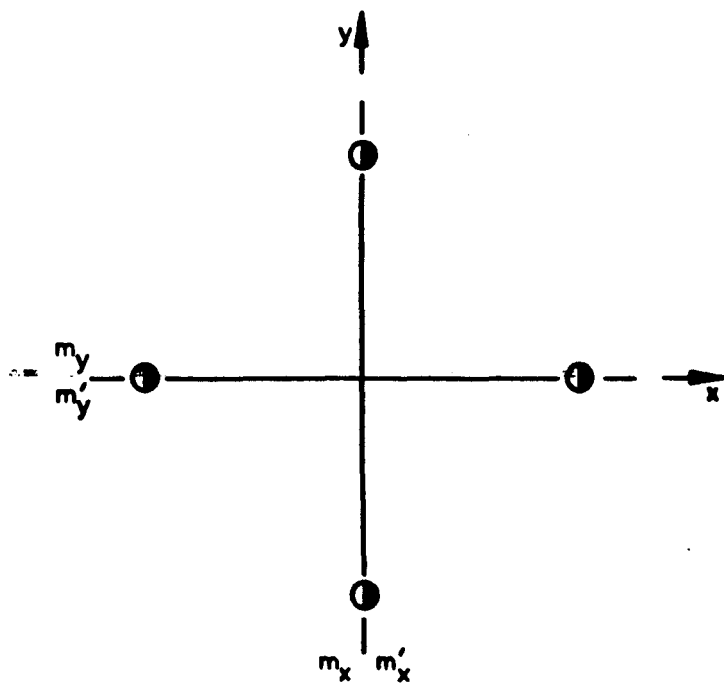
It is seen by comparing the composites in figures 6.1.1a and 6.1.1b that the shifting of the components relative to each another results in a composite with lower symmetry. This holds, however, only for the cases of holosymmetric composites, i.e. composites exhibiting the highest possible symmetry which can be created by the superposition of two given components in a given misorientation relationship. For two given components and for a given misorientation there exists a unique translational position of the two components leading to the holosymmetric composite. The symmetry group of the latter is isomorphous to either the point group of the components or to a subgroup/supergroup of it (depending on the misorientation of the two components) and this can be found by applying the procedure in section 4.3.

In the following text the composite with  $\underline{t}=0$  (see section 3.1) is taken to be always the holosymmetric one, unless specifically stated to

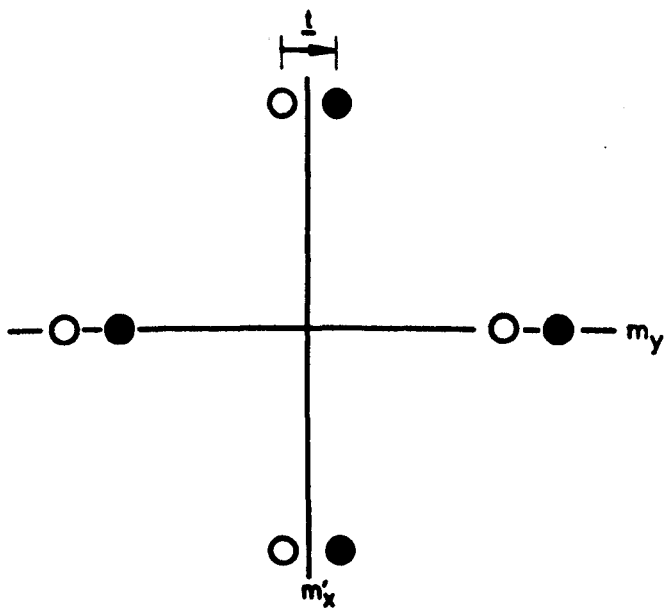
Figure 6.1.1

It shows the variation of the point symmetry with displacement. The original composite is shown in (a); its symmetry is  $4mm1'$ . When the black component is displaced by  $\underline{t}$  the symmetry is reduced to  $m'm2'$  (b). Note the shift of the mirror plane  $m'_x$ . The coordinate system for expressing the symmetry operations and displacements is shown in (a); the z-axis is out of the plane of the paper.

(a)



(b)



be otherwise. In this case the point symmetry of the composite after displacement is a subgroup of the point group of the holosymmetric composite. First of all, it is a group by virtue of the restrictions placed upon the conservation of its elements. No product of elements in the set can be unrelated to the particular geometric relationship of the two components, and all elements of the initial composite related to this relationship are included in the set. Secondly, it is a subgroup because in displacing the black component symmetry elements are removed, but not added (as long as the initial composite is the holosymmetric one).

The consideration of a holosymmetric composite for  $\underline{t}=0$  provides a way to check that all the symmetries of 'displaced' composites have been found. This is because only certain symmetries, which are amongst the subgroups of the particular point group, can be created by displacing the black component.

Having established the relationship between the point groups of the composites before and after displacement the analytical approach for studying the point symmetry variation can be derived. For this the colour-reversing and ordinary symmetry operations are considered separately.

### 6.1.2 Conservation of colour-reversing symmetry operations

Colour-reversing symmetry operations arise by the geometrical relationships existing between the white and black components. Thus, any displacement  $\underline{t}$  which does not alter the particular relationship conserves the respective operation which, however, is shifted by  $\underline{t}/2$ . Referring to figure 6.1.1b, for an example, the mirror plane  $s'_x$  has been shifted after the displacement  $\underline{t}=(x,0,0)$ , by  $(x/2,0,0)$  relative to its original

position.

When the black component is displaced by  $\underline{t}$  the origin of the coordinate system has, therefore, to be displaced by  $\underline{t}/2$  in order to retain the form of the symmetry operation matrix representations (this coordinate system is called the 'displaced coordinate system'). Alternatively stated, it can be considered that the black component is displaced by  $\underline{t}/2$  and at the same time the white component by  $-\underline{t}/2$ . In this case the conserved symmetry elements remain in their initial positions and, hence, they are expressed relative to the original coordinate system.

Let  $\underline{S}$  be a colour-reversing symmetry operation which is conserved after displacement  $\underline{t}$ . Since  $\underline{S}$  is present in the initial composite there is at least a pair of points belonging to the white and black components -their positions in the original composite are denoted by  $\underline{x}_w$  and  $\underline{x}_b$  respectively- for which:

$$\underline{S}\underline{x}_w = \underline{x}_b$$

If the black and white components are displaced by  $\underline{t}/2$  and  $-\underline{t}/2$  the positions of the above points (relative to the original coordinate system) are  $\underline{x}_w - \underline{t}/2$  and  $\underline{x}_b + \underline{t}/2$  respectively. The symmetry relationship between the two points is now expressed by:

$$\underline{S}(\underline{x}_w - \underline{t}/2) = \underline{x}_b + \underline{t}/2$$

Consequently, a colour-reversing symmetry operation is conserved only if:

$$\underline{S}(-\underline{t}/2) = \underline{t}/2 \quad (6.1.1)$$

where the displacement  $\underline{t}/2$  is expressed relative to the coordinate system of the original composite.

### 6.1.3 Conservation of ordinary symmetry operations

Ordinary symmetry operations result by the coincidence of identical operations in the two components (see section 4.1). Thus, a displacement

$\underline{t}$  conserves an ordinary symmetry operation only when it leaves these symmetry elements in coincidence. If the original composite contains, say, a  $u$ -fold rotation axis, obtained by the superposition of two  $u$ -fold axes of the components, then this axis is conserved only for displacements along its direction.

Let  $\underline{S}_0$  an ordinary symmetry operation which is conserved when the two components are displaced relative to each other. In the initial composite there is at least a pair of white points,  $\underline{x}_w$  and  $\underline{x}'_w$ , as well as a pair of black points,  $\underline{x}_b$  and  $\underline{x}'_b$ , for which:

$$\underline{S}_0 \underline{x}'_w = \underline{x}_w$$

and

$$\underline{S}_0 \underline{x}'_b = \underline{x}_b$$

After displacement the positions of the points in the white component become  $\underline{x}_w - \underline{t}/2$  and  $\underline{x}'_w - \underline{t}/2$  and those in the black component  $\underline{x}_b + \underline{t}/2$  and  $\underline{x}'_b + \underline{t}/2$  respectively. Therefore, the symmetry relationships of the two pairs of points are given by:

$$\underline{S}_0 (\underline{x}'_w - \underline{t}/2) = \underline{x}_w - \underline{t}/2$$

and

$$\underline{S}_0 (\underline{x}'_b + \underline{t}/2) = \underline{x}_b + \underline{t}/2$$

Consequently, an ordinary symmetry operation is conserved by a displacement only if:

$$\underline{S}_0 (\underline{t}/2) = \underline{t}/2 \quad (6.1.2)$$

A displacement, therefore, conserves only these ordinary symmetry elements which satisfy relation (6.1.2); for the same displacement the colour-reversing elements present in the composite are given by relation (6.1.1).

#### 6.1.4 Conservation of (ordinary or colour-reversing) symmetry elements

Relations (6.1.1) and (6.1.2) give the conditions under which symmetry operations of the composite are conserved by displacements of

the black component. For determining the displacements conserving a symmetry element all the symmetry operations associated to it must be considered. The displacement conserving a particular symmetry element is then the one for which all the associated symmetry operations are invariant. In other words, in the case of a symmetry element, of order  $n$ , the displacement conserving it is determined by the solution of the system:

$$\sum_i [(-1)^k \underline{t}/2] = \underline{t}/2 \quad (6.1.3)$$

where  $\underline{S}_i$  ( $i=1,2,\dots,n$ ) are the matrices of the symmetry operations associated to the symmetry element and  $k=1$  for colour-reversing or  $k=2$  for ordinary symmetry operations. Under this convention equations (6.1.1) and (6.1.2) allow the determination of displacements conserving the symmetry elements of the original composite.

Concluding this section it is of interest to give the general rules of symmetry element conservation with displacement:

**Rule 6.1.1:** The ordinary identity operation is conserved by any displacement whereas no translation conserves the antisymmetry operation.

**Rule 6.1.2:** An ordinary rotation axis or mirror plane is conserved only by displacements parallel to this axis or plane of symmetry.

**Rule 6.1.3:**  $u$ -fold ( $u \geq 2$ ) colour-reversing rotation axes are destroyed by any displacement. However, colour-reversing axes  $2'$  or planes  $m'$  are conserved by displacements which are perpendicular to these rotation axes and symmetry planes.

**Rule 6.1.4:** The ordinary inversion centre is destroyed by any displacement whereas the colour-reversing one is always conserved.



The displacement associated with the identity operation is rather obvious; there is no displacement destroying the symmetrical relation of a point to itself. In contrast, the colour-reversing centre of symmetry is destroyed by any displacement because the inversion centres in the two components are brought out of coincidence. The way of deriving the remaining of the above rules is demonstrated in the next section.

- - -

- Footnotes
- 1: No new symmetry operations can be created by a displacement (see section 6.1.1).
  - 2: The symbol  $\underline{t}=(x,0,0)$  denotes the vector  $\underline{t}=x\underline{i}+0\underline{j}+0\underline{k}$  with  $\underline{i}$ ,  $\underline{j}$ ,  $\underline{k}$  the unit vectors along the x-, y- and z-axes of the coordinate system Oxyz indicated in figure 6.1.1a.
  - 3: Order of a symmetry element is the number of symmetry operations associated with this particular element; for example, the order of the  $\bar{4}$ -fold rotation axis is equal to 4.

## 6.2 Example of point symmetry variation

The application of the method outlined in section 6.1 is now demonstrated with reference to a particular example. For this a bicoloured composite is considered and its point symmetry variation is studied by allowing the two components to be displaced relative to one another

Let both the white and black components be non-periodic<sup>1</sup> with symmetry 4/mmm and let these be superposed so the obtained composite has the symmetry 4/mm'm'. This point group contains the following symmetry operations (see table A1.3):

ordinary operations: 1,  $4_z^1$ ,  $4_z^3$ ,  $2_z^1$ , i,  $\bar{4}_z^1$ ,  $\bar{4}_z^3$ ,  $s_z$

colour-reversing operations:  $2_x^{1'}$ ,  $2_y^{1'}$ ,  $2_\alpha^{1'}$ ,  $2_\beta^{1'}$ ,  $s_x'$ ,  $s_y'$ ,  $s_\alpha'$ ,  $s_\beta'$ .

The z-axis of the orthogonal coordinate system used for expressing

the matrix representations of the symmetry operations (and the displacements) is along the 4-fold axis. The x- and y-axes, on the other hand, coincide with two mutually orthogonal 2-fold axes of the point group.

The considered composite exhibits the highest possible symmetry created by the given components in the given misorientation, i.e. it is the holosymmetric composite. Consequently, only certain symmetries can be created by displacing the black component. These symmetries are among the subgroups of the point group  $4/mm'm'$  given in table 6.2.1 (note that all the crystallographically non-equivalent subgroups of  $4/mm'm'$  are included in this table).

#### 6.2.1 Conservation of symmetry elements

The next stage in the procedure is to determine the displacement(s) for which each of the symmetry operations of  $4/mm'm'$  is invariant. Colour-reversing operations are conserved by the displacements obtained as solutions of the equation (6.1.1); these are given in table 6.2.2. On the other hand, the displacements conserving ordinary operations are, according to equation (6.1.2), these in table 6.2.3.

In applying the results of tables 6.2.2 and 6.2.3 it must be born in mind that they correspond to symmetry operations. The translation(s) conserving a particular symmetry element is(are) the displacement(s) for which all the symmetry operations associated to this element are invariant (see section 6.1.4). The ordinary 4-fold axis, for example, involves the presence of the four symmetry operations:  $1$ ,  $4_z^1$ ,  $2_z^1$ ,  $4_z^3$ . All these operations are conserved for displacements parallel to the z-axis and, hence, the 4-fold ordinary axis is conserved for  $\underline{t}=(0,0,z)$ . As far as the ordinary axis  $\bar{4}$  is concerned, it contains the symmetry operations:  $1$ ,  $\bar{4}_z^1$ ,  $2_z^1$ ,  $\bar{4}_z^3$  and, therefore, it is destroyed by any displacement (table 6.2.3).

TABLE 6.21

Subgroups of the black-white point group  $4mm'm'$

number	subgroup	1	$4_z^1$	$4_z^3$	$2_z^1$	$2_x^1$	$2_y^1$	$2_\alpha^1$	$2_\beta^1$	l	$z_z^1$	$z_z^3$	$s_z$	$s_x$	$s_y$	$s_\alpha$	$s_\beta$
1	$4mm'm'$	X	X	X	X	X	X	X	X	X	X	X	X	X	X	X	X
2	$\bar{4}2'm'$	X	X	X	X	X	X										X
3	$\bar{4}2'm'$	X	X	X	X			X	X					X	X		
4	$4m'm'$	X	X	X	X									X	X	X	X
5	$42'2'$	X	X	X	X	X	X	X	X								
6	$4/m$	X	X	X	X					X	X	X	X				
7	$\bar{4}$	X			X						X	X					
8	$4$	X	X	X	X												
9	$m'm'm'$	X			X	X	X			X			X	X	X		
10	$m'm'm'$	X			X			X	X	X			X			X	X
11	$m'm'2'$	X					X						X	X			
12	$m'm'2'$	X				X							X		X		
13	$m'm'2'$	X						X					X			X	
14	$m'm'2'$	X						X					X				X
15	$2'/m'$	X				X				X				X			
16	$2'/m'$	X					X			X					X		
17	$2'/m'$	X						X		X							X
18	$2'/m'$	X							X	X							X
19	$2/m$	X			X					X			X				
20	$m'm'2$	X			X									X	X		
21	$m'm'2$	X			X											X	X
22	$22'2'$	X			X	X	X										
23	$22'2'$	X			X			X	X								
24	$\bar{1}$	X								X							
25	$m'$	X												X			
26	$m'$	X													X		
27	$m'$	X														X	
28	$m'$	X															X
29	$2'$	X				X											
30	$2'$	X					X										
31	$2'$	X						X									
32	$2'$	X							X								
33	$m$	X											X				
34	$2$	X			X												
35	$1$	X															

Note: all the subgroups are given; from the total 35 subgroups only 19 are crystallographically non-equivalent

TABLE 6.2.2

Solutions of the equation  $\underline{S}(-\underline{t}/2)=\underline{t}/2$  for the colour-reversing symmetry operations of the black-white point group  $4/\text{mm}'\text{m}'$

Symmetry element	Matrix equation	Solution
$2_x^{1'}$	$\begin{pmatrix} 1 & 0 & 0 \\ 0 & -1 & 0 \\ 0 & 0 & -1 \end{pmatrix} \begin{pmatrix} -t_x/2 \\ -t_y/2 \\ -t_z/2 \end{pmatrix} = \begin{pmatrix} t_x/2 \\ t_y/2 \\ t_z/2 \end{pmatrix}$	$t_x=0$ $t_y$ : no condition $t_z$ : no condition
$2_y^{1'}$	$\begin{pmatrix} -1 & 0 & 0 \\ 0 & 1 & 0 \\ 0 & 0 & -1 \end{pmatrix} \begin{pmatrix} -t_x/2 \\ -t_y/2 \\ -t_z/2 \end{pmatrix} = \begin{pmatrix} t_x/2 \\ t_y/2 \\ t_z/2 \end{pmatrix}$	$t_x$ : no condition $t_y=0$ $t_z$ : no condition
$2_\alpha^{1'}$	$\begin{pmatrix} 0 & 1 & 0 \\ 1 & 0 & 0 \\ 0 & 0 & -1 \end{pmatrix} \begin{pmatrix} -t_x/2 \\ -t_y/2 \\ -t_z/2 \end{pmatrix} = \begin{pmatrix} t_x/2 \\ t_y/2 \\ t_z/2 \end{pmatrix}$	$t_x=-t_y$ (*) $t_z$ : no condition
$2_\beta^{1'}$	$\begin{pmatrix} 0 & -1 & 0 \\ -1 & 0 & 0 \\ 0 & 0 & -1 \end{pmatrix} \begin{pmatrix} -t_x/2 \\ -t_y/2 \\ -t_z/2 \end{pmatrix} = \begin{pmatrix} t_x/2 \\ t_y/2 \\ t_z/2 \end{pmatrix}$	$t_x=t_y$ (**) $t_z$ : no condition
$s_x'$	$\begin{pmatrix} -1 & 0 & 0 \\ 0 & 1 & 0 \\ 0 & 0 & 1 \end{pmatrix} \begin{pmatrix} -t_x/2 \\ -t_y/2 \\ -t_z/2 \end{pmatrix} = \begin{pmatrix} t_x/2 \\ t_y/2 \\ t_z/2 \end{pmatrix}$	$t_x$ : no condition $t_y=0$ $t_z=0$
$s_y'$	$\begin{pmatrix} 1 & 0 & 0 \\ 0 & -1 & 0 \\ 0 & 0 & 1 \end{pmatrix} \begin{pmatrix} -t_x/2 \\ -t_y/2 \\ -t_z/2 \end{pmatrix} = \begin{pmatrix} t_x/2 \\ t_y/2 \\ t_z/2 \end{pmatrix}$	$t_x=0$ $t_y$ : no condition $t_z=0$
$s_\alpha'$	$\begin{pmatrix} 0 & 1 & 0 \\ 1 & 0 & 0 \\ 0 & 0 & 1 \end{pmatrix} \begin{pmatrix} -t_x/2 \\ -t_y/2 \\ -t_z/2 \end{pmatrix} = \begin{pmatrix} t_x/2 \\ t_y/2 \\ t_z/2 \end{pmatrix}$	$t_x=t_y$ (**) $t_z=0$
$s_\beta'$	$\begin{pmatrix} 0 & -1 & 0 \\ -1 & 0 & 0 \\ 0 & 0 & 1 \end{pmatrix} \begin{pmatrix} -t_x/2 \\ -t_y/2 \\ -t_z/2 \end{pmatrix} = \begin{pmatrix} t_x/2 \\ t_y/2 \\ t_z/2 \end{pmatrix}$	$t_x=-t_y$ (*) $t_z=0$

(\*)  $t_x=-t_y$  means a displacement perpendicular to the  $xy$ -direction

(\*\*)  $t_x=t_y$  denotes a displacement perpendicular to the  $xy$ -direction

TABLE 6.2.3

Solutions of the equation  $\underline{S}(t/2)=t/2$  for the ordinary symmetry operations of the black-white point group  $4/mm'm'$

Symmetry element	Matrix equation	Solution
1	$\begin{pmatrix} 1 & 0 & 0 \\ 0 & 1 & 0 \\ 0 & 0 & 1 \end{pmatrix} \begin{pmatrix} t_x/2 \\ t_y/2 \\ t_z/2 \end{pmatrix} = \begin{pmatrix} t_x/2 \\ t_y/2 \\ t_z/2 \end{pmatrix}$	$t_x$ : no condition $t_y$ : no condition $t_z$ : no condition
$4_z^1$	$\begin{pmatrix} 0 & -1 & 0 \\ 1 & 0 & 0 \\ 0 & 0 & 1 \end{pmatrix} \begin{pmatrix} t_x/2 \\ t_y/2 \\ t_z/2 \end{pmatrix} = \begin{pmatrix} t_x/2 \\ t_y/2 \\ t_z/2 \end{pmatrix}$	$t_x=0$ $t_y=0$ $t_z$ : no condition
$4_z^3$	$\begin{pmatrix} 0 & 1 & 0 \\ -1 & 0 & 0 \\ 0 & 0 & 1 \end{pmatrix} \begin{pmatrix} t_x/2 \\ t_y/2 \\ t_z/2 \end{pmatrix} = \begin{pmatrix} t_x/2 \\ t_y/2 \\ t_z/2 \end{pmatrix}$	$t_x=0$ $t_y=0$ $t_z$ : no condition
$2_z^1$	$\begin{pmatrix} -1 & 0 & 0 \\ 0 & -1 & 0 \\ 0 & 0 & 1 \end{pmatrix} \begin{pmatrix} t_x/2 \\ t_y/2 \\ t_z/2 \end{pmatrix} = \begin{pmatrix} t_x/2 \\ t_y/2 \\ t_z/2 \end{pmatrix}$	$t_x=0$ $t_y=0$ $t_z$ : no condition
i	$\begin{pmatrix} -1 & 0 & 0 \\ 0 & -1 & 0 \\ 0 & 0 & -1 \end{pmatrix} \begin{pmatrix} t_x/2 \\ t_y/2 \\ t_z/2 \end{pmatrix} = \begin{pmatrix} t_x/2 \\ t_y/2 \\ t_z/2 \end{pmatrix}$	$t_x=0$ $t_y=0$ $t_z=0$
$\bar{4}_z^1$	$\begin{pmatrix} 0 & -1 & 0 \\ 1 & 0 & 0 \\ 0 & 0 & -1 \end{pmatrix} \begin{pmatrix} t_x/2 \\ t_y/2 \\ t_z/2 \end{pmatrix} = \begin{pmatrix} t_x/2 \\ t_y/2 \\ t_z/2 \end{pmatrix}$	$t_x=0$ $t_y=0$ $t_z=0$
$\bar{4}_z^3$	$\begin{pmatrix} 0 & 1 & 0 \\ -1 & 0 & 0 \\ 0 & 0 & -1 \end{pmatrix} \begin{pmatrix} t_x/2 \\ t_y/2 \\ t_z/2 \end{pmatrix} = \begin{pmatrix} t_x/2 \\ t_y/2 \\ t_z/2 \end{pmatrix}$	$t_x=0$ $t_y=0$ $t_z=0$
$s_z$	$\begin{pmatrix} 1 & 0 & 0 \\ 0 & 1 & 0 \\ 0 & 0 & -1 \end{pmatrix} \begin{pmatrix} t_x/2 \\ t_y/2 \\ t_z/2 \end{pmatrix} = \begin{pmatrix} t_x/2 \\ t_y/2 \\ t_z/2 \end{pmatrix}$	$t_x$ : no condition $t_y$ : no condition $t_z=0$

The colour-reversing mirrors  $s'_\alpha$  and  $s'_\beta$ , on the other hand, are invariant for displacements which do not change the respective mirror relationships of the two components, that is, for displacements  $(x,x,0)$  and  $(-x,x,0)$  respectively (rule 6.1.3). These considerations indicate the way by which the rules in the previous section were derived.

### 6.2.2 Conservation of sets of symmetry operations

Attention is now focused on displacements which conserve sets of symmetry elements. In other words, the displacements leading to a composite with symmetry described by any one of the subgroups of the point group  $4/mm'm'$  are determined. For this, each one of the subgroups given in table 6.2.1 is considered (starting with those of higher symmetry). For each subgroup a displacement conserving all the group elements can be established. This is, in fact, equivalent to solving the system of  $r$  equations:  $S_{\underline{i}}(-\underline{t}/2) = \underline{t}/2$  ( $i=1,2,\dots,r/2$ ) and  $S_{\underline{j}}(\underline{t}/2) = \underline{t}/2$  ( $j=1,2,\dots,r/2$ ) where  $S_{\underline{i}}$  and  $S_{\underline{j}}$  are respectively the matrix representations of the colour-reversing and ordinary elements of the particular subgroup of order  $r$ .

For example, consider the subgroup  $42'2' = \{1, 4_z^1, 2_z^1, 4_z^3, 2_x^1, 2_y^1, 2_\alpha^1, 2_\beta^1\}$ . The 4-fold axis is conserved by a displacement  $(0,0,z)$ , whereas the axes  $2_x^1, 2_y^1, 2_\alpha^1, 2_\beta^1$  are conserved by the displacements  $(0,y,z), (x,0,z), (-x,x,z), (x,x,z)$  respectively. Therefore, the only displacement conserving all the elements of  $42'2'$  are of the form  $(0,0,z)$ . Similar considerations give the displacements which conserve each of the remaining subgroups in table 6.2.1. These displacements and the associated point groups are given in table 6.2.4<sup>2</sup>. Since the point group of the composite for  $\underline{t} \neq 0$  is restricted to be a subgroup of the point group  $4/mm'm'$  and since all the subgroups were considered it is clear

TABLE 6.2.4

Point symmetry variation of a composite  
with symmetry  $4/m\bar{m}'m'$

Fractional coordinates of displacement	Point group	
	Number*	Symbol
000	1	$4/m\bar{m}'m'$
00z	5	$42'2'$
0y0	11	$m'm2'$
x00	12	$m'm2'$
xx0	13	$m'm2'$
$\bar{x}x0$	14	$m'm2'$
x0z	29	$2'$
0yz	30	$2'$
xxz	31	$2'$
$\bar{x}xz$	32	$2'$
xy0	33	m
xyz	35	1

(\*) see table 6.2.1

that table 6.2.4 covers all the possible composites obtained from the original holosymmetric one.

When the displacements conserving the elements of a subgroup are determined, the following must be kept in mind:

- 1) Since the ordinary identity operation is conserved by any displacement, there is no need to account for this operation.
- 2) Certain subgroups are not invariant by displacements  $\underline{t} \neq \underline{0}$ . The subgroup  $42'm'$ , for example, is conserved by the displacement  $\underline{t} = (0,0,0)$  only.
- 3) Certain subgroups are formed by displacements which at the same time conserve another subgroup of higher symmetry.

The latter is a consequence of the conservation of various symmetry elements by the same displacement. For example, both subgroups  $42'2'$  and  $4$  are formed by a displacement of the form  $(0,0,z)$ . This happens when the two groups contain common elements, or, in other words, when the group of lower symmetry is a subgroup of the one of higher symmetry. In such cases, however, the symmetry of the dichromatic complex or bicrystal is described by the highest order subgroup (highest symmetry). This explains why the subgroup list must be considered in a sequence of decreasing group order.

### 6.2.3 Equivalent composites

Table 6.2.4 shows that certain subgroups can be created by more than one crystallographically equivalent displacement<sup>3</sup>. This occurs in the cases where a subgroup adopts more than one crystallographically equivalent orientation in the point group of the composite with  $\underline{t} = \underline{0}$ . The subgroup  $m'$ , for example, adopts two different, but equivalent, orientations in  $4/mm'm'$ ; the two orientations are related by symmetry



operations of the initial composite. As it can be seen from table 6.2.4 the displacements leading to the corresponding composites are also related by symmetry operations of the initial composite.

Pond & Bollmann (1979) have shown that whenever a composite with  $t=0$  contains point symmetry higher than 1, there exists a set of dichromatic patterns or bicrystals, obtained from the original composite by displacements of the black component, which are related by the symmetry of the initial composite. They called the composites of such sets equivalent dichromatic patterns and equivalent bicrystals. Similar considerations indicate that the same holds for dichromatic complexes, and, following Pond & Bollmann (1979), such sets are called here 'equivalent dichromatic complexes'.

The symmetry relationships between the sets of equivalent dichromatic complexes and bicrystals will be further examined in section 7.3.

- - -

- Footnotes 1: The consideration of non-periodic components (and, hence, non-periodic composites) has no significance except that it implies that point symmetry only is taken into account. The method is, however, identically applied for studying the point symmetry variation of periodic composites.
- 2: In table 6.2.4 only displacements  $t \neq 0$  (and the associated subgroups) are included.
- 3: It is possible that composites with identical symmetry can be created by crystallographic non-equivalent displacements. These cases, however, must be treated separately; this is a situation where the need to distinguish between crystallographically non-equivalent subgroups arises.

### 6.3 Variation of the spatial symmetry

The discussion in the previous sections was confined to non-periodic components. This allowed the effect of the relative displacement on the

point symmetry to be analysed. Dichromatic complexes and bicrystals can, however, be periodic. Thus, attention is now focused on infinite components and the variation of their symmetry is studied.

### 6.3.1 Displacements conserving a periodic composite

The consideration of periodicity implies that there are displacements which conserve the original composite. These are due to the translational symmetry of the components, but for a periodic composite additional displacements exist as well. Thus, two categories of displacements are distinguished.

The first contains displacements for which the obtained composite differs in no way from the original one; they recreate the composite at the original position. Displacements of this category are equal to the translation vectors of the respective component. In the case of CSL based dichromatic complexes and bicrystals, where the two components have a common superlattice, the vectors of this superlattice represent displacements of either component which conserve the original composite. Thus, the displacements of the first category can further be classified into:

- (a) displacements which can be applied to the respective component in order to recreate the initial composite, and,
- (b) vectors which represent shifting of either component.

For displacements of the second category the composite is conserved as far as the configuration of points is concerned but it is displaced relative to its original position. The displacements of the second category are, in fact, equal to the DSC lattice vectors (Bollmann, 1970). Bollmann has shown that these vectors form a sublattice of the composite lattice and, in fact, it is this sublattice which represents the periodic

variation of the composite symmetry.

### 6.3.2 Displacement vector set for dichromatic complexes and bicrystals

The displacements of the above two categories can be represented in an integrated way by means of the vector space, a concept introduced by Buerger (1950a,b) in connection with the solution of the Patterson function in X-ray crystallography. For the purposes of the symmetry variation studies the vector space is considered as the space containing the displacement vector set of the associated dichromatic complex or bicrystal.

The vector space is formed by drawing vectors between all points in the dichromatic complex or bicrystal (disregarding the different colours). These vectors are then assembled at common origin and the unit cell of the periodic vector is established. The unit-translations of the vector set correspond to the displacements which recreate the original composite<sup>1</sup>. In other words, the translation symmetry of the vector set represents the periodicity of the spatial symmetry variation. Consequently, it is adequate to investigate the spatial symmetry variation due to displacements which fall within the Wigner-Seitz cell of the associated vector set.

It is evident, from the construction of the vector set, that the fundamental set and the vector set have the same number of translation axes. In the case of dichromatic complexes or bicrystals with no translational symmetry the Wigner-Seitz cell has zero volume. For complexes or bicrystals with one- or two-dimensional periodicity the unit cell of the vector set is linear or planar respectively. In the case of dichromatic complexes based in CSL the Wigner-Seitz cell is three-dimensional and has a volume that decreases as  $\Sigma$  increases.

### 6.3.3 General and special displacements

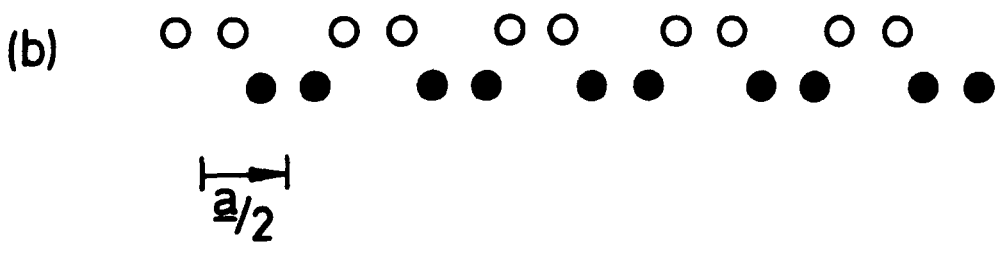
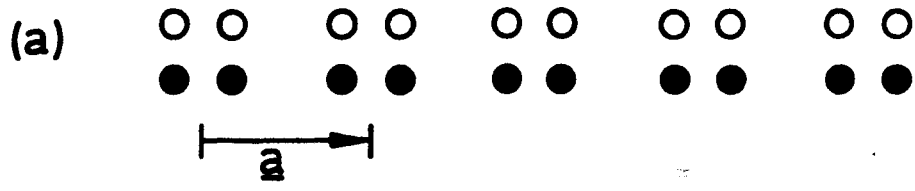
An implication of the periodic variation of the spatial symmetry of dichromatic complexes and bicrystals is the possibility of displacements for which rotation axes and/or mirror planes of the original composite become screw axes and/or glide mirror planes (or vice versus). Consider, for example, figure 6.3.1. An infinitely small displacement of the black component away from the reference position destroys the mirror plane  $m'_y$  present originally in the composite. Thus, all the composites corresponding to displacements  $\underline{t} \neq 0$  do not possess this mirror plane. The displacement  $\underline{t} = \underline{a}/2$ , however, brings the white and black components in a glide-reflection relationship (figure 6.3.1b). Such displacements correspond, usually, to vectors with end-points lying midway two lattice points of the DSC lattice.

The periodicity of the spatial symmetry variation, therefore, implies that there are displacements resulting in spatial symmetry groups which have the same point symmetry but where some (if not all) of the translation-free rotation axes or mirror planes have been changed to screw axes or glide mirror planes (or vice versus). Displacements with this property or displacements which conserve the composite will be called 'special displacements' while the remaining are designated 'general displacements'.

Special displacements correspond to dichromatic complexes or bicrystals whose symmetry is uniquely determined by the displacement vector. Any infinitely small deviation away from the special position results in a change in the symmetry of the composite. The displacement of the black component does not alter the configuration of either the black or the white component but it changes their relative position only. There-

Figure 6.3.1

- (a) It shows an composite with one-dimensional periodicity; the unit translation is indicated by the vector  $\underline{a}$ . Open and filled circles represent points of the white and black (one-dimensional) components respectively. The composite exhibits a symmetry  $\rho_{mm}2'$ .
- (b) The composite obtained by displacing the black component by  $\underline{t}=\underline{a}/2$ . The symmetry of this composite is  $\rho_{ma}2'$ . The axes of the orthogonal coordinate system are: x-axis along the translation axis, y-axis on the plane of the paper and z-axis out of the page.



fore, only colour-reversing axes and/or mirror planes can be transformed to their associated translation-coupled counterparts (or vice versus) by a special displacement.

General displacements, on the other hand, are associated with dichromatic complexes or bicrystals whose symmetry remains unchanged over wide limits of displacement. Examples of general displacements are the vectors  $0 < t < a/2$  in figure 6.3.1.

Both general and special displacements change the spatial and/or point symmetry of the dichromatic complex or of the bicrystal. The variation of the point symmetry has been investigated in section 6.1; it remains, therefore, to give the procedure for the determination of the spatial symmetry variation. The method is based on the fact that a displacement can never modify the periodicity of the dichromatic complex or bicrystal. This means that the spatial symmetry group of the composite with  $t \neq 0$  must be a subgroup<sup>2</sup> of that corresponding to  $t=0$ ; but the two groups must have the same translations.

#### 6.3.4 Determination of the spatial groups for general displacements

The spatial symmetry of a composite obtained by a general displacement is described by a group which exhibits:

- (a) point symmetry which is a subgroup of the original composite (section 6.1), and,
- (b) the same translational symmetry as the original composite.

General displacements correspond, therefore, to spatial subgroups in which the descent in symmetry has only affected the rotations and reflections but not the accompanying translations in the unit cell. Hermann (1929b) designated such groups 'zellengleichen subgroups' (an analysis of Hermann's approach is given in appendix 11 since no full

exposition in the English language exists).

### 6.3.5 Determination of the spatial groups for special displacements

The spatial symmetry obtained by a special displacement corresponds to a spatial group which:

- (a) has a point group belonging to the same class as a subgroup (including the trivial ones) of the reference composite,
- (b) has the same set of translation vectors as the reference composite, and,
- (c) may contain translation-coupled symmetry elements corresponding to translation-free elements in the original composite (or vice versus).

Consequently, special displacements correspond to spatial subgroups where the translations and not the types of symmetry are affected. These subgroups are the 'klassengleichen subgroups' in Hermann's (1929b) terminology<sup>3</sup>.

As was mentioned above special displacements correspond to vectors connecting the origin to 'special' points in the unit cell of the DSC lattice. Such 'special' points are usually the vertices, centres of faces or edges and points lying midway between them. The following rules facilitate the determination of the special displacements:

Rule 6.3.1: The special displacements follow the rules of symmetry element conservation given in section 6.1.

Rule 6.3.2: A special displacement creates a translation-coupled symmetry operation from a translation-free one (or vice versus). The latter is present in the initial composite but is not conserved by the



particular displacement. Moreover, it is always a colour-reversing operation.

Rule 6.3.3: From all the operations of the initial composite which may create a translation-coupled/translation-free symmetry element only those which are compatible with the special displacement form such an element.

For example, if the original composite contains a 4-fold colour-reversing axis and the special displacement is equal to the half-period along the axis direction, then a  $4_2$  axis can be created but not a  $4_1$  or a  $4_3$  one.

- - -

Footnotes 1: It is possible that such displacements recreate the original composite in a new position, but this is not important as far as its symmetry is concerned.

2: A subgroup of a given spatial group is a group of lower symmetry obtained by the removal of certain symmetry operations from the given spatial group (see appendix 11).

3: This does not include the special displacements for which the original composite is reformed. The spatial group of these composites is, obviously, identical to that of the original composite, or, according to Hermann's (1929b) approach it is the trivial zellen-gleiche subgroup. The vectors of such displacements, however, 'end' outside the Wigner-Seitz cell of the DSC lattice.

#### 6.4 Example of spatial symmetry variation

In this section the procedure for studying the spatial symmetry variation of dichromatic complexes<sup>1</sup> is demonstrated by giving an example. For this the dichromatic pattern formed by two f.c.c. lattices rotated

relative to each another by  $[001]/36.9^\circ$  ( $\Sigma=5$ ) is used as an illustration. The space group of this holosymmetric dichromatic pattern is  $I4/m'm'$  (figure 5.2.2c).

The point symmetry variation has already been considered in section 6.2 and, hence, table 6.2.4 gives the general displacements and the point groups of the associated patterns.

As far as the space groups of the dichromatic patterns associated to general displacements are concerned they can be found by applying the principles outlined in section 6.3. For this the list of the zellengleichen subgroups of the space group  $I4/m'm'$  (table A11.1) is considered. For each of the general displacements the point symmetry of the obtained pattern is given in table 6.2.4; the corresponding space group is then the one in table A11.1 which belongs to the particular symmetry class. For example consider the dichromatic pattern obtained by a displacement  $\underline{t}=(0,0,z)$ ; its point group is  $42'2'$ . Referring to table A11.1 it is seen that the zellengleiche subgroup of the class  $42'2'$  is  $I42'2'$ ; this is the space group of the dichromatic pattern with  $\underline{t}=(0,0,z)$ .

When this procedure is applied regard must be given for the cases where the point group adopts more than one crystallographically non-equivalent orientation in the point group of the original pattern. In this case different zellengleichen subgroups might correspond to the non-equivalent subgroups. The ambiguity can be resolved by considering which symmetry operations of the original pattern are conserved by the particular general displacement. Thus, it is possible to establish the point subgroups corresponding to these dichromatic patterns and thus the appropriate zellengleichen subgroups are determined.

Let, for example, the dichromatic patterns obtained by  $\underline{t}=(x,0,0)$

and  $\underline{t}=(x,x,0)$ . It is shown in section 6.2 that a displacement of the form  $\underline{t}=(x,0,0)$  conserves the subgroup  $m'm2'=\{1, 2_y^{1'}, s_z, s_x'\}$  and according to the table A11.1 the respective space group is  $Im'm2'$ . If the displacement  $\underline{t}=(x,x,0)$  is, however, considered the conserved symmetry operations form the subgroup  $m'm2'=\{1, 2_p^{1'}, s_z, s_x'\}$  and, hence, the space group of the dichromatic pattern with  $\underline{t}=(x,x,0)$  is  $Fm'm2'$ . In a similar manner the space symmetry of the dichromatic patterns for the other general displacements is determined.

The special displacements can be found by applying the rules given in section 6.3. Thus, the displacement  $\underline{t}=(\frac{1}{2},0,0)$ , for example, conserves the subgroup  $m'2'_m=\{1, s_z, s_x', 2_y^{1'}\}$  while destroying the rest of the symmetry operations in the initial pattern, i.e. the operations of the set  $4_z^1, 2_z^1, 4_z^3, 2_x^1, 2_\alpha^1, 2_\beta^1, i, \bar{4}_z^1, \bar{4}_z^3, s_y', s_\alpha', s_\beta'$ . In this set only the elements  $2_x^1$  and  $s_y'$  satisfy the conditions given in section 6.3 and, hence, a displacement of the black component by  $\underline{t}=(\frac{1}{2},0,0)$  creates a glide-mirror plane normal to the y-axis and a 2-fold screw axis along the x-direction.

In order to determine the special displacements it is necessary to determine, first of all, the possible space groups associated with such displacements. These are klassengleichen subgroups of either the space group of the dichromatic pattern with  $\underline{t}=\underline{0}$ , or of a zellengleiche subgroup of it. Moreover, these klassengleichen subgroups must have translational vectors identical to that of the original dichromatic pattern; these groups are listed in the first coloumn of table 6.4.1. In fact, this table gives the klassengleichen subgroups of the (classical) space group  $I4/mmm$  instead of the two-coloured  $I4/mm'm'$ . This is because the procedure for the determination of the klassengleichen

TABLE 6.4.1

Klassengleichen subgroups of  $I4/m\bar{m}m$  which correspond to special displacements for the  $\Sigma=5$  dichromatic pattern formed by two f.c.c. lattices

Space group	Comments
$I4/m\bar{c}m$	
$I4_1/amd$	$4_1$ and a-plane are ordinary elements
$I4_1/acd$	$4_1$ and a-plane are ordinary elements
$I4_1/22$	$4_1$ is an ordinary element
$I422$	zellengleiche subgroup
$I4_1/cd$	$4_1$ is an ordinary element
$I4_1/md$	$4_1$ is an ordinary element
$I4cm$	
$I4mm$	zellengleiche subgroup
$I\bar{4}2d$	$\bar{4}$ is an ordinary axis
$I\bar{4}2m$	zellengleiche subgroup
$I\bar{4}c2$	$\bar{4}$ is an ordinary element
$I\bar{4}m2$	zellengleiche subgroup
$I4_1/a$	$4_1$ and a-plane are ordinary elements
$I4/m$	zellengleiche subgroup
$I4_1$	$4_1$ is an ordinary axis
$I4$	zellengleiche subgroup
$I\bar{4}$	zellengleiche subgroup
$Imma$	
$Ibca$	$m_z$ is an ordinary mirror plane
$Ibam$	b- and a-plane are normal to the x- and y-axis respectively and there is no displacement creating simultaneously the a- and b-planes
$Immm$	zellengleiche subgroup
$Fmmm$	zellengleiche subgroup
$I2_1^2 2_1^2 2_1^2$	$2_2$ axis is an ordinary element
$I222$	zellengleiche subgroup
$F222$	zellengleiche subgroup
$Ima2$	
$Iba2_1$	see the comment for $Ibam$
$Imm2$	zellengleiche subgroup
$Fdd2$	there is no displacement creating simultaneously the two d-planes
$Fmm2$	zellengleiche subgroup

subgroups is fairly complicated and the only available listing of such subgroups (Boyle & Lawrenson, 1972b) deals with the classical space groups.

Some of the groups given in table 6.4.1 must be excluded from further considerations because, as it was mentioned in section 6.3, the only symmetry operations present to the initial pattern which can be changed to translation-coupled/translation-free are the colour-reversing operations. Thus, since the initial point group contains an ordinary 4-fold axis klassengleichen subgroups containing  $4_1$ ,  $\bar{4}$  or  $2_1$  axes (the latter if it is parallel to the 4-fold axis) must be excluded. Similar considerations (see table 6.4.1) for the remaining subgroups indicate that the only subgroups which must be taken into account are the  $I4/mc'm'$ ,  $I4c'm'$ ,  $Imm'a'$  and  $Ima'2'$ . But,  $I4c'm'$  and  $Ima'2'$  are zellengleichen subgroups of the space groups  $I4/mc'm'$  and  $Imm'a'$  respectively. Therefore, special displacements give patterns with space groups  $I4/mc'm'$  or  $Imm'a'$  (this is further examined below).

The next step in the procedure is the determination of the special displacements. This is based on the rule given by Pond & Bollmann (1979) (see also section 7.3) concerning the conservation of symmetry of dichromatic patterns (and bicrystals). According to them the variation of the symmetry obeys the following conservation rule: "the product  $n_j r_j$  is invariant with relative displacement, where  $n_j$  is the order of the point symmetry for the pattern created by a given relative displacement away from the holosymmetric pattern and  $r_j$  is the number of crystallographically equivalent patterns obtained by symmetry related displacements". According to this rule, the rank of a special displacement is equal to  $n_h/n_k$  where  $n_h$  and  $n_k$  are the orders of the point groups of the dichro-

matic patterns before and after displacement respectively.

For example, the rank of the displacement leading to a dichromatic pattern with symmetry  $I4/mc'm'$  ( $n_k=16$ ) must be equal to 1 since  $n_h=16$ . Inspection of the holosymmetric dichromatic pattern shows that the only displacement with rank 1 is the  $\underline{t}=(0,0,\frac{1}{2})$  (or its translation-equivalent  $\underline{t}=(\frac{1}{2},\frac{1}{2},0)$ ). This means that a dichromatic pattern with symmetry  $I4/mc'm'$  is formed by the special displacement  $\underline{t}=(\frac{1}{2},\frac{1}{2},0)$ . Similarly, the rank of the displacement leading to a dichromatic pattern with symmetry  $Imm'a'$  is equal to  $n_h/n_k=16/8=2$  and the special displacement associated with this group is  $(\frac{1}{2},0,0)$ .

The above rule enables, additionally, to decide whether a particular klassengleichen subgroup corresponds to a special displacement or not. This is the case for the group  $I4c'm'$  which as mentioned above must be excluded. If a special displacement creates a dichromatic pattern with space symmetry  $I4c'm'$  then its rank has to be equal to 2. But the only displacement of rank 2 is the  $\underline{t}=(\frac{1}{2},0,0)$  and it can not correspond to the above group since it does not conserve the 4-fold axis.

Table 6.4.2 summarizes the variation of the space symmetry of the  $Z=5$  dichromatic pattern formed by two f.c.c. lattices.

- - -

Footnote 1: The procedure for bicrystals is identical.

TABLE 6.4.2

Spatial symmetry variation of the dichromatic pattern  
 $\Sigma=5$  formed by two f.c.c. lattices

Fractional coordinates of displacements	Rank	Point group	Space group
000	1	4/mn'm'	I4/mn'm'
$\frac{1}{2}\frac{1}{2}0$	1	4/mn'm'	I4/mc'm'
$\frac{1}{2}00$ $0\frac{1}{2}0$	2	mn'm'	Imm'a'
00z $00\bar{z}$	2	42'2'	I42'2'
x00 $0x0$ $\bar{x}00$ $0\bar{x}0$	4	m'm2'	Im'm2'
xx0 $\bar{x}x0$ $x\bar{x}0$ $\bar{x}\bar{x}0$	4	m'm2'	Fm'm2'
x0z $0xz$ $\bar{x}0z$ $0\bar{x}z$ $x0\bar{z}$ $0x\bar{z}$ $\bar{x}0\bar{z}$ $0\bar{x}\bar{z}$	8	2'	C2'
xxz $\bar{x}xz$ $\bar{x}xz$ $\bar{x}\bar{x}z$ $xx\bar{z}$ $\bar{x}\bar{x}\bar{z}$ $\bar{x}xz$ $\bar{x}\bar{x}z$	8	2'	C2'
xy0 $yx0$ $\bar{x}\bar{y}0$ $y\bar{x}0$ $\bar{x}\bar{y}0$ $\bar{y}\bar{x}0$ $\bar{x}y0$ $\bar{y}x0$	8	m	Cm
xyz $\bar{x}yz$ $\bar{x}\bar{y}z$ $\bar{x}\bar{y}z$ $yxz$ $\bar{y}xz$ $\bar{y}\bar{x}z$ $\bar{y}\bar{x}z$ $xy\bar{z}$ $\bar{x}y\bar{z}$ $\bar{x}y\bar{z}$ $\bar{x}y\bar{z}$ $yx\bar{z}$ $\bar{y}x\bar{z}$ $\bar{y}x\bar{z}$ $\bar{y}x\bar{z}$	16	1	P1

## Chapter 7

### GENERAL RELATIONS OF DICHROMATIC SYMMETRY AND BICRYSTAL SYMMETRY

#### Introduction

The symmetry of a bicrystal depends on: (a) the misorientation and the translational position of its components (see chapters 3-6), and, (b) the orientation of the interface. The effect of the latter on the interfacial symmetry can be understood in terms of the procedure used for manufacturing a bicrystal (see section 3.1). The selection of the boundary plane and the location of the appropriate motifs (atom complexes) on each side of this plane imply that some of the symmetry elements present in the respective dichromatic complex may be eliminated. Such changes in the symmetry are considered in this chapter.

In section 7.1 a procedure is given for the determination of the point and/or spatial symmetry of all possible bicrystals manufactured from a given dichromatic complex. The procedure is, subsequently, applied in section 7.2 for deriving some geometrical features of the interfacial symmetry.

An important conclusion reached by employing the above method is that sets of bicrystals with boundary planes related by the symmetry of the corresponding dichromatic complex have symmetry related (i.e. energetically degenerate) structures. This is similar to the occurrence of equivalent dichromatic complexes or bicrystals (Pond & Bollmann, 1979). As it is explained in section 7.3 these cases can be described in terms of group-theoretical considerations.

#### 7.1 Bicrystal symmetry for a given misorientation

The determination of the (point and/or spatial) bicrystal symmetry is based on the fact that it corresponds to a section of the (point and/or



spatial) symmetry group of the dichromatic complex taken in the boundary position. This section must be taken through the group (point and/or spatial) of the respective dichromatic complex in a position corresponding to that of the boundary plane in both orientation and translation.

In taking this section only those symmetry elements which transform the geometrical section into itself are retained. These include (as has been mentioned in section 5.3):

- (1) perpendicular to the plane: non-translation-coupled ordinary elements (the only exception being the colour-reversing rotoinversion axes),
- (2) parallel to the plane: only two-fold colour-reversing elements, and,
- (3) inclined to the plane: no elements.

The set of symmetry elements in the section is a group by virtue of the restrictions placed upon the selection of its elements. Thus, no product of elements in the set can be unrelated to the plane, and, all elements related to the plane, in the dichromatic group, were included in the sectional set. In addition, symmetry elements were removed, but not added, in taking the section of the dichromatic group. Hence, the set of symmetry elements in the section is a subgroup of the dichromatic group.

#### 7.1.1 Determination of the point symmetry

The determination of the bicrystal point groups for a given dichromatic complex is based on the subgroup relation just mentioned; the point group of the section (bicrystal point group) is a subgroup of the dichromatic point group. Consequently, the procedure for finding the bicrystal point group is as follows.

First of all, the subgroups<sup>1</sup> of the dichromatic point group are determined (subgroup tables of the two-coloured point groups have been published by Ascher & Lammer, 1965). However, not all of these subgroups correspond to bicrystal symmetry. This is so because of the restrictions imposed on the symmetry elements of a bicrystal (see section 5.3). Therefore, using table 5.3.1, the subgroups which are not permissible bicrystal groups must be rejected. For each of the remaining subgroups a boundary plane can be established in order to have colour-reversing symmetry elements on this plane and ordinary symmetry elements perpendicular to the plane (except for colour-reversing rotoinversion axes; see above). This is, in fact, equivalent to the requirement of plane invariance as it has been discussed in section 5.3.

After the elimination of the non-permissible subgroups, it is advisable to consider the subgroup list in a sequence of decreasing group order. The reason for this is that for a given orientation of the boundary plane some lower order subgroups will give different bicrystal symmetry than higher order subgroups. This is because the boundary plane does not separate elements of symmetry arbitrarily, but only by considering the defining plane. The lower order bicrystal class would correspond to either the same or to a different translational position of the interface in the dichromatic complex. In the former case the lower symmetry group is a subgroup of the section group of the dichromatic group. As was explained in sections 6.1 and 6.3, however, the higher symmetry subgroup corresponds to the holosymmetric bicrystal (for the given translational position of the components) from which the remaining bicrystal symmetries for the given boundary plane orientation can be determined by the method presented in chapter 6.

An example will serve to outline the matter of derivation of the bicrystal point symmetry. Consider the dichromatic pattern formed by two f.c.c. lattices and corresponding to the  $\Sigma=5$ ,  $[001]/36.9^\circ$  misorientation relationship (figure 5.2.2c); the space group of this pattern is  $I4/m'm'$ . In table 7.1.1 the investigation of the point symmetry of bicrystals associated with this dichromatic pattern is given. The first column in this table lists the subgroups of the point group  $4/m'm'$  according to the tables by Ascher & Lammer (1965). The second and third columns give the number and the elements of symmetry equivalent groups corresponding to each subgroup in the first column. The next column gives the boundary plane for each of the subgroups which are permissible bicrystal classes. The next, fifth, column is reserved for comments.

It is seen from table 7.1.1 that for a boundary plane parallel to  $(001)_c$ , say, bicrystals with point symmetries  $42'2'$ ,  $4$ ,  $22'2'$  can be created. It is evident that since  $22'2'$  is a subgroup of the  $42'2'$  containing the same symmetry elements perpendicular to the section plane these two groups correspond to the same location of the interface but to different relative displacements of the components (see below). On the other hand, the bicrystal with point symmetry  $4$  is obtained when the interface plane does not pass through the origin. This is, however, explained in a more comprehensive way in terms of the sectional plane.

### 7.1.2 Sectional-plane method

As was already mentioned the symmetry elements conserved after locating the boundary plane form a group. For  $n$ -dimensional periodic dichromatic complexes ( $n \leq 3$ ) this group is an infinite group of an  $m$ -dimensional periodic discontinuum (where  $m=0,1,2$ ), and is designated a 'sectional group' (Holser, 1958a). The possible sectional groups

TABLE 7.1.1

Holosymmetric bicrystal symmetry based on the  $\Sigma=5$  dichromatic pattern formed by two f.c.c. lattices

Subgroup	No of sym. equivalent groups(+)	Symmetry elements in the subgroup (+)	Boundary plane(++)	Comments
$4/mm'm'$	1	$1, 4_z^1, 4_z^3, 2_z^1, 2_x^1, 2_y^1, 2_\alpha^1, 2_\beta^1$ $i, 4_z^1, 4_z^3, s_z, s_x', s_y', s_\alpha', s_\beta'$		(*)
$\bar{4}2'm'$	1	$1, 4_z^1, 4_z^3, 2_z^1, 2_x^1, 2_y^1, s_\alpha', s_\beta'$		(*)
$\bar{4}2'm'$	1	$1, 4_z^1, 4_z^3, 2_z^1, 2_\alpha^1, 2_\beta^1, s_x', s_y'$		(*)
$4m'm'$	1	$1, 4_z^1, 4_z^3, 2_z^1, s_x', s_y', s_\alpha', s_\beta'$		(*)
$42'2'$	1	$1, 4_z^1, 4_z^3, 2_z^1, 2_x^1, 2_y^1, 2_\alpha^1, 2_\beta^1$	$(001)_c$	
$4/m$	1	$1, 4_z^1, 4_z^3, 2_z^1, i, 4_z^1, 4_z^3, s_z$		(*)
4	1	$1, 4_z^1, 4_z^3, 2_z^1$	$(001)_c$	
$m'm'm$	1	$1, 2_z^1, 2_x^1, 2_y^1, i, s_z, s_x', s_y'$		(*)
$m'm'm$	1	$1, 2_z^1, 2_\alpha^1, 2_\beta^1, i, s_z, s_\alpha', s_\beta'$		(*)
$m'm2'$	2	$1, s_z, s_y', 2_x^1$	$(100)_c$	
		$1, s_z, s_x', 2_y^1$	$(010)_c$	
$m'm2'$	2	$1, s_z, s_\beta', 2_\alpha^1$	$(110)_c$	
		$1, s_z, s_\alpha', 2_\beta^1$	$(\bar{1}10)_c$	
$2'/m'$	2	$1, 2_x^1, i, s_x'$		(*)
		$1, 2_y^1, i, s_y'$		(*)
$2'/m'$	2	$1, 2_\alpha^1, i, s_\alpha'$		(*)
		$1, 2_\beta^1, i, s_\beta'$		(*)
$2/m$	1	$1, 2_z^1, i, s_z'$		(*)

TABLE 7.1.1-continued

Subgroup	No of sym. equivalent groups(+)	Symmetry elements in the subgroup (+)	Boundary plane(++)	Comments
$m'm'2$	1	$1, 2_z^1, s'_x, s'_y$		(*)
$m'm'2$	1	$1, 2_z^1, s'_\alpha, s'_\beta$		(*)
$22'2'$	1	$1, 2_z^1, 2_x^{1'}, 2_y^{1'}$	$(001)_c$	
$22'2'$	1	$1, 2_z^1, 2_\alpha^{1'}, 2_\beta^{1'}$	$(001)_c$	
$\bar{1}$	1	$1, i$		(*)
$m'$	2	$1, s'_x$	$(100)_c$	
		$1, s'_y$	$(010)_c$	
$m'$	2	$1, s'_\alpha$	$(\bar{1}10)_c$	
		$1, s'_\beta$	$(110)_c$	
$2'$	2	$1, 2_x^{1'}$	$(0k1)_c$	
		$1, 2_y^{1'}$	$(h01)_c$	
$2'$	2	$1, 2_\alpha^{1'}$	$(hhl)_c$	
		$1, 2_\beta^{1'}$	$(\bar{h}hl)_c$	
$m$	1	$1, s_z$	$(hk0)_c$	
$2$	1	$1, 2_z^1$	$(001)_c$	
$1$	1	$1$	$(hkl)_c$	

(+) When considering the subgroups of the black-white point group, it is advisable to distinguish not only the crystallographically non-equivalent groups but also the different orientations that may occur with respect to the given group

(++) Referred to the CSL coordinate system

(\*) Non-permissible bicrystal point group

depend on the dichromatic complex group, the orientation of the plane and its location. The procedure for the determination of the sectional groups as well as their use in the study of the bicrystal symmetry are demonstrated by the following example.

Consider the above mentioned dichromatic pattern with symmetry  $I4/m\bar{m}'m'$ . The planes of possible interest have directions of say  $(001)_c$ ,  $(010)_c$ ,  $(100)_c$ ,  $(110)_c$ ,  $(101)_c$ ,  $(011)_c$  and so on. However, for a given plane orientation, say  $(001)_c$ , only certain locations give distinct sectional groups. Thus, at the edge of the unit cell of the dichromatic pattern the sectional plane  $(001)_c$  contains the symmetry  $p42'2'$ , where the first part of the symbol indicates the lattice type, the second part, 4, indicates the symmetry in a direction normal to the plane, the third and fourth parts indicate the symmetry in two directions (in this case the x- and y-axes) lying in  $(001)_c$ . At  $z=a/2$  the plane  $(001)_c$  has the same symmetry as just described for  $(001)_c$ . On the other hand, at  $z=a/4$  or  $z=3a/4$  it has symmetry  $p42'_12$ . All other planes in this orientation do not intersect any symmetry elements except the ordinary 4-fold axis and thus these planes have symmetry  $p4$ . The sectional groups for various orientations and positions in the space group  $I4/m\bar{m}'m'$  are listed in table 7.1.2.

Symmetry elements are lost as one moves from special to more general sectional orientations, as in the sequence  $(001)_c$ ,  $(011)_c$ , etc.; this is particularly true in space groups of low symmetry. The special positions of the sectional plane in the space group lie in not more than four elevations for a given orientation of the section; in many cases the 0 and  $\frac{1}{2}$  elevations as well as the  $\frac{1}{4}$  and  $\frac{3}{4}$  elevations are equivalent pairs. Any other elevation is general and can contain only a few

TABLE 7.1.2

Sectional plane groups in the space group  $I4/m'm'$

Location* Direction+	$0, \frac{1}{2}$	$\frac{1}{4}, \frac{3}{4}$	others
$(001)_c$	$p42'2'$	$p42'_12'$	$p4$
$(010)_c$	$pmm'2'$	$pmm'2'$	$pm$
$(100)_c$	$pmm'2'$	$pmm'2'$	$pm$
$(110)_c$	$pmm'2'$	$pmm'2'$	$pm$
$(\bar{1}10)_c$	$pmm'2'$	$pmm'2'$	$pm$
$(011)_c$	$c2'$	$p1$	$p1$
$(101)_c$	$c2'$	$p1$	$p1$
$(0k1)_c$	$p2'$	$p1$	$p1$
$(h01)_c$	$p2'$	$p1$	$p1$
$(hh1)_c$	$p2'$	$p1$	$p1$
$(\bar{h}h1)_c$	$p2'$	$p1$	$p1$
$(h01)_c$	$p2$	$p1$	$p1$
$(0k1)_c$	$p2$	$p1$	$p1$
$(hk0)_c$	$pm$	$p1$	$p1$
$(hkl)_c$	$p1$	$p1$	$p1$

\* Location is given in terms of fractional distance between the planes with listed indices (origin at  $mm'm'$  intersection)

+ The subscript denotes that the directions refer to the CSL coordinate system

particular symmetry elements. This explains why, in cases where a particular interface orientation corresponds to more than one group having common elements perpendicular to the sectional plane, the one with the highest symmetry must be considered.

The above considerations fully determine the symmetry of bicrystals created from the  $Z=5$ ,  $[001]_1/36.9^\circ$  dichromatic pattern formed by two f.c.c. lattices (table 7.1.3). The results in this table are in complete agreement with the table given by Pond & Bollmann (1979). The terms in the last column are explained in the next section.

- - -

Footnotes 1: This includes the crystallographically equivalent, as well as the trivial, subgroups.

2: The subscript means that the coordinate system of the CSL unit is used.

## 7.2 Characteristic features of bicrystals

The discussion in 7.1 indicates that the use of the sectional group concept provides the most comprehensive method for studying bicrystal symmetry for a given dichromatic complex. The spatial symmetry of a bicrystal can, in most cases, be predicted without relying on the sectional plane provided that the boundary plane and the associated bicrystal point group are known. This method, although not very useful for a general study of the bicrystal symmetry, can be used for demonstrating a very important feature of the interfacial symmetry.

### 7.2.1 Rigid and non-rigid interfaces

The translational symmetry of a bicrystal is restricted by the orientation of the interface and for a dichromatic complex exhibiting  $n$ -dimensional periodicity the interface must contain  $m \leq n - 1$  non-parallel translation axes. Hence, in the case of bicrystals manufactured from one-dimensional dichromatic complexes there will be no translational symmetry in the bicrystal unless the interface contains the periodicity



**TABLE 7.1.3**

Holosymmetric bicrystal symmetry based on the  $\Sigma=5$  dichromatic pattern with  $\underline{t}=0$  (the component lattices are f.c.c.; plane indices refer to the coordinate system of the CSL)

Interface plane	Rank	Layer group of holosymmetric bicrystal	Order	Interface category
$(001)_c$	1	$p42_1'2'$	8	rigid
$(100)_c$ $(010)_c$	2	$pmm'2'$	4	rigid
$(110)_c$ $(\bar{1}\bar{1}0)_c$	2	$pmm'2'$	4	rigid
$(hk0)_c$ $(\bar{h}\bar{k}0)_c$ $(kh0)_c$ $(k\bar{h}0)_c$	4	$pm11$	2	non-rigid
$(h01)_c$ $(h0\bar{1})_c$ $(0h1)_c$ $(0h\bar{1})_c$	4	$p12'1$	2	non-rigid
$(hh1)_c$ $(\bar{h}\bar{h}1)_c$ $(hh\bar{1})_c$ $(\bar{h}\bar{h}\bar{1})_c$	4	$p12'1$	2	non-rigid
$(hk1)_c$ $(\bar{h}\bar{k}1)_c$ $(\bar{h}\bar{k}1)_c$ $(hk1)_c$ $(\bar{k}h1)_c$ $(k\bar{h}1)_c$ $(kh1)_c$ $(\bar{k}\bar{h}1)_c$	8	$p1$	1	non-rigid

axis. For bicrystals manufactured from CSL based dichromatic complexes crystallographic planes must contain two non-parallel translation axes.

For three-dimensional dichromatic complexes, therefore, if the subgroup implies that the interface is a rational plane<sup>2</sup> then the translational symmetry of the bicrystal is two-dimensional. For example, the subgroup  $pmm'2'$  in the above mentioned case restricts the interface to be parallel to the  $(010)_c$  plane. Therefore, the associated bicrystal exhibits a two-dimensional periodicity. On the other hand, if the subgroup necessitates the definition of a crystallographic direction, or when the dichromatic complex has one-dimensional periodicity, a one-dimensional periodic bicrystal could be created (the axis of translation is, in this case, the defined crystallographic direction). Hence, the interfaces can be divided into the following two categories.

The first category comprises the interfaces whose planes are uniquely determined by the bicrystal group. Boundary planes perpendicular to a well-defined orientation, say  $(001)_c$  or  $(120)_c$ , are characteristic of such interfaces. The second category comprises those interfaces with planes being not uniquely determined by the bicrystal group. An example of this category is an interface required by the bicrystal symmetry to contain a given crystallographic direction  $[hkl]$ . In this case the interface is any plane in the zone of  $[hkl]$ .

If the orientation of the interface in the dichromatic complex is given by three (two) crystallographic directions, then the interface will belong to the first category. These interfaces will be arbitrarily called 'rigid' since when the plane is rotated by an arbitrarily small angle about any direction the symmetry of the bicrystal changes. If the orientation of the interface is given by a single direction in the dichromatic pattern or in the general case is not connected with any

direction (bicrystal groups 1 and  $\bar{1}$ ') then rotation about a given direction by an arbitrarily small angle does not change the bicrystal symmetry. Such interfaces belong to the second category and will be called 'non-rigid'. Thus, in table 7.1.3 the designation non-rigid for an interface means that the boundary can have lower translational (but the same point symmetry) if the boundary plane is irrational. In contrast, for the rigid interfaces both the periodicity and point symmetry are changed simultaneously.

### 7.2.2 Parity-related interfaces

The most important conclusion reached by investigating the bicrystal symmetry in terms of the sectional plane is, perhaps, the discovery that bicrystals with degenerate structures due to the appropriate orientation of the interface can exist.

Let, for example, the case of the  $\Sigma=5$  f.c.c./f.c.c dichromatic pattern considered in section 7.1. It can be seen from table 7.1.2 that for  $(100)_c$  and  $(010)_c$  the sectional groups are identical ( $pmm'2'$ ). Furthermore, it is possible to show that the two sectional planes as well as the bicrystals with interfaces  $(100)_c$  and  $(010)_c$  are related by the point symmetry of the dichromatic pattern (see figure 7.3.1). This means that the rank<sup>3</sup>,  $r$ , of the sectional group  $pmm'2'$  is equal to 2, and since the order,  $n$ , of the sectional point group is equal to 4,  $n.r=8$ . The same is true for any other sectional group. Consider the set of planes  $(h0l)_c$ ,  $(0kl)_c$ ,  $(\bar{h}0l)_c$  and  $(0\bar{k}l)_c$ . These planes correspond to the sectional group  $p2$  and hence this group has rank  $r=4$  and its order is  $n=2$ , i.e. again  $n.r=8$ .

Consequently, the symmetry of the sectional plane (or equivalently of the bicrystal) changes according to the conservation rule:  $n_i r_i = n_j r_j$ .

This is investigated in detail in section 7.3. Here it is sufficient to notice that whenever a dichromatic pattern contains point symmetry higher than 1 there exists a set of bicrystals, obtained by a proper choice of the boundary plane, which are related by the symmetry of the associated dichromatic complex. Bicrystals with this property will be called 'parity-related bicrystals'; their existence is due to the symmetry of the dichromatic complex and the restrictions imposed upon the symmetry elements of the bicrystal.

- - -

Footnotes 1: The equality does not hold for  $n=3$ .

2: Expressed relative to the coordinate system of the CSL unit cell.

3: Rank is the number of crystallographically equivalent groups (in this case of the sectional groups).

### 7.3 Group-theoretical considerations concerning equivalent dichromatic complexes and energetically degenerate bicrystals

As was mentioned in section 7.2 the occurrence of parity-related bicrystals can be formulated in group-theoretical terms. Here, this is further examined and it is shown that not only the formation of parity-related bicrystals but also that of the equivalent dichromatic complexes as well as equivalent bicrystals can be expressed by these principles.

#### 7.3.1 Originating configurations and variant sets

The set of the equivalent dichromatic complexes or equivalent bicrystals or parity-related bicrystals will be termed the set of variants and its elements simply variants. In all these cases there exists an initial configuration generating the variants. This configuration will be called the 'reference' or 'originating' configuration.

The following notations will be introduced: the point group of the reference configuration will be represented by  $G$ , of order  $p$  with elements  $g_i$ . It has been shown that the process of creating a variant is accompanied by a decrease in symmetry in such a way that the point group  $H$  of the variant of order  $q$  is a subgroup of  $G$ .

It will be assumed that (a) all the symmetry operations relating the variants are contained in the point group of the originating configuration, (b) any element of the point group of the originating configuration is to be a symmetry operation for the variant or, speaking more exactly, when  $f$  is an element of the point group of the originating configuration and  $V$  is a variable formed by operating of  $f$  on  $V'$ ,  $V$  is always to be a possible variant as  $V'$  (this second item prevents the originating configuration having superfluous symmetry elements not connected with the formation of variants and, on the other hand, defines a complete set of orientation states).

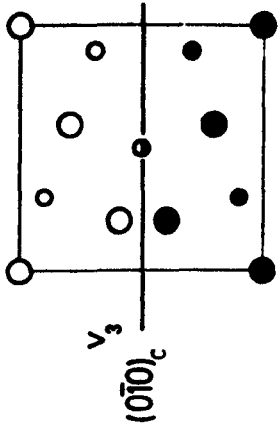
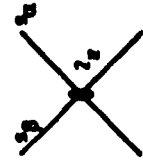
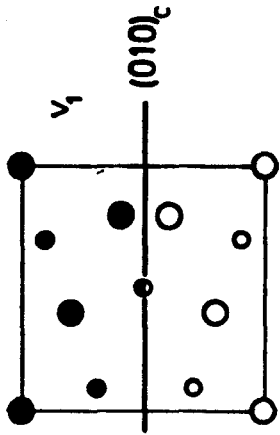
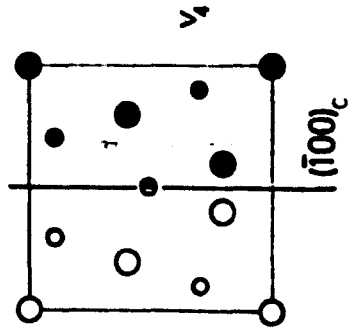
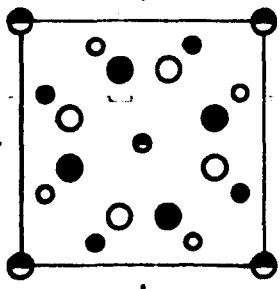
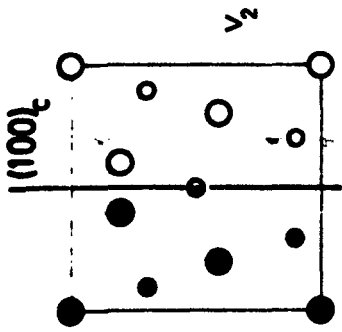
The structure of the different variants will be denoted by  $V_j$  and their point groups by  $H_j$ ; the  $H_j$  can only differ in the orientation of their elements. It is also clear that the structures as well as the point groups are related by operations of  $G$  which are not elements of  $H$ . Consider, for example, figure 7.3.1 showing the variants obtained by locating the boundary plane parallel to  $\{100\}_c$  in the dichromatic pattern  $L=5$  formed by two f.c.c. lattices. The variants  $V_1$  and  $V_2$ , on one hand, are related by the mirror  $s'_\alpha$  of the reference pattern, while the  $2_z^1$  axis, on the other hand, relates the variants  $V_1$  and  $V_3$ .

### 7.3.2 Group-theoretical approach

When  $H_i$  is a variant and  $g$  is a symmetry operation the result from the performance of  $g$  upon  $H_i$  is expressed as  $gH_i$ . The notation

Figure 7.3.1

The four variants with symmetry  $mm'2'$  obtained by locating the boundary plane parallel to  $\{100\}_c$  in the dichromatic pattern  $\Sigma=5$  formed by two f.c.c. lattices in the  $[001]/36.9^\circ$  misorientation. The insert shows the symmetry operations of the dichromatic pattern which transforms each variant to the remaining ones.



$H_i=H_j$  is to denote that a variant  $H_i$  is identical with the variant  $H_j$ .

The following theorems hold (see e.g. Aizu, 1970; Tendeloo, van & Amelinckx, 1974a,b):

**Theorem 7.3.1:** If  $H_i$  and  $H_j$  are the point groups of two variants  $V_i$  and  $V_j$ , and  $g$  is an element of the point group of the originating configuration such that it transforms  $V_i$  to  $V_j$  (i.e.  $gV_i=V_j$ ), then the set of operations transforming  $V_i$  to  $V_j$  is given by  $gV_i$  or  $V_jg$ .

**Theorem 7.3.2:** When  $H_i$  is the point group of a variant  $V_i$  and  $g$  is an operation of  $G$  relating  $V_i$  to another variant  $V_j$  the point group  $H_j$  of  $V_j$  is equal to  $gH_i g^{-1}$ , i.e. the point groups of all the variants are conjugate in  $G$ .

If for all  $g \in G$ ,  $H_i=H_j$  the subgroup  $H$  is invariant in  $G$ . This is often not the case; moreover, the configuration of the elements of  $H$  generally adopt different orientations with respect to the elements of  $G$  (as in the case of figure 7.3.1).

**Theorem 7.3.3:** The number of variants equals the order  $p$  of the point group  $G$  of the originating configuration divided by the order  $q$  of the point group  $H$  of the variant.

Symbolically this can be expressed by:

$$G = g_1 H + g_2 H + \dots + g_p H$$

In group theory this is called the resolution of  $G$  into left cosets with respect to  $H$  (see e.g. Higman, 1955). This conforms to the well-known theorem of Lagrange (Janseen, 1973), and hence the number of variants,  $n$ , is given by  $n=p/q$ . Moreover, the above relation indicates that the set of operations that generates all variants can be obtained



by taking one operation from each coset in the development of  $G$  into cosets of  $H$ .

### 7.3.3 Symmetry degenerate configurations

The example given in section 6.2 is now worked out according to the above group-theoretical considerations. This example concerns the equivalent patterns associated with the  $\Sigma=5$  dichromatic pattern formed by two f.c.c. lattices. The point group of this pattern is  $4/mm'm'$  and it contains 16 elements in ten classes:

$$\{1\}, \{2_x^{1'}, 2_y^{1'}\}, \{2_x^{1'}, 2_p^{1'}\}, \{s_x', s_y'\}, \{s_x', s_p'\}, \{4_z^1, 4_z^3\}, \\ \{\bar{4}_z^1, \bar{4}_z^3\}, \{i\}, \{s_z\}, \{2_z^1\}.$$

Let the subgroup  $H$  be  $mm'2'$ ; it contains four elements in four classes:

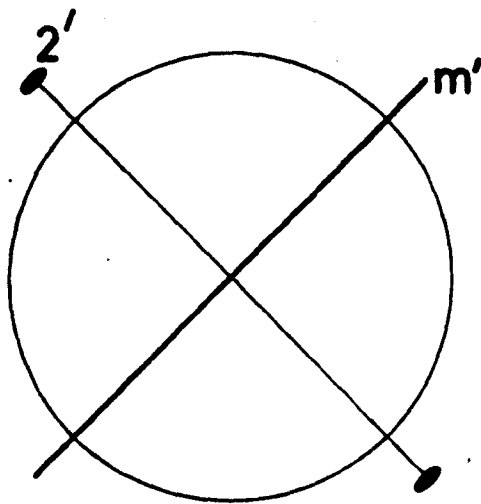
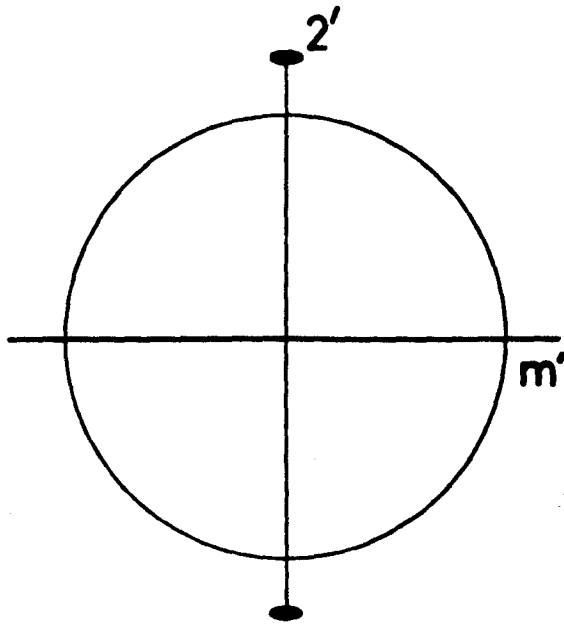
$$\{1\}, \{s_z\}, \{s_x'\}, \{2_x^{1'}\}.$$

Since  $H$  contains classes of  $G$ ,  $H$  is an invariant subgroup of  $G$  (see e.g. Higman, 1955). The group  $H$  adopt four different orientations in  $G$  differing over an angle  $45^\circ$  about the 4-fold axis; two of these orientations are not crystallographically equivalent and they are shown in figure 7.3.2. Only the first orientation is considered in detail, since the second case can be treated in exactly the same way.

The ratios of the order of the groups  $G$  and  $H$  is equal to 4 and, therefore, four equivalent dichromatic patterns with point symmetry  $mm'2'$  can be formed. It should be understood that these variants correspond to the first orientation of the point group  $mm'2'$  and that further variants might be obtained by considering the crystallographically non-equivalent orientation (see below). However, the sets of variants arising by non-equivalent subgroups are not related by symmetry elements of the originating configuration and hence each of the non-equivalent

Figure 7.3.2

Stereograms illustrating the two orientations of  $H=mm'2'$  within  $G=4/mm'm'$ . They differ by a rotation over  $45^\circ$  along the four-fold axis.



subgroups must be considered separately.

The symmetry relations between the variants of the first orientation are determined by decomposing the group  $G$  in the following manner (this is indicated explicitly in table 7.3.1):

$$G = 1.H + s'_\alpha.H + s'_\beta.H + 2^1_z.H$$

Therefore, the variants are related by the symmetry operations of the group  $m'm'2 = \{1, s'_\alpha, s'_\beta, 2^1_z\}$ . A dichromatic pattern with point symmetry  $mm'2' = \{1, s'_z, s'_x, 2^1_x\}$  is created by a displacement  $\underline{t} = (x, 0, 0)$  (see table 6.2.4), the displacements leading to the remaining dichromatic patterns can be found by operating the elements of the group  $\{1, s'_\alpha, s'_\beta, 2^1_z\}$  on the displacement  $\underline{t} = (x, 0, 0)$ . Thus, the four equivalent dichromatic patterns are associated to the displacements  $(x, 0, 0)$ ,  $(0, x, 0)$ ,  $(\bar{x}, 0, 0)$ ,  $(0, \bar{x}, 0)$ . It is easy to find that the corresponding patterns are also related by the symmetry operations of the group  $m'm'2 = \{1, s'_\alpha, s'_\beta, 2^1_z\}$ ; thus  $^1V_{x00} = 1.V_{x00} = s'_\beta.V_{0x0} = 2^1_z.V_{\bar{x}00} = s'_\alpha.V_{0\bar{x}0}$ .

Considering, now, the second orientation of the group  $mm'2'$  (figure 7.3.2) it can be seen from table 6.2.4 that a variant with this point symmetry is obtained by a displacement  $(x, x, 0)$ . In this case  $H = \{1, s'_z, s'_\beta, 2^1_x\}$  and, hence,  $G = 1.H + s'_x.H + s'_y.H + 2^1_z.H$ . Therefore, the displacements  $(x, x, 0)$ ,  $(\bar{x}, x, 0)$ ,  $(\bar{x}, \bar{x}, 0)$  and  $(x, \bar{x}, 0)$  give rise to another set of equivalent dichromatic patterns with point symmetry  $mm'2'$ . The variants of this set are related by the symmetry elements  $1, s'_x, s'_y, 2^1_z$ .

- - -

Footnote 1: The subscripts indicate the displacements associated to each variant. Thus,  $V_{x00}$  denotes the variant obtained by the displacement  $\underline{t} = (x, 0, 0)$ .

**TABLE 7.3.1**

The decomposition of  $G=4/m\bar{m}'2'$   
 into left cosets with respect  
 to  $H=mm'2'$

$\begin{array}{c} H \\ g_i \end{array}$	1	$s_z$	$s'_x$	$2^1_x$
1	1	$s_z$	$s'_x$	$2^1_x$
$s'_x$	$s'_x$	$2^1_p$	$4^1_z$	$4^3_z$
$s'_p$	$s'_p$	$2^1_\alpha$	$4^3_z$	$4^1_z$
$2^1_z$	$2^1_z$	1	$s'_y$	$2^1_y$

## Chapter 8

### CONCLUDING REMARKS CONCERNING THE INTERFACIAL SYMMETRY

#### 8.1 Crystallography of grain boundaries

In the previous chapters the interfacial symmetry (and associated concepts) was studied. This involved the investigation of the symmetry of bicrystals while taking into account the eight degrees of geometrical freedom associated with them (section 3.1). Alternatively stated, given two identical crystals separated by the grain boundary it was sought to determine the symmetry of the whole for various relative orientations and positions of the two crystals as well as orientations and positions of the interface.

Thus, the bicrystal symmetry was initially studied in terms of the misorientation relationship between the two crystals; secondly, the variation of the symmetry so obtained was examined with respect to the position of the components and, finally, changes in the interfacial symmetry due to the orientation of the boundary plane were accounted for. In order to investigate the effect of these factors on the bicrystal symmetry a geometrical model was developed (chapter 3) without any particular reference to a grain boundary structure theory. This model permits the study of the bicrystal symmetry by considering each one of the above factors in turn.

An important feature of the just mentioned model is the concept of the 'dichromatic complex' (section 3.1). This was defined as the configuration of two interpenetrating lattice-complexes and as such it permits to study the bicrystal symmetry in a direct correlation to the symmetry of the single-crystal structure. Moreover, it is immediately clear that the dichromatic complex can be used for expressing the sym-

metry in terms of the orientation and position of the two components (chapters 4,5 and 7).

The concept of the dichromatic complex is, by definition, more general than that of the dichromatic pattern (Pond & Bollmann, 1979). Such a generalization was necessary in order to account for the symmetry of bicrystals in structures with symmetry lower than that of the respective lattice. If the approach of Pond & Bollmann (1979) is to be used for determining the symmetry of the configuration in figure 3.1.1a, for example, the appropriate dichromatic pattern (figure 3.1.1b) must be initially obtained. Then the appropriate bases are to be filled (in the appropriate misorientation) and the symmetry of the obtained configuration to be determined. This procedure is simplified, however, by considering the corresponding dichromatic complex (figure 3.1.1a); in this case the decrease in symmetry due to the atomic basis is already taken into account in the lattice-complex. Thus, the advantages of the proposed approach are apparent. It should be noticed, however, that the dichromatic complex is a purely mathematical concept and that no physical meaning is to be assigned to it at this stage.

Another aspect introduced in connection with the crystallographic treatment of the interfacial symmetry is the employment of antisymmetry groups. The introduction of these groups, first proposed by Pond & Bollmann (1979) was due to the fact that dichromatic complexes and bicrystals were described as sets of white and black points. The white/black designation, used for distinguishing between points belonging to different components, is quite arbitrary, but as was proved in this thesis the approach yields a comprehensive way for studying various aspects of symmetry. Although this was considered in conjunction with grain boundaries

the white/black approach can be shown to be useful in several other situations as well. First of all, it facilitates the determination of the symmetry classes of interphase boundaries; this is examined in the next section. More significantly, however, the use of two-coloured symmetry simplifies the study of the variation of the symmetry of a figure consisting of two components; in this respect most of the considerations in chapter 6 hold. As an example the  $\{111\}$  planar defects in  $L1_2$  structures are now considered.

### 8.1.1 Symmetry considerations of planar defects in superlattices

In binary alloys the ordered distribution of the atoms can lead to superlattices<sup>1</sup>; atoms of one kind occupy one or more sets of sites, and atoms of another kind occupy different sets of sites. In the case of f.c.c. structure the superlattices derived are known as  $L1_0$  (composition AB) and  $L1_2$  (composition  $A_3B$ ) in the Strukturbericht notation. The unit cell of each contains the four atoms found in the cubic unit cell of the disordered structure, but  $L1_0$  has tetragonal symmetry.

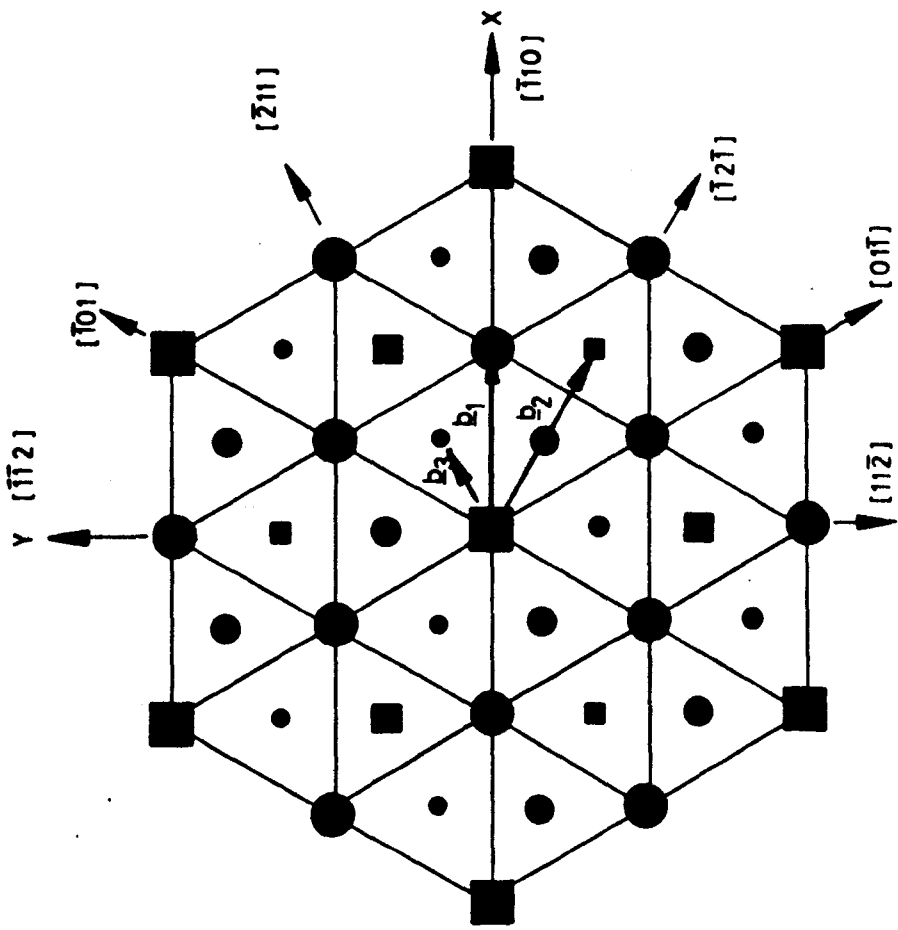
The  $L1_2$  structure corresponds to the ideal composition  $A_3B$ . The B atoms are in the 000 (and translational equivalent) positions, and A atoms in the remaining positions of the conventional unit cell of the f.c.c. structure. The atomic arrangement on the (111) plane in an  $A_3B$  alloy with the  $L1_2$  structure is shown in figure 8.1.1, where circles and squares represent A and B atoms respectively. The layers normal to  $[111]$  are composed of large, medium and small symbols.

On the basis of a hard sphere model and geometrical considerations three possible planar faults on  $\{111\}$  have been considered in the literature. These are the antiphase domain boundary (APB), superlattice intrinsic stacking fault (SISF) and complex stacking fault (CSF) consisting



Figure 8.1.1

The three (111) planes of an  $A_3B$  alloy. Circles represent A atoms and squares represent B atoms. Large, medium and small symbols represent the ...ABCABCAB... stacking along [111]. The vectors  $\underline{b}_1$ ,  $\underline{b}_2$ ,  $\underline{b}_3$  represent the displacements corresponding to the antiphase domain boundary, superlattice intrinsic stacking fault and complex stacking fault respectively.



of the APB and the SISF. In the case of the (111) plane the displacement vectors characterizing these faults are, for example,  $1/2[\bar{1}10]$ ,  $1/3[\bar{1}2\bar{1}]$ , and  $1/6[\bar{2}11]$  respectively (see figure 8.1.1). Yamaguchi, Vitek & Pope (1980) studied the dependence of fault energy on displacement in  $L1_2$  structures by means of computer simulation. They found that the SISF is always stable while the APB and CSF can be unstable.

Here the symmetry variation of the  $L1_2$  structure with displacements on the  $\{111\}$  plane is investigated by means of the method given in chapter 6. For this the structure is considered to consist of two  $L1_2$  structures, one white and the other black, in complete coincidence. Thus, the symmetry of the  $A_3B$  structure is  $Pm3m1'$  (grey group). The isomorphous point group contains 96 elements, half of them are ordinary while the remaining are their colour-reversing counterparts. By applying the procedure given in section 6.1 the displacements which conserve any one of the subgroups of  $m3m1'$  are determined<sup>2</sup>. Then, the spatial symmetry is considered (table 8.1.1).

The study of symmetry variation for planar defects is different from that for bicrystals or dichromatic complexes in a rather important aspect. This is because the concept of the DSC lattice is not applicable and therefore it is not clear, at first sight, that the symmetry of the composite changes periodically with the displacement. It is this situation in which the employment of the vector set can be useful. If the fundamental set is a lattice (as in the particular case) then the vector set and the lattice are identical. Hence, the vector set associated to a lattice represents all the displacements which create an identical fundamental set. Any other displacement corresponds to a fundamental set which is different to the original. Therefore, the composite sym-

TABLE 8.1.1

Symmetry variation of the  $A_3B$  structure with relative displacement

(the coordinate system for specifying the displacements has axes along the edges of the unit cell of the  $A_3B$  structure)

Fractional coordinates of symmetry equivalent displacements	Rank:	Point group	Point group order	Space group
000	1	$m\bar{3}m1'$	96	$Pm\bar{3}m1'$
$1/6[\bar{2}11]$ $1/6[2\bar{1}\bar{1}]$ $1/6[211]$	8	$\bar{3}'m$	12	$R\bar{3}'m$
$1/6[\bar{2}\bar{1}\bar{1}]$ $1/6[\bar{2}11]$ $1/6[2\bar{1}\bar{1}]$				
$1/6[2\bar{1}\bar{1}]$ $1/6[\bar{2}11]$				
$xxx$ $\bar{x}\bar{x}$ $\bar{x}\bar{x}$ $\bar{x}\bar{x}$	8	$\bar{3}'m$	12	$R\bar{3}'m$
$\bar{x}\bar{x}\bar{x}$ $\bar{x}\bar{x}\bar{x}$ $\bar{x}\bar{x}$ $\bar{x}\bar{x}$				
$x00$ $0x0$ $00x$ $\bar{x}00$ $0\bar{x}0$ $00\bar{x}$	6	$4/m'mm$	16	$P4/m'mm$
$0xx$ $x0x$ $xx0$ $0x\bar{x}$ $\bar{x}0x$ $x\bar{x}0$	12	$mmm'$	8	$Pmmm'$
$0\bar{x}\bar{x}$ $\bar{x}0\bar{x}$ $\bar{x}\bar{x}0$ $0\bar{x}x$ $x0\bar{x}$ $\bar{x}x0$				
$0yz$ $z0y$ $yz0$ $0zy$ $y0z$ $zy0$	24	$2'/m$	4	$P2'/m$
$0\bar{y}\bar{z}$ $\bar{z}0\bar{y}$ $\bar{y}\bar{z}0$ $0\bar{z}\bar{y}$ $\bar{y}0\bar{z}$ $\bar{z}\bar{y}0$				
$0y\bar{z}$ $z0\bar{y}$ $\bar{y}\bar{z}0$ $0z\bar{y}$ $y0\bar{z}$ $\bar{z}\bar{y}0$				
$0\bar{y}z$ $\bar{z}0y$ $\bar{y}z0$ $0\bar{z}y$ $\bar{y}0z$ $\bar{z}y0$				
$xxz$ $zxx$ $xzx$ $\bar{x}\bar{x}\bar{z}$ $\bar{z}\bar{x}\bar{x}$ $\bar{x}\bar{z}\bar{x}$	24	$2'/m$	4	$P2'/m$
$\bar{x}\bar{x}\bar{z}$ $\bar{z}\bar{x}\bar{x}$ $\bar{x}\bar{z}\bar{x}$ $\bar{x}\bar{x}\bar{z}$ $\bar{z}\bar{x}\bar{x}$ $\bar{x}\bar{z}\bar{x}$				
$\bar{x}\bar{x}\bar{z}$ $\bar{z}\bar{x}\bar{x}$ $\bar{x}\bar{z}\bar{x}$ $\bar{x}\bar{x}\bar{z}$ $\bar{z}\bar{x}\bar{x}$ $\bar{x}\bar{z}\bar{x}$				
$\bar{x}\bar{x}\bar{z}$ $\bar{z}\bar{x}\bar{x}$ $\bar{x}\bar{z}\bar{x}$ $\bar{x}\bar{x}\bar{z}$ $\bar{z}\bar{x}\bar{x}$ $\bar{x}\bar{z}\bar{x}$				
$xyz$ $zxy$ $yzx$ $xzy$ $yxz$ $zyx$	48	$\bar{1}'$	2	$P\bar{1}'$
$\bar{x}\bar{y}\bar{z}$ $\bar{z}\bar{x}\bar{y}$ $\bar{y}\bar{z}\bar{x}$ $\bar{x}\bar{z}\bar{y}$ $\bar{y}\bar{x}\bar{z}$ $\bar{z}\bar{y}\bar{x}$				
$\bar{x}\bar{y}\bar{z}$ $\bar{z}\bar{x}\bar{y}$ $\bar{y}\bar{z}\bar{x}$ $\bar{x}\bar{z}\bar{y}$ $\bar{y}\bar{x}\bar{z}$ $\bar{z}\bar{y}\bar{x}$				
$\bar{x}\bar{y}\bar{z}$ $\bar{z}\bar{x}\bar{y}$ $\bar{y}\bar{z}\bar{x}$ $\bar{x}\bar{z}\bar{y}$ $\bar{y}\bar{x}\bar{z}$ $\bar{z}\bar{y}\bar{x}$				
$\bar{x}\bar{y}\bar{z}$ $\bar{z}\bar{x}\bar{y}$ $\bar{y}\bar{z}\bar{x}$ $\bar{x}\bar{z}\bar{y}$ $\bar{y}\bar{x}\bar{z}$ $\bar{z}\bar{y}\bar{x}$				
$\bar{x}\bar{y}\bar{z}$ $\bar{z}\bar{x}\bar{y}$ $\bar{y}\bar{z}\bar{x}$ $\bar{x}\bar{z}\bar{y}$ $\bar{y}\bar{x}\bar{z}$ $\bar{z}\bar{y}\bar{x}$				
$\bar{x}\bar{y}\bar{z}$ $\bar{z}\bar{x}\bar{y}$ $\bar{y}\bar{z}\bar{x}$ $\bar{x}\bar{z}\bar{y}$ $\bar{y}\bar{x}\bar{z}$ $\bar{z}\bar{y}\bar{x}$				
$\bar{x}\bar{y}\bar{z}$ $\bar{z}\bar{x}\bar{y}$ $\bar{y}\bar{z}\bar{x}$ $\bar{x}\bar{z}\bar{y}$ $\bar{y}\bar{x}\bar{z}$ $\bar{z}\bar{y}\bar{x}$				

metry changes periodically and thus displacements in the Wigner-Seitz cell have to be considered only. The Wigner-Seitz cell in this particular case is a two-dimensional cell on the (111) plane. Table 8.1.2 gives the symmetry variation with displacements within this cell; in this case, since only displacement on the (111) plane are considered, the point group of the initial configuration can be taken to be  $\bar{P}3m1'$ .

It can be seen from table 8.1.1 and 8.1.2 that the conservation rule 'rank.order=constant' holds in this case as well. This can be treated in terms of the group-theoretical considerations given in section 7.3. A crystallographic space or point group may be decomposed into non-intersecting (except for the identity operator) subgroups, called direct factors, whose product is the original group (Kurosh, 1955). In this context, a product is understood as the sum of all products of elements of the subgroups one by one. The decomposition generally is not unique, a decomposable group can be represented as the product of only two subgroups. Let the initial group  $G$  be decomposed into two factors, one of the subgroups is chosen to be the group  $H$  of the composite with  $t \neq 0$  and designate the other as  $G_g$ . Even this decomposition is not unique, however, so that for a given  $G$  and  $H$ ,  $G_g$  may be chosen in a number of ways  $G_{g,i}$ . Each such  $G_{g,i}$  represents a set of operations, all independent of  $H$ , which relate composites created by symmetry related displacements.

In the particular case the point group of the originating configuration is  $\bar{3}m1'$  (order 24), thus:  $G=K+1'.K$ , where

$$K = \{1, 3_z^1, 3_z^2, 2_x^1, 2_A^1, 2_B^1, i, \bar{3}_z^1, \bar{3}_z^2, s_x, s_A, s_B\}.$$

$$\text{Let the subgroup } H = \bar{3}'m = \{1, 3_z^1, 3_z^2, 2_x^{1'}, 2_A^{1'}, 2_B^{1'}, i', \bar{3}_z^{1'}, \bar{3}_z^{2'}, s_x, s_A, s_B\}$$

(order 12);  $H$  adopts one orientation. Then:  $G=1.H+i.H$ .

TABLE 8.1.2

Symmetry variation of the  $A_3B$  structure with relative displacements on the (111) plane

(the coordinate system for specifying the general displacements has x- y- and z-axes along the  $[\bar{1}10]$ ,  $[\bar{1}\bar{1}2]$  and  $[111]$  directions)

Fractional coordinates of symmetry equivalent displacements	Rank	Point group	Point group order	Space group
000	1	$\bar{3}m1'$	24	$P\bar{3}m1'$
$1/6[\bar{2}11]$ $1/6[2\bar{1}\bar{1}]$	2	$\bar{3}'m$	12	$R\bar{3}'m$
$x, 2x, 0; \bar{x}, 2\bar{x}, 0; x, \bar{x}, 0;$ $\bar{x}, x, 0; 2x, x, 0; 2\bar{x}, \bar{x}, 0$	6	$2'/m$	4	$C2'/m$
$x, 0, 0; \bar{x}, 0, 0; 0, \bar{x}, 0;$ $0, x, 0; x, x, 0; \bar{x}, \bar{x}, 0$	6	$2/m'$	4	$C2/m'$
$x, y, 0; \bar{y}, x-y, 0; y-x, \bar{x}, 0;$ $y, x, 0; \bar{x}, y-x, 0; x-y, \bar{y}, 0;$ $\bar{x}, \bar{y}, 0; y, y-x, 0; x-y, x, 0;$ $\bar{y}, \bar{x}, 0; x, x-y, 0; y-x, y, 0$	12	$\bar{1}'$	2	$P\bar{1}'$

Therefore, the variants are related by the symmetry operations of the group  $\bar{1}=\{1, i\}$ . Hence, the symmetry related displacements are:  $1/6[\bar{2}11]$  and  $1/6[2\bar{1}\bar{1}]$  (rank 2).

Let, now, the subgroup  $H=2'/m=\{1, 2_x^{1'}, s_x, i'\}$  (order 4); H adopts three orientations, but these orientations are crystallographically equivalent (i.e. they are related to each another by symmetry elements  $g_i$  of the group G with  $g_i \notin H$ ). Then:

$$G = 1H + 1'H + 3\frac{1}{z}H + 3\frac{1}{z}H + 3\frac{2}{z}H + 3\frac{2}{z}H$$

Therefore, the variants are related by the symmetry operations of the group  $31'=\{1, 1', 3_z^1, 3_z^{1'}, 3_z^2, 3_z^{2'}\}$ ; the symmetry related displacements are those given in the table 8.1.2.

Similarly, the symmetry displacements for the subgroups  $H_1=2/m'$  and  $H_2=\bar{1}'$  can be found by taking into account that:

$$G = 1H_1 + 1'H_1 + 3\frac{1}{z}H_1 + 3\frac{2}{z}H_1 + 3\frac{1}{z}H_1 + 3\frac{2}{z}H_1$$

and

$$G = 1H_2 + 1'H_2 + 3\frac{1}{z}H_2 + 3\frac{1}{z}H_2 + 3\frac{2}{z}H_2 + 3\frac{2}{z}H_2 + 2\frac{1}{x}H_2 + 2\frac{1}{x}H_2 + 2\frac{1}{A}H_2 + 2\frac{1}{A}H_2 + 2\frac{1}{B}H_2 + 2\frac{1}{B}H_2$$

respectively.

- - -

Footnotes 1: This term results from an unfortunate mistranslation of the German "Überstruktur" or "overstructure". In its commonest usage 'superlattice' is synonymous with 'multiple-cell structure'. However, it must not be confused with the term 'superlattice' used in the lattice geometry to refer to a lattice obtained from an original lattice by means of a transformation matrix having integral elements and determinant larger than unity (Santoro & Mighell, 1972; Bucksch, 1971, 1972; Cassels, 1959).

2: No details are given since the point group  $m3m1'$  contains 418 subgroups.

## 8.2 Crystallography of interphase boundaries

An interphase boundary is the surface<sup>1</sup> separating two crystals with different structures; its structure is similar in many ways to that of a grain boundary. In the general case, five degrees of freedom are associated with an interphase boundary. Three degrees of geometrical freedom are needed to specify the relative orientations of the two lattices, but of course it is no longer possible to carry one lattice into the other by means of a pure rotation. The additional two degrees of freedom are associated with the specification of the interface plane.

In order to study the symmetry of interphase boundaries the conventions made in chapter 3 are considered. Thus, one of the semi-infinite structures across a general interphase boundary is designated 'white' and the other 'black'. For symmetry considerations the atomic structure of the adjacent crystals can be disregarded. The interphase boundary is, then, considered as the geometrical plane separating the black and white semi-infinite lattice-complexes<sup>2</sup>.

The relative orientation of the two lattices<sup>3</sup> across an interphase boundary can be described as follows. The white lattice is considered fixed in space and is used as reference. Then, the relative orientation is considered to arise by the appropriate transformation of the black lattice. This transformation describing the relation between the white and black lattices is a general linear transformation  $\underline{R}\underline{P}$  where  $\underline{P}$  is a pure strain and  $\underline{R}$  a pure rotation<sup>4</sup>; it may also be described by any other linear transformation  $\underline{S}_i \underline{R} \underline{P} \underline{S}_j$  where  $\underline{S}_i$  and  $\underline{S}_j$  represent symmetry operations of either lattice.

### 8.2.1 Point symmetry of interphase boundaries

The point symmetry of interphase boundaries can be determined by a way similar to that employed for grain boundaries. The interphase



boundary is, from the crystallographic point of view, a unique plane which must be invariant under the transformations of the point group. Thus, the symmetry classes possess three-dimensional highest invariance (since the bicrystal is 'in' three-dimensional space) and, additionally, a two-dimensional invariance (in view of the presence of the unique plane). Therefore, the point symmetry of interphase boundaries is described by groups of the class  $G_{3,2,0}^2$ , i.e. the two-coloured, two-sided rosettes.

However, not all of the rosette groups are consistent with the geometry of interphase boundaries. For instance, centrosymmetrical rosette groups are not permissible since the inversion centre implies that both sides of the unique plane are neutral (see section 5.3). Furthermore, unlike grain boundaries, the antiinversion operation is not consistent with interphase boundaries. As was explained in section 5.3 a centre of colour reversal, although leaving the unique plane invariant (without interchanging its two sides), it imposes continuation conditions on the lattices across the interface. In other words, the white and black lattices must be identical and in complete coincidence, which, clearly is not the case with interphase boundaries.

Further restrictions on the symmetry operations are imposed by the fact that the interphase boundary separates two different structures. This means that there is no symmetry operation which transforms the white lattice-complex to the black one or vice versus. Therefore, no colour-reversing symmetry elements are consistent with the geometry of interphase boundaries. It is at this point where the crucial difference between grain and interphase boundaries, as far as the symmetry is concerned, arises. Consequently, the only permissible symmetry operations are ordi-

nary ones lying perpendicular to the boundary plane.

The point symmetry classes are given in table 8.2.1; these are the two-dimensional point groups (Niggli, 1959). The coordinate system, relative to which the group symbols are given has an axis a perpendicular to the plane, while the axes b and c are orthogonal to the axis a and make a right or oblique angle with each other, depending on the class of rosette symmetry. The letters or numbers in the first, second, and third positions of the symbol indicate that a particular symmetry element coincides with the coordinate axes in the order a, b, c (for the lower symmetry classes) or with (and in this order) the axes a, b and the bisector of the angle between the axes b and c (for the senior classes).

### 8.2.2 Spatial symmetry of interphase boundaries

In discussing the symmetry of interphase boundaries, it is convenient to distinguish three types of interface which are described as incoherent, semi-coherent and coherent respectively. For the case of incoherent phase boundaries there is no continuity condition for the lattice vectors or planes across the interface. In the fully coherent interface, on the other hand, the lattices match exactly at the interface, and 'corresponding' lattice planes and directions are continuous across the interface, although they change direction as they pass from one structure to another<sup>5</sup>.

It is not generally possible, however, to find a coherent interface between two arbitrary structures. If the matching condition is nearly satisfied, two phases may be forced elastically into coherence across an interphase boundary<sup>6</sup>. This is usually possible only when one (included) crystal is very small, since the stress at any point increases with the

TABLE 8.2.1

Point groups describing the symmetry of  
interphase boundaries

Number	Point group	
	Full symbol	Short symbol
1	111	1
2	211	21
3	1m1	1m <sup>+</sup>
4	2mm	2mm
5	411	4
6	4mm	4mm
7	3m1	3m
8	311	3
9	611	6
10	6mm	6mm

+ In the international notation the (third position) symbol 1 in the class 1m (short symbol) is omitted because of confusion that might occur in later two-dimensional space-group nomenclature, in which 1 may occur in the second or third position of the symbol.

size of the crystal. Forced elastic coherence of this kind may exist at the nucleation in early growth stage of a transformation. By contrast, the semi-coherent interface consists of regions in which the two structures may be regarded as being in forced elastic coherence, separated by regions of misfit.

The above considerations indicate that interphase boundaries can have one- or two-dimensional periodicity. This immediately implies that their symmetry is described by band and layer symmetry groups respectively. The permissible groups are determined by considering the combination of the point symmetry groups (table 8.2.1) with translational symmetry. The procedure for establishing the spatial symmetry is, therefore, to consider the lists of the two-coloured, two-sided band or layer groups and to delete those groups which are not isomorphous to a bicrystal point group (table 8.2.1). Tables 8.2.2 and 8.2.3 give the symmetry groups of one- and two-dimensional interphase boundaries.

### 8.2.3 Examples of interphase boundary symmetry

Three examples related to epitaxial growth of II-VI components are now mentioned in order to indicate the symmetry classification of interphase boundaries. All the epitaxial orientation relations for II-VI compounds<sup>7</sup> grown on cubic crystal substrates are of two types only (Pashley, 1956, 1965). The sphalerite structure films always grow in the parallel orientation and the wurtzite structure films in the quasi-parallel orientation<sup>8</sup> on these substrates. The P orientation corresponds to:  $(hkl)_{\text{film}}$  parallel to  $(hkl)_{\text{substrate}}$  with  $[uvw]_{\text{film}}$  parallel to  $[uvw]_{\text{substrate}}$ , where  $[uvw]$  is a direction in the  $(hkl)$  plane. The P' orientation, on the other hand, occurs when  $(0001)_{\text{film}}$  is parallel to  $(111)_{\text{substrate}}$  and  $[11\bar{2}0]_{\text{film}}$  parallel to  $[110]_{\text{substrate}}$ . In both

TABLE 8.2.2

Band groups describing the symmetry of  
interphase boundaries

Number	Band group	Number	Band group
1	$\rho 111$	7	$\rho 112$
2	$\rho 121$	8	$\rho m11$
3	$\rho 1m1$	9	$\rho ma2$
4	$\rho 1a1$	10	$\rho 11m$
5	$\rho m2m$	11	$\rho 11a$
6	$\rho m2a$	12	$\rho mm2$

TABLE 8.2.3

Layer groups describing the symmetry of  
interphase boundaries

Number	Layer group	Number	Layer group
1	p1	9	cmm2
2	p112	10	p4
3	p1m1	11	p4mm
4	p1a1	12	p3
5	c1m1	13	p3m1
6	pmm2	14	p31m
7	pbm2	15	p6
8	pba2	16	p6mm

the P' orientation and its geometrically equivalent P orientation (namely  $(111)_{\text{film}} // (111)_{\text{substrate}}$  with  $[0\bar{1}1]_{\text{film}} // [0\bar{1}1]_{\text{substrate}}$ ) hexagonal arrays of atoms in the substrate surface and in the interface plane of the film are parallel. This can be seen in considering the ZnS growth on (111) surfaces of silicon. Figure 8.2.1 shows the two interface planes; during growth (0001) planes of wurtzite-type-structure ZnS are deposited onto (111) planes of silicon. From this figure it can be easily found that the symmetry of the interphase boundary is  $3m$  (group no. 7 in table 8.2.1).

The second example of epitaxially grown interphase boundaries refers to the vacuum evaporation of CdS (sphalerite structure) onto NaCl. The latter has a f.c.c. lattice ( $a=5.63\text{\AA}$ ) and the basis has one  $\text{Na}^+$  ion at 000 and one  $\text{Cl}^-$  ion at  $\frac{1}{2}\frac{1}{2}\frac{1}{2}$ . Cadmium sulfide is also based on the f.c.c. lattice ( $a=5.82\text{\AA}$ ) with a basis containing a S atom at 000 and a Cd atom at  $\frac{1}{4}\frac{1}{4}\frac{1}{4}$ . The (001) projections of NaCl and CdS are shown in figure 8.2.2. Chopra & Khan (1967) have found that moderately high temperature epitaxial growth of CdS on rock salt follows the parallel (P) orientation:  $(001)_{\text{CdS}} // (001)_{\text{NaCl}}$  with  $[110]_{\text{CdS}} // [110]_{\text{NaCl}}$ . In this case the symmetry of the interface is described by the point group  $2mm$ ; the mirror planes are normal to  $[110]_{\text{NaCl}}$  and  $[\bar{1}10]_{\text{NaCl}}$  while the 2-fold axis is along the normal to the interface.

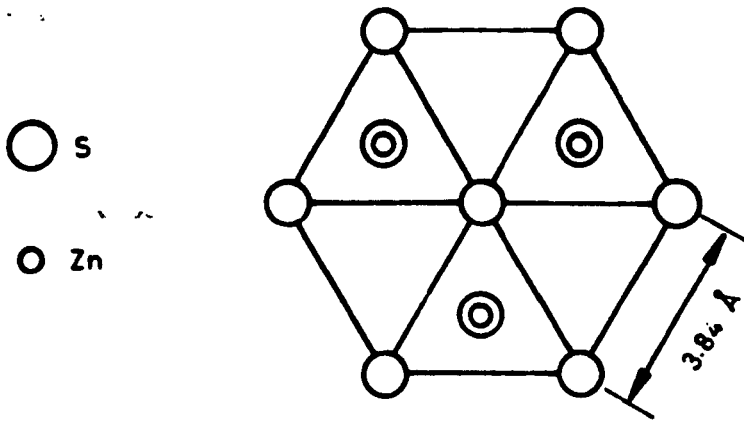
Finally, epitaxial films of CdS onto (110) surfaces of germanium have been found (Holt & Wilcox, 1971; Abdalla, Holt & Wilcox, 1973) to be in parallel alignment with the substrate, i.e.:  $(110)_{\text{CdS}} // (110)_{\text{Ge}}$  and  $[\bar{1}10]_{\text{CdS}} // [\bar{1}10]_{\text{Ge}}$ . Figure 8.2.3 shows the (110) projections of CdS and Ge; it is clear that if the two structures are superimposed on the (110) planes, then the point symmetry of the interphase boundary

Figure 8.2.1

The (00.1) surface of ZnS and (111) surface of Si



$\alpha$ -ZnS structure (00.1)



Si structure (111)

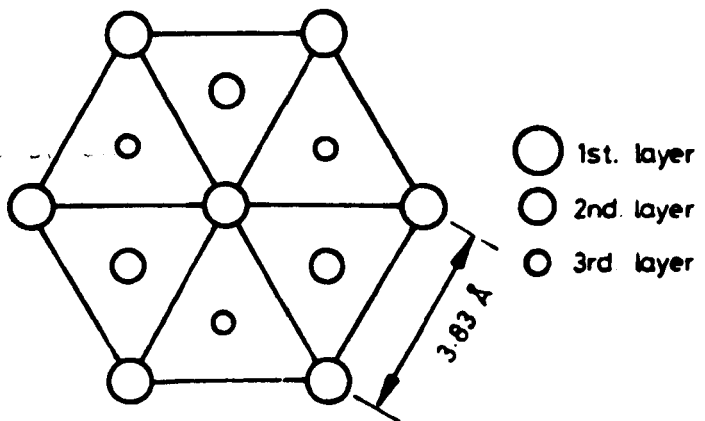
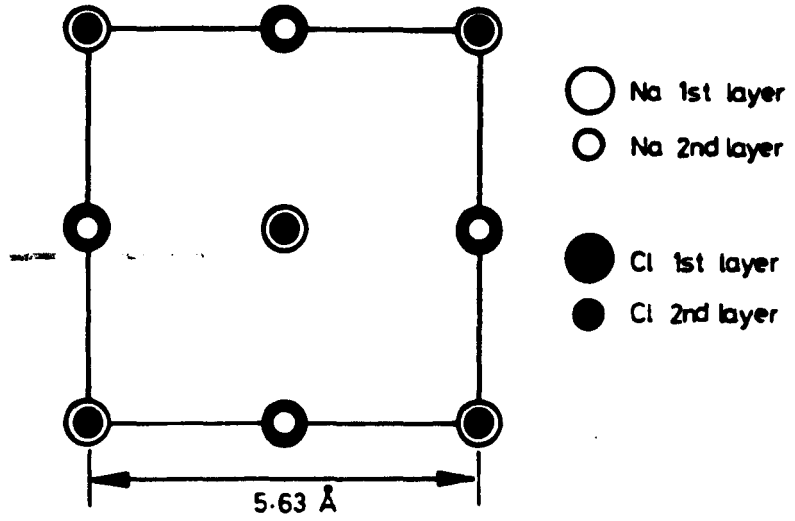


**Figure 8.2.2**

**The (001) surfaces of NaCl and CdS**

NaCl structure (001)



CdS structure (001)

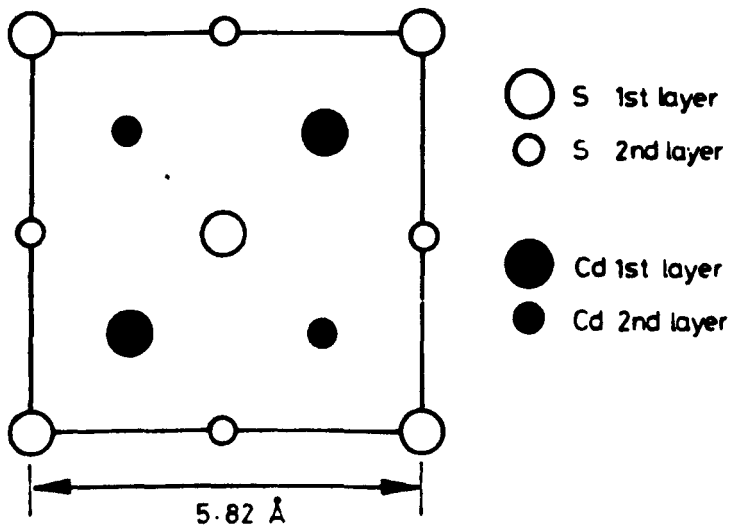
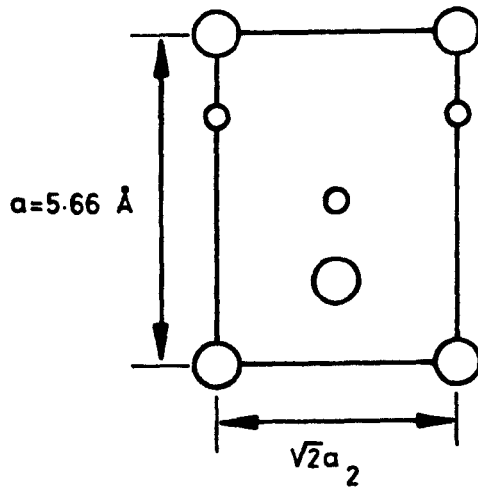




Figure 8.2.3

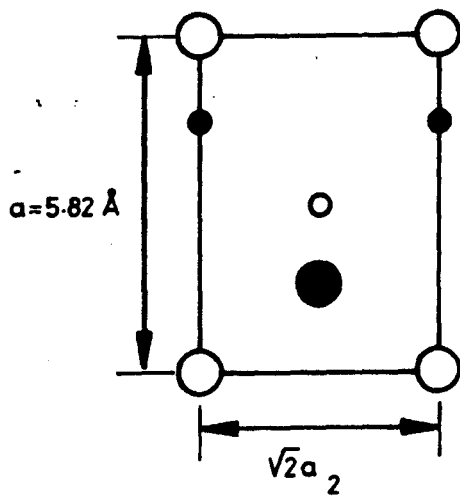
The (110) surfaces of Ge and CdS





Ge structure (110)



-  Ge 1st layer
-  Ge 2nd layer

CdS structure (110)



-  S 1st layer
-  S 2nd layer
-  Cd 1st layer
-  Cd 2nd layer

is  $lm$  (i.e. a mirror plane normal to the common  $[\bar{1}10]$  direction). The examples given above cover most of the usual cases of epitaxial growth as listed in table 8.2.4.

- - -

Footnotes 1: In the present treatment the interphase boundary is considered planar.

2: Unlike grain boundaries, the two lattice-complexes are not identical in the case of interphase boundaries.

3: Since the two structures across the interphase boundary are different, a misorientation relationship is not uniquely defined as in the case of grain boundaries. Thus, the term 'relative orientation' is used instead.

4: Obviously, for  $\underline{P}=\underline{I}$ ,  $\underline{I}$  being the  $3 \times 3$  unit matrix, the grain boundary case is obtained.

5: A coherent interface in the sense in which it is used here does not necessarily imply a rational interface.

6: The best known example of nearly exact matching is this involving f.c.c. and h.c.p. structures with virtually identical interatomic distances in the octahedral and basal planes respectively.

7: The structure of II-VI components is either hexagonal wurtzite or cubic zinc-blend type (see, e.g. Holt, 1974).

8: These orientation relationships are denoted by the letters  $P$  and  $P'$  respectively.

### 8.3 Discussion

The foregoing considerations have shown how the spatial and/or point symmetry of grain or interphase boundaries can be classified. The application of the symmetry scheme so determined is discussed in the present section and future work is proposed<sup>1</sup>.

Pond & Bollmann (1979) have already pointed out that the consideration of bicrystal symmetry can be useful for the investigation of interfacial structure. For instance, the tessellated form of secondary

TABLE 8.2.4

Point symmetry of epitaxial interphase boundaries of II-VI compounds on cubic substrates

Compound	Substrate orientation	Film structure and orientation <sup>+</sup>	Point symmetry	Reference
ZnSe	GaAs (100)	S,P	2mm	(1)
CdS	NaCl (100)	S,P	2mm	(2)
	NaCl (110)	S,P	m	
	NaCl (111)	W,P'	3m	
	BaF <sub>2</sub> (111)	W,P'	3m	
CdS	Ge (100)	S,P	2mm	(3)
	Ge (110)	S,P	m	
	Ge (111)	W,P'	3m	
ZnTe	Ge (100)	S,P	2mm	(4)
	Ge (110)	S,P	m	
CdTe	Ge (100)	S,P	2mm	(5)
	Ge (111)	W,P'	3m	
CdTe	Si (111)	W,P'	3m	(6)
CdSe	Ge (100)	S,P	2mm	(7)

+ In the epitaxial orientation column S signifies the sphalerite structure, W the wurtzite structure, P the parallel orientation and P' the quasi-parallel orientation for the wurtzite structure as discussed in section 8.2.

References: (1) Genthe & Aldrich, 1971

(2) Chopra & Khan, 1967; Wilcox & Holt, 1969;

Holt & Wilcox, 1971; Wilcox, 1970

TABLE 8.2.4-continued

(3) Holt & Wilcox, 1971; Abdalla, Holt & Wilcox, 1973

(4) Multi & Holt, 1972

(5) Abdalla & Holt, 1973

(6) Abdalla, 1973

(7) Gejji & Holt, 1975



dislocation networks accommodating small angular deviations from coincidence misorientations could give information concerning the presence of equivalent interfacial structures. The same authors have indicated how the bicrystal symmetry can be used for the investigation of interfacial structure by atomistic computer simulation. In general the nature of atomistic relaxations will depend on the symmetry of the bicrystal (see e.g. Smith et al. 1977; Pond & Vitek, 1977; Pond et al. 1979).

Here, the discussion is somewhat more general in the sense that the implications of symmetry on the physical properties of bicrystals is considered. It must be born in mind that at least some of the physical properties of bicrystals are not identical to those of single crystals with identical chemical composition and structure. The differentiation of the physical properties can be contributed by:

- (1) factors that are inherent to the complex geometrical relations defining each grain and its tensor properties with respect to its neighbors, e.g. size and shape of grains, relative lattice orientation, etc.,
- (2) factors that are intrinsic properties of the internal boundary surfaces, i.e. grain boundaries bounding individual grains from their neighbours, e.g. grain boundary structure, strength, energy, diffusion, etc.

The factors of both categories are related to the symmetry of the grain boundary and therefore it is evident that considerations of interfacial symmetry yield an important insight of both the structure and properties of polycrystalline materials.

If the point or spatial symmetry group of a bicrystal is established experimentally, it can be said that the minimum symmetry of its possible

physical properties has also been established. This provides a basis for deriving descriptive structural classifications and grouping of bicrystals in classes by appropriate sets of criteria. In exactly the same way, physics classifies elementary particles, atomic and molecular spectra, normal vibrations, etc. These symmetry classifications are based on the various groups of permissible transformations carried out on the elements of the corresponding bicrystal. The problem of classification is a primary one, so that symmetry, which establishes structural invariants, constitutes an essential technique for interfacial investigations.

However, this is not the most important aspect. More important for 'bicrystal physics' is the fact that it is possible to relate a unique coordinate system to the symmetry elements of a bicrystal and thus ensure uniqueness of description for its physical properties, which generally<sup>2</sup> depend on the direction of measurement. Having settled the choice of axes (appendix 1) it can be asserted without ambiguity that along a specific direction the bicrystal will have such and such physical properties. Thus, measurements of the physical properties of bicrystals of one particular material are only comparable when they are referred to the same coordinate system. Knowing the symmetry group of the bicrystal it is possible to limit the range of measurements of physical properties along specified directions<sup>3</sup>. This greatly reduces the number of measurements required to reveal anisotropy, i.e. the dependence of the physical properties on the direction of measurement.

Another important implication is that the bicrystal symmetry group (which is closely connected to the symmetry groups of the physical quantities—Neumann's principle) enables us to establish the number of

independent constants characterizing every property. In other words, it can always be stated how many measurements (along different directions) will have to be made in order to obtain a complete characterization of a particular property of the bicrystal. The number of measurements depends on the nature of the property under consideration and on the law governing the transformation of the corresponding physical quantity.

The use of symmetry methods may be still more effective in the studies of the electron structure or structural analysis of bicrystals. If translational symmetry do not exist for bicrystals, the analysis of the physical properties of the corresponding atomic system containing about  $10^{23}$  particles/cm<sup>3</sup> would be extremely difficult. However, bicrystals<sup>4</sup> can be periodic and thus their structure can be described by the (periodic) repetition of an elementary atomic motif usually consisting of a small number of particles. This motif (occupying the unit cell) plays the part of the 'molecule' in the structure of bicrystal. Hence, in the study of the physical properties of bicrystals, it is (roughly speaking) sufficient to study the behaviour of an aggregate of particles within a single unit cell, since the properties of the whole may be judged from the properties of the part. In quantum mechanical terms the properties of the whole are reflected in the properties of the translationally periodic part through Bloch's theorem and its equivalent.

In other words, the link between the interfacial symmetry and quantum mechanics comes about through the transformation properties of the Hamiltonian operator, whose eigenvalues play an extremely important role in quantum mechanics. In the single crystal case it is well-known (see e.g. Cornwell, 1969) that all transformations leaving the Hamiltonian operator invariant form a group which is isomorphic to the group of the crystal. Consider, now, electrons in the vicinity of the interface. Within the

'one-electron' approximation every electron of mass  $m$  has associated with it a Hamiltonian of the simple form:

$$H(\underline{r}) = -\frac{\hbar^2}{2m} \left\{ \frac{\partial^2}{\partial x^2} + \frac{\partial^2}{\partial y^2} + \frac{\partial^2}{\partial z^2} \right\} + V(\underline{r})$$

where the potential energy term  $V(\underline{r})$  contains the field caused by the nuclei and the average field of all the other electrons acting on the electron under consideration.

In the general case of a bicrystal the form of  $V(\underline{r})$  is not known because:

(1) intrinsic difficulties in calculating  $V(\underline{r})$  for an array of atoms, and,

(2) more significantly, because the actual structure of the interface is not known.

However, one can draw very important conclusions without knowing the precise form of  $V(\underline{r})$ . This is based on the fact that:

$$V(\{R/\underline{t}\}\underline{r}) = V(\underline{r})$$

or, in other words, the potential energy has the symmetry of the spatial group of the bicrystal<sup>5</sup>. Hence, for an electron in the vicinity of an interface, its Hamiltonian is invariant with respect to the spatial symmetry group of the interface.

The implication of this is that by using basic functions of representations of the group of the Schrödinger equation it is possible to simplify significantly several important types of quantum mechanical calculations. In analogy to the single crystal cases (see e.g. Wigner, 1930; Chen, 1967; Maradudin & Vosko, 1968) it can be seen that such calculations are only feasible when group theoretical arguments are used to exploit the symmetry to the full.

Of course, before the interfacial symmetry is applied to quantum

mechanical calculations account must be given to the significance of the colour-reversing operations. One way that this can be done is as follows. The potential energy  $V(\underline{r})$  in the vicinity of the interface can be calculated in principle by the corresponding potentials of the two components  $V_1(\underline{r})$  and  $V_2(\underline{r})$ , i.e.:

$$V(\underline{r}) = V_1(\underline{r}) + V_2(\underline{r})$$

Let  $G$  the symmetry group of the interface and  $G_1$  and  $G_2$  the respective groups of each component. In general, not every operation of  $G_1$  or  $G_2$  will leave  $V(\underline{r})$  invariant although every transformation of  $G$  will leave  $V_1(\underline{r})$  and  $V_2(\underline{r})$  invariant (in view of the fact that  $G$  is a subgroup/supergroup of  $G_1$  and  $G_2$ ). Therefore, the colour-reversing elements of  $G$  can be considered as the symmetry operations which express the misorientation contribution of  $V_1(\underline{r})$  and  $V_2(\underline{r})$  in  $V(\underline{r})$ .

Concluding this section it is, perhaps, of interest to indicate another aspect of the bicrystal symmetry. This refers to electron contrast simulations of planar coincidence-site lattice interfaces. Such simulations are complicated and in the general case it is impossible to take into account the dynamical interactions between primary and secondary beams arising from interfaces which do not conserve the reciprocal lattice. However, symmetry considerations show that this problem can be exactly solved for the case of CSL boundaries. In this case, whereas the direct crystals are merely in contact with one another (semi-infinite crystals), the extent of a reciprocal lattice is independent of the size of the crystal and pervades all the reciprocal space. Therefore, the reciprocal lattices of the two individuals of the bicrystal occupy the same space. Thus, the reciprocal lattice  $L_c$  of the bicrystal is described as the intersection (common subgroup) of the reciprocal space groups  $L_1$  and  $L_2$

of the components. Gratiias & Portier (1979) proposed that in this case the scattering matrices (Howie—Whelan formulation)  $S_{\underline{1}}$  and  $S_{\underline{2}}$  are then built up on this common basis by computing the structure factors in the group  $L_c$  for the two different sets of Wyckoff positions of the atoms corresponding to the two crystals (see also Guan & Sass, 1973a,b; Sass, 1980).

- - -

Footnotes 1: These considerations are primarily referred to grain boundaries. Extension to interphase boundaries is, in principle, possible provided that their particular nature is taken into account.

2: For non-scalar properties

3: These directions form a solid angle which 'cut' the bicrystal into symmetrically independent regions.

The choice of the directions of measurement is based on the fact that the number of symmetrically independent (or symmetrically equal) regions into which a symmetrical figure may be divided equals the order of its symmetry group.

4: Or, at least, bicrystals with special properties.

5: This leads to the above mentioned theorem of Bloch (1928).

## Chapter 9

### ELECTRON MICROSCOPY OF GRAIN BOUNDARIES

#### Introduction

In the last twenty years optical, electron, field-ion and X-ray microscopy has been used to study grain boundaries in a wide variety of materials (table 9.1.1). Critical examination of these methods indicates that, at present, the transmission electron microscope allows considerable flexibility in operation, as well providing the essential image contrast and diffraction information necessary for the elucidation of grain boundary structure.

The interpretation of image contrast across grain boundaries, based on the dynamical theory of diffraction (see e.g. Hirsch et al. 1965), is generally more complicated than in the single crystal cases. This is mainly due to the presence of the interface. The surface separating the two crystals corresponds, in first approximation, to the junction of two elastically isomorphic half-spaces. Thus, the displacement field of a grain-boundary dislocation, say, must be determined for each crystal, and numerical values in the Howie-Whelan (1960, 1961) equations will be different on either side of the interface (see e.g. Tucker, 1969).

Further complications arise due to the misorientation relationship across the interface which causes different diffraction modes to occur (see e.g. Pond, Smith & Clark, 1974). Each of the beams excited in the upper crystal is incident on the lower one and can give rise to further diffracted beams in that crystal. Thus, the total number of beams propagating in the lower crystal can be substantial, and unlike the single crystal case, all these beams are not necessarily coupled to each other (Sutton & Pond, 1978). The effect is that: (a) the specimen can be

TABLE 9.1.1

Methods of interface examination and specific  
properties investigated

---

Optical metallography	-faceted or non-faceted boundaries
X-ray Laue	-orientation relationships
Thermionic emission	-interface migration mechanisms
Electron microscopy	-interface structure and crystallography
Field-ion microscopy	-atomic structure of boundary

---

---



orientated for one of several diffraction conditions, and, (b) multi-beam dynamical theory must be employed to interpret the images of interfaces (Corbett & Sheinin, 1976; Sheinin & Corbett, 1976; Sutton & Pond, 1978).

Geometrically speaking the occurrence of the various diffraction modes depends on which set of atomic planes and in which crystal are orientated for diffraction. The various diffraction conditions are illustrated in figure 9.1.1 (for a review see Pond, 1980). Humble & Forwood (1975) pointed out that the 'one-crystal-diffraction' mode can only be obtained approximately. On the other hand, they obtained excellent agreement for comparisons of experimental observations, obtained by simultaneous two-beam conditions, to simulations using the two-beam equations. This diffraction mode is particularly important for investigating interfacial imperfections while the 'same  $g$  condition' is very useful for studying the structure of grain boundaries between coincidence related crystals (Sutton & Pond, 1978; Pond, 1979).

Although the above mentioned factors influence the interpretation of the interfacial contrast, the electron microscope can be used successfully for the determination of (a) the geometrical parameters of grain boundaries (see section 9.2), and, (b) the investigation of grain boundary imperfections, as well as of physical processes such as grain-boundary sliding or segregation, and, (c) the study of grain-boundary structure.

### 9.1 Determination of the geometrical parameters

As the models of grain boundary structure, outlined in section 1.2, depend very sensitively on the crystallography of the interface and the crystals which form it, it is important to determine the grain boundary parameters with the highest possible accuracy. These parameters are the misorientation relationship and the interface plane; their determination

**Figure 9.1.1**

Schematic representation of the diffraction modes in a sample containing a grain boundary:

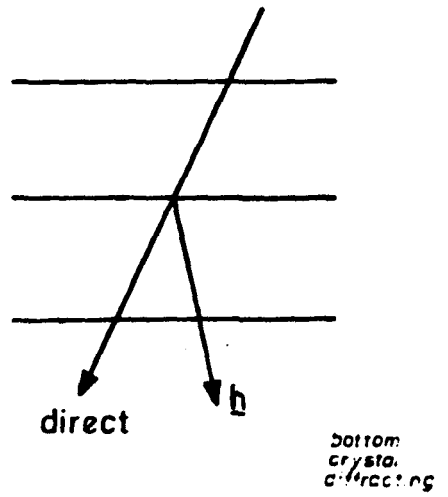
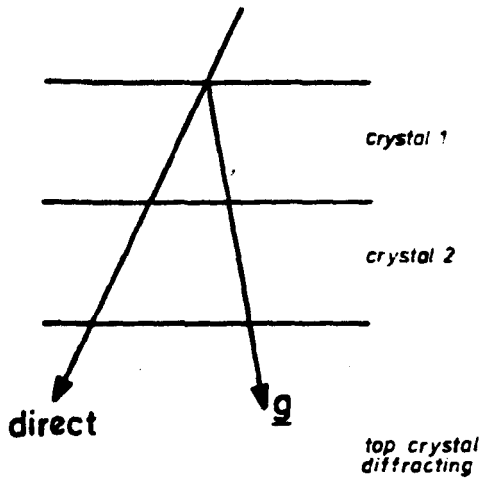
(a) one-crystal diffracting,

(b) simultaneous two-beam condition,

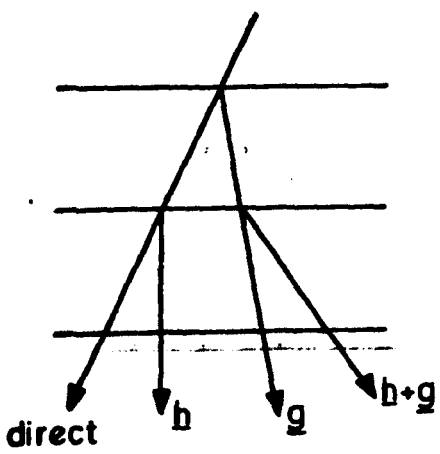
(c) same  $\underline{g}$  condition (this mode is a special case of (b) for  $\underline{g} + \underline{h} = \underline{g}' + \underline{h}'$  and the two crystals are CSL related).

In all diagrams the reciprocal space vector of a reflection from the upper crystal is called  $\underline{g}$  and from the lower crystal  $\underline{h}$ ).

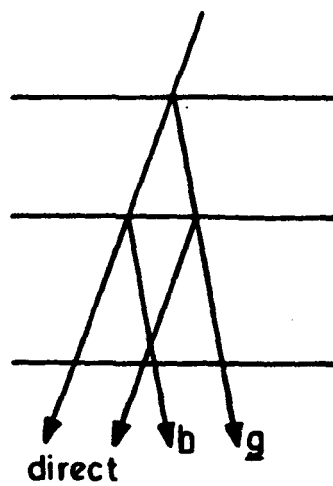
(after Pond, 1980a)



(a)



(b)



(c)

is a significant part of any experimental project concerned with grain boundaries.

### 9.1.1 The determination of the misorientation matrix<sup>1</sup>

Misorientation relationships across an interface are generally expressed in one of the following two ways:

- (1) a pair of parallel directions in a pair of parallel planes; this is normally used for epitaxial interphase boundaries, and,
- (2) as a matrix describing the vector transformation from one crystal to the other; physically this corresponds to an axis/angle pair, and it is mainly used for grain boundaries.

The technique used to determine the misorientation relationship between two grains depends upon the type of misorientation, the accuracy of information required, and the limitations imposed by the specimen and/or the instrument. Two approaches are commonly used:

- (1) Spot patterns from both grains may be used either because strain effects prevent the formation of Kikuchi lines or because the crystallographic relationship is particularly simple<sup>2</sup>.
- (2) Kikuchi lines may be employed to improve the accuracy of the misorientation determination since the spot pattern is clearly an inaccurate representation of the beam direction.

The minimum information required to calculate a misorientation matrix is the indices of two pairs of parallel directions, with one of each pair in each crystal (Goux, 1974). A third pair of such directions follows automatically from the vector cross-product of the first two, but additional pairs of directions will overdetermine the relationship

and allow an estimate of the error in the procedure to be obtained (see appendix 13). In practice the determination of the misorientation matrix is carried out in two stages. Firstly, the pairs of parallel directions are obtained, then the misorientation relationship is determined either graphically as an axis/angle pair<sup>3</sup> or by calculating the misorientation matrix.

The most accurate analysis for indexing Kikuchi patterns is that due to von Heimendahl et al. (1964) and requires a minimum of three non-parallel Kikuchi line pairs to obtain the beam direction unambiguously from one pattern. This method is based on the relationship between the three Kikuchi line pairs and the central beam spot. The measurement of the directions of the triangle, and its relation to the beam spot clearly limit the accuracy of the method, and considerable care must be taken to ensure that the error is kept to a minimum. An analysis (see appendix 12) of the factors limiting the accuracy indicates that in all of today's methods comparitably large errors arise by the uncertainty in the exact position of the centre of the diffraction pattern. In order to eliminate such errors a new technique was developed during this work (appendix 12). This method, though in its second phase similar to that described by von Heimendahl and co-workers (Heimendahl von et al. 1964; Heimendahl von, 1971), is more accurate than the latter. The exact direction of the electron beam is determined in an accuracy of the order of 1' provided that the area selected for diffraction is not deformed. The advantage of the proposed method is that no geometrical constructions are necessary for finding the position of the points required for the indexing procedure.

It is, however, not feasible to determine precisely the beam direction of a Kikuchi pattern. Thus, in the experimental situation error may

reside in any or all of the beam directions derived from the Kikuchi patterns, and, thus, the calculated matrix  $\underline{R}$  is subject to experimental errors. Consequently, it is important to use as many independently obtained directions as possible in order to prevent the propagation of systematic errors among the components of  $\underline{R}$ . It is usual practice to overdetermine  $\underline{R}$  by providing excess information for the solution and find the matrix best fitting to the available data. Such an adjustment of  $\underline{R}$ , associated with a non-linear least-squares problem, is, however, by no means straightforward. A detailed analysis of the problem is given in appendix 13 where a least-squares method for the determination of the best fitting matrix  $\underline{R}$  subjected to orthogonality constraints is developed.

#### 9.1.2 Determination of the boundary plane

The most general method for determining the boundary plane is the trace analysis (see e.g. Edington, 1974, vol. 3, p. 55). Using this approach errors in the boundary plane of  $\pm 5^\circ$  may occur primarily because the method relies on measurements of some dimension of the interface, usually the projected width, taken from the image and such measurements are prone to error. Uncertainty in the boundary plane is introduced by the following factors:

- (1) the boundary may not be exactly planar, particularly near the surfaces of the specimen, and,
- (2) diffraction effects frequently make the accurate measurements of the interface dimensions difficult, by obscuring the intersections of the boundary and the foil surface with thickness fringes, for example.

A more reliable approach is available in electron microscopes where specimen tilting in large angles is possible. The principle of this

technique, often called 'edge-on technique', is to tilt the specimen such that the boundary plane lies parallel to the electron beam, that is minimum width of the image. The procedure of the above approach is as follows:

- (1) determine the foil normal by obtaining a diffraction pattern at zero tilt from the area of interest
- (2) set the tilt axis parallel to the line of intersection of the foil and boundary planes
- (3) tilt the specimen in a known sense until the defect is edge on (minimum image thickness)
- (4) obtain image and diffraction patterns at this tilt and determine the crystallographic directions on the image.

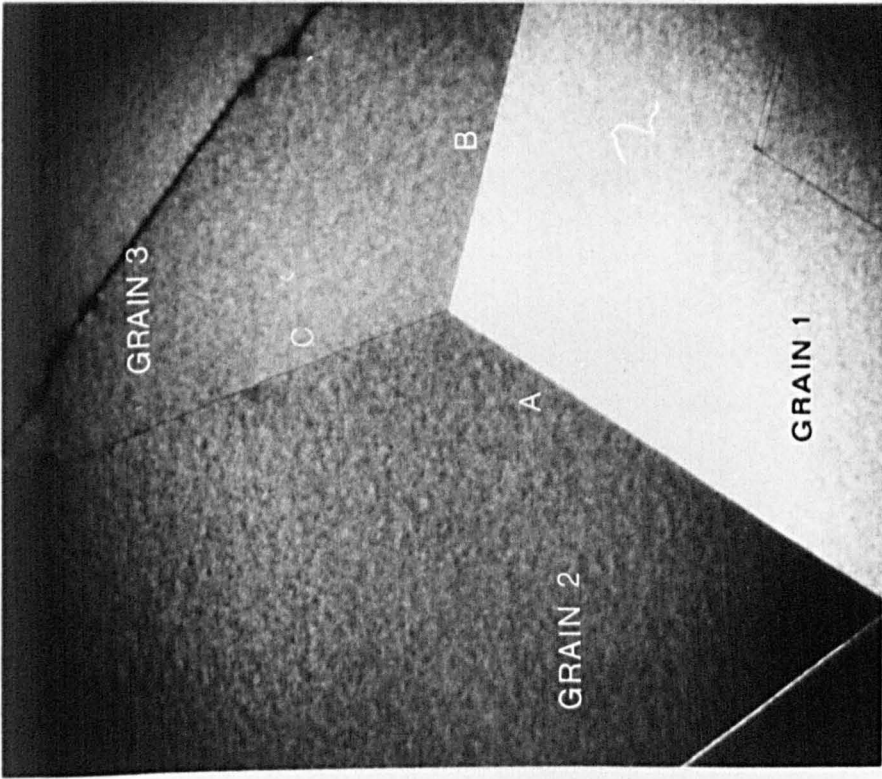
The 'edge-on technique' must be used in all cases where the geometry of the specimen permits it. Errors are generally  $\pm 0.5^\circ$ ; significant errors will always arise because the image of the boundary is influenced by the diffracting conditions and may remain constant over several degrees of tilt. For maximum accuracy a series of pictures and diffraction patterns should be taken at different angles of tilt and the projected width of the boundary measured to determine the position of minimum image width.

The 'edge-on technique' is now demonstrated by giving an example. Figure 9.1.2 shows the intersection of three grains being set in dynamical diffraction. The misorientation relationship across the boundary A as well as across the interface B was determined to be the CSL  $\langle 011 \rangle / 70.53^\circ$ ,  $\Sigma=3$  rotation. On the other hand, the misorientation relationship between grains 2 and 3 was found to correspond to  $\langle 011 \rangle / 38.94^\circ$   $\Sigma=9$ . The foil normal was determined for each crystal from a diffraction

Figure 9.1.2

A bright-field electron micrograph of an intersection of three growth twins in silicon. All the grains are diffracting. The boundaries A and B are coherent twins whereas the misorientation across the plane C is  $[011]/38.94^\circ, \Sigma=9$ .





0.5 μm

pattern at zero tilt. Then, the specimen was tilted (in a known direction) until the boundary plane width was a minimum (figure 9.1.2) In the diffraction pattern at the angle of tilt the  $\underline{g}=[11\bar{1}]_2$  reflection was (after allowing for image/diffraction pattern rotation) within  $1^\circ$  of the perpendicular to the trace of the twin boundary A. Furthermore, the angle of tilt measured on the goniometer stage was within  $1^\circ$  of the angle between the foil normal and  $(11\bar{1})_2$ . Consequently, the boundary plane was concluded to be  $(11\bar{1})_2$  which is the coherent twin plane in diamond-structure-type materials (Köhn, 1958; Fontaine & Rocher, 1979). Similarly, the normal to the boundary plane C was determined to be  $[\bar{1}2\bar{2}]_2/[\bar{1}2\bar{2}]_3$ ; this is in full agreement to the observation by Krivanek, Isoda & Kobayashi (1977) as was pointed out by Pond (1980a).

- - -

- Footnotes 1: The treatment given here refers to the more general case. A number of special techniques have, however, been developed relying on particular diffraction conditions being satisfied (see, for example, Lange, 1967; Young, Steele & Lytton, 1973; Clark, 1976).
- 2: In the latter case the interface plane as well as particular image characteristics often provide a check of the misorientation relationship.
- 3: The graphical method (due to Goux, 1961, 1974) is only accurate to  $1^\circ$  at best, which is not sufficient for reliable analysis of grain boundary structure.
- 4: The subscript denotes the crystal system relative to which the directions (and planes) are expressed.

## 9.2 Method for measuring the rigid-body translation across a grain boundary

It was mentioned above that due to the misorientation relationship across the interface various diffraction modes may occur depending on

which set of atomic planes and in which crystal are orientated for diffraction. Here the 'same  $\underline{g}$  condition' is considered and its application is briefly examined.

### 9.2.1 The principle of the method

The same  $\underline{g}$  condition is of great importance in the case of interfaces between coincidence related crystals and it can be used when there are two parallel, low-index, directions in the two crystals<sup>1</sup>. When these planes are set into Bragg condition then, if they are continuous across the interface, no contrast is observed. Any rigid-body translation,  $\underline{R}$ , between the two crystals (that is not a DCS lattice vector) will give rise to stacking-fault-like fringes in the plane (Pond & Smith, 1974) equivalent to that of a stacking fault or anti-phase boundary in a single crystal, and exhibiting the same quantitative behaviour (Pond, Smith & Clark, 1974). Relative translation,  $\underline{R}$ , between the crystals is known to be an important mode of relaxation in grain boundaries (Pond & Vitek, 1977).

The features expected in the interface image where there is a rigid-body translation  $\underline{R}$  are summarized in table 9.2.1. They can be deduced by the following considerations. The existence of  $\underline{R}$  involves that the planes used for imaging the boundary are offset on either side of the boundary plane. This introduces a phase shift between the Bloch waves traveling in the upper crystal, and those below the interface in the lower crystal and consequently the amplitudes of the diffracted components of the Bloch waves at the interface are modulated by a factor  $\exp(i\alpha)$ , where  $\alpha=2\pi\underline{ngR}$  the phase factor due to the rigid-body displacement.

The nature of the relative displacement  $\underline{R}$  can be understood in terms of the structural model of CSL boundaries by reference to figure 9.2.1.

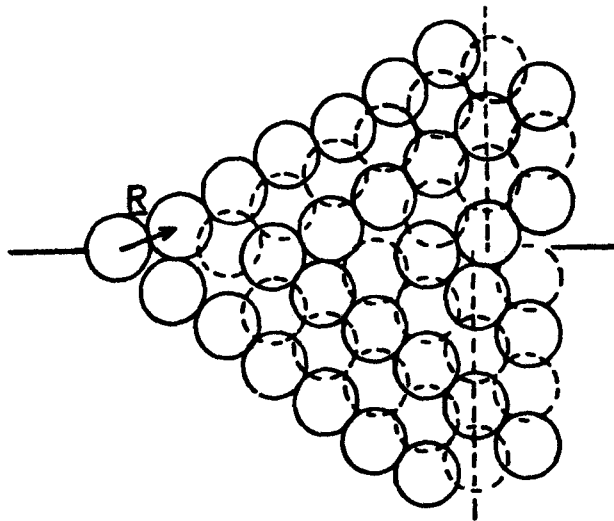
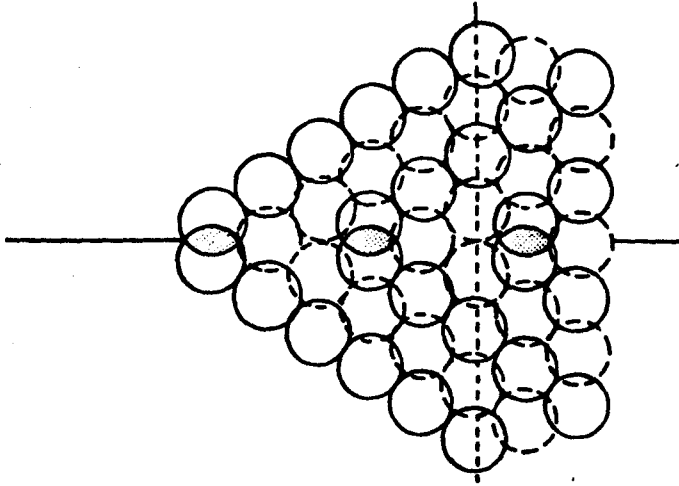
TABLE 9.3.1

Characteristics of the boundary image where there is a rigid-body translation  $\underline{R}$

Bright field image	Dark field image
Fringes parallel to the intersection of the interface and the foil surface	As in bright field image
Symmetrical image, absorption dampens out fringe contrast in the centre of the foil	Asymmetrical image
Performed by $\underline{g}_c$	If performed by $\underline{g}_c$ then the fringe at the top of the foil is the same as in bright field; the fringe at the bottom shows opposite contrast as in bright field image
Fringe contrast is a function of $\underline{E}_g$ , $w$ , and total thickness of the specimen	As in bright field image
In thin sample area the profile consists of a superposition of two sets of fringes, one having periodicity $\underline{E}_g^{eff}$ , the other $\underline{E}_g^{eff}/2$	
On a positive print the fringe at the top is bright for $\underline{g}\underline{R} > 0$ and dark for $\underline{g}\underline{R} < 0$	

**Figure 9.3.1**

The structure of a CSL grain boundary. In the top figure the boundary separating the two crystals is drawn with the atoms represented as hard spheres. Dashed spheres are  $\pm a/4 [110]_{1/2}$  out of the page. Atoms from the two crystals overlap at the boundary in the hatched region and this might be expected to increase the boundary energy. A means of avoiding the overlap is to displace one crystal relative to the other by  $\underline{R}$  (bottom figure). It is emphasized, however, that this figure does not represent an exact solution (no relaxations of individual atoms have been superimposed on the translation, for example), but is merely intended to illustrate qualitatively the type of translation that may occur.



Computer simulation indicates that the configuration in figure 9.2.1a has a high energy mainly because of the 'overlapping' of atoms. Furthermore, it was found that a major reduction in interfacial energy can be achieved by a rigid-body relaxation (figure 9.2.1b).

The vector  $\underline{R}$  can be resolved into two components:  $\underline{R} = \underline{t}' + \underline{e}$ . The displacement  $\underline{t}'$  corresponds to a vector which shifts the lower crystal away from the coincidence position in a direction parallel to the interface while the component  $\underline{e}$  represents a local expansion normal to the boundary plane<sup>2</sup> (i.e. it introduces excess volume into the interface compared to a perfect crystal).

### 9.2.2 Limitations of the method

Using the above experimental technique the total displacement  $\underline{R}$  can be measured, and in certain circumstances the constituent components can be measured separately. Three experimental requirements are, however, essential for a reliable determination of  $\underline{R}$  (Pond & Smith, 1974; Pond, 1979):

- (1) the adjacent crystals must be orientated very close to a coincidence relationship. Deviation from the exact CSL misorientation introduces complications in image contrast due to the presence of dislocations or moiré effects.
- (2) it is important that only common beams are excited. Sutton & Pond (1978) have shown that if there are non-common reflections present in the diffraction pattern (other than 000) then two sets of thickness fringes are expected and in this case no information about the translation at the boundary can be obtained.
- (3) the common reflections used must be relatively low index

or fringe intensity is low and ambiguity in the determination of  $|\underline{g}_c \cdot \underline{R}|$  may arise (Pond, 1979).

The translation  $\underline{R}$  does not, in general, have low indices, and, hence, it may not be possible to satisfy the ' $\underline{g} \cdot \underline{R} = 0$  criterion' for two, or sometimes even for one, reflection. Therefore, the direction and magnitude of  $\underline{R}$  must be confirmed by other means<sup>3</sup>. This can be achieved by comparing the observed fringes with those calculated from multi-beam dynamical theory, using the boundary parameters as input (Sutton, 1977; Pond, 1979). The calculated fringes may be output as fringe profiles (Humphreys, Howie & Booker, 1967) and matched to microdensitometer traces of the micrographs or the 'half-tone' method of Head *et al.* (1973) may be employed. Both these techniques will determine  $\underline{R}$  fully provided that the following two conditions are satisfied.

Firstly, the values of  $\underline{g} \cdot \underline{R}$  must be determined absolutely, and not just simply expressed modulus 1. Pond (1979) has outlined the limits of  $\underline{g} \cdot \underline{R}$  for which  $\underline{R}$  may be considered unambiguously determined. For the  $\Sigma=3$  boundary these limits are  $-0.5 < \underline{g} \cdot \underline{R} < 0.5$  for  $\underline{g}=111$  type,  $-1/3 < \underline{g} \cdot \underline{R} < 1/3$  for  $\underline{g}=220$  type and  $-1/12 < \underline{g} \cdot \underline{R} < 1/12$  for  $\underline{g}=311$  type.

Secondly, the boundary must be imaged in three non-coplanar diffracting vectors  $\underline{g}_i$  ( $i=1,2,3$ ). The value of  $\underline{g}_i \cdot \underline{R}$  is then determined for each reflection either by obtaining  $\underline{g}_i \cdot \underline{R} = n_i$  or by image matching for  $\underline{g}_i \cdot \underline{R} \neq n_i$ . Let  $\underline{G}$  the  $3 \times 3$  matrix with the  $\underline{g}_i$  vectors in orthogonal coordinates written as rows,  $\underline{R}$  the column vector with the components of  $\underline{R}$  in orthogonal coordinates and  $\underline{U}$  the column vector with the values of the scalar products  $\underline{g} \cdot \underline{R}$ , then  $\underline{G} \cdot \underline{R} = \underline{U}$ . The latter matrix equation yields a (non-trivial) solution for  $\underline{R}$  only when  $\det(\underline{G}) \neq 0$ , or, in other terms, when the diffracting vectors are non-coplanar.



### 9.2.3 The sensitivity of the technique

Concluding this section it is appropriate to indicate the sensitivity of the technique in determining  $\underline{R}$ . Theoretical calculations undertaken by Humphreys et al. (1967) show that a detectable change in contrast (minimum  $\pm 10\%$  of background) could be obtained from values of  $\underline{g}\cdot\underline{R}$  which differ from an integer by  $\pm 0.02$  or more. This implies that for a  $\langle 220 \rangle$  type vector displacements as small as  $0.03\text{\AA}$  could be detected. In other words, a resolution comparable with the wavelength of the 100kV electrons.

It is emphasized, in view of the earlier remarks made about the sensitivity of the fringes to  $E_g$ ,  $w$  and the foil thickness that these quantities must be determined accurately in order to maximize the overall sensitivity of the method. Provided that this is done the sensitivity in determining  $\underline{R}$  depends on:

- (1) the  $\Delta(\underline{g}_c \cdot \underline{R})$  value, i.e. the change of  $\underline{g}_c \cdot \underline{R}$  which is necessary to produce a certain change of contrast of any fringe (whether subsidiary or main) in the simulation profile, and,
- (2) the finite size of the slit width in the microdensitometer which influences directly the sensitivity of the instrument.

The effect of these factors on the overall sensitivity in determining  $\underline{R}$  has been considered by Sutton (1977) who concluded that it is not possible to define a generalized sensitivity for the method.

- - -

- Footnotes
- 1: These directions correspond to planes of the CSL.
  - 2: The complete crystallographic formulation has been given by Pond (1977).
  - 3: At a grain boundary  $\underline{R}$  must be determined absolutely and not, unlike the stacking fault displacements, be distinguished between several values.

## Chapter 10

### TWIN BOUNDARIES IN SILICON

#### Introduction

The observations reported herein were made on silicon specimens prepared from bulk of polycrystalline silicon kindly supplied by Dr. A.G. Cullis of the Royal Signals and Radar Establishment (the sample preparation methods are discussed in appendix 15). The specimen was examined in a JEOL, model JEM 200B, scanning-transmission electron microscope operating at 150 kV. Thus, the accelerating voltage was well below the threshold voltage for electron bombardment damage in silicon of  $\approx 180$  kV (Fraser, 1977).

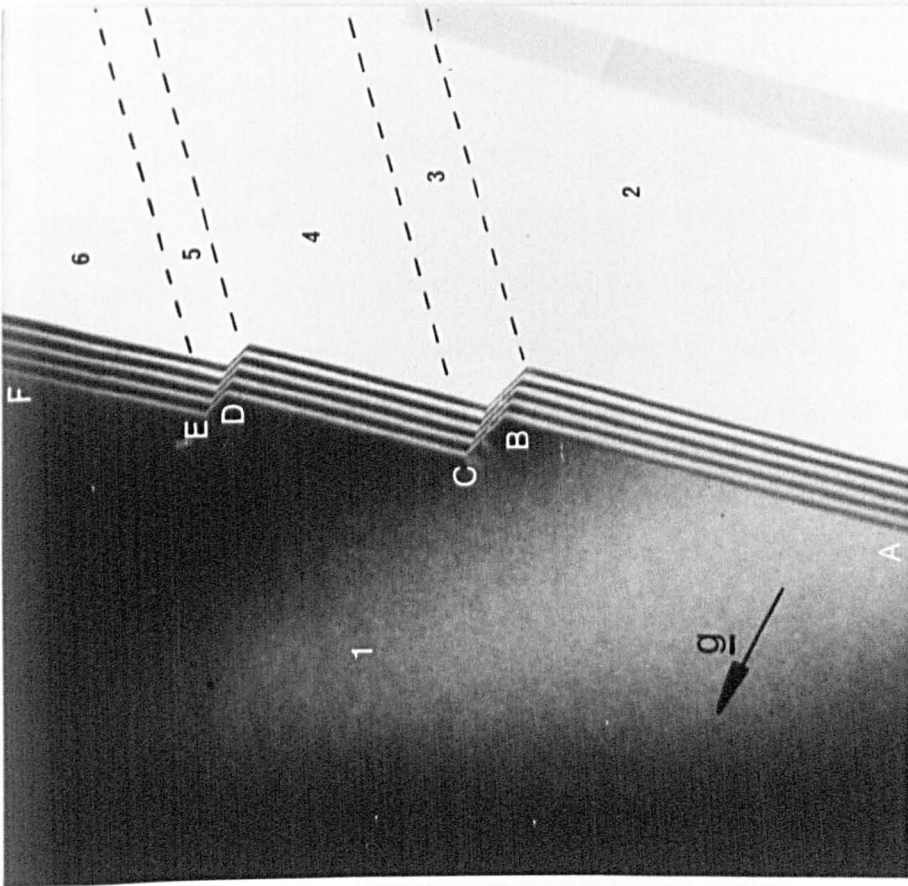
The main objective of the experimental work was the investigation of the structure of the twin boundaries in silicon. Speaking more accurately, it was sought to establish: (1) the geometrical parameters, and, (2) the rigid-body displacements for twin boundaries. The need to determine the former is self-explanatory and the techniques outlined in section 9.2 were used for this. The measurement of the rigid-body displacements is necessary, apart from the geometrical parameters, for an unambiguous determination of the grain-boundary structure. This is carried out by employing the method in section 9.3 and the determination of the rigid-body movement for two  $\Sigma=3$  boundaries is given in this chapter. In the first case the interface is the coherent twin while the second example refers to the  $\{211\}$  incoherent twin boundary.

#### 10.1 The $\Sigma=3$ , $\{111\}$ twin

The coherent twin in silicon being a simple case, from the crystallographic point of view, is the first case presented. Micrograph 10.1.1 shows a sample area where six grains meet. The interfaces AB, BC, CD,

Figure 10.1.1

A bright-field electron micrograph of growth twins in silicon. Grain 1 is in a two-beam diffraction condition and the other is diffracting negligibly. The boundary planes AB, CD, and EF have been indexed as  $(111)_1$  planes.



0.5 μm

DE and EF are inclined relative to the electron beam and are imaged with two-beam dynamical conditions in grain 1 and kinematical conditions in the other grains, that is  $g$  is very large on all reflections. Under these conditions the boundaries are visible as conventional thickness fringes (Pond, Smith & Clark, 1974).

#### 10.1.1 Determination of the interfacial crystallography

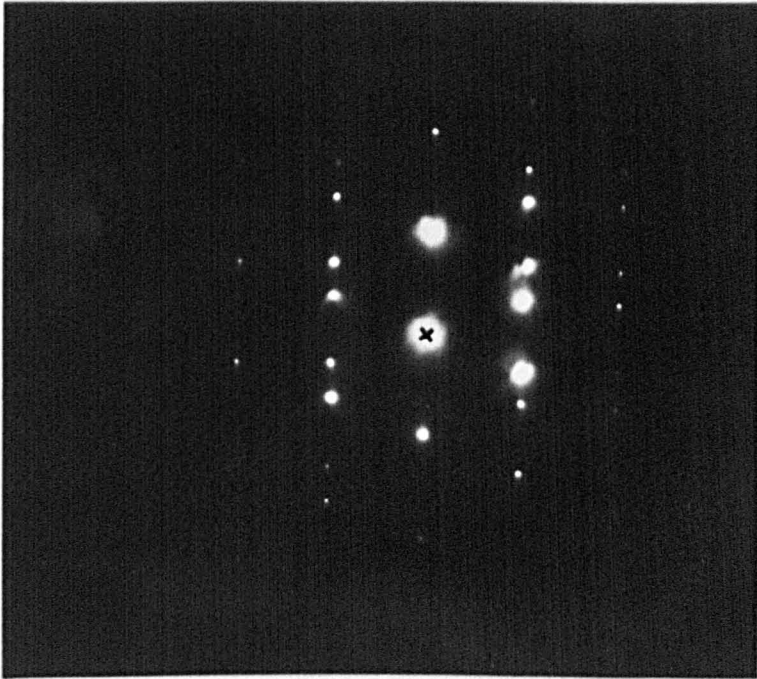
The misorientation between crystals 1 and 2 has been calculated from four pairs of parallel directions plus their cross-products. All the beam directions have been determined by the method of appendix 12 and the misorientation matrix has been calculated by the least-squares method in appendix 13. This matrix indicates no detectable deviation from the exact coincidence orientation  $[011]/70.53^\circ$ ,  $\Sigma=3$ . Since no dislocations of any kind were observed in this interface at any time during the course of this experiment the misorientation was taken to be the exact  $\Sigma=3$  CSL misorientation.

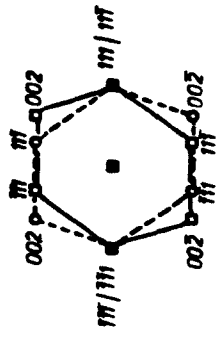
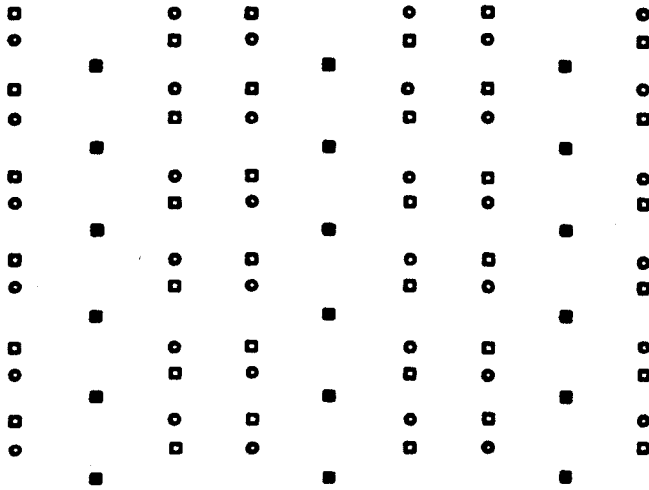
Similarly, the misorientation between crystals 1 and 4 as well as between 1 and 6 were found to be related by a rotation of  $70.53^\circ$  about a common  $\langle 011 \rangle$  axis. The misorientation relationships are not expressed by the lower angle description  $\langle 111 \rangle / 60^\circ$  (see e.g. Acton & Bevis, 1971); this is because the geometry of the particular specimen allowed the rotation axis to be determined unambiguously. The diffraction pattern in figure 10.1.2a has been recorded by placing the selected area aperture across the interface AB. This pattern corresponds to a superposition of two  $[1\bar{1}0]$  diffraction patterns related by a rotation  $70.53^\circ$  along the common  $[1\bar{1}0]$  axis (figure 10.1.2b).

The misorientation across the other interfaces could not be measured since grains 3 and 5, being in fact microtwins, were considerably narrow.

Figure 10.1.2

- (a) Diffraction pattern from silicon twinned on (111); the beam direction  $\underline{B} = [\bar{1}\bar{1}0]$  is common to both the matrix and the twin crystals
- (b) A schematic representation of the spot pattern. Matrix spots are shown by open squares, twin spots as open circles and common spots by filled squares. The two superimposed spot patterns are related by a rotation  $70.52^\circ$  along the beam direction (insert).





$B = [1\bar{1}0]_{\text{common}}$



An attempt to record diffraction patterns with the selected area aperture straddling the boundary was not successful because the intensity of the Kikuchi lines originated from grain 3 was very low and the required exposure times involved that the strong Kikuchi lines from crystal 2, say, overlapped the weak ones.

In order to determine the boundary planes the specimen was set so the interfaces AB, CD, and EF were parallel to the tilt axis of the microscope and the foil normal was determined from the diffraction pattern at zero tilt. Then the specimen was tilted in a known direction until the boundary plane width was a minimum (figure 10.1.3). In the diffraction pattern at the angle of tilt the  $111_1$  reflection<sup>1</sup> was very strong and, after allowing for image rotation  $111_1$  was within  $1^\circ$  of the perpendicular to the line of the twin boundary. Furthermore, the angle of tilt measured on the goniometer stage was within  $1^\circ$  of the angle between the foil normal and  $111_1$ . Consequently, the boundary plane may be concluded to be  $(111)_1$  which is the coherent twin plane in diamond-structure-type materials (Köhn, 1958; Fontaine & Rocher, 1979). The latter indicates that the established interface planes are in complete agreement with the measured misorientation relationship across the boundaries AB, CD, EF.

#### 10.1.2 Determination of the rigid-body displacement

Figure 10.1.4 shows the CSL unit cell in the  $\Sigma=3$  system; this is hexagonal with the  $[111]_1/[1\bar{1}\bar{1}]_2$  direction along the c-axis. In reciprocal space a lattice of common diffraction spots exists (figure 10.1.4b) whose orientation, symmetry and dimensions are related to those of the CSL. Figure 10.1.5 shows the schematic representation of the  $(11\bar{2})_1/(\bar{1}\bar{1}2)_2$  diffraction pattern; all the reflections in this pattern are common to

Figure 10.1.3

Bright-field image in which the boundaries are tilted edge on.  
All the boundaries are diffracting; the diffraction pattern across  
the interface AB is shown in figure 10.1.2.

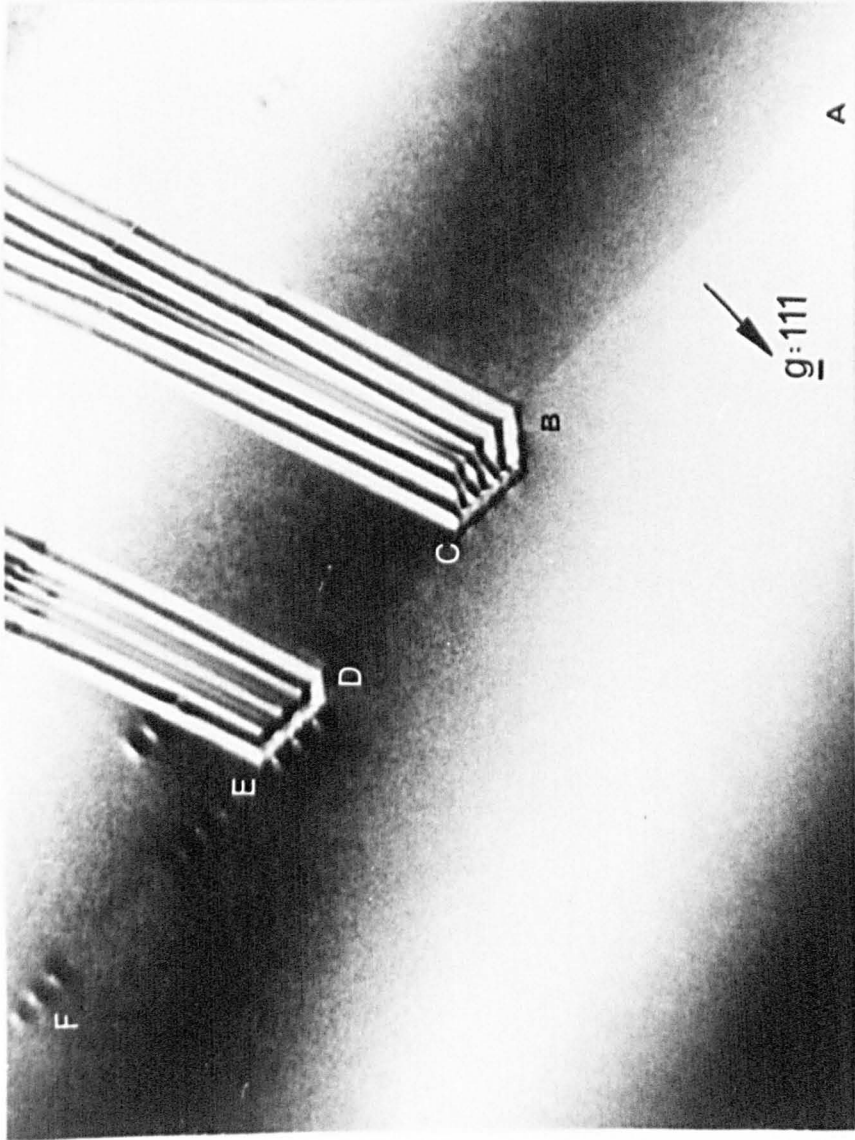


Figure 10.1.4

- (a) The geometry of the  $\Sigma=3$  coincidence lattice cell in silicon.  
The height of the cell is three (111) interplanar spacings
- (b) The geometry of the lattice of common diffraction spots for the  $\Sigma=3$  twin.

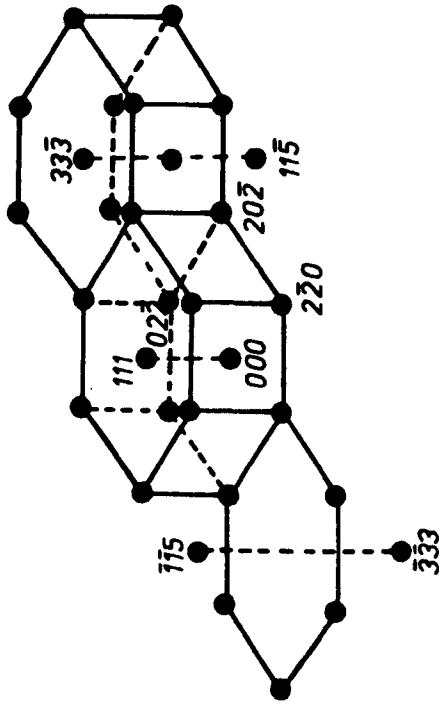
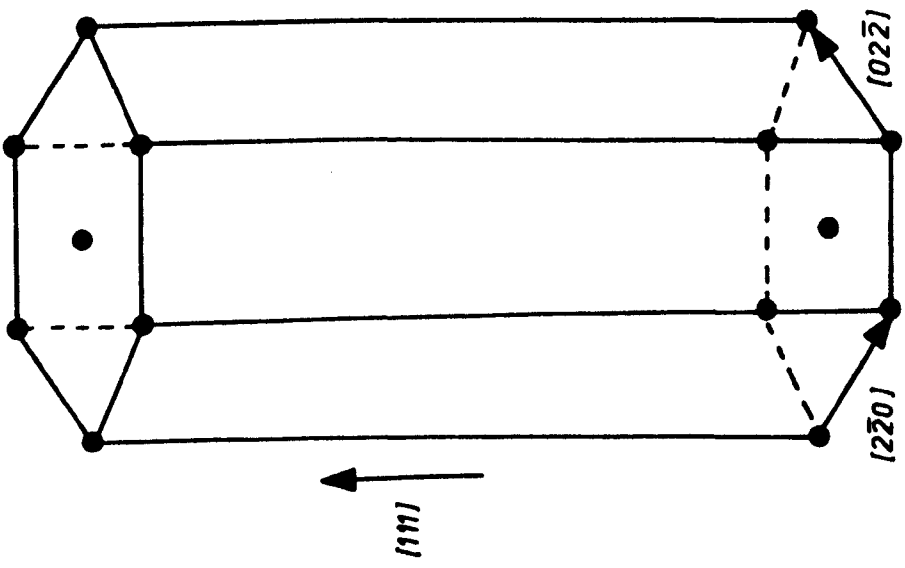
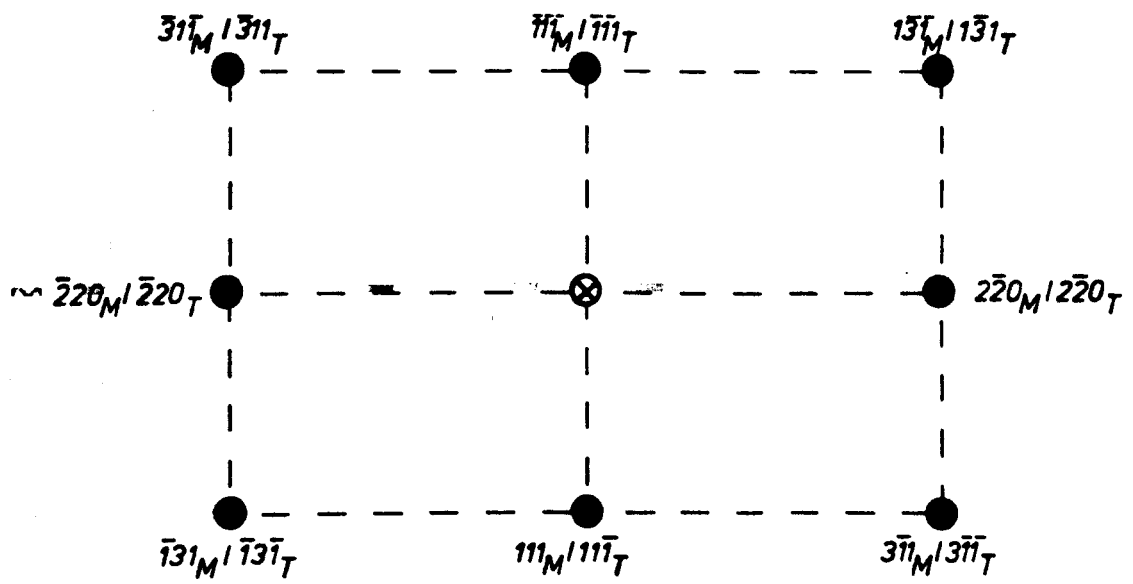


Figure 10.1.5

Schematic representation of  $(11\bar{2})_M / (\bar{1}\bar{1}2)_T$  diffraction pattern.



$$B = [\bar{1}1\bar{2}] / [\bar{1}\bar{1}\bar{2}]$$

both crystals. Thus, these spots may be used to image the boundary in order to detect any rigid-body translation.

The analysis of the translation fringes was undertaken in two stages, as the discussion in section 9.2 might suggest. Firstly, the boundary was examined in reflections such as  $2\bar{2}0_1/2\bar{2}0_2$  which are orthogonal to the  $(111)_1/(1\bar{1}\bar{1})_2$  plane. From the image behaviour in these reflections the in-plane translation,  $\underline{t}$ , is determined. The images in figure 10.1.6 were taken by using the common reflection  $\underline{g}_c = 2\bar{2}0$  (i.e.  $\underline{g}_c$  is perpendicular to the coherent boundary normal  $[111]_1$ ). No stacking-fault-like fringes are observed in the boundary and therefore there is no component of displacement parallel to  $[2\bar{2}0]_{1,2}$ . Similarly, no fringes were detected using  $\underline{g}_c = 2\bar{2}0_1$ . This means that no relative displacement parallel to the interface exists.

In order to detect any displacement normal to the boundary common planes inclined to the interface were used. The image in figure 10.1.7 shows the contrast observed using  $\underline{g}_c = 1\bar{3}1_1/3\bar{1}1_2$ , and again no fringes are detectable across the boundary. Taking into account the sensitivity of the method (see, for example, Sutton, 1977) it is concluded that if there is a normal displacement then this must be less than 5% of the interplanar spacing of  $\{113\}$  planes. Therefore, in the case of coherent twins in silicon no (parallel or normal) relative displacement exists. This is now examined in terms of the interfacial structure.

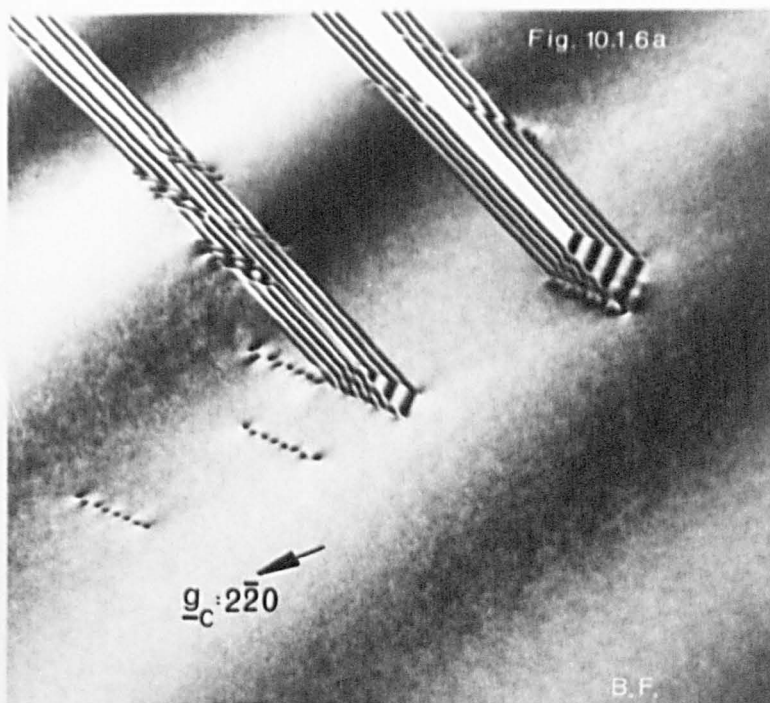
### 10.1.3 The structure of the coherent twin in silicon

The structure of the coherent twin in diamond-structure materials, projected on  $(1\bar{1}0)$ , is shown in figure 10.1.8. The large circles are atoms in the  $(1\bar{1}0)$  plane passing through the origin of the unit cell; the small ones are atoms in a  $(\bar{1}\bar{1}0)$  plane separated from the first by



Figure 10.1.6

Bright- and dark-field micrographs in a common two-beam condition of the coherent twin in silicon. No fringe contrast is visible along the  $(111)_1$  interfaces.



0.5  $\mu\text{m}$

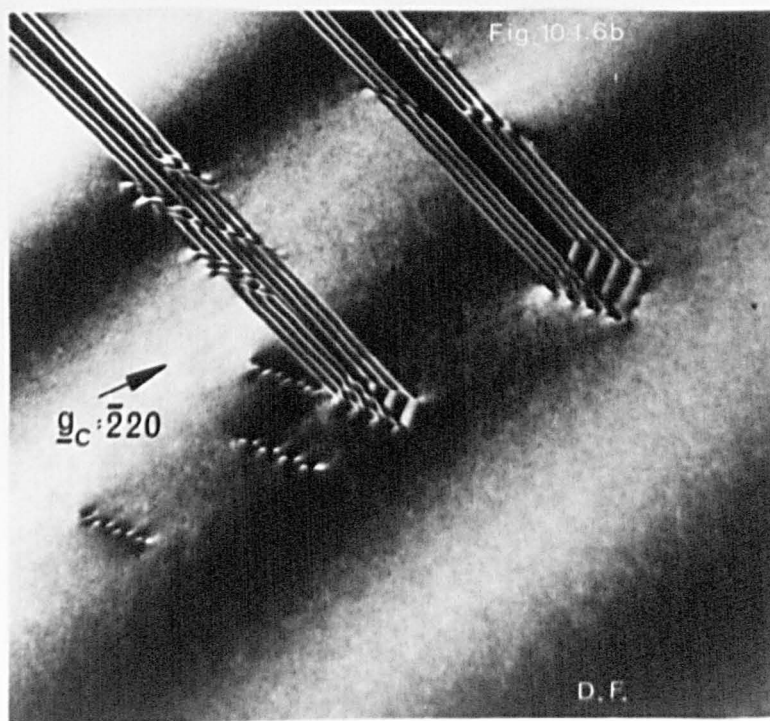
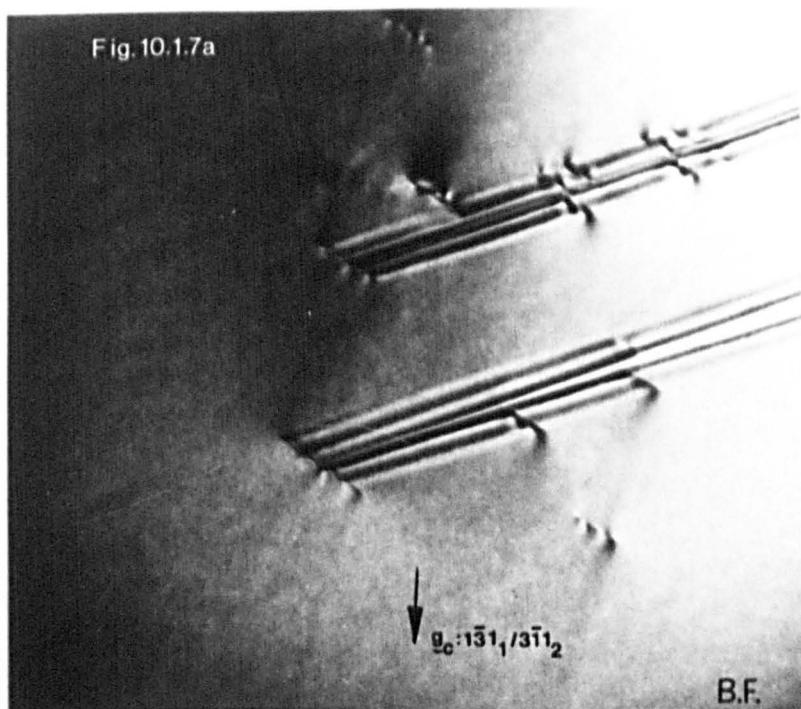


Fig. 10.1.7a



0.5  $\mu\text{m}$

Fig. 10.1.7b

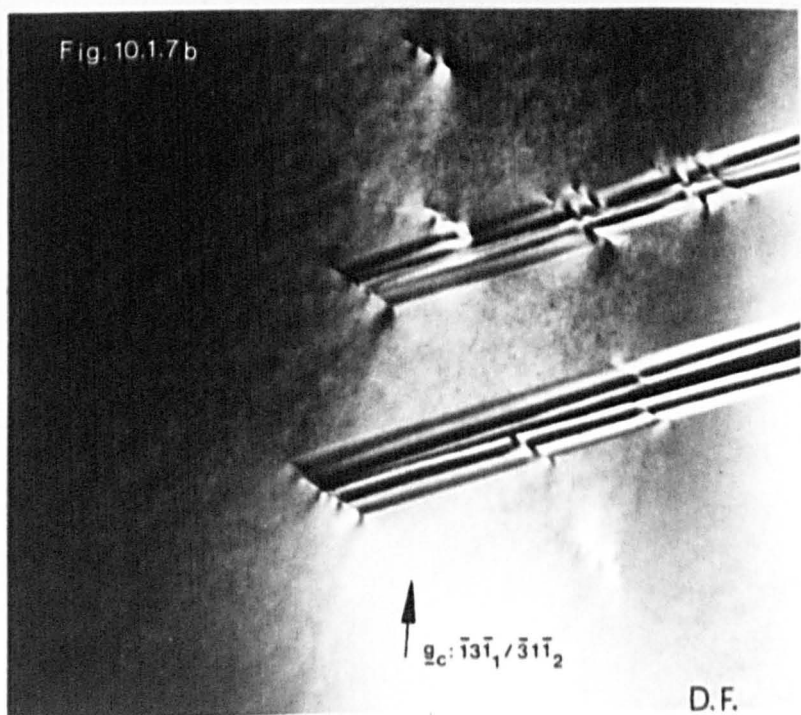
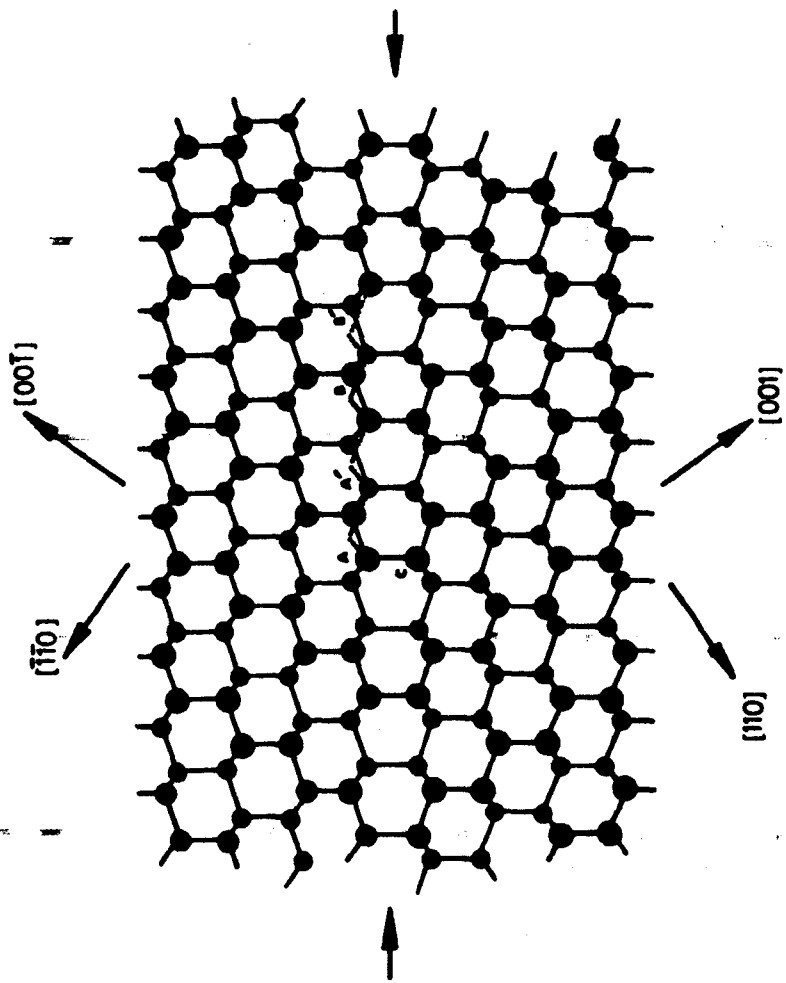


Figure 10.1.8

The atomic configuration of the coherent twin boundary (indicated by the arrows) in diamond-structure type silicon projected along  $[1\bar{1}0]$ .

Key: Large circles: sites in page

Small circles: sites  $\sqrt{2}a/4$  above page



a quarter of a cell diagonal. The matrix and the twin are related by a rotation of  $70.52^\circ$  about the normal to the figure. The following can be seen from this figure.

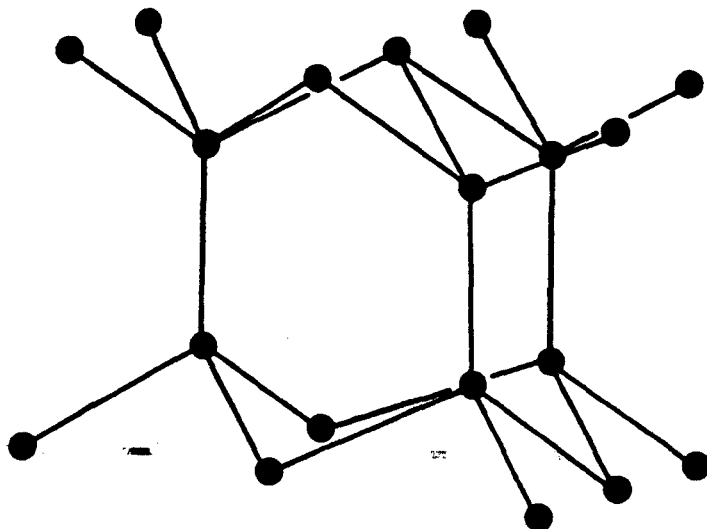
The atomic configuration of the single crystal can be described as six-sided arrays of atoms along the  $[011]$ . Along the unit length of the twin boundary the proposed structure offers, instead, an altered six-sided array. Any atom in the vicinity of the boundary has four nearest neighbors and, there are no dangling bonds across the coherent twin. It can be concluded, therefore, on the grounds of the discussion on the covalent bond energy given in appendix 16, that the energy of this interface is very similar to that of the single crystal.

A relative small increase in energy can be easily predicted in terms of deviations in the direction and/or the length of the bonds along the interface. At the atomic positions where such changes have taken place, the 'undistorted' bond direction is indicated by dotted lines in the figure 10.1.8. At points designated A and A' the bond has been rotated respectively into and out of the plane of the figure by  $57.1^\circ$ . The same occurs in points B and B'. The lengths of all these bonds are, however, unchanged (the twin plane is a mirror plane passing midway atoms A and C). If nearest neighbour interactions are only considered, then it is seen that the energy of each of the atoms A and B is identical to that of an atom in the untwinned material. For an atom in a single crystal the angles between the bonds are equal to  $109^\circ 28'$  and the bond lengths are  $0.433a$  ( $a$  is the lattice parameter). In the case of atom A (and B) the bond angles and lengths are identical but the bonds are differently orientated (figure 10.1.9). They are related to the undistorted configuration by a rotation  $[111]/180^\circ$  (an alternative

Figure 10.1.9

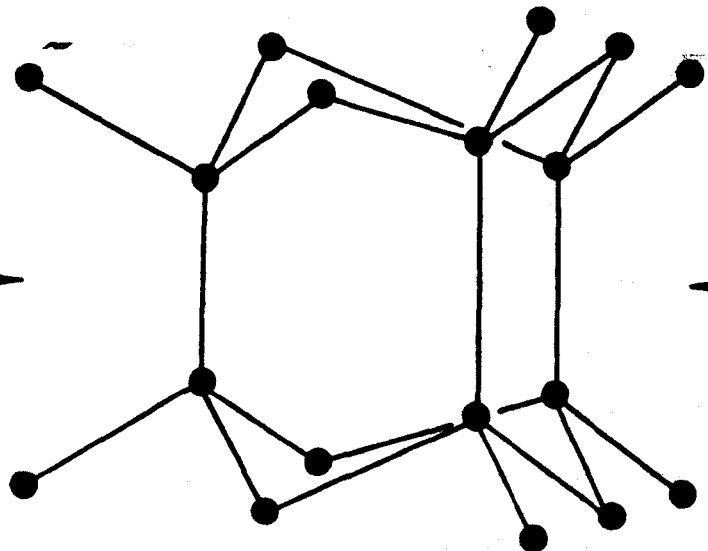
Atomic bonding in silicon: (a) single crystal

(b) across the coherent twin



(a)

boundary  
plane  
trace →



(b)



description of the  $\Sigma=3$  misorientation).

If interactions between atoms of second (and higher) coordinations are now considered the energy of the interfacial configuration increases; deviations from the undistorted structure occur for second (and higher) coordinations. As was, however, mentioned in appendix 16 the increases in the energy due to such deviations is relatively low. Its influence is so remote that it seems most unlikely that it could affect the structure (Buerger, 1945).

It is, therefore, concluded that the structure of the coherent twin in silicon is that given in figure 10.1.8. The low energy of this twin is due to the fact that the nearest neighbours are the same as in the perfect crystal. A similar situation can be found in the  $\Sigma=3$ ,  $\{111\}$  twins in f.c.c. metals. In the case of aluminium (Pond & Smith, 1974) and stainless steel (Pond, Smith & Clark, 1974) no relative displacement at all was observed. Negligible increase in the energy has been reported for coherent twins in copper (McLean, 1973) and nickel (Murr et al. 1970). Inasmuch as the diamond-structure-type materials are concerned no direct experimental evidence is to-day available. However, it is well-known that in diamond-structure-type materials twinning in  $\{111\}$  planes is very common (Slawson, 1950; Köhn, 1958; Fontaine & Rocher, 1979); this is easily explained by the low energy of the coherent twin. Furthermore, there have been several reports of results which support the low energy configuration of the coherent twins in silicon. The majority of such evidences are related to investigations of electrical behaviour of polycrystalline silicon. These studies are discussed in section 10.3.

- - -

Footnote 1: The subscript denotes the crystal coordinate system relative to which the particular direction is expressed.

## 10.2 The {211} incoherent twin

The second example of a  $\Sigma=3$  boundary in silicon refers to an incoherent twin. The micrograph 10.2.1 shows the area of observation; the interfaces are imaged with the common [011] axis parallel to the electron beam.

### 10.2.1 Determination of the interfacial crystallography

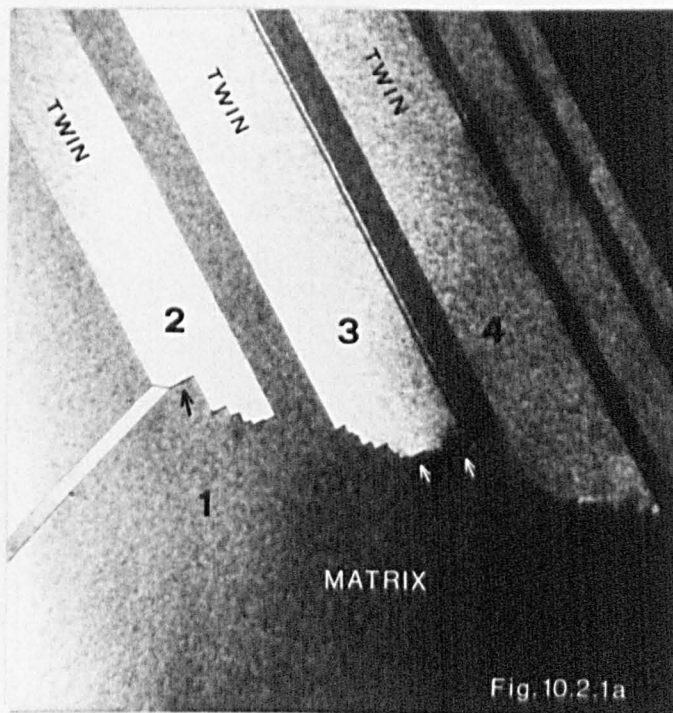
The misorientation between crystals 1 and 2, as well as between 1 and 3, and, 1 and 4 has been determined by the method given in appendices 12, 13 and 14. Again, no detectable deviation from the exact coincidence orientation  $\Sigma=3$  was detected, and, hence, it was taken to be the exact CSL misorientation.

In a study of this nature, where the proposed rigid-body translation is a function of the boundary plane, the accuracy with which the boundary plane may be indexed is of fundamental importance. In this case it was possible to tilt the specimen sufficiently to align the interfaces parallel to the electron beam, and, index them directly from the diffraction pattern (see figure 10.2.1). The relevant plane and line directions so determined are given in figure 10.2.1b.

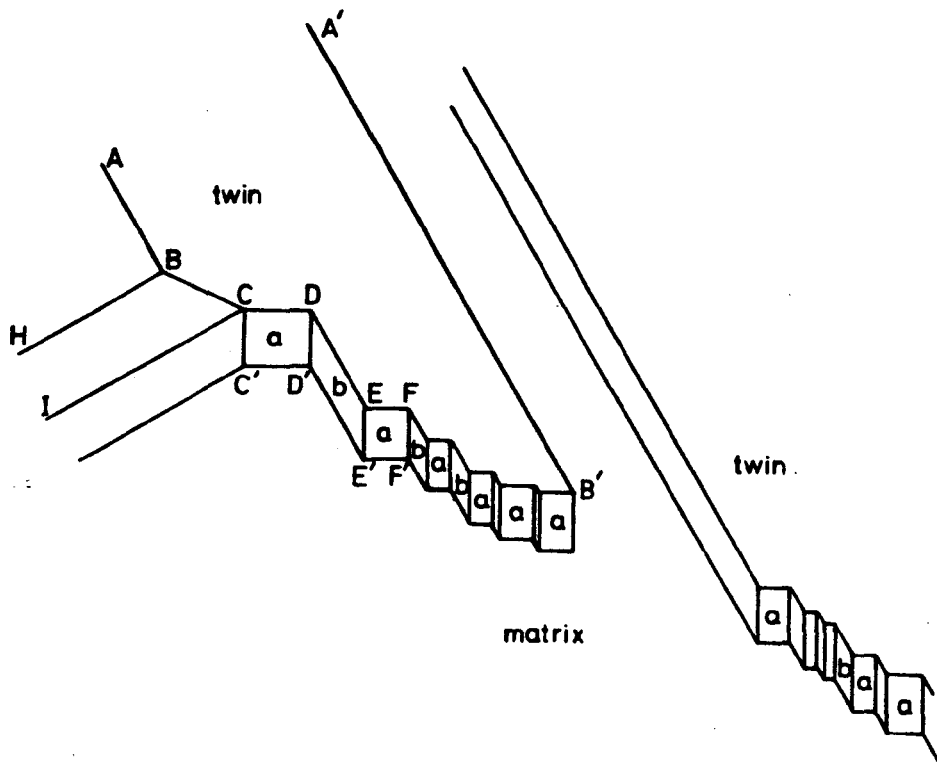
As an additional check the trace analysis (see section 9.1) was employed for the segments marked by arrows in figure 10.2.1a; the boundary planes were determined from 10 estimates for each facet, involving three separate tilts of the specimen in the microscope. The magnitudes of the tilts employed were large ( $\pm 40^\circ$ ) giving substantial variations in the length of defined vectors in the boundary plane, and increasing thus the accuracy of the method. Facets had the same boundary plane normal ( $2\bar{1}1$ ). In all cases the deviations were found to be less than  $\pm 1.0^\circ$ , which indicates a high degree of accuracy for a boundary plane determi-

**Figure 10.2.1**

- (a) Bright-field micrograph of coherent and incoherent twin boundary facets in silicon; all crystals are diffracting**
- (b) Sketch of the boundary geometry**



0.5  $\mu\text{m}$



Lines  $CC', DD', EE', FF'$ :  $[011]_M$

Lines  $AB, DE, GF, D'E'$ :  $[2\bar{1}\bar{1}]_M$

Faces  $a$ :  $(21\bar{1})_M$

Faces  $b$ :  $(1\bar{1}1)_M$

Face  $ICC'$ :  $(\bar{1}\bar{1}1)_M$

nation. It is concluded, therefore, that these facets are  $(21\bar{1})$  incoherent twins.

### 10.2.2 Determination of the rigid-body displacement

In order to determine the rigid-body displacement for the  $(21\bar{1})$  incoherent interfaces they were imaged by using reflections common to both the matrix and twin crystals. A wide variety of these spots were used to study the fringe behaviour as fully as possible. Since the reciprocal CSL lattices of the coherent and incoherent twins are identical the spots in the diffraction pattern of figure 10.2.2 are common and these spots can be used for determining the rigid-body translation in the incoherent twin.

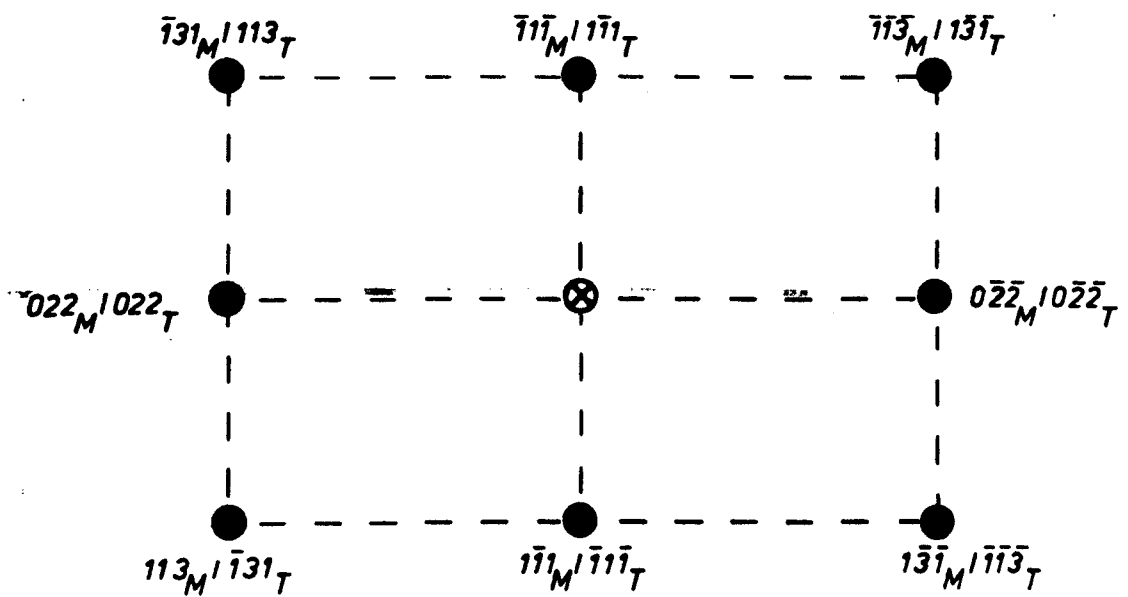
Figure 10.2.3 shows the bright and dark field micrographs obtained by using the common reflection  $\underline{g}_c = 1\bar{1}1_1 / \bar{1}1\bar{1}_2$ . The vector  $\underline{g}_c$  lies in the plane of the boundary  $(21\bar{1})$ . The observation of fringes for this reflection yields immediately that the two grains across the interface are displaced relative to one another. Moreover, since  $\underline{g}_c$  is in the interface plane, there is a component of the rigid-body translation parallel to the plane.

For the unambiguous determination of the total rigid-body displacement the translations giving rise to fringes for, at least, three non-coplanar diffraction vectors must be determined (see section 9.2). The specimen was, thus, orientated for the two-beam condition with  $\underline{g}_c = 022_1$ . No fringe contrast was observed for this setting. Since  $\underline{g}_c$  is on the boundary plane it is concluded that the only rigid-body displacement parallel to the interface is along the  $[1\bar{1}1]_1 / [\bar{1}1\bar{1}]_2$  direction.

Finally, the interfaces were imaged for  $\underline{g}_c = \bar{1}\bar{1}3_1 / \bar{3}11_2$  (figure 10.2.4); in this case  $\underline{g}_c$  is inclined to the boundary plane. The

Figure 10.2.2

Schematic representation of  $(2\bar{1}\bar{1})_M / (\bar{2}11)_T$  diffraction pattern

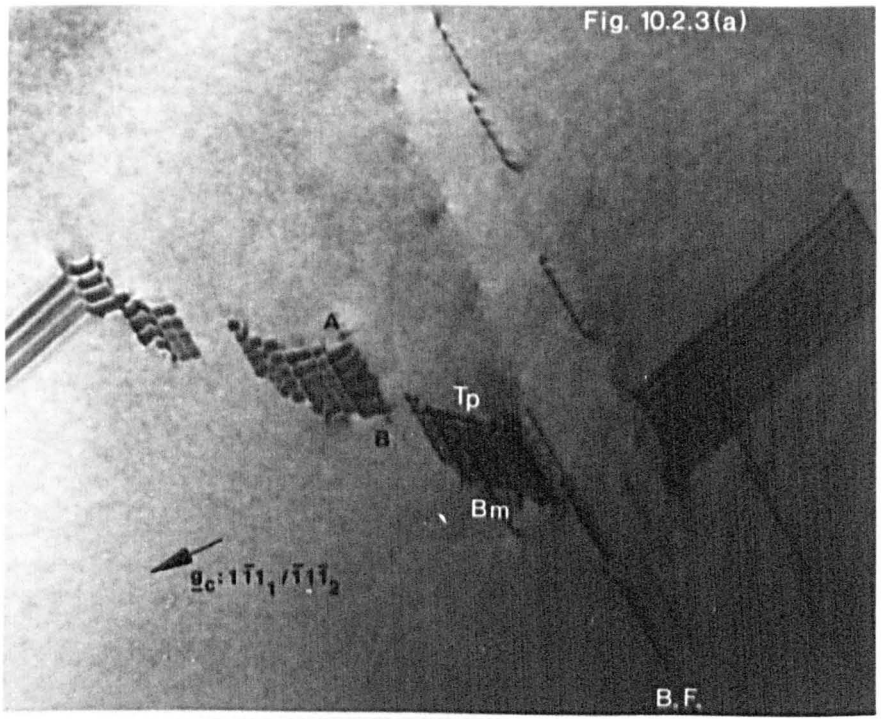


$$\underline{B} = [21\bar{1}] / [\bar{2}\bar{1}1]$$



**Figure 10.2.3**

Bright- and dark-field micrographs of the boundaries shown in figure 10.2.1 but with a common diffraction spot  $\underline{g}_c$  operating. The  $(2\bar{1}\bar{1})$  segments show stacking-fault like fringes and the  $(\bar{1}\bar{1}1)$  segments are out of contrast



0.5  $\mu\text{m}$

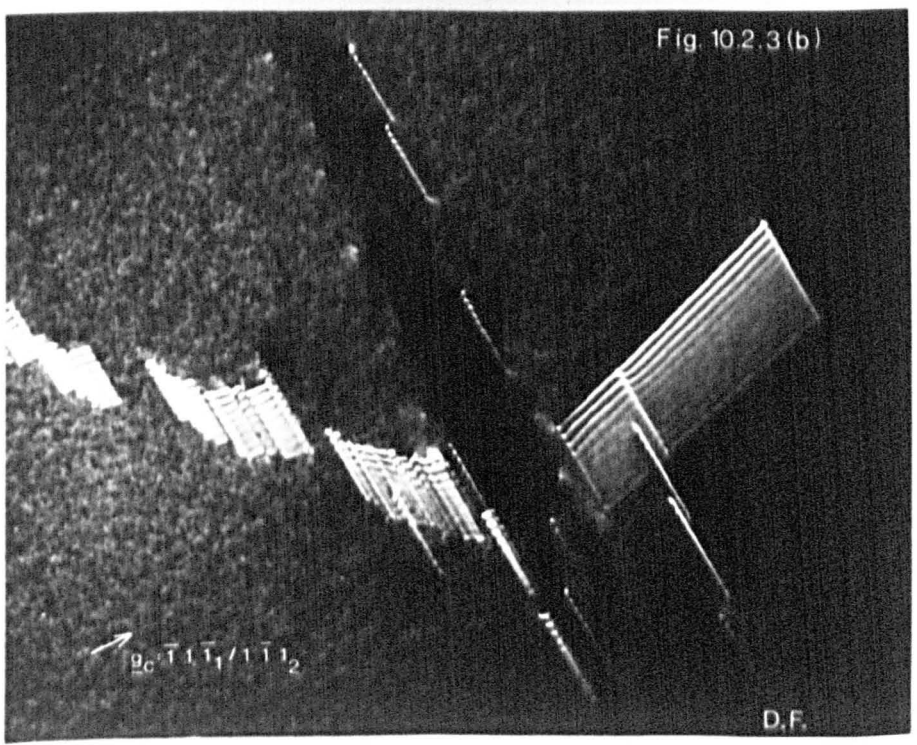
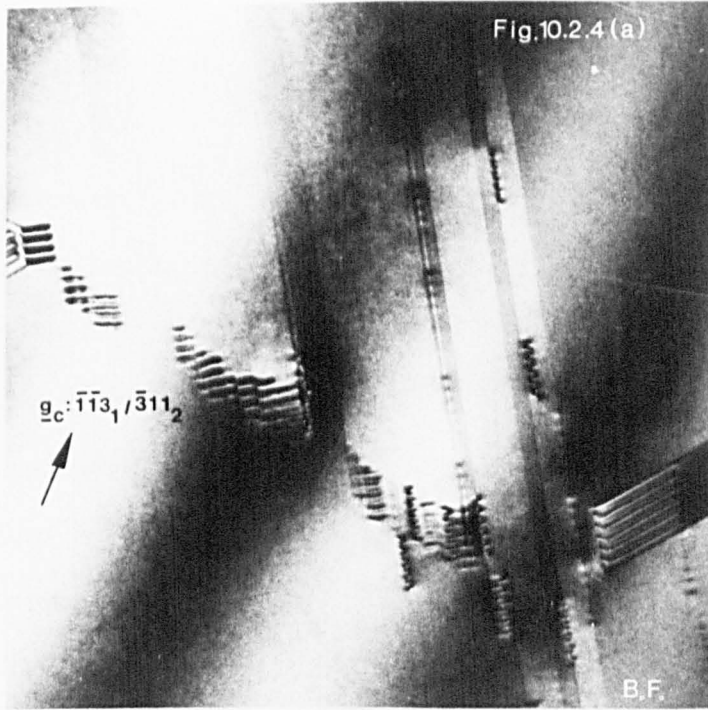
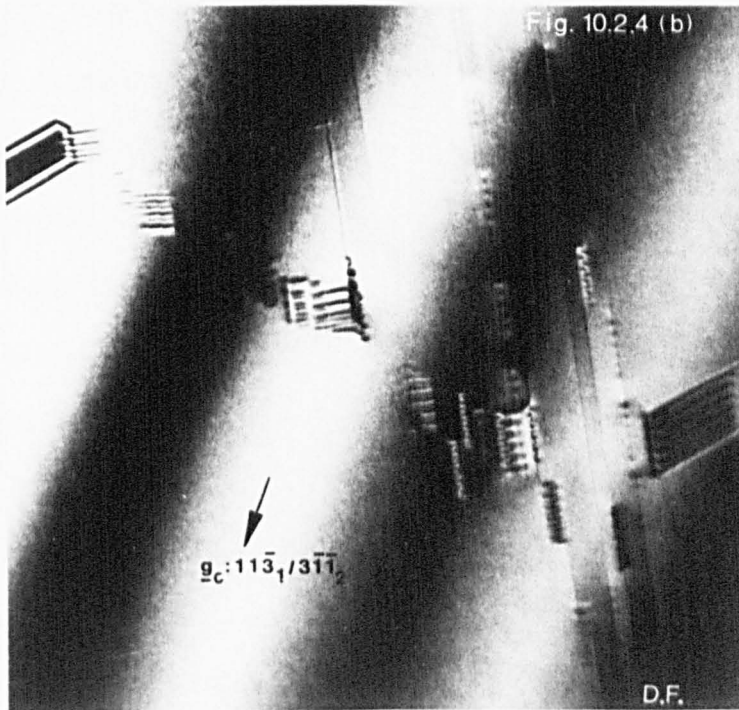


Figure 10.2.4

Bright- and dark-field micrigraps obtained with the 'same g  
condition' where g is inclined to the boundary planes



0.5  $\mu\text{m}$



presence of stacking-fault-like fringes to the boundary for this reflection yields that there may be a rigid-body translation perpendicular to the interface. This displacement (if exists) corresponds to an expansion; see section 9.2.

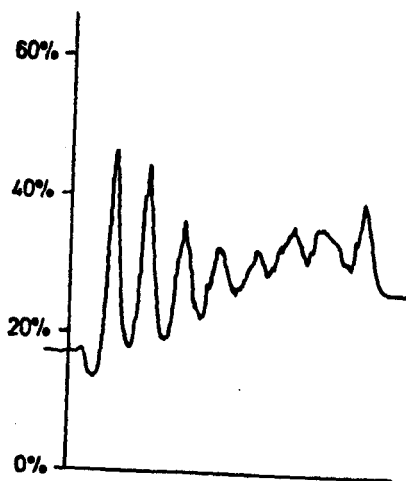
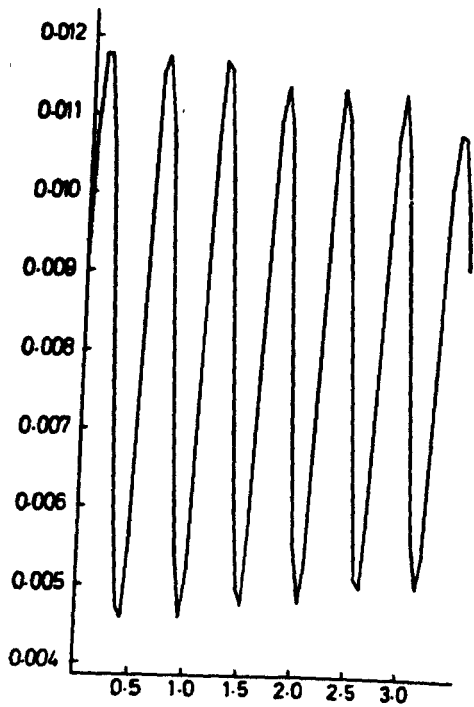
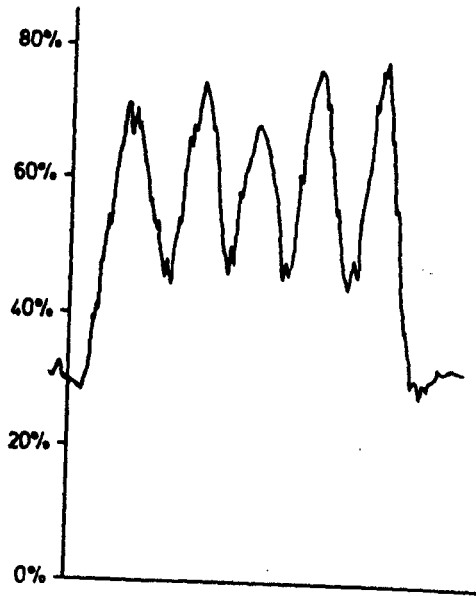
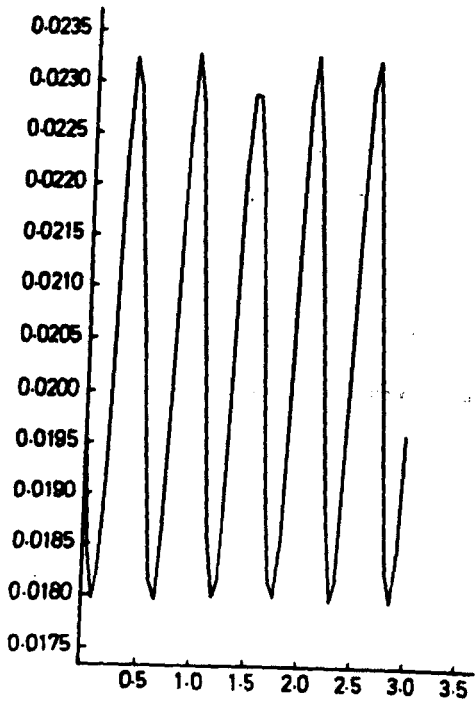
The components of the rigid-body displacement are determined by matching experimental and computer simulated intensity profiles. Figure 10.2.5 is a series of calculated intensity profiles and microdensitometer traces of the experimental fringes illustrated in figures 10.2.3 and 10.2.4. Microdensitometer traces were taken for the micrographs using a Hilger-Jaco machine. The slit width used to illuminate the photographic plates was 60  $\mu\text{m}$  which was typically 10% of the fringe width. The same scan across the plates was chosen for producing the traces and is from A to B in figure 10.2.3.

The computer simulated intensity profiles were calculated by a FORTRAN computer program, called STACKFAULT, written by Dr. P. Rez. This program uses many beam dynamical theory and the required input data are listed in table 10.2.1. The value of  $K_x$  (the component of the incident electron wave vector parallel to the surface of the foil) was calculated for each micrograph from the Kikuchi line positions on the corresponding diffraction patterns (see appendix 17). The thickness was measured by multiplying the number of fringes on micrographs obtained from good two-beam conditions by the relevant extinction distance; it was found to be  $4500 \pm 150 \text{ \AA}$ . Numerical values for the relevant extinction distances and anomalous absorption coefficients are given in appendix 17. The number of calculated points on each simulation was 100 (Sutton, 1977). The details of the simulations are given in table 10.2.3. By matching of the simulated and experimental profiles it was found that

Figure 10.2.5

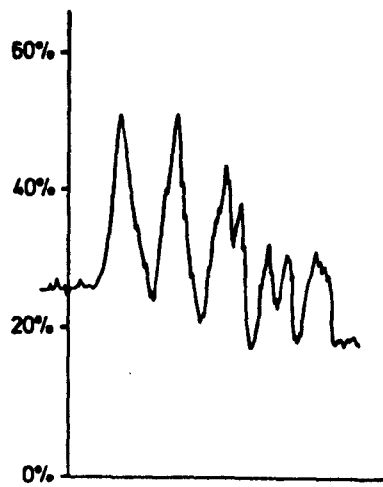
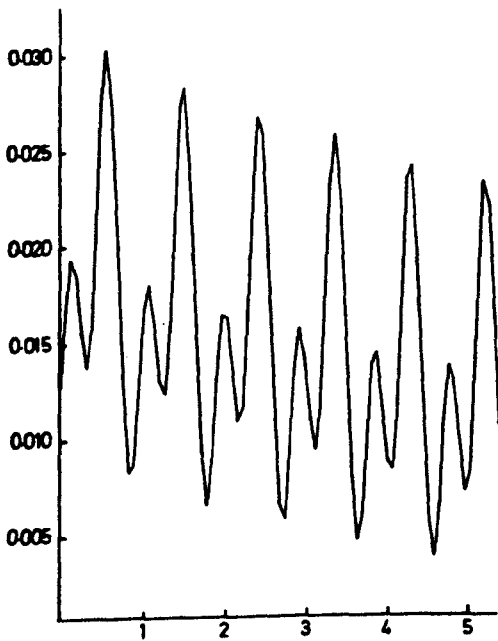
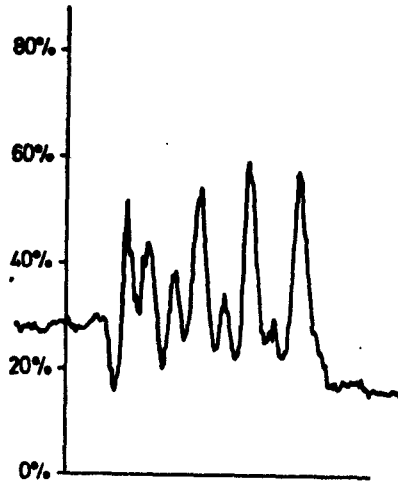
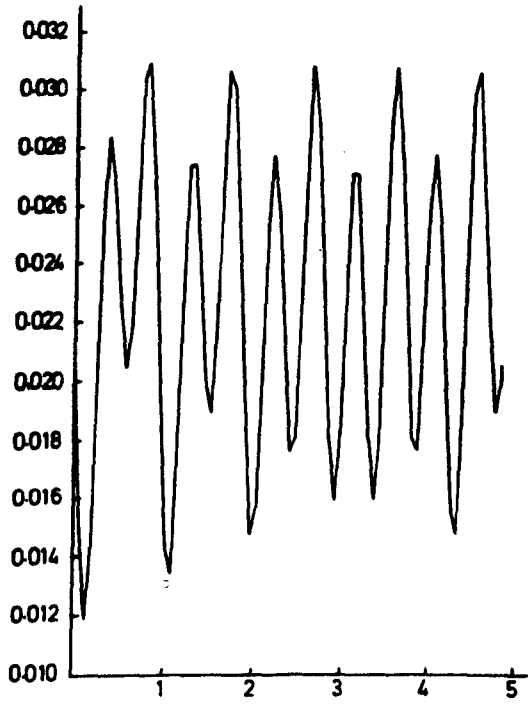
Theoretical and experimental intensity profiles for the incoherent boundaries in silicon. Microdensitometer traces were taken along the line AB in figure 10.2.3. The vertical axis of the simulation is the ratio of transmitted to incident beam intensity, and the horizontal axis is scaled in units of the extinction distance of the most strongly excited beam. The vertical axis of the microdensitometer traces is in percentage of transmitted light.

(10.2.3a)



(10.2.3b)

(10.2.4a)



(10.2.4b)



TABLE 10.2.1

Input data for STACKFAULT program

---



---

Number of beams
Accelerating voltage (in kV)
$\underline{K}_x$ (+)
Indices of beams
Extinction distances ( $\underline{\epsilon}_g$ and $\underline{\epsilon}'_g$ )
Lattice parameter (in $\text{\AA}$ )
Thickness (in $\text{\AA}$ )
Number of points on each intensity profile

---



---

(+)  $\underline{K}_x$  is the component of the incident electron wave vector parallel to the surface of the foil. For a reflection  $\underline{g}$ , in a systematic row,  $\underline{K}_x$  is given by:

$$-\underline{K}_x = \underline{g} \left( \frac{1}{2} + \frac{sk}{g} \right)$$

where  $k$  the magnitude of the electron wave vector corrected for the mean inner potential of the crystal, and  $s$  the deviation parameter for  $\underline{g}$ .

TABLE 10.2.2

Diffraction parameters for micrographs of figures 10.2.3 and 10.2.4

Fig.	B.F./D.F.	$\underline{g}_c$	w	Beams inserted in input data (relative to crystal 1)
10.2.3a	B.F.	$1\bar{1}1_1/\bar{1}1\bar{1}_2$	0.52	$\bar{1}\bar{1}\bar{1}, 000, 1\bar{1}\bar{1}, 2\bar{2}\bar{2}$
10.2.3b	D.F.	$\bar{1}\bar{1}\bar{1}_1/111_2$	0.14	$1\bar{1}\bar{1}, 000, \bar{1}\bar{1}\bar{1}, \bar{2}\bar{2}\bar{2}$
10.2.4a	B.F.	$\bar{1}\bar{1}3_1/\bar{3}11_2$	0.26	$000, \bar{1}\bar{1}3$
10.2.4b	D.F.	$11\bar{3}_1/3\bar{1}\bar{1}_2$	0.65	$11\bar{3}, 000$

$\underline{R} = [-0.188, 0.218, -0.218]$ . This rigid-body displacement can be resolved as  $\underline{t} = [-0.208, 0.208, -0.208]$ ,  $\underline{e} = [0.020, 0.010, -0.010]$ , or as  $\underline{t} = 0.208[\bar{1}1\bar{1}]$  and  $\underline{e} = 0.010[21\bar{1}]$ .

### 10.2.3 The structure of the $\{211\}$ incoherent twin

As was mentioned earlier the  $\Sigma=3$  misorientation relationship is described by a rotation  $\langle 110 \rangle / 70.52^\circ$  or equivalently as a rotation  $180^\circ$  about a  $\langle 111 \rangle$  axis. Figure 10.2.6 shows a (110) projection of a twinned diamond-structure-type material with twin plane been the  $(21\bar{1})$  plane. The latter passes through coincidence sites (Ellis & Treuting, 1951).

However, under this construction atoms on the coincidence plane have alternatively seven, five, six and five (altered) nearest neighbours, a circumstance that presumably requires some adjustment along such a boundary. Ellis & Treuting (1951) have proposed that imperfections are required in order to satisfy nearest neighbour distance requirements across such boundaries. The experimental evidence, however, indicates that this is not the case and that nearest neighbours requirements are satisfied by a rigid-body translation.

Figure 10.2.7 shows the atomic structure of the  $\{112\}$  twin where now the two crystals are shifted by  $\underline{R} = [-0.188, 0.218, -0.218]$ . It is seen from this figure that all the atoms near the boundary have four fold coordination and hence the energy of the configuration must be less than that of figure 10.2.6. However, the trans-boundary structure is not completely restored. For each boundary segment there are atomic configurations having seven, four and six sides. The directions and/or the lengths of a number of bonds are now altered (for example A and B in figure 10.2.7). This leads, of course, to an increase in the energy but the total interfacial energy is less than that of a general (non-

Figure 10.2.6

(011) projection of the atomic configuration across the  $(2\bar{1}\bar{1})$  twin boundary in silicon (indicated by the arrows). The two crystals are mirror images of each other with respect to  $(2\bar{1}\bar{1})$ .

Key: Large circles: sites in page

Small circles: sites  $\sqrt{2}a/4$  above page

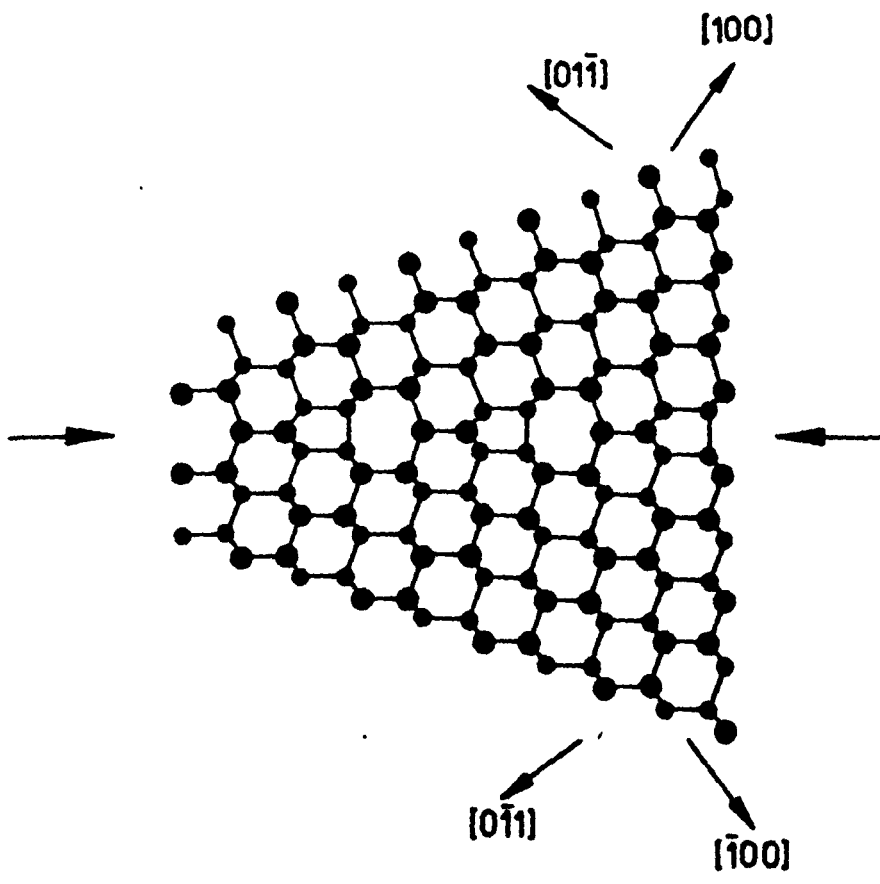
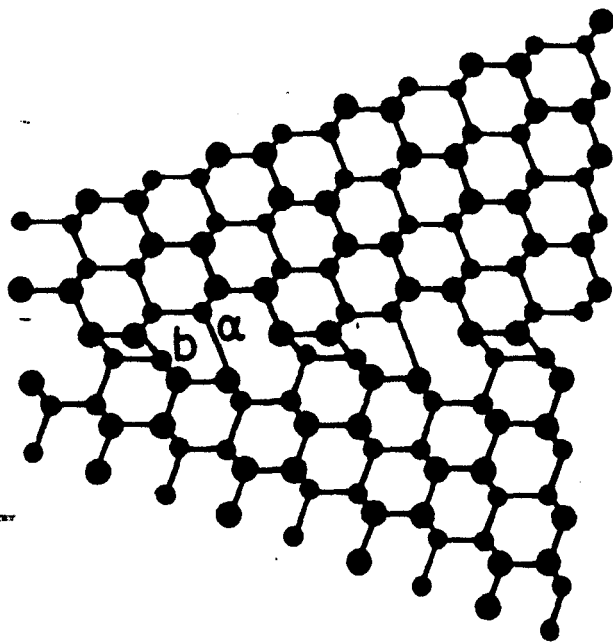


Figure 10.2.7

Low energy structure of the  $(21\bar{1})$  twin boundary in silicon. The arrow shows the displacement of the lower crystal with respect to the upper one. Symbols as in figure 10.2.6.



H

-twin-related) grain boundary. This is explained by the following considerations.

The energy of a covalent bond is largely the energy of resonance of two electrons between two atoms. Examination of the form of the resonance integral (see e.g. Pauling, 1967) shows that the resonance energy increases in magnitude with decrease in the overlapping of the two atomic orbitals involved in the formation of the bond. Consequently, it is expected that if two  $sp^3$  atomic orbitals in two atoms are only partially overlapped, the bond formed (i.e. the molecular orbital) will tend to have a higher energy than in the case of complete overlap. The two extremes in the bonding energy are the coincidence of the two atomic orbitals (low energy) and non-coincidence (high energy). Thus, either in the case of partial overlap the energy is relatively low; in other words, it is the requirement of non-existence of dangling bonds than the changes in angles/or directions which influence the energy predominally.

It can be said, therefore, that the  $\{112\}$  incoherent twins are intermediate in energy between the coherent and a general grain boundary. This will be further examined in the next section. The actual equilibrium position for the boundary is most probably one corresponding to a configuration where atomic adjustments occur in order to accommodate these abnormalities.

### 10.3 The use of polycrystalline silicon for solar cells

The study of the structure of grain boundaries in silicon is of great importance for the construction of solar cells (section 1.3). In this context the experimental results are discussed in this section. But before that the boundary effect on the electric behaviour of the material is briefly discussed.



### 10.3.1 Electrical characteristics of solar cells

To understand the grain boundary effects, the mechanism of the photovoltaic effect (Adams & Day, 1877; Chapin, Fuller & Pearson, 1954; Reynolds et al. 1954) must be born in mind. Photons absorbed in a semiconductor release their energies to electrons in the valence band, causing them to rise to the conducting band. Thus, electron-hole pairs are created, giving an excess above the equilibrium concentration. Once excess electron-hole pairs are generated they must be separated, moved to an edge of the semiconductor and removed to an external circuit before useful power may be obtained from the incident photons. To effect the separation an electrostatic field (potential barrier) must be supplied; the conventional technique is to create an p-n junction by diffusion at one surface of the semiconductor.

The most important factor which influences the effeciency of a solar cell is the lifetime of the carriers. This is defined as the average period before a minority carrier recombines with a majority carrier. Grain boundary effects are also important since they can short circuit the junction or barrier, and often lifetimes in general boundaries are very short. Such effects yield a low efficiency of the device. Moreover, some authors (Cowher & Sedgwick, 1972) have suggested that in polycrystalline layers a loss of doping occurs due to the impurity segregation at grain boundaries; this contributes to a lower conductivity. However, recent experimental evidence (see e.g. Graef et al. 1979) indicates that the decrease in the conductivity has to be explained in terms of the segregation of electrons and holes, and not the segregation of dopant atoms. Therefore, the electrical behaviour is solely determined by energy barriers at the grain boundaries.

### 10.3.2 Discussion of the electrical properties of twins in silicon

It is well recognized by now (Hovel, 1975; Palz, 1979) that the cost of silicon sheet has to be substantially reduced in order to meet the requirements of low-cost terrestrial solar cell arrays. Several low-cost silicon sheet technologies are currently being developed (see e.g. Overstraeten van & Palz, 1979). The quality of the silicon produced by any of the processes is less than perfect (see e.g. Koliwan, Daud & Liu, 1979). Thus, considerable effort has been put forward to determine the electrical characteristics of these low-cost silicon sheet.

Schwuttke (1977) studied the structural perfection as well as its effect on the lifetime distributions of silicon ribbons produced by the edge-defined film-fed growth. He concluded that the perfection of ribbons so obtained is dominated by simple parallel twinning. Such ribbon sections display excellent lifetime properties and in this respect compare well with lifetime distributions observed in Czochralski wafers. The majority of interfaces in Schwuttke's specimens were coherent twins.

Similar are the results obtained by Daud, Koliwad & Allen (1978) and Koliwad, Daud & Liu (1979). These authors measured the diffusion length in the vicinity of a planar defect and showed that this is considerably reduced in a general grain boundary but not in twins. The quantitative differentiation of general grain boundaries and twins was recently demonstrated by Helmreich & Seiter (1979). They investigated the characteristics of polycrystalline silicon and were able to show that the behaviour degradation due to coherent and incoherent twins (8% and 12% respectively) is appreciably less than that of general grain boundaries (40%). The unique behaviour of twins, and in particular of coherent twins, can be explained in terms of the twin structure as it was determined in this work.

It can be seen from figures 10.1.8 and 10.2.7 that no dangling bonds or elastic deformation of the lattice occur in the twin boundary region. The absence of dangling bonds implies that no extra energy levels are introduced in the gap and hence the capture cross-section for incident carriers will be similar to that in a single crystal. Moreover, the 'smooth' trans-boundary structure is associated with a constant-width-forbidden gap across the twin boundaries. In other words, no additional defect-acceptor-levels are introduced by the existence of twins and consequently the carrier lifetime is not altered in the vicinity of twin boundaries. A detailed analysis of the electrical properties across a high-angle grain boundary has been given by Mataré (1956) but his approach was based on the low-angle dislocation model. An extension to electrical properties of high-angle grain boundaries was recently proposed by Brown (1977a-e). However, neither of the two approaches gives a comprehensive relation between atomic structure and electrical properties of grain boundaries.

**APPENDICES**

## Appendix 1

### NOMENCLATURE OF SYMMETRY GROUPS, ELEMENTS AND OPERATIONS

The main function of this appendix is to give an outline of the nomenclature used in this thesis. Symbols are chiefly and frequently employed for point groups, spatial groups, symmetry elements as well as operations of symmetry. Additional mathematical data are also given providing the essential background for group-theoretical calculations.

Before explaining the nomenclature it must be mentioned that in the present work concepts from two-coloured symmetry are extensively used. Thus, it is necessary to discriminate between one- and two-coloured point groups, spatial groups, symmetry operations or symmetry elements. The symbols of the two-coloured point and spatial groups are constructed according to the 'international' or Hermann-Mauguin extended scheme, the fundamentals of which are given by Koptsik (1966) and Shubnikov & Koptsik (1974). Each of the elements of symmetry designated in symbols may be ordinary or colour-reversing. The latter are designated by a 'prime'.

In chapter 4 it is explained that some non-crystallographic symmetry groups must also be included in symmetry considerations of dichromatic complexes and bicrystals. In this case, however, the use of the symbol 12 can be misinterpreted. This is because of the possibility of confusing the 12-fold axis with the two-sided, one-coloured rosette group (see group no. 6 in table A3.1). For this the 12-fold axis is designated by a line underneath the symbol, i.e. 12.

As regards the symbols of the symmetry operations it is imperative to discriminate between them and the symbols of symmetry elements. According to a scheme proposed by Donnay & Donnay (1972) the Hermann-Mauguin

symbols that normally refer to symmetry axes also represent symmetry operations and their matrix representations, provided the power of the operation be explicitly stated. It must be noted that the sense of rotation is necessary to be also defined in order the scheme of Donnay & Donnay represents unambiguously the rotational symmetry operations. By convention the rotation of the symmetry axes (and therefore of the corresponding symmetry operations) is considered in the right-handed (anticlockwise) sense. Subscripts are used to indicate the direction of the symmetry axis<sup>1</sup>. As to inversion and reflection the letters *i* (for inversion) and *s* (for Spiegelung=reflection)<sup>2</sup> provide self-explanatory symbols; whereas the subscript for the mirror operation (or mirror element) shows the normal of the mirror plane. Symbols of some symmetry operations are given briefly below demonstrating the above scheme:

$1$  = identity operation

$i$  = inversion operation

$2_z^1$  = rotation through  $\pi$  about  $Oz$

$3_x^2$  = right-handed rotation through  $4\pi/3$  about  $Ox$

$\bar{4}_y^3$  = inversion followed by rotation through  $3\pi/2$  about  $Oy$   
in the right-handed sense

$\bar{6}_z^5$  = inversion followed by rotation through  $5\pi/3$  about  $Oz$   
in the right-handed sense

$8_x^1$  = right-handed rotation through  $\pi/4$  about  $Ox$

$\underline{12}_y^1$  = right-handed rotation through  $\pi/12$  about  $Oy$

Colour-reversing symmetry operations are designated by a prime which implies that the ordinary symmetry operation is followed by colour change. Thus,  $2'_z$  is the symbol of a 2-fold colour-reversing rotation along the  $z$ -axis of the coordinate system.

In applying the equations derived in this thesis it is necessary to know the symmetry operations (and their matrix representations) associated with the point group in question. Matrix representations of the symmetry operations included in the 32 point groups have been given by Billings (1969). Table A1.1 gives the comparison between the notation used in the present work and that by Billings. According to the latter

$(000)_{-1}$  signifies inversion

$(abc)^{1/n}$  signifies one n-fold rotational operation in the anticlockwise sense about the line joining  $(0,0,0)$  to  $(a,b,c)$

$(abc)_m$  signifies a mirror reflection in the plane perpendicular to the line joining  $(0,0,0)$  to  $(a,b,c)$

$(abc)^{1/n}_{-1}$  signifies  $(abc)^{1/n}(000)_{-1}$

In a similar way the symmetry operations (and their matrix representations) of the 8- and 12-fold symmetry classes are given in table A1.2. On the other hand, in table A1.3 the symmetry operations associated with the 32 crystal classes are listed (a similar table for the 8- and 12-fold classes is given in appendix 9).

Finally, it must be mentioned that the stereographic representations of point groups are given throughout the present work by using the notation by Nye (1957). All rotational axes pass through the space origin and are shown on the stereogram at the position corresponding to the intersection between the axis and a sphere centred on the origin. The directions of the coordinate axes  $x$ ,  $y$ ,  $z$  are as follows: the  $z$ -axis is always perpendicular to the plane of the drawing, while the  $x$ - and  $y$ -axes are orthogonal to the  $z$ -axis and make a right angle with each other. These

TABLE A1.1

Comparison of the notations of symmetry operations

Donnay & Donnay symbols	Billings symbols	Donnay & Donnay symbols	Billings symbols
1	$(000)_1$	$s_y$	$(010)_m$
i	$(000)_{-1}$	$s_z$	$(001)_m$
$2_x^1$	$(100)^{\frac{1}{2}}$	$s_\alpha$	$(110)_m$
$2_y^1$	$(010)^{\frac{1}{2}}$	$s_\beta$	$(1\bar{1}0)_m$
$2_z^1$	$(001)^{\frac{1}{2}}$	$s_A$	$(\bar{1}\sqrt{3}0)_m$
$2_\alpha^1$	$(110)^{\frac{1}{2}}$	$s_B$	$(1\sqrt{3}0)_m$
$2_\beta^1$	$(1\bar{1}0)^{\frac{1}{2}}$	$s_r$	$(\sqrt{3}10)_m$
$2_A^1$	$(\bar{1}\sqrt{3}0)^{\frac{1}{2}}$	$s_\Delta$	$(\sqrt{3}\bar{1}0)_m$
$2_B^1$	$(1\sqrt{3}0)^{\frac{1}{2}}$	$s_\gamma$	$(101)_m$
$2_r^1$	$(\sqrt{3}10)^{\frac{1}{2}}$	$s_\theta$	$(10\bar{1})_m$
$2_\Delta^1$	$(\sqrt{3}\bar{1}0)^{\frac{1}{2}}$	$s_\kappa$	$(01\bar{1})_m$
$2_\gamma^1$	$(101)^{\frac{1}{2}}$	$s_\lambda$	$(011)_m$
$2_\theta^1$	$(10\bar{1})^{\frac{1}{2}}$	$3_z^1$	$(001)^{\frac{1}{3}}$
$2_\kappa^1$	$(01\bar{1})^{\frac{1}{2}}$	$3_z^2$	$(001)^{\frac{2}{3}}$
$2_\lambda^1$	$(011)^{\frac{1}{2}}$	$3_x^1$	$(1\bar{1}1)^{\frac{1}{3}}$
$s_x$	$(100)_m$	$3_x^2$	$(1\bar{1}1)^{\frac{2}{3}}$



TABLE A1.1-continued

Donnay & Donnay symbols	Billings symbols	Donnay & Donnay symbols	Billings symbols
$3\frac{1}{6}$	$(111)^{\frac{1}{3}}$	$4\frac{1}{x}$	$(100)^{\frac{1}{4}}$
$3\frac{2}{6}$	$(111)^{\frac{2}{3}}$	$4\frac{3}{x}$	$(100)^{\frac{3}{4}}$
$3\frac{1}{6}$	$(\bar{1}\bar{1}\bar{1})^{\frac{1}{3}}$	$4\frac{1}{y}$	$(010)^{\frac{1}{4}}$
$3\frac{2}{6}$	$(\bar{1}\bar{1}\bar{1})^{\frac{2}{3}}$	$4\frac{3}{y}$	$(010)^{\frac{3}{4}}$
$3\frac{1}{4}$	$(11\bar{1})^{\frac{1}{3}}$	$4\frac{1}{z}$	$(001)^{\frac{1}{4}}$
$3\frac{2}{4}$	$(11\bar{1})^{\frac{2}{3}}$	$4\frac{3}{z}$	$(001)^{\frac{3}{4}}$
$\bar{3}\frac{1}{z}$	$(001)^{\frac{1}{3}} = (001)^{\frac{1}{3}}(000)_{-1}$	$\bar{4}\frac{1}{x}$	$(100)^{\frac{1}{4}}_{-1}$
$\bar{3}\frac{2}{z}$	$(001)^{\frac{2}{3}} = (001)^{\frac{2}{3}}(000)_{-1}$	$\bar{4}\frac{3}{x}$	$(100)^{\frac{3}{4}}_{-1} = (100)^{\frac{3}{4}}(000)_{-1}$
$\bar{3}\frac{1}{y}$	$(1\bar{1}\bar{1})^{\frac{1}{3}} = (1\bar{1}\bar{1})^{\frac{1}{3}}(000)_{-1}$	$\bar{4}\frac{1}{y}$	$(010)^{\frac{1}{4}}_{-1} = (010)^{\frac{1}{4}}(000)_{-1}$
$\bar{3}\frac{2}{y}$	$(1\bar{1}\bar{1})^{\frac{2}{3}} = (1\bar{1}\bar{1})^{\frac{2}{3}}(000)_{-1}$	$\bar{4}\frac{3}{y}$	$(010)^{\frac{3}{4}}_{-1} = (010)^{\frac{3}{4}}(000)_{-1}$
$\bar{3}\frac{1}{6}$	$(111)^{\frac{1}{3}} = (111)^{\frac{1}{3}}(000)_{-1}$	$\bar{4}\frac{1}{z}$	$(001)^{\frac{1}{4}}_{-1} = (001)^{\frac{1}{4}}(000)_{-1}$
$\bar{3}\frac{2}{6}$	$(111)^{\frac{2}{3}} = (111)^{\frac{2}{3}}(000)_{-1}$	$\bar{4}\frac{3}{z}$	$(001)^{\frac{3}{4}}_{-1} = (001)^{\frac{3}{4}}(000)_{-1}$
$\bar{3}\frac{1}{6}$	$(\bar{1}\bar{1}\bar{1})^{\frac{1}{3}} = (\bar{1}\bar{1}\bar{1})^{\frac{1}{3}}(000)_{-1}$	$6\frac{1}{z}$	$(001)^{1/6}$
$\bar{3}\frac{2}{6}$	$(\bar{1}\bar{1}\bar{1})^{\frac{2}{3}} = (\bar{1}\bar{1}\bar{1})^{\frac{2}{3}}(000)_{-1}$	$6\frac{5}{z}$	$(001)^{5/6}$
$\bar{3}\frac{1}{4}$	$(11\bar{1})^{\frac{1}{3}} = (11\bar{1})^{\frac{1}{3}}(000)_{-1}$	$\bar{6}\frac{1}{z}$	$(001)^{1/6}_{-1} = (001)^{1/6}(000)_{-1}$
$\bar{3}\frac{2}{4}$	$(11\bar{1})^{\frac{2}{3}} = (11\bar{1})^{\frac{2}{3}}(000)_{-1}$	$\bar{6}\frac{5}{z}$	$(001)^{5/6}_{-1} = (001)^{5/6}(000)_{-1}$

TABLE A1.2

Symmetry operations associated with the 8- and 12-fold classes

$$8_z^1 = (001)^{1/8} = \begin{pmatrix} \sqrt{2}/2 & \sqrt{2}/2 & 0 \\ -\sqrt{2}/2 & \sqrt{2}/2 & 0 \\ 0 & 0 & 1 \end{pmatrix}$$

$$8_z^3 = (001)^{3/8} = (001)^{1/8} (001)^{1/4} = 8_z^1 \cdot 4_z^1$$

$$8_z^5 = (001)^{5/8} = (001)^{1/8} (001)^{1/2} = 8_z^1 \cdot 2_z^1$$

$$8_z^7 = (001)^{7/8} = (001)^{1/8} (001)^{3/4} = 8_z^1 \cdot 4_z^3$$

$$\bar{8}_z^1 = (001)_{-1}^{1/8} = (001)^{1/8} (000)_{-1} = 8_z^1 \cdot i$$

$$\bar{8}_z^3 = (001)_{-1}^{3/8} = (001)^{3/8} (000)_{-1} = 8_z^3 \cdot i$$

$$\bar{8}_z^5 = (001)_{-1}^{5/8} = (001)^{5/8} (000)_{-1} = 8_z^5 \cdot i$$

$$\bar{8}_z^7 = (001)_{-1}^{7/8} = (001)^{7/8} (000)_{-1} = 8_z^7 \cdot i$$

$$2_p^1 = (\sqrt{2+\sqrt{2}}, \sqrt{2-\sqrt{2}}, 0)^{1/2} = (001)^{1/8} (110)^{1/2} = 8_z^1 \cdot 2_p^1$$

$$2_r^1 = (\sqrt{2+\sqrt{2}-\sqrt{2-\sqrt{2}}}, \sqrt{2+\sqrt{2}+\sqrt{2-\sqrt{2}}}, 0)^{1/2} = (001)^{3/8} (1\bar{1}0)^{1/2} = 8_z^3 \cdot 2_p^1$$

$$2_y^1 = (-\sqrt{2-\sqrt{2}}, \sqrt{2+\sqrt{2}}, 0)^{1/2} = (001)^{5/8} (110)^{1/2} = 8_z^5 \cdot 2_p^1$$

$$2_x^1 = (-\sqrt{2+\sqrt{2}-\sqrt{2-\sqrt{2}}}, \sqrt{2+\sqrt{2}-\sqrt{2-\sqrt{2}}}, 0)^{1/2} = (001)^{7/8} (1\bar{1}0)^{1/2} = 8_z^7 \cdot 2_p^1$$

$$s_p = (\sqrt{2+\sqrt{2}}, \sqrt{2-\sqrt{2}}, 0)_m = (\sqrt{2+\sqrt{2}}, \sqrt{2-\sqrt{2}}, 0)^{1/2} (000)_{-1} = 2_p^1 \cdot i$$

$$s_r = (\sqrt{2+\sqrt{2}-\sqrt{2-\sqrt{2}}}, \sqrt{2+\sqrt{2}+\sqrt{2-\sqrt{2}}}, 0)_m = (\sqrt{2+\sqrt{2}-\sqrt{2-\sqrt{2}}}, \sqrt{2+\sqrt{2}+\sqrt{2-\sqrt{2}}}, 0)^{1/2} (000)_{-1} = 2_r^1 \cdot i$$

$$s_y = (-\sqrt{2-\sqrt{2}}, \sqrt{2+\sqrt{2}}, 0)_m = (-\sqrt{2-\sqrt{2}}, \sqrt{2+\sqrt{2}}, 0)^{1/2} (000)_{-1} = 2_y^1 \cdot i$$

$$s_x = (-\sqrt{2+\sqrt{2}-\sqrt{2-\sqrt{2}}}, \sqrt{2+\sqrt{2}-\sqrt{2-\sqrt{2}}}, 0)_m = (-\sqrt{2+\sqrt{2}-\sqrt{2-\sqrt{2}}}, \sqrt{2+\sqrt{2}-\sqrt{2-\sqrt{2}}}, 0)^{1/2} (000)_{-1} = 2_x^1 \cdot i$$

$$\frac{12}{z}^1 = (001)^{1/12} = \begin{pmatrix} \sqrt{3}/2 & 1/2 & 0 \\ -1/2 & \sqrt{3}/2 & 0 \\ 0 & 0 & 1 \end{pmatrix}$$

TABLE A1.2-continued

$$\underline{12}_z^5 = (001)^{5/12} = (001)^{1/12} (001)^{1/3} = \underline{12}_z^1 \cdot \underline{3}_z^1$$

$$\underline{12}_z^7 = (001)^{7/12} = (001)^{1/12} (001)^{1/2} = \underline{12}_z^1 \cdot \underline{2}_z^1$$

$$\underline{12}_z^{11} = (001)^{11/12} = (001)^{1/12} (001)^{1/3} (001)^{1/2} = \underline{12}_z^1 \cdot \underline{3}_z^1 \cdot \underline{2}_z^1$$

$$\overline{12}_z^1 = (001)_{-1}^{1/12} = (001)^{1/12} (000)_{-1} = \underline{12}_z^1 \cdot i$$

$$\overline{12}_z^5 = (001)_{-1}^{5/12} = (001)^{5/12} (000)_{-1} = \underline{12}_z^5 \cdot i$$

$$\overline{12}_z^7 = (001)_{-1}^{7/12} = (001)^{7/12} (000)_{-1} = \underline{12}_z^7 \cdot i$$

$$\overline{12}_z^{11} = (001)_{-1}^{11/12} = (001)^{11/12} (000)_{-1} = \underline{12}_z^{11} \cdot i$$

$$2_E^1 = (\sqrt{2+\sqrt{3}}, \sqrt{2-\sqrt{3}}, 0)^{1/2} = (001)^{1/12} (\sqrt{3}i0)^{1/2} = \underline{12}_z^1 \cdot \underline{2}_r^1$$

$$2_H^1 = (\sqrt{2+\sqrt{3}} - \sqrt{3}\sqrt{2-\sqrt{3}}, \sqrt{3}\sqrt{2+\sqrt{3}} + \sqrt{2-\sqrt{3}}, 0)^{1/2} = (001)^{5/12} (\sqrt{3}i0)^{1/2} = \underline{12}_z^5 \cdot \underline{2}_\Delta^1$$

$$2_\Theta^1 = (-\sqrt{2-\sqrt{3}}, \sqrt{2+\sqrt{3}}, 0)^{1/2} = (001)^{7/12} (\sqrt{3}i0)^{1/2} = \underline{12}_z^7 \cdot \underline{2}_r^1$$

$$2_\Lambda^1 = (-\sqrt{3}\sqrt{2+\sqrt{3}} - \sqrt{2-\sqrt{3}}, \sqrt{2+\sqrt{3}} - \sqrt{3}\sqrt{2-\sqrt{3}}, 0)^{1/2} = (001)^{11/12} (\sqrt{3}i0)^{1/2} = \underline{12}_z^{11} \cdot \underline{2}_\Delta^1$$

$$s_E = (\sqrt{2+\sqrt{3}}, \sqrt{2-\sqrt{3}}, 0)_m = (\sqrt{2+\sqrt{3}}, \sqrt{2-\sqrt{3}}, 0)^{1/2} (000)_{-1} = \underline{2}_E^1 \cdot i$$

$$s_H = (\sqrt{2+\sqrt{3}} - \sqrt{3}\sqrt{2-\sqrt{3}}, \sqrt{3}\sqrt{2+\sqrt{3}} + \sqrt{2-\sqrt{3}}, 0)_m =$$

$$= (\sqrt{2+\sqrt{3}} - \sqrt{3}\sqrt{2-\sqrt{3}}, \sqrt{3}\sqrt{2+\sqrt{3}} + \sqrt{2-\sqrt{3}}, 0)^{1/2} (000)_{-1} = \underline{2}_H^1 \cdot i$$

$$s_\Theta = (-\sqrt{2-\sqrt{3}}, \sqrt{2+\sqrt{3}}, 0)_m = (-\sqrt{2-\sqrt{3}}, \sqrt{2+\sqrt{3}}, 0)^{1/2} (000)_{-1} = \underline{2}_\Theta^1 \cdot i$$

$$s_\Lambda = (-\sqrt{3}\sqrt{2+\sqrt{3}} - \sqrt{2-\sqrt{3}}, \sqrt{2+\sqrt{3}} - \sqrt{3}\sqrt{2-\sqrt{3}}, 0)_m =$$

$$= (-\sqrt{3}\sqrt{2+\sqrt{3}} - \sqrt{2-\sqrt{3}}, \sqrt{2+\sqrt{3}} - \sqrt{3}\sqrt{2-\sqrt{3}}, 0)^{1/2} (000)_{-1} = \underline{2}_\Lambda^1 \cdot i$$

TABLE A1.3

Groups of transformations associated with the 32 crystal classes

Number	Crystal class description	Order	Minimum symmetry transformations to define group	Other symmetry transformations in group (excluding identity transformation)
1	1	1	1	
2	$\bar{1}$	2	i	
3	m	2	$s_z$	
4	2	2	$2_z^1$	
5	2/m	4	$2_z^1, s_z$	i
6	mm2	4	$s_x, s_y$	$2_z^1$
7	222	4	$2_x^1, 2_y^1$	$2_z^1$
8	mmm	8	$s_x, s_y, s_z$	$i, 2_x^1, 2_y^1, 2_z^1$
9	4	4	$4_z^1, 4_z^3$	$2_z^1$
10	$\bar{4}$	4	$\bar{4}_z^1, \bar{4}_z^3$	$2_z^1$
11	4/m	8	$4_z^1, 4_z^3, s_z$	$i, 2_z^1, \bar{4}_z^1, \bar{4}_z^3$
12	$\bar{4}2m$	8	$\bar{4}_z^1, \bar{4}_z^3, 2_x^1$	$2_y^1, 2_z^1, s_x, s_y$
13	4mm	8	$s_x, s_y$	$4_z^1, 4_z^3, 2_z^1, s_y, s_x$
14	422	8	$2_x^1, 2_y^1$	$4_z^1, 4_z^3, 2_z^1, 2_y^1, 2_x^1$
15	4/mmm	16	$s_y, s_z, s_x$	$i, 4_z^1, 4_z^3, 2_z^1, 2_x^1, 2_y^1, 2_z^1, 2_x^1, 2_y^1, 2_z^1, \bar{4}_z^1, \bar{4}_z^3, s_x, s_y$
16	3	3	$3_z^1, 3_z^2$	

TABLE A1.3-continued

Number	Crystal class description	Order	Minimum symmetry transformations to define group	Other symmetry transformations in group (excluding identity transformation)
17	$\bar{3}$	6	$\bar{3}_z^1, \bar{3}_z^2$	$i, 3_z^1, 3_z^2$
18	3m	6	$3_z^1, 3_z^2, s_x$	$s_A, s_B$
19	32	6	$3_z^1, 3_z^2, 2_x^1$	$2_A^1, 2_B^1$
20	$\bar{3}m$	12	$\bar{3}_z^1, \bar{3}_z^2, s_x$	$i, 3_z^1, 3_z^2, s_A, s_B, 2_A^1, 2_B^1, 2_x^1$
21	6	6	$6_z^1, 6_z^5$	$3_z^1, 3_z^2, 2_z^1$
22	$\bar{6}$	6	$\bar{6}_z^1, \bar{6}_z^5$	$3_z^1, 3_z^2, s_z$
23	6/m	12	$6_z^1, 6_z^5, s_z$	$i, 2_z^1, 3_z^1, 3_z^2, \bar{3}_z^1, \bar{3}_z^2, \bar{6}_z^1, \bar{6}_z^5$
24	$\bar{6}2m$	12	$\bar{6}_z^1, \bar{6}_z^5, s_x$	$3_z^1, 3_z^2, 2_y^1, 2_\Gamma^1, 2_\Delta^1, s_z, s_A, s_B$
25	6mm	12	$6_z^1, 6_z^5, s_x$	$2_z^1, 3_z^1, 3_z^2, s_y, s_A, s_B, s_\Gamma, s_\Delta$
26	622	12	$6_z^1, 6_z^5, 2_x^1$	$2_z^1, 3_z^1, 3_z^2, 2_y^1, 2_A^1, 2_B^1, 2_\Gamma^1, 2_\Delta^1$
27	6/mmm	24	$s_z, s_y, s_B$	$i, 2_z^1, 3_z^1, 3_z^2, 6_z^1, 6_z^5, 2_y^1, 2_x^1,$ $2_A^1, 2_B^1, 2_\Gamma^1, 2_\Delta^1, s_x, s_A,$ $s_\Gamma, s_\Delta, \bar{3}_z^1, \bar{3}_z^2, \bar{6}_z^1, \bar{6}_z^5$
28	23	12	$2_x^1, 3_\delta^1, 3_\epsilon^2$	$2_y^1, 2_z^1, 3_\delta^1, 3_\delta^2, 3_\epsilon^1, 3_\epsilon^2,$ $3_\tau^1, 3_\tau^2$
29	m3	24	$s_x, 3_\delta^1, 3_\epsilon^2$	$i, 2_x^1, 2_y^1, 2_z^1, 3_\delta^1, 3_\delta^2, 3_\epsilon^1,$ $3_\epsilon^2, 3_\tau^1, 3_\tau^2, \bar{3}_\delta^1, \bar{3}_\delta^2, \bar{3}_\epsilon^1, \bar{3}_\epsilon^2$ $\bar{3}_\tau^1, \bar{3}_\tau^2, \bar{3}_\delta^1, \bar{3}_\delta^2, s_y, s_z$

TABLE A1.3-continued

Number	Crystal class description	Order	Minimum symmetry transformations to define group	Other symmetry transformations in group (excluding identity transformation)
30	$\bar{4}3m$	24	$\bar{4}_z^1, \bar{4}_z^3, s_x,$ $3_s^1, 3_s^2$	$2_x^1, 2_y^1, 2_z^1, 3_x^1, 3_y^2, 3_z^1, 3_z^2,$ $3_z^1, 3_z^2, \bar{4}_x^1, \bar{4}_x^3, \bar{4}_y^1, \bar{4}_y^3, s_p,$ $s_\gamma, s_\delta, s_\kappa, s_\lambda$
31	432	24	$3_s^1, 3_s^2, 2_\alpha^1$	$2_\gamma^1, 2_\lambda^1, 2_\rho^1, 2_\psi^1, 2_\kappa^1, 3_y^1, 3_y^2,$ $3_z^1, 3_z^2, 3_z^1, 3_z^2, 4_z^1, 4_z^3, 4_y^1,$ $4_y^3, 4_x^1, 4_x^3, 2_x^1, 2_y^1, 2_z^1$
32	m3m	48	$s_x, 3_s^1, 3_s^2,$ $s_\kappa$	$3_y^1, 3_y^2, 3_z^1, 3_z^2, 3_z^1, 3_z^2, 2_\alpha^1,$ $2_\rho^1, 2_\gamma^1, 2_\psi^1, 2_\kappa^1, 2_\lambda^1, 4_z^1, 4_z^3,$ $4_y^1, 4_y^3, 4_x^1, 4_x^3, 2_x^1, 2_y^1, 2_z^1,$ $i, \bar{3}_y^1, \bar{3}_y^2, \bar{3}_z^1, \bar{3}_z^2, \bar{3}_z^1, \bar{3}_z^2,$ $\bar{3}_z^1, \bar{3}_z^2, s_p, s_\gamma, s_\delta, s_\kappa, s_\lambda,$ $\bar{4}_x^1, \bar{4}_x^3, \bar{4}_y^1, \bar{4}_y^3, \bar{4}_z^1, \bar{4}_z^3, s_y, s_z$

axes consist the coordinate system relative to which all the matrix representations are expressed (alias expressions). Stereograms of the two-coloured point groups have been given by Koptsik (1966), Billings (1969) and Joshua (1974)<sup>3</sup>.

- - -

- Footnotes
- 1: The symbols used for denoting the various directions of rotation axes and normals to mirror planes are explained in table A1.1.
  - 2: Note that the symmetry element of mirror reflection is represented by *m* while the mirror symmetry operation by *s*. This is, in fact, the only departure from the Hermann-Mauguin notation.
  - 3: Joshua (1974) introduced new symbols of colour-reversing operations in order to avoid the use of two different colours (usually black and red) for printing the stereograms.

Appendix 2

THE 'DIMENSIONAL' DESCRIPTION OF SYMMETRY GROUPS

After the introduction of the concept of antisymmetry by Heesch (1930), and later by Shubnikov (1951), symmetry groups are generally classified in terms of antisymmetry or extensions of this idea. A symmetry group belongs, therefore, to either the one-coloured or the (generalized) two-coloured class. However, another aspect of the symmetry groups can serve as a basis of classification as well. The principle of this classification is the dimensions of the space which is invariant under the operations of each particular group in the class. With this viewpoint a 'dimensional' description of symmetry groups may be established. This scheme has been considered by Neronova & Belov (1961) and independently by Holser (1961) for indicating relations among some categories of one- or two-coloured classes.

The space (point, line, plane, cell or some combination of them) is invariant under all operations<sup>1</sup> of the symmetry groups in a class. Thus, as Holser (1961) pointed out, the dimensions of the space, or its general symmetry, is a description of the symmetry class. The symbol  $G_{r,s,\dots,t}^1$  (or  $G_{r,s,\dots,t}$ ) is introduced (following Bohm, 1963; Bohm & Domberger-Schiff, 1966) to denote the (isometric) symmetry group of an  $r$ -dimensional geometrical space if this group simultaneously transforms the (periodic or non-periodic) subspaces of this space with dimensions  $s,\dots,t$  ( $r>s>\dots>t$ ) into themselves. If  $n$ -coloured is considered, the symbol  $G_{r,s,\dots,t}^p$  is used (Shubnikov & Koptsik, 1974); the meaning of the lower indices is as above, while the upper index determines the number of colours in the group<sup>2</sup>. Thus, the two-coloured groups are



represented by the symbol  $G_{r,s,\dots,t}^2$ .

The term 'invariance' is used to express the fact that any symmetry operation of the group acting on any subspace gives it back unchanged. Translational symmetry is necessarily restricted to the lowest dimension of invariance. On the other hand, if a group is 'in' n-dimensional space, the n-dimensional space must be invariant with respect to this group; this is the highest dimension of invariance. From this point of view all the classes of groups may be designated in terms of their dimensional invariance. Thus, the one-coloured point groups of finite (or infinite) figures acquire the symbol  $G_{3,0}^1$  since while transforming a three-dimensional space into itself they keep only a singular point (zero-dimensional space) invariant.

The classification of one- and two-coloured crystallographic groups (up to three dimensions) according to this dimensional description are given in tables 2.1.1 and 2.2.1 respectively. All the dimensions listed are invariant with respect to any group in the class; the group lies in the space of highest dimension and has translation along the lowest dimension.

- - -

Footnotes 1: This includes translations as well as rotations and reflections.

2: Attention must be given with respect to the meaning of the upper index. Some authors (see e.g. Koptsik, 1967) define the upper index as the group of equality (i.e. colour) substitutions. Thus, according to the latter definition the two-coloured groups are represented by  $G_{r,s,\dots,t}^1$ .

### Appendix 3

#### TWO-SIDED, TWO-COLOURED ROSETTE GROUPS

The 31 point groups and their isomorphic 80 plane groups related to a two-sided, one-coloured plane were independently derived by Hermann (1929a), Alexander & Herrmann (1929), Heesch (1929). These groups are based on one of the four<sup>1</sup> two-dimensional lattices with the addition of those symmetry elements that are invariant with respect to the plane. Thus, the 31 point groups of a two-sided, one coloured plane are the 32 crystallographic groups minus the 5 cubic groups and plus alternative orientations for the 4 crystallographic groups 2, m, 2/m, and mm2. They are relisted in table A3.1 in a notation consistent with the Hermann-Mauguin scheme.

The coordinate system, relative to which the group symbols are given, has an axis a perpendicular to the plane, while axes b and c are orthogonal to the axis a and make a right or oblique angle with each other, depending on the class of rosette symmetry. The letters in the first, second and third positions of the symbol indicate that a particular symmetry element coincides with the coordinate axes in the order a, b, c (for the lower symmetry classes) or with (and in this order) the axes a, b and the bisector of the angle between the axes b and c (for the senior classes). If no symmetry axes or normals to symmetry planes coincide with a coordinate axes the number 1 is placed in the corresponding position (for the full symbol) or the position is left vacant. According to this notation the symbol 211 means a two-fold axis normal to the plane, while m11 denotes a mirror plane parallel to the plane.

The two-sided, two-coloured rosette groups are obtained as extensions of the classical two-sided, one-coloured groups of table A3.1. The 125

TABLE A3.1

Point groups of a two-sided  
one-coloured plane

Number	Two-sided one-coloured rosette groups	
	Short symbol	Full symbol
1	1	111
2	$\bar{1}$	$\bar{1}11$
3	21	211
4	m1	m11
5	2/m1	2/m11
6	12	121
7	1m	1m1
8	12/m	12/m1
9	222	222
10	2mm	2mm
11	m2m	m2m
12	mmm	mmm
13	4	411
14	$\bar{4}$	$\bar{4}11$
15	4/m	4/m11
16	422	422
17	4mm	4mm
18	$\bar{4}2m$	$\bar{4}2m$
19	4/mmm	4/mmm
20	3	311
21	$\bar{3}$	$\bar{3}11$
22	32	321
23	3m	3m1
24	$\bar{3}m$	$\bar{3}m1$
25	6	611
26	$\bar{6}$	$\bar{6}11$
27	6/m	6/m11
28	622	622
29	6mm	6mm
30	$\bar{6}m2$	$\bar{6}m2$
31	6/mmm	6/mmm

groups were derived by starting with the 31 'generating' groups (in the sense of Zamorzaev, 1957) considered as two-sided but one-coloured and simply or severally changing ordinary operations by colour-reversing ones.

The two-coloured, two-sided rosette groups are listed in table A3.2. The second column contains the symbols of the 31 generating groups. The 31 grey groups, those for which every point is bicoloured, are indicated by adding 1' to the symbol and are given in the third column. The remaining 63 groups, in which particular symmetry operations or groups of operations involve colour change are symbolized in the last column of the table.

Alternatively, the derivation of the two-coloured, two-sided rosette groups has been carried out by employing Boyle's (1969) method (see also appendix 9). Another derivation of the crystallographic two-sided, two-coloured rosette groups can be devised by selecting the 158 point groups from the 530 two-coloured, two-sided layer groups given by Neronova & Belov (1961). The 33 of these 158 groups have reoriented counterparts leaving only 125 crystallographically non-equivalent rosette groups.

- - -

Footnote 1: Five two-dimensional lattices if centred rectangular is allowed.

TABLE A3.2

Point groups of a two-sided, two-coloured plane

Number	Two-sided, two-coloured rosette groups		
	Classical	Neutral	Black-white
1 (1-2)	1	1'	
2 (3-5)	$\bar{1}$	$\bar{1}1'$	$\bar{1}'$
3 (6-8)	21	21'	2'1
4 (9-11)	m1	m1'	m'1
5 (12-16)	2/m1	2/m1'	2/m'1, 2'/m1, 2'/m'1
6 (17-19)	12	121'	12'
7 (20-22)	1m	1m1'	1m'
8 (23-27)	12/m	12/m1'	12/m', 12'/m, 12'/m'
9 (28-31)	222	2221'	2'2'2, 22'2'
10 (32-35)	2mm	2mm1'	2'm'm, 2m'm'
11 (36-40)	m2m	m2m1'	m2'm', m'2m', m'2'm
12 (41-47)	mmm	mmm1'	m'm'm, mm'm, m'm'm', m'mm, mm'm'
13 (48-50)	4	41'	4'
14 (51-53)	$\bar{4}$	$\bar{4}1'$	$\bar{4}'$
15 (54-58)	4/m	4/m1'	4/m', 4'/m, 4'/m'
16 (59-62)	422	4221'	42'2', 4'2'2
17 (63-66)	4mm	4mm1'	4m'm', 4'm'm
18 (67-71)	$\bar{4}2m$	$\bar{4}2m1'$	$\bar{4}2'm', \bar{4}'2m', \bar{4}'2'm$
19 (72-78)	4/mmm	4/mmm1'	4/m'm'm', 4/m'mm, 4'/m'm'm, 4'/mmm', 4'/mm'm'
20 (79-80)	3	31'	
21 (81-83)	$\bar{3}$	$\bar{3}1'$	$\bar{3}'$
22 (84-86)	32	321'	32'
23 (87-89)	3m	3m1'	3m'
24 (90-94)	$\bar{3}m$	$\bar{3}m1'$	$\bar{3}'m', \bar{3}'m, \bar{3}m'$
25 (95-97)	6	61'	6'
26 (98-100)	$\bar{6}$	$\bar{6}1'$	$\bar{6}'$
27 (101-105)	6/m	6/m1'	6/m', 6'/m', 6'/m
28 (106-109)	622	6221'	6'2'2, 62'2'
29 (110-113)	6mm	6mm1'	6'm'm, 6m'm'
30 (114-118)	$\bar{6}m2$	$\bar{6}m21'$	$\bar{6}'m'2, \bar{6}m'2', \bar{6}'m2'$
31 (119-125)	6/mmm	6/mmm1'	6/m'm'm', 6/m'mm, 6'/mmm', 6'/m'm'm, 6'/mm'm'

Appendix 4

TWO- SIDED, TWO-COLOURED BAND GROUPS

Bands are infinite figures with a singular plane and a singular translation axis lying on the plane. The one-sided bands are special cases in which the singular plane is polar; its 'face' is different from its 'back'. One-sided bands might, therefore, be defined as figures without singular points but with a singular polar plane and a singular translation axis. For bands in general, however, the singular plane can be nonpolar, i.e. transformations making the two sided coincide with each other are permitted. The consideration of the additional permissible transformations means that the number of symmetry classes is increased

The seven one-sided, one-coloured band groups are, apart from the point groups, the simplest symmetry class. Lists of these groups have been given by Polyá (1924) and Niggli (1926). The 31 two-sided, one-coloured band groups were first enumerated by Speiser (1924); these groups are listed in table A4.1. The group symbols are given according to the international notation. The coordinate axis a is directed perpendicular to the band plane, and the axes b and c are orthogonal to the axis a and make a right angle with each other; the b-axis coincides with the translation direction. In the notation of bands, the symbol  $\rho$  of the one-dimensional translation group is given first, the letters or numbers in the second, third and fourth positions of the symbol indicate that a particular symmetry element coincides with the coordinate axes in the order a, b, c. If no symmetry axes or normals to symmetry planes coincide with a coordinate axis the number 1 is placed in the corresponding position of the symbol or the position is left vacant.

TABLE A4.1

One-coloured, two-sided band groups

Number	Group	Number	Group
1*	$\rho 111$	16	$\rho 112/m$
2	$\rho \bar{1}11$	17	$\rho 112/b$
3	$\rho 211$	18	$\rho 222$
4	$\rho 121$	19	$\rho 22_1 2$
5	$\rho 12_1 1$	20	$\rho 2mm$
6*	$\rho 112$	21	$\rho 2mb$
7*	$\rho m11$	22	$\rho m2m$
8*	$\rho b11$	23	$\rho b2b$
9*	$\rho 1m1$	24	$\rho b2_1 m$
10	$\rho 11m$	25	$\rho m2_1 b$
11	$\rho 11b$	26*	$\rho mm2$
12	$\rho 2/m11$	27*	$\rho bm2$
13	$\rho 2/b11$	28	$\rho mmm$
14	$\rho 12/m1$	29	$\rho bmm$
15	$\rho 12_1/m1$	30	$\rho mmb$
		31	$\rho bmb$

Note: Asterisks mark the one-coloured, one-sided band groups

These groups are considered as the 31 'generating' groups (in the sense of Zamorzaev, 1957) in order to derive the two-sided, two-coloured band groups. The groups in table A4.2 were derived by starting with the generating groups and simply or severally changing operations to their colour-reversing counterparts. At the same time the possibility of .. coloured translation is taken also into account; this involves the consideration of a second one-dimensional lattice, designated  $\rho'$ . This lattice having a basic period  $\underline{t}$  contains a coloured translation  $\underline{t}'$  ( $|\underline{t}'| = \frac{1}{2}|\underline{t}|$ ) as well.

The first two columns in table A4.2 give the 31 'generating' classical and the 31 grey groups. The remaining 117 black-white groups are symbolized in the third column. The 31 of these groups correspond to the black-white lattice whereas in the remaining 86 groups particular symmetry operations are colour-reversing ones.

Asterisks in table A4.2 mark the 31 classes of one-sided, two-coloured band groups whose list and pictorial representations were given by Shubnikov (1930). These groups differ in their symmetry elements but not in the orientation of these symmetry elements with respect to the singular plane. The remaining 148 classes describe the symmetry of the two-sided, two-coloured bands.

Another deviation of the two-sided, two-coloured band groups can be devised by selecting from among the 394 two-coloured rod groups (Neronova & Belov, 1961) the 119 which do not have 3-, 4- or 6-fold axes. Among these there are 60 which symmetry operation in only one of the axial directions normal to the rod axis. To each of these there correspond two among the two-sided, two-coloured band groups, e.g.  $\rho 2'/m11$  and  $\rho 112'/m$  in the orientation here adopted. A comparable



TABLE A4.2

Two-sided, two-coloured band groups

Number	Band group symbols		
	One-coloured groups	Neutral (grey) groups	Two-coloured groups
1 * (1-3)	$\rho 111$	$\rho 1111'$	$\rho'111$
2 (4-7)	$\rho \bar{1}11$	$\rho \bar{1}111'$	$\rho' \bar{1}11, \rho \bar{1}'11$
3 (8-11)	$\rho 211$	$\rho 2111'$	$\rho'211, \rho 2'11$
4 (12-15)	$\rho 121$	$\rho 1211'$	$\rho'121, \rho 12'1$
5 (16-19)	$\rho 12_1 1$	$\rho 12_1 11'$	$\rho'12_1 1, \rho 12_1' 1$
6 * (20-23)	$\rho 112$	$\rho 1121'$	$\rho'112, \rho 112'$
7 * (24-27)	$\rho m11$	$\rho m111'$	$\rho'm11, \rho m'11$
8 * (28-31)	$\rho b11$	$\rho b111'$	$\rho'b11, \rho b'11$
9 * (32-35)	$\rho 1m1$	$\rho 1m11'$	$\rho'1m1, \rho 1m'1$
10 (36-39)	$\rho 11m$	$\rho 11m1'$	$\rho'11m, \rho 11m'$
11 (40-43)	$\rho 11b$	$\rho 11b1'$	$\rho'11b, \rho 11b'$
12 (44-49)	$\rho 2/m11$	$\rho 2/m111'$	$\rho'2/m11, \rho 2'/m11, \rho 2/m'11,$ $\rho 2'/m'11$
13 (50-55)	$\rho 2/b11$	$\rho 2/b111'$	$\rho'2/b11, \rho 2'/b11, \rho 2/b'11,$ $\rho 2'/b'11$
14 (56-61)	$\rho 12/m1$	$\rho 12/m11'$	$\rho'12/m1, \rho 12'/m1, \rho 12/m'1,$ $\rho 12'/m'1$
15 (62-67)	$\rho 12_1/m1$	$\rho 12_1/m11'$	$\rho'12_1/m1, \rho 12_1'/m1,$ $\rho 12_1/m'1, \rho 12_1'/m'1$
16 (68-73)	$\rho 112/m$	$\rho 112/m1'$	$\rho'112/m, \rho 112'/m, \rho 112/m',$ $\rho 112'/m'$

TABLE A4.2-continued

Number	Band group symbols		
	One-coloured groups	Neutral (grey) groups	Two-coloured groups
17 (74-79)	$\rho_{112/b}$	$\rho_{112/b1'}$	$\rho'_{112/b}, \rho_{112'/b}, \rho_{112/b'}$ , $\rho_{112'/b'}$
18 (80-85)	$\rho_{222}$	$\rho_{2221'}$	$\rho'_{222}, \rho_{22'2'}$ , $\rho_{2'22'}$ , $\rho_{2'2'2}$
19 (86-91)	$\rho_{22_1 2}$	$\rho_{22_1 21'}$	$\rho'_{22_1 2}, \rho_{22_1 2'}$ , $\rho_{2'2_1 2'}$ , $\rho_{2'2_1 2}$
20 (92-97)	$\rho_{2mm}$	$\rho_{2mm1'}$	$\rho'_{2mm}, \rho_{2m'm'}$ , $\rho_{2'mm'}$ , $\rho_{2'm'm}$
21 (98-103)	$\rho_{2mb}$	$\rho_{2mb1'}$	$\rho'_{2mb}, \rho_{2m'b'}$ , $\rho_{2'mb'}$ , $\rho_{2'm'b}$
22 (104-109)	$\rho_{m2m}$	$\rho_{m2m1'}$	$\rho'_{m2m}, \rho_{m2'm'}$ , $\rho_{m'2m'}$ , $\rho_{m'2'm}$
23 (110-115)	$\rho_{b2b}$	$\rho_{b2b1'}$	$\rho'_{b2b}, \rho_{b2'b'}$ , $\rho_{b'2b'}$ , $\rho_{b'2'b}$
24 (116-121)	$\rho_{b2_1 m}$	$\rho_{b2_1 m1'}$	$\rho'_{b2_1 m}, \rho_{b2_1 m'}$ , $\rho_{b'2_1 m'}$ , $\rho_{b'2_1 m}$
25 (122-127)	$\rho_{m2_1 b}$	$\rho_{m2_1 b1'}$	$\rho'_{m2_1 b}, \rho_{m2_1 b'}$ , $\rho_{m'2_1 b'}$ , $\rho_{m'2_1 b}$
26* (128-133)	$\rho_{mm2}$	$\rho_{mm21'}$	$\rho'_{mm2}, \rho_{mm'2'}$ , $\rho_{m'm2'}$ , $\rho_{m'm'2}$
27* (134-139)	$\rho_{bm2}$	$\rho_{bm21'}$	$\rho'_{bm2}, \rho_{bm'2'}$ , $\rho_{b'm2'}$ , $\rho_{b'm'2}$

TABLE A4.2—continued

Number	Band group symbols		
	One-coloured groups	Neutral (grey) groups	Two-coloured groups
28 (140-149)	$\rho m m n$	$\rho m m n 1'$	$\rho' m m n, \rho m m' m', \rho m' m m',$ $\rho m' m' m, \rho m' m n, \rho m m' m,$ $\rho m m n', \rho m' m' m'$
29 (150-159)	$\rho b m n$	$\rho b m n 1'$	$\rho' b m n, \rho b m' m', \rho b' m n',$ $\rho b' m' m, \rho b' m n, \rho b m' m,$ $\rho b m n', \rho b' m' m'$
30 (160-169)	$\rho m m b$	$\rho m m b 1'$	$\rho' m m b, \rho m m' b', \rho m' m b',$ $\rho m' m' b, \rho m' m b, \rho m m' b,$ $\rho m m b', \rho m' m' b'$
31 (170-179)	$\rho b m b$	$\rho b m b 1'$	$\rho' b m b, \rho b m' b', \rho b' m b',$ $\rho b' m' b, \rho b' m b, \rho b m' b,$ $\rho b m b', \rho b' m' b'$

Note: Asterisks mark the two-coloured, one-sided band groups

situation arises in selecting symbols for the 80 two-sided (one-coloured) plane groups from among the symbols of the 230 Fedorov groups (classical space groups).

## Appendix 5

### GRAPHICAL REPRESENTATION OF POINT GROUPS SUPERPOSITION

The best way to demonstrate graphically the combination of point groups is by considering the corresponding stereograms. Stereographic projections of symmetry groups represent which symmetry elements are contained in a given symmetry group and how these symmetry elements are disposed relative to one another. In an alternative way, the stereogram can be considered as the totality of all points which can be derived from a given point, xyz ('starting' point) by the operation of all the symmetry operations of the given point group. This concept is the basis for the representation of the superposition of two point groups.

The combination of two point groups is represented by the superposition of the corresponding stereograms. In order to account for the relative misorientation the superposed stereograms are rotated by the appropriate angle relative to each other along the appropriate axis. This is demonstrated below.

Referring to the superposition of the cubic point group  $m\bar{3}m$  and the tetragonal group  $4/m\bar{3}m$ , considered in section 4.1, their misorientation results by rotation about the (common) 4-fold axis. Figures A5.1a and A5.1b show the stereograms of the two groups where the normal to the page of the paper coincides with the 4-fold axis in each group. Any misorientation is, therefore, expressed as a rotation about the normal to the paper.

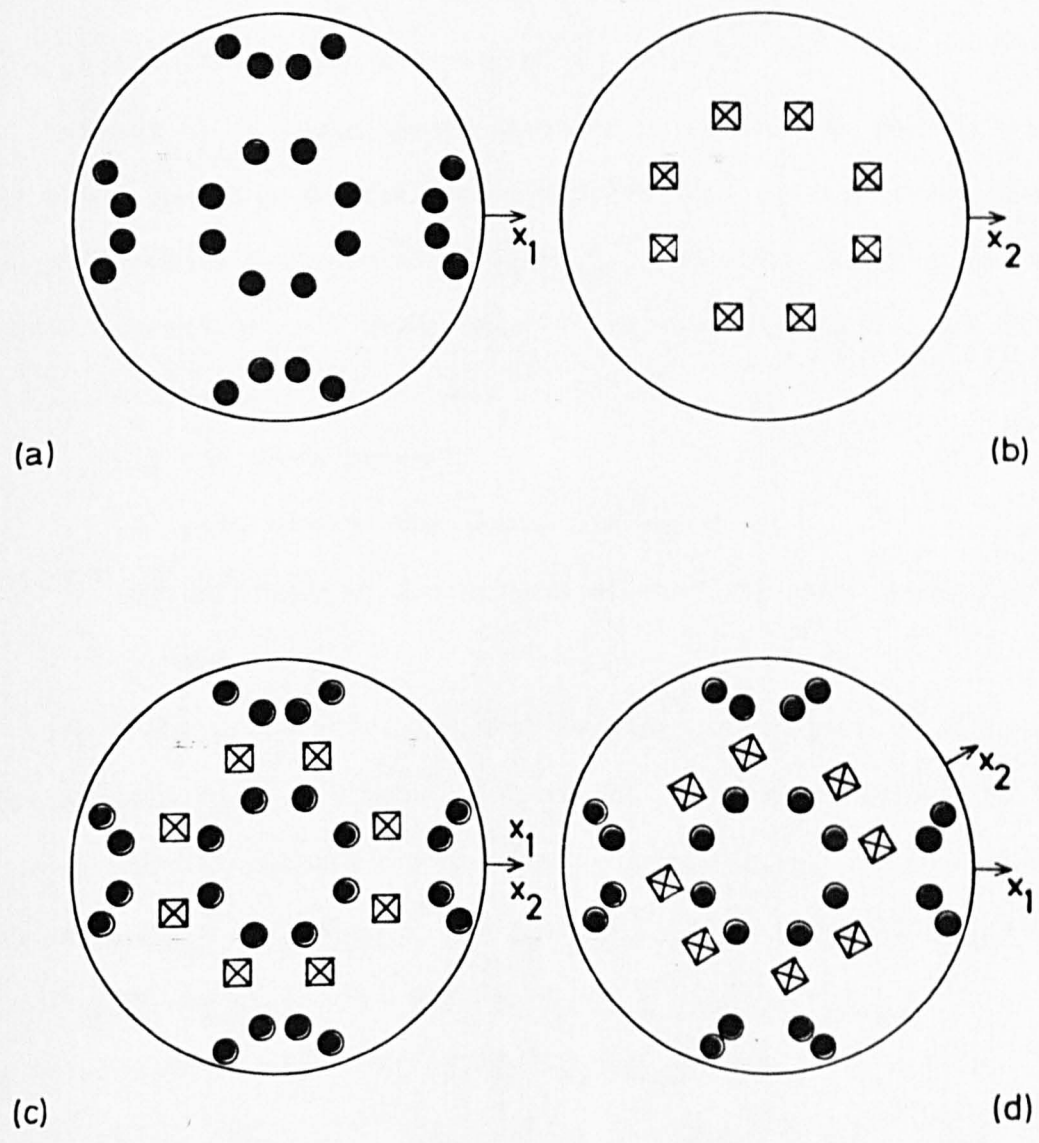
Consider the misorientation to be  $\theta=0^\circ$ . Then, the mirror planes of the two groups coincide; this is shown in figure A5.1c. It is evident that the conserved symmetry operations shown in this figure correspond to the point group  $4/m\bar{3}m$ .

Figure A5.1

Representation of point group superposition by means of stereograms:

- (a) stereogram of the point group  $m\bar{3}m$  (filled and open circles represent points above and below the page respectively)
- (b) stereogram of the point group  $4/m\bar{3}m$  (squares and crosses represent points above and below the page plane respectively)
- (c) superposition of stereograms (a) and (b) for  $\theta=0^\circ$
- (d) superposition of stereograms (a) and (b) for  $\theta \neq n\pi/2$   
( $n$ =integer)

On the other hand, the stereogram in Figure 21.14 corresponds to the superposition of the two point groups for  $S_6/2$  (invariant), the planes of symmetry passing through the 4-fold axes are not destroyed. In this case the 6-fold axis and the mirror perpendicular to it are only conserved and thus the composite symmetry is  $C_{2h}$ .



On the other hand, the stereogram in figure A5.1d corresponds to the superposition of the two point groups for  $\theta \neq n\pi/2$  ( $n$ =integer); the planes of symmetry passing through the 4-fold axes are now misaligned. In this case the 4-fold axis and the mirror plane perpendicular to it are only conserved and thus the composite symmetry is  $4/m$ .



### Appendix 6

#### THE PROOF OF THEOREMS 4.2.1 AND 4.2.2

In this appendix it is proved that the ordinary operations present in a dichromatic point group form a subgroup of the original point group  $G_o$ . In other terms, it must be proved that:

- (1) the set  $D_o$  is a group by itself, and,
- (2) it contains elements of  $G_o$  only.

The set  $D_o$  of the ordinary symmetry operations in the dichromatic point group contains all the symmetry operations of the white point group which satisfy the relation  $\underline{g}_i = R \underline{g}_j R^{-1}$  (relation 4.2.1). The set of these operations is a group only if its elements fulfill the following three postulates (see e.g. McWeeny, 1963):

- (1) the group property
- (2) existence of the identity element
- (3) existence of the inverse element for each element of the set.

The group property states that (a) the combination of any two elements (including an element with itself) is also an element of the set, and, (b) the element combination is associative. In the particular case, if  $\underline{g}_1 = R \underline{g}_a R^{-1}$ ,  $\underline{g}_2 = R \underline{g}_b R^{-1}$  and  $\underline{g}_3 = R \underline{g}_c R^{-1}$ , then it should  $\underline{g}_1 \underline{g}_2 \in D_o$  and  $(\underline{g}_1 \cdot \underline{g}_2) \cdot \underline{g}_3 = \underline{g}_1 \cdot (\underline{g}_2 \cdot \underline{g}_3)$ . But  $\underline{g}_1 \underline{g}_2 = \underline{g}_1 \cdot \underline{g}_2 = R \underline{g}_a R^{-1} \cdot R \underline{g}_b R^{-1} = R \underline{g}_a \underline{g}_b R^{-1}$ , i.e.  $\underline{g}_1 \underline{g}_2$  is an element of  $D_o$  and  $(\underline{g}_1 \cdot \underline{g}_2) \cdot \underline{g}_3 = (R \underline{g}_a R^{-1} \cdot R \underline{g}_b R^{-1}) \cdot R \underline{g}_c R^{-1} = R \underline{g}_a \underline{g}_b R^{-1} \cdot R \underline{g}_c R^{-1} = R \underline{g}_a \underline{g}_b \underline{g}_c R^{-1} = R \underline{g}_a \underline{g}_c R^{-1} \cdot R \underline{g}_b R^{-1} = R \underline{g}_a R^{-1} \cdot (R \underline{g}_b R^{-1} \cdot R \underline{g}_c R^{-1}) = \underline{g}_1 \cdot (\underline{g}_2 \cdot \underline{g}_3)$ . Therefore, the elements of  $D_o$  satisfy the group property.

The second postulate is also satisfied since  $\underline{I} = R R^{-1} = R^{-1} R$  (where  $\underline{I}$  is the identity element, i.e. the 3x3 unit matrix). The last axiom requires the existence of the inverse element for each element of  $D_o$ .

In other words, if  $\underline{g}_i = R \underline{g}_k R^{-1}$  then there must be an element  $\underline{g}_j \in D_0$  so  $\underline{g}_i \underline{g}_j = I$  or  $R \underline{g}_k R^{-1} \cdot \underline{g}_j = I$  or  $\underline{g}_j = R \underline{g}_k^{-1} R^{-1}$ . Thus, for each element of  $D_0$  its inverse element belongs also to  $D_0$ .

Consequently, the set  $D_0$  is a group and since  $D_0$  contains only elements of the white group  $G_w$ ,  $D_0$  is a subgroup of the  $G_w$ . The latter proves theorem 4.2.1.

This theorem is now used for deriving the relation between the orders of the dichromatic point group ( $r$ ) and of the white point group ( $r_w$ ). According to the analysis in section 4.2 ordinary elements belong to the dichromatic point group only if they relate white and at the same time black points. Thus, the number of general points ( $n_d$ ) in the dichromatic point group is twice the order  $r_0$  of  $D_0$ . Alternatively stated, the point symmetry of the dichromatic complex is described by the set of the  $2r_0$  general points. But the number of the general points is equal to the order of the dichromatic point group and thus  $r = 2r_0$ . The group  $D_0$  is, however, a subgroup of the white point group  $G_w$  and according to the Lagrange's theorem (see e.g. Buerger, 1963) the order of a subgroup is a factor of the group, i.e.  $r_0 = r_w/k$  where  $k$  is an integer. The latter proves theorem 4.2.2.

## Appendix 7

### THE PROOF OF THEOREMS 4.2.3 AND 4.2.4

It has been shown in section 4.2 that the set of the symmetry operations in a dichromatic point group is  $D = D_o + D_c$ . In this appendix the conditions under which the set  $D = D_o + D_c$  forms a group are investigated.

The combination law between elements of the set  $D$  is based on the fundamental property of the colour-reversing operations: two consecutive colour-reversing transformations are equivalent to one uncoloured operation. On the other hand, the combination of an ordinary and a colour-reversing operation is equivalent to another colour-reversing operation. Therefore, regarding the nature of the product between elements of the set  $D$  the following relations occur:  $OxO=O$ ,  $CxC=O$ ,  $OxC=C$ ,  $CxO=C$ , where  $O$  and  $C$  denote ordinary and colour-reversing operations.

The investigation of the conditions for which the set  $D = D_o + D_c$  is a group must be carried out in two stages. This is because two cases must be distinguished for the element  $\underline{g}$  entering the relation 4.2.2, namely:

- (1)  $\underline{g}$  is an element of  $D_o$ , and,
- (2)  $\underline{g}$  is not an element of  $D_o$ .

The former case is called 'doubled symmetry case' while the latter is the 'single symmetry case'.

#### A7.1 The doubled symmetry case

In this case the colour-reversing operations are given by  $C_{\underline{1}} = h_{\underline{1}} R^{-1}$  with  $h_{\underline{1}} \in D_o$ ; thus the set  $D$  contains the elements:

$$D = \{h_{\underline{1}}, h_{\underline{2}}, \dots, C_{\underline{1}}, C_{\underline{2}}, \dots\}$$

and the conditions for the formation of a dichromatic point group are

derived by requiring these elements to fulfil the group postulates (see appendix 6). The group property holds for the products between ordinary elements since the set  $D_0$  is a group (theorem 4.2.1). Additionally, it must be satisfied for the product of two colour-reversing elements, say,  $C_{i=i} = h_i R^{-1}$  and  $C_{j=j} = h_j R^{-1}$ , i.e. their product must be an ordinary element belonging to the set  $D$ . Thus, it must be:  $C_{i=i} \cdot C_{j=j} = h_i R^{-1} \cdot h_j R^{-1} = h_k$ . But, from the relation (4.2.1)  $R^{-1} h_j = h_{j=1} R^{-1}$  and the last relation can be written  $C_{i=i} \cdot C_{j=j} = h_i h_{j=1} R^{-1} R^{-1} = h_k$ .

Therefore, in order the closure property to be satisfied for the colour-reversing elements, the operation  $\underline{RR}$  must be equivalent to an operation of the set  $D_0$ . Let  $\underline{RR} = h_p$ ; then, the closure property holds for all the colour-reversing elements of  $D$ , since:  $C_{i=i} \cdot C_{j=j} = h_i h_{j=1} R^{-1} R^{-1} = h_{i=1} h_{j=1} h_p$ .

It remains, now, to check if the closure property holds for the combination of an ordinary and a colour-reversing element. In other words, it must be checked that the products  $h_{i=j} C_j$  and  $C_{j=i} h_i$  belong to the set  $D$ . But:

$$h_{i=j} C_j = h_{i=j} h_j R^{-1} = h_{k=k} R^{-1} \in D$$

and,

$$C_{j=i} h_i = h_{j=i} R^{-1} h_i = h_{l=l} R^{-1} \in D$$

since from the relation (4.2.1) it holds that  $R^{-1} h_i = h_{i=m} R^{-1}$ .

Therefore, the closure property holds for the set  $D$  only when the operation  $\underline{RR}$  is equivalent to an ordinary operation of the set  $D_0$ . The products of elements of  $D$  satisfy the associative law as it is indicated below:

(a)  $(h_{1=1} \cdot h_{2=2}) \cdot h_{3=3} = h_{1=1} \cdot (h_{2=2} \cdot h_{3=3})$  since  $D_0$  is a group (theorem 4.2.1)

(b)  $(h_{1=1} \cdot h_{2=2}) \cdot C_{3=3} = (h_{1=1} \cdot h_{2=2}) \cdot h_{3=3} R^{-1} = h_{1=1} h_{2=2} \cdot h_{3=3} R^{-1} = h_{1=1} h_{2=2} h_{3=3} R^{-1} = h_{1=1} \cdot h_{2=2} h_{3=3} R^{-1} = h_{1=1} \cdot (h_{2=2} \cdot h_{3=3} R^{-1}) = h_{1=1} \cdot (h_{2=2} \cdot C_{3=3})$

$$(c) \quad (\underline{h}_1 \cdot \underline{C}_2) \cdot \underline{h}_3 = (\underline{h}_1 \cdot \underline{h}_2 \underline{R}^{-1}) \cdot \underline{h}_3 = \underline{h}_1 \underline{h}_2 \underline{R}^{-1} \cdot \underline{h}_3 = \underline{h}_1 \underline{h}_2 \underline{R}^{-1} \underline{h}_3 = \underline{h}_1 \cdot \underline{h}_2 \underline{R}^{-1} \underline{h}_3 = \underline{h}_1 \cdot (\underline{h}_2 \underline{R}^{-1} \cdot \underline{h}_3) = \underline{h}_1 \cdot (\underline{C}_2 \cdot \underline{h}_3)$$

$$(d) \quad (\underline{C}_1 \cdot \underline{h}_2) \cdot \underline{h}_3 = (\underline{h}_1 \underline{R}^{-1} \cdot \underline{h}_2) \cdot \underline{h}_3 = \underline{h}_1 \underline{R}^{-1} \underline{h}_2 \cdot \underline{h}_3 = \underline{h}_1 \underline{R}^{-1} \underline{h}_2 \underline{h}_3 = \underline{h}_1 \underline{R}^{-1} \cdot \underline{h}_2 \underline{h}_3 = \underline{h}_1 \underline{R}^{-1} \cdot (\underline{h}_2 \cdot \underline{h}_3) = \underline{C}_1 \cdot (\underline{h}_2 \cdot \underline{h}_3)$$

$$(e) \quad (\underline{h}_1 \cdot \underline{C}_2) \cdot \underline{C}_3 = (\underline{h}_1 \cdot \underline{h}_2 \underline{R}^{-1}) \cdot \underline{h}_3 \underline{R}^{-1} = \underline{h}_1 \underline{h}_2 \underline{R}^{-1} \cdot \underline{h}_3 \underline{R}^{-1} = \underline{h}_1 \underline{h}_2 \underline{R}^{-1} \underline{h}_3 \underline{R}^{-1} = \underline{h}_1 \cdot \underline{h}_2 \underline{R}^{-1} \underline{h}_3 \underline{R}^{-1} = \underline{h}_1 \cdot (\underline{h}_2 \underline{R}^{-1} \cdot \underline{h}_3 \underline{R}^{-1}) = \underline{h}_1 \cdot (\underline{C}_2 \cdot \underline{C}_3)$$

$$(f) \quad (\underline{C}_1 \cdot \underline{h}_2) \cdot \underline{C}_3 = (\underline{h}_1 \underline{R}^{-1} \cdot \underline{h}_2) \cdot \underline{h}_3 \underline{R}^{-1} = \underline{h}_1 \underline{R}^{-1} \underline{h}_2 \cdot \underline{h}_3 \underline{R}^{-1} = \underline{h}_1 \underline{R}^{-1} \underline{h}_2 \underline{h}_3 \underline{R}^{-1} = \underline{h}_1 \underline{R}^{-1} \cdot \underline{h}_2 \underline{h}_3 \underline{R}^{-1} = \underline{h}_1 \underline{R}^{-1} \cdot (\underline{h}_2 \cdot \underline{h}_3 \underline{R}^{-1}) = \underline{C}_1 \cdot (\underline{h}_2 \cdot \underline{C}_3)$$

$$(g) \quad (\underline{C}_1 \cdot \underline{C}_2) \cdot \underline{h}_3 = (\underline{h}_1 \underline{R}^{-1} \cdot \underline{h}_2 \underline{R}^{-1}) \cdot \underline{h}_3 = \underline{h}_1 \underline{R}^{-1} \underline{h}_2 \underline{R}^{-1} \cdot \underline{h}_3 = \underline{h}_1 \underline{R}^{-1} \underline{h}_2 \underline{R}^{-1} \underline{h}_3 = \underline{h}_1 \underline{R}^{-1} \cdot \underline{h}_2 \underline{R}^{-1} \underline{h}_3 = \underline{h}_1 \underline{R}^{-1} \cdot (\underline{h}_2 \underline{R}^{-1} \cdot \underline{h}_3) = \underline{C}_1 \cdot (\underline{C}_2 \cdot \underline{h}_3)$$

$$(h) \quad (\underline{C}_1 \cdot \underline{C}_2) \cdot \underline{C}_3 = (\underline{h}_1 \underline{R}^{-1} \cdot \underline{h}_2 \underline{R}^{-1}) \cdot \underline{h}_3 \underline{R}^{-1} = \underline{h}_1 \underline{R}^{-1} \underline{h}_2 \underline{R}^{-1} \cdot \underline{h}_3 \underline{R}^{-1} = \underline{h}_1 \underline{R}^{-1} \underline{h}_2 \underline{R}^{-1} \underline{h}_3 \underline{R}^{-1} = \underline{h}_1 \underline{R}^{-1} \cdot \underline{h}_2 \underline{R}^{-1} \underline{h}_3 \underline{R}^{-1} = \underline{h}_1 \underline{R}^{-1} \cdot (\underline{h}_2 \underline{R}^{-1} \cdot \underline{h}_3 \underline{R}^{-1}) = \underline{C}_1 \cdot (\underline{C}_2 \cdot \underline{C}_3)$$

Taking into account theorem 4.2.1 it is clear that the set D contains the identity element as well as the inverse element of each ordinary symmetry operation. The set D contains also the inverse element of each colour-reversing element, since there are two ordinary elements  $\underline{h}_1$  and  $\underline{h}_k$  such so  $\underline{C}_i \underline{C}_j = \underline{h}_i \underline{R}^{-1} \cdot \underline{h}_j \underline{R}^{-1} = \underline{h}_i \underline{h}_j \underline{R}^{-1} \underline{R}^{-1} = \underline{h}_i \underline{h}_j \underline{R}^{-1} \underline{R}^{-1} = \underline{h}_i \underline{h}_j = \underline{I}$  for all the elements  $\underline{C}_i, \underline{C}_j$ .

Therefore, in the doubled symmetry case the set D forms a group only when the rotation  $\underline{R}$  is such so the transformation  $\underline{R}\underline{R}$  is equivalent to one of the ordinary elements of the group  $G_w$ .

The dichromatic point group contains  $2r_o$  points, half of them white and the rest black. Thus, according to theorem 4.2.2 the  $r_w$  white points of the group  $G_w$  can be dispersed into  $i=2/k$  subsets each containing  $r_o$  points, and the same can be done for the black points. The following

notation is introduced:

white point subsets:  $Z_1, Z_2, \dots, Z_i$

black point subsets:  $U_1, U_2, \dots, U_i$

Moreover, it is considered that the points in  $Z_1$  and  $U_1$  are given by the operation of the ordinary symmetry elements  $D_0$  on a general point (which is  $\underline{x}$  for the white and  $\underline{Rh}_0 \underline{x}$  for the black points;  $h_0 \in D_0$ ). The points in the remaining subsets are given by the operation of the symmetry elements belonging to the set  $\{G_0 - D_0\}$  on the same starting points.

Thus:

$$Z_1 = \{ \underline{h}_1 \underline{x}, \underline{h}_2 \underline{x}, \dots, \underline{h}_r \underline{x} \}, \quad Z_2 = \{ \underline{g}_{r_0+1} \underline{x}, \dots, \underline{g}_{2r_0} \underline{x} \}, \quad \dots$$

$$U_1 = \{ \underline{Rh}_1 \underline{h}_0 \underline{x}, \underline{Rh}_2 \underline{h}_0 \underline{x}, \dots, \underline{Rh}_r \underline{h}_0 \underline{x} \}, \quad U_2 = \{ \underline{Rg}_{r_0+1} \underline{x}, \dots, \underline{Rg}_{2r_0} \underline{x} \}, \quad \dots$$

It is now clear that the colour-reversing symmetry operations in the doubled symmetry case have been obtained by considering relations between points of the subsets  $Z_1$  and  $U_1$ . However, if a colour-reversing symmetry element is obtained by considering relations between points of the subsets  $Z_k$  and  $U_k$  with  $k \neq 1$ , then it is given by  $\underline{g}_{k=1} R^{-1}$  with  $\underline{g}_k \in D_0$ . Therefore, in the doubled symmetry case the colour-reversing symmetry elements are given by  $\underline{g}_{n=1} R^{-1}$  with  $\underline{g}_n$  any element of the white point group  $G_w$ . This implies that the order of the dichromatic point group in the doubled symmetry case is twice the order of the white point group.

But, the transformation  $\underline{R}$  can be written as  $\underline{PI}'$  ( $= \underline{I}' \underline{P}$ ) where  $\underline{I}'$  is the antiidentity operation and  $\underline{P}$  is to be understood as the ordinary rotation 'equivalent' to  $\underline{R}$ . Hence, the colour-reversing elements are given by  $\underline{g}_i \underline{P}^{-1} \underline{I}'$  ( $= \underline{I}' \underline{g}_i \underline{P}^{-1}$ ), and the group  $D$  can be written as  $D = G_w + \underline{I}' G_w \underline{P}^{-1}$ . This group is, obviously, a supergroup of  $G_w$  of factor 2. Therefore, in the doubled symmetry case a dichromatic point group is formed only when an isomorphic ordinary point group exists.

It should be noticed that in this case the ordinary operations are given by a relation of the form  $\underline{g}_i = R \underline{g}_j R^{-1}$ . Moreover, all the elements of the white group satisfy necessarily the above relation and therefore the transformation  $\underline{R}$  is a similarity transformation of the white point group. Hence, the relation  $\underline{R} \underline{R} = \underline{g}_i$  gives the rotations which leave the white point group invariant. The last involves that in theorem 4.2.1 the trivial subgroups must be included as well.

#### A7.2 The single symmetry case

The colour-reversing elements of the set  $D = D_0 + D_c$  are given, in the single symmetry case, by  $\underline{C}_i = \underline{g}_j R^{-1}$  with  $\underline{g}_j \in D_0$ . Thus, the set  $D$  contains the elements:

$$D = \{ \underline{h}_1, \underline{h}_2, \dots, \underline{C}_1, \underline{C}_2, \dots \}$$

In order this set to form a group the fundamental postulates must be satisfied. The fulfilment of these postulates imposes certain conditions on the form of the transformation  $\underline{R}$ . Moreover, additional conditions are imposed on the operations  $\underline{g}_i$ . This is because, according to theorem 4.2.2, the number of elements of the set  $D$  is  $2r_0$  where  $r_0$  is the order of the group  $D_0$ , and hence the number of colour-reversing elements in  $D$  is  $r_0$ . However, since the number of elements  $\underline{g}_i \in D_0$  is greater than  $r_0$ , it is necessary to investigate the conditions imposed on the  $\underline{g}_i$ 's under which the set  $D$  is a group.

Initially, it is examined whether the elements of  $D$  satisfy the closure property. Since the ordinary symmetry operations form a group  $D_0$ , the product of any two ordinary elements is another ordinary operation of  $D_0$  and therefore of  $D = D_0 + D_c$ . Considering, now, the product of two colour-reversing elements  $\underline{C}_i = \underline{g}_i R^{-1}$  and  $\underline{C}_j = \underline{g}_j R^{-1}$  it is required that their product must be an ordinary element  $\underline{h}_k$ , i.e.:

$$\underline{C}_i \underline{C}_j = \underline{g}_i R^{-1} \cdot \underline{g}_j R^{-1} = \underline{h}_k \quad \text{or} \quad R^{-1} \underline{g}_j R^{-1} = \underline{g}_i^{-1} \underline{h}_k$$

But,  $R^{-1} \underline{g}_j R^{-1}$  corresponds necessarily to an ordinary operation (two consecutive colour transformations). Therefore, the operation  $\underline{g}_i^{-1} \underline{h}_k$  must be an ordinary operation of  $D_0$ , i.e.  $\underline{g}_i^{-1} \underline{h}_k = \underline{h}_m$ . The last relation means that the set of operations  $\{\underline{h}_1, \underline{h}_2, \dots, \underline{g}_1, \underline{g}_2, \dots\}$  must be a group. But, since the elements  $\{\underline{h}_1, \underline{h}_2, \dots\}$  form a group and because the number of  $\underline{g}_i$ 's is equal to the number of  $\underline{h}_i$ , the group  $\{\underline{h}_1, \underline{h}_2, \dots, \underline{g}_1, \underline{g}_2, \dots\}$  is a supergroup of  $D_0$  of factor 2. Moreover, since all the elements of this group are elements of  $G_w$ ,  $\{\underline{h}_1, \underline{h}_2, \dots, \underline{g}_1, \underline{g}_2, \dots\}$  is a subgroup of  $G_w$ . This supergroup will be symbolized by  $D_2$ . Therefore, in the single symmetry case a dichromatic point group is formed when the isomorphic ordinary point group exists. In other words, no new ordinary point groups are introduced.

It follows that the set  $D$  is a group when the relation  $\underline{Rg}_i R = \underline{g}_j$  is satisfied for any element belonging to the set  $\{D_2 - D_0\}$ . However, this condition can be further restricted. Let  $\underline{C}_1 = \underline{g}_1 R^{-1}$  and  $\underline{C}_2 = \underline{g}_2 R^{-1}$  are two colour-reversing elements such that  $\underline{C}_1 \cdot \underline{C}_2 = \underline{h}$  where  $\underline{h}$  is an ordinary symmetry element. The condition for the set  $D$  to be group states that the relation  $\underline{Rg}_i R = \underline{g}_j$  must hold for any pair of  $\underline{g}_i, \underline{g}_j$  where  $\underline{g}_i \in \{D_2 - D_0\}$  and  $\underline{g}_j \in \{D_2 - D_0\}$ . Therefore, the relations  $\underline{Rg}_1 R = \underline{g}_2$  and  $\underline{Rg}_2 R = \underline{g}_1$  hold. Accounting for the relation  $\underline{C}_1 \underline{C}_2 = \underline{h}$  it holds respectively:  $\underline{g}_1 \underline{g}_1 = \underline{h}$  and  $\underline{g}_2 \underline{g}_2 = \underline{h}$ . The two last relations impose that  $\underline{g}_1 = \underline{g}_2$ . Therefore, the set  $D$  is a group only when the relation  $\underline{Rg}_i R = \underline{g}_i$  is satisfied for all the elements of the set  $\{D_2 - D_0\}$ .

It should be noticed that as far as the products of an ordinary element  $\underline{h}_i$  and a colour-reversing element  $\underline{C}_j = \underline{g}_j R^{-1}$  are concerned it



holds that:

$$h_i \cdot C_j = h_i \cdot g_j R^{-1} = g_k R^{-1}$$

and

$$C_j \cdot h_i = g_j R^{-1} \cdot h_i = g_j h_i R^{-1} = g_m R^{-1}$$

where the relation (4.2.1) is taken into account for the second relation and with  $g_k$  and  $g_m$  being elements of the group  $D_2$ .

Therefore, the condition mentioned above is the only one required for the fulfilment of the closure property. It can be proved easily that the associative property is also satisfied. Taking into account theorem 4.2.1, the set  $D$  contains the unit element as well as the inverse of each ordinary symmetry operation. Moreover, the set  $D$  contains also the inverse elements of the colour-reversing elements, since there are two elements  $g_i, g_j$  belonging to the set  $\{D_2 - D_0\}$  such that  $g_i R^{-1} \cdot g_j R^{-1} = g_i g_j = I$  for all the elements  $C_i = g_i R^{-1}$  and  $C_j = g_j R^{-1}$ .

Therefore, in the single symmetry case, the set  $D$  forms a group only when there is a factor 2 supergroup of the group  $D_0$  being subgroup of  $G_0$  and the rotation  $R$  is such that the relation  $R g_i R = g_i$  holds for all the elements of the set  $\{D_2 - D_0\}$ .

## Appendix 8

### EXAMPLES OF POINT SYMMETRY SUPERPOSITION

The coordinate system used for the calculations in this appendix is that of the white point group, except if it is otherwise stated. This orthogonal coordinate system is considered to have the standard orientation (see International Tables of X-ray Crystallography, 1969) relative to the symmetry operations of the white point group. The symmetry operations are denoted according to the scheme given in appendix 1.

#### A8.1 Superposition in monoclinic hemihedral holoaxial class

In the case of the monoclinic group  $2 = \{1, 2_z^1\}$  both doubled and single symmetry dichromatic groups are likely to be formed. The latter arise since the monoclinic group has two subgroups (corresponding to the trivial ones), namely,  $1 = \{1\}$  and  $2 = \{1, 2_z^1\}$ .

The doubled symmetry rotations are  $[xyz]/180^\circ$  and  $[00z]/90^\circ$ , obtained from  $\underline{\underline{RR}} = \underline{\underline{1}}$  and  $\underline{\underline{RR}} = \underline{\underline{2}}_z^1$  respectively. A  $[00z]/90^\circ = 4_z^1$  misorientation creates a dichromatic point group isomorphic to  $4' = \{1, 2_z^1, 4_z^{1'}, 4_z^{3'}\}$  since  $\underline{\underline{1}} \cdot \underline{\underline{R}}^{-1} = \underline{\underline{4}}_z^{3'}$  and  $\underline{\underline{2}}_z^1 \underline{\underline{R}}^{-1} = \underline{\underline{4}}_z^{1'}$ . Similarly, the improper rotation  $[00z]/90^\circ$  corresponds to the dichromatic point group  $\bar{4}'$ .

The rotation  $[xyz]/180^\circ$  yields a dichromatic point group only when it transforms the white group into itself, i.e. only when  $\underline{\underline{2}}_z^1 = \underline{\underline{R}} \underline{\underline{2}}_z^1 \underline{\underline{R}}^{-1}$ . The solutions of this equation are the rotations  $[00z]/180^\circ$  and  $[xy0]/180^\circ$ . However,  $[00z]/180^\circ$  is a symmetry operation of the white group and thus it creates a  $21'$  point group. The dichromatic point group formed by proper and improper rotations  $[00z]/180^\circ$ ,  $[xy0]/180^\circ$  and  $[00z]/90^\circ$  are given in table A8.1.

TABLE A8.1

Dichromatic point groups created by the superposition of two  
monoclinic groups  $2 = \{1, 2_z^1\}$

Rotation	Ordinary elements	Colour-reversing elements	Dichromatic point group
Proper			
$xyz/0^\circ$	$1, 2_z^1$	$1', 2_z^1$	$21'$
$00z/180^\circ$	$1, 2_z^1$	$1', 2_z^1$	$21'$
$xy0/180^\circ$	$1, 2_z^1$	$2_x^1, 2_y^1$	$2'2'2$
$00z/90^\circ$	$1, 2_z^1$	$4_z^1, 4_z^3$	$4'$
$xy0/\theta^\circ$	1	$2_z^1$	$2' (*)$
Improper			
$xyz/0^\circ$	$1, 2_z^1$	$i', s_z'$	$2/m'$
$00z/180^\circ$	$1, 2_z^1$	$i', s_z'$	$2/m'$
$xy0/180^\circ$	$1, 2_z^1$	$s_x', s_y'$	$2m'm'$
$00z/90^\circ$	$1, 2_z^1$	$\bar{4}_z^1, \bar{4}_z^3$	$\bar{4}'$
$xy0/\theta^\circ$	1	$s_z'$	$m' (*)$

(\*) Relative to the dichromatic coordinate system

In the single symmetry case the subgroup  $D_0 = 1 = \{1\}$  is considered only. The next step is to determine its supergroup  $D_2$ ; reference to figure A9.2 indicates that only the ordinary point group  $2 = \{1, 2_z^1\}$  can be considered as  $D_2$  and thus only one dichromatic point group corresponds to the single symmetry case. In order to determine the single symmetry rotation(s) the equation  $\underline{\underline{R}}_{\underline{\underline{z}}}^{\underline{\underline{1}}} \underline{\underline{R}}_{\underline{\underline{z}}}^{\underline{\underline{2}}^1} = \underline{\underline{2}}^1$  is solved. The solution of this equation corresponds to any rotation about a direction normal to the z-axis, i.e.:

$$\underline{\underline{R}} = \begin{pmatrix} \cos\theta + m_1^2(1 - \cos\theta) & m_1 m_2(1 - \cos\theta) & -m_2 \sin\theta \\ m_1 m_2(1 - \cos\theta) & \cos\theta + m_2^2(1 - \cos\theta) & m_1 \sin\theta \\ m_2 \sin\theta & -m_1 \sin\theta & \cos\theta \end{pmatrix}$$

The colour-reversing element relative to the white coordinate system is given by:

$$\underline{\underline{2}}_{\underline{\underline{z}}}^{\underline{\underline{1}}} \underline{\underline{R}}^{-1} = \begin{pmatrix} -\cos\theta - m_1^2(1 - \cos\theta) & -m_1 m_2(1 - \cos\theta) & m_2 \sin\theta \\ -m_1 m_2(1 - \cos\theta) & -\cos\theta - m_2^2(1 - \cos\theta) & -m_1 \sin\theta \\ m_2 \sin\theta & -m_1 \sin\theta & \cos\theta \end{pmatrix}$$

or expressed relative to the dichromatic coordinate system:

$$\underline{\underline{T}}_{\underline{\underline{z}}}^{\underline{\underline{2}}^1} \underline{\underline{R}}^{-1} \underline{\underline{T}}^{-1} = \begin{pmatrix} -1 & 0 & 0 \\ 0 & -1 & 0 \\ 0 & 0 & 1 \end{pmatrix}$$

where

$$\underline{\underline{T}} = \begin{pmatrix} \cos\theta/2 + m_1^2(1 - \cos\theta/2) & m_1 m_2(1 - \cos\theta/2) & m_2 \sin\theta/2 \\ m_1 m_2(1 - \cos\theta/2) & \cos\theta/2 + m_2^2(1 - \cos\theta/2) & -m_1 \sin\theta/2 \\ m_2 \sin\theta/2 & m_1 \sin\theta/2 & \cos\theta/2 \end{pmatrix}$$

Therefore, any rotation about an axis normal to the z-axis creates a dichromatic point group  $2' = \{1, 2_z^{1'}\}$ . It should be emphasized, however, that in this case the position of the colour-reversing operation  $2_z^{1'}$  is expressed relative to the dichromatic coordinate system which is

not coincident with the white one. For the improper rotation  $[hkl]/\theta$ , the corresponding dichromatic point group is  $m' = \{1, s'_z\}$  where again the position of the mirror operation is expressed relative to the dichromatic coordinate system.

Table A8.1 summarizes the dichromatic point groups obtained by the superposition of two monoclinic hemihedral-holoaxial groups.

### A8.2 Superposition in hexagonal tetartohedral class

For the case of doubled symmetry of the superposition of hexagonal tetartohedral groups the solution of the equations  $RR = g_1$  is given in table A8.2 for each of the elements of the group  $6 = \{1, 2_z^1, 3_z^1, 3_z^2, 6_z^1, 6_z^5\}$ . Therefore, only the rotations corresponding to the solutions no. 1b, 2 and 5 must be considered in order to determine the colour-reversing elements obtained by both proper and improper rotations (table A8.3).

Considering the single symmetry cases the subgroups of the point group 6 are:  $1 = \{1\}$ ,  $2 = \{1, 2_z^1\}$ , and  $3 = \{1, 3_z^1, 3_z^2\}$ . But, only rotations  $[xyz]/180^\circ$ , corresponding to the subgroup 2, give a dichromatic point group.

The possible dichromatic point groups formed by the superposition of hexagonal tetartohedral groups are those in table A8.4. The study of the superposition of point groups belonging to planar symmetry classes appears to be more complicated. The case of the white point group  $4mm$  will be presented in detail while the superposition of the other planar symmetry groups can be treated in a similar matter.

### A8.3 Superposition in tetragonal antihemihedral class

The point group  $4mm$  contains the symmetry operations  $1, 4_z^1, 4_z^3, 2_z^1, s_x, s_y, s_\alpha, s_\beta$ . In table A8.5 the rotations corresponding to the doubled symmetry case are derived. It can be seen from this table that only

TABLE A8.2

Solution of the equation  $\underline{\underline{RR}}=\underline{\underline{g}}_i$  for the elements of the group

$$\{1, 2_z^1, 3_z^1, 3_z^2, 6_z^1, 6_z^5\}$$

No	Element $\underline{\underline{g}}_i$	Solution of $\underline{\underline{RR}}=\underline{\underline{g}}_i$	Remarks
1a	1	00z/180° (*)	symmetry operation of G <sub>o</sub>
1b	1	xy0/180° (*)	
2	2 <sub>z</sub> <sup>1</sup>	00z/90°	
3	3 <sub>z</sub> <sup>1</sup>	00z/60°	symmetry operation of G <sub>o</sub>
4	3 <sub>z</sub> <sup>2</sup>	00z/120°	symmetry operation of G <sub>o</sub>
5	6 <sub>z</sub> <sup>1</sup>	00z/30°	
6	6 <sub>z</sub> <sup>5</sup>	00z/150°	related by symmetry to solution no. 5

(\*) Rotations conserving the white point group

TABLE A8.3

Colour-reversing symmetry operations created by the rotations in table A8.2

Rotation	$\underline{\underline{1R}}^{-1}$	$\underline{\underline{2^1R}}^{-1}$	$\underline{\underline{3^1R}}^{-1}$	$\underline{\underline{3^2R}}^{-1}$	$\underline{\underline{6^1R}}^{-1}$	$\underline{\underline{6^5R}}^{-1}$
proper						
xy0/180°	$2_x^{1'}$	$2_r^{1'}$	$2_A^{1'}$	$2_y^{1'}$	$2_B^{1'}$	$2_\Delta^{1'}$
00z/90°	$4_z^{3'}$	$\underline{\underline{12}}_z^{11'}$	$\underline{\underline{12}}_z^{7'}$	$4_z^{1'}$	$\underline{\underline{12}}_z^{1'}$	$\underline{\underline{12}}_z^{5'}$
00z/30°	$\underline{\underline{12}}_z^{11'}$	$\underline{\underline{12}}_z^{1'}$	$4_z^{3'}$	$\underline{\underline{12}}_z^{5'}$	$4_z^{1'}$	$\underline{\underline{12}}_z^{7'}$
improper						
xyz/0°	$i'$	$\bar{6}_z^{1'}$	$\bar{6}_z^{5'}$	$s'_z$	$\bar{3}_z^{1'}$	$\bar{3}_z^{2'}$
xy0/180°	$2_x^{1'}$	$2_r^{1'}$	$2_A^{1'}$	$2_y^{1'}$	$2_B^{1'}$	$2_\Delta^{1'}$
00z/90°	$\bar{4}_z^{3'}$	$\underline{\underline{12}}_z^{11'}$	$\underline{\underline{12}}_z^{7'}$	$\bar{4}_z^{1'}$	$\underline{\underline{12}}_z^{1'}$	$\underline{\underline{12}}_z^{5'}$
00z/30°	$\underline{\underline{12}}_z^{11'}$	$\underline{\underline{12}}_z^{1'}$	$\bar{4}_z^{3'}$	$\underline{\underline{12}}_z^{5'}$	$\bar{4}_z^{1'}$	$\underline{\underline{12}}_z^{7'}$

TABLE A8.4

Dichromatic point groups created by the superposition of two

groups  $\{1, 2_z^1, 3_z^1, 3_z^2, 6_z^1, 6_z^5\}$

Proper rotation	Dichromatic point group	Improper rotation	Dichromatic point group
$00z/30^\circ$	$\underline{12}'$	$xyz/0^\circ$	$6/m'$
$00z/60^\circ$	$61'$	$00z/30^\circ$	$\underline{\bar{12}}'$
$00z/90^\circ$	$\underline{12}'$	$00z/60^\circ$	$6/m'$
$00z/180^\circ$	$61'$	$00z/90^\circ$	$\underline{\bar{12}}'$
$xy0/180^\circ$	$62'2'$	$00z/180^\circ$	$6/m'$
$xy0/\theta^\circ$	$2'$	$xy0/180^\circ$	$62'2'$
		$xy0/\theta^\circ$	$m'$



**TABLE A8.5**

Solution of the equation  $\underline{RR}=\underline{g}_i$  for the elements of the group

$$\{1, 4_z^1, 4_z^3, 2_z^1, s_x, s_y, s_\alpha, s_\beta\}$$

No	Element $\underline{g}_i$	Solution of $\underline{RR}=\underline{g}_i$	Remarks
1a	1	$00z/180^\circ$ (*)	symmetry operation of $G_o$
1b	1	$xy0/180^\circ$	
2	$2_z^1$	$00z/90^\circ$	symmetry operation of $G_o$
3	$4_z^1$	$00z/45^\circ$	
4	$4_z^3$	$00z/135^\circ$	related by symmetry to solution no. 3

(\*) Rotation conserving the white point group

the  $[xy0]/180^\circ$  and  $[00z]/45^\circ$  proper and improper rotations must be considered. Additionally, since the point group  $4mm$  does not contain a centre of symmetry the pure inversion must be included in the set of the improper rotations. The table A8.6 gives the created colour-reversing symmetry operations and the corresponding dichromatic point group for each of the above rotations.

To establish the dichromatic point groups corresponding to the single symmetry case, the subgroups of the white group  $G_w$  must be determined. Moreover, for each subgroup of  $G_w$  its supergroup of index 2 which at the same time is a subgroup of  $G_w$  must be found. The deviation of the single symmetry groups is shown in table A8.7.

Finally, improper rotations of the single symmetry case must be considered in addition to those in table A8.7. Table A8.8 gives the dichromatic point groups resulting by such rotations together with those derived above.

TABLE A8.6

Colour-reversing symmetry operations created by the rotations in table A8.5

Rotation	$\underline{1R}^{-1}$	$\underline{4^1R}^{-1}$ $\underline{=z}$	$\underline{4^3R}^{-1}$ $\underline{=z}$	$\underline{2^1R}^{-1}$ $\underline{=z}$	$\underline{sR}^{-1}$ $\underline{=x}$	$\underline{sR}^{-1}$ $\underline{=y}$	$\underline{sR}^{-1}$ $\underline{=x}$	$\underline{sR}^{-1}$ $\underline{=p}$	Dichromatic point group
Proper									
xy0/180°	$\underline{2^1_x}$	$\underline{2^1_\alpha}$	$\underline{2^1_\beta}$	$\underline{2^1_y}$	$i'$	$\underline{s'_z}$	$\underline{4^3'_z}$	$\underline{4^1'_z}$	4/m'mm
00z/45°	$\underline{8^7_z}$	$\underline{8^1_z}$	$\underline{8^5_z}$	$\underline{8^3_z}$	$\underline{s'_y}$	$\underline{s'_p}$	$\underline{s'_\tau}$	$\underline{s'_\tau}$	8'mm'
Improper									
xyz/0°	$i'$	$\underline{4^3_z}$	$\underline{4^1_z}$	$\underline{s'_z}$	$\underline{2^1_x}$	$\underline{2^1_y}$	$\underline{2^1_\alpha}$	$\underline{2^1_\beta}$	4/m'mm
00z/45°	$\underline{8^7_z}$	$\underline{8^1_z}$	$\underline{8^5_z}$	$\underline{8^3_z}$	$\underline{2^1_y}$	$\underline{2^1_p}$	$\underline{2^1_\tau}$	$\underline{2^1_\tau}$	$\underline{8^1_m2'}$

Note: The improper rotation xy0/180° corresponding to a symmetry operation of the white point group  $G_0$  is not included in the above table

TABLE A8.7

Investigation of the dichromatic point groups created by the superposition of two point groups 4mm

No	Subgroup $D_0$	Elements	Supergroup $D_2$	$D_2-D_0$	Solutions of $Rg, R=g_i$	Colour-reversing elements	Dichromatic point group	Remarks
1	4	$1, 4_z^1, 4_z^3, 2_z^1$	4mm	$s_x, s_y, s_\alpha, s_\beta$	$00z/\mathcal{I}^\circ$	$s_x, s_y, s_\alpha, s_\beta$	4m'm'	relative to the dichromatic system
2	mm2	$1, 2_z^1, s_x, s_y$	4mm	$s_\alpha, s_\beta, 4_z^1, 4_z^3$	$00z/180^\circ$	—	—	$00z/180^\circ = 2_z^1$ , symmetry operation of $G_0$
3	mm2	$1, 2_z^1, s_\alpha, s_\beta$	4mm	$s_x, s_y, 4_z^1, 4_z^3$	$00z/180^\circ$	—	—	$00z/180^\circ = 2_z^1$ , symmetry operation of $G_0$
4	m	$1, s_x$	mm2	$s_y, 2_z^1$	$00z/180^\circ$ $0y0/180^\circ$ $x00/\mathcal{I}^\circ$	— — $s_y, 2_z^1$	— — mm'2'	$00z/180^\circ = 2_z^1$ , symmetry operation of $G_0$ $0y0/180^\circ$ conserves $G_0$ relative to the dichromatic system
5	m	$1, s_y$	mm2	$s_x, 2_z^1$	$00z/180^\circ$ $x00/180^\circ$ $0y0/\mathcal{I}^\circ$	— — $s_x, 2_z^1$	— — mm'2'	$00z/180^\circ = 2_z^1$ , symmetry operation of $G_0$ $x00/180^\circ$ conserves $G_0$ relative to the dichromatic system
6	m	$1, s_\alpha$	mm2	$s_\beta, 2_z^1$	$00z/180^\circ$ $\bar{x}x0/180^\circ$ $xx0/\mathcal{I}^\circ$	— — $s_\beta, 2_z^1$	— — mm'2'	$00z/180^\circ = 2_z^1$ , symmetry operation of $G_0$ $\bar{x}x0/180^\circ$ conserves $G_0$ relative to the dichromatic system
7	m	$1, s_\beta$	mm2	$s_\alpha, 2_z^1$	$00z/180^\circ$ $xx0/180^\circ$ $\bar{x}x0/\mathcal{I}^\circ$	— — $s_\alpha, 2_z^1$	— — mm'2'	$00z/180^\circ = 2_z^1$ , symmetry operation of $G_0$ $xx0/180^\circ$ conserves $G_0$ relative to the dichromatic system
8	2	$1, 2_z^1$	mm2	$s_x, s_y$	$x00/180^\circ$ $0y0/180^\circ$ $00z/\mathcal{I}^\circ$	— — —	— — —	$x00/180^\circ$ conserves $G_0$ $0y0/180^\circ$ conserves $G_0$ see no.1
9	2	$1, 2_z^1$	mm2	$s_\alpha, s_\beta$	$xx0/180^\circ$ $\bar{x}x0/180^\circ$ $00z/\mathcal{I}^\circ$	— — —	— — —	$xx0/180^\circ$ conserves $G_0$ $\bar{x}x0/180^\circ$ conserves $G_0$ see no.1
10	1	1	2	$2_z^1$	$xy0/\mathcal{I}^\circ$	$2_z^1$	2'	relative to the dichromatic system
11	1	1	m	$s_x$	$0yz/\mathcal{I}^\circ$	$s_x$	m'	relative to the dichromatic system
12	1	1	m	$s_y$	$x0z/\mathcal{I}^\circ$	$s_y$	m'	relative to the dichromatic system
13	1	1	m	$s_\alpha$	$xx0/\mathcal{I}^\circ$	$s_\alpha$	m'	relative to the dichromatic system
14	1	1	m	$s_\beta$	$\bar{x}x0/\mathcal{I}^\circ$	$s_\beta$	m'	relative to the dichromatic system

TABLE A8.8

Dichromatic point groups created by the superposition of two

groups  $\{1, 4_2^1, 4_2^3, 2_2^1, \sigma_x, \sigma_y, \sigma_\alpha, \sigma_\beta\}$

Proper rotation	Dichromatic point group	Improper rotation	Dichromatic point group
$xy0/180^\circ$	$4/m'mm$	$xyz/0^\circ$	$4/m'mm$
$00z/45^\circ$	$8'mm'$	$00z/45^\circ$	$\bar{8}'m2'$
$00z/\theta^\circ$	$4m'm'$	$00z/\theta^\circ$	$42'2'$
$x00/\theta^\circ$	$mm'2'$	$x00/\theta^\circ$	$mm'2'$
$0y0/\theta^\circ$	$m'm2'$	$0y0/\theta^\circ$	$m'm2'$
$\bar{x}x0/\theta^\circ$	$mm'2'$	$\bar{x}x0/\theta^\circ$	$mm'2'$
$xx0/\theta^\circ$	$m'm2'$	$xx0/\theta^\circ$	$m'm2'$
$xy0/\theta^\circ$	$2'$	$xy0/\theta^\circ$	$m'$

### Appendix 9

#### POINT GROUPS CONTAINING 8- OR 12-FOLD ROTATION

#### (OR ROTOINVERSION) AXES

It has been pointed out in section 4.3 that 8- or 12-fold rotation (or rotoinversion) groups must be included in the symmetry classes of dichromatic complexes with (zero- or) one-dimensional translational symmetry (see also section 5.1). These symmetry classes are derived in this appendix (the one-dimensional groups are considered in appendix 10).

Initially, the complete list of the ordinary point groups containing 8- or 12-fold symmetry operations is deduced. For this, combinations among the symmetry elements 8,  $\bar{8}$ ,  $\underline{12}$ ,  $\overline{12}$  and the crystallographic symmetry elements must be considered. The procedure for determining these combinations is similar to the one yielding the 32 classical point groups. Thus, applying the method of the conventional crystallography (see e.g. Buerger, 1963) it is found that the only combinations with the 2-fold rotation axis and the mirror plane are permissible. Working on these lines the ordinary point groups containing an 8- or 12-fold symmetry operation are derived. These are given in table A9.1, whereas their geometrical representations are shown in figure A9.1.

Having deduced the ordinary point groups a complete enumeration of the corresponding grey and black-white point groups is feasible. The most comprehensive procedure for the determination of the new groups is the one proposed by Boyle (1969)<sup>1</sup> for the construction of non-crystallographic antisymmetry groups.

The basic principle of Boyle's procedure is the classification of the 32 ordinary point groups into families of 'halving subgroups'<sup>2</sup> and thus forming the halving subgroup diagrams. The construction of

TABLE A9.1

The ordinary classes of 8- and 12-fold rotation or  
rotoinversion axes

Group	Order	Halving subgroups
8	8	4
$\bar{8}$	8	4
8/m	16	4/m, 8, $\bar{8}$
8mm	16	4mm, 8
$\bar{8}m2$	16	422, 4mm, $\bar{8}$
822	16	422, 8
8/mmm	24	4/mmm, 8/m, 8mm, $\bar{8}m2$ , 822
$\underline{12}$	12	6
$\overline{12}$	12	6
$\underline{12}/m$	24	6/m, $\underline{12}$ , $\overline{12}$
$\underline{12}mm$	24	6mm, $\underline{12}$
$\overline{12}m2$	24	622, 6mm, $\overline{12}$
$\underline{12}22$	24	622, $\underline{12}$
$\underline{12}/mmm$	48	6/mmm, $\underline{12}/m$ , $\underline{12}mm$ , $\overline{12}m2$ , $\underline{12}22$

Notes: (1) The elements of each of the above groups are given in tables A9.1a and A9.1b.

(2) The new symbolism is built up on the following principles: each symbol gives from one to three symbols for the elements which lie along special directions. The latter are: the principal axis (along which the non-crystallographic axis lies), the secondary axis perpendicular to it and an axis which is also perpendicular to the principal axis and cuts the secondary axis at  $22.5^\circ$  (for 8-fold groups) or  $15^\circ$  (for 12-fold groups).

**TABLE A91a**

**Symmetry operations of the 8-fold point groups**

	$C_8$	$C_4$	$C_2$	$C_2$	$C_2$	$C_2$	$C_2$		$C_8$	$C_4$	$C_2$	$C_2$	$C_2$	$C_2$	$C_2$	$C_2$
	1	2	3	4	5	6	7		1	2	3	4	5	6	7	
1	X	X	X	X	X	X	X	$I$			X				X	
$C_8^1$	X		X	X		X	X	$C_8^1$		X	X		X		X	
$C_8^3$	X		X	X		X	X	$C_8^3$		X	X		X		X	
$C_8^5$	X		X	X		X	X	$C_8^5$		X	X		X		X	
$C_8^7$	X		X	X		X	X	$C_8^7$		X	X		X		X	
$C_4^1$	X	X	X	X	X	X	X	$C_4^1$			X				X	
$C_4^3$	X	X	X	X	X	X	X	$C_4^3$			X				X	
$C_2^1$	X	X	X	X	X	X	X	$S_z$			X				X	
$C_2^x$						X	X	$S_x$				X	X		X	
$C_2^y$						X	X	$S_y$				X	X		X	
$C_2^a$						X	X	$S_a$				X	X		X	
$C_2^b$						X	X	$S_b$				X	X		X	
$C_2^v$					X	X	X	$S_v$				X			X	
$C_2^{\xi}$					X	X	X	$S_{\xi}$				X			X	
$C_2^p$					X	X	X	$S_p$				X			X	
$C_2^t$					X	X	X	$S_t$				X			X	



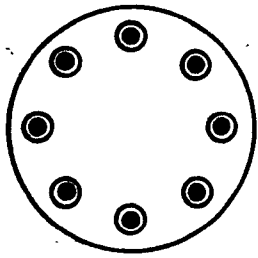
TABLE A9.10

Symmetry operations of the 12-fold point groups

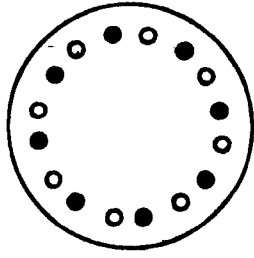
	$12$	$\bar{12}$	$12/m$	$12/m\bar{m}$	$\bar{12}m2$	$12/22$	$12/mmm$		1	2	3	4	5	6	7
1	X	X	X	X	X	X	X	$2^1_x$						X	X
$12^1_z$	X		X	X		X	X	$2^1_y$						X	X
$12^5_z$	X		X	X		X	X	$2^1_A$						X	X
$12^7_z$	X		X	X		X	X	$2^1_B$						X	X
$12^{11}_z$	X		X	X		X	X	$2^1_\Gamma$						X	X
$6^1_z$	X	X	X	X	X	X	X	$2^1_\Delta$						X	X
$6^5_z$	X	X	X	X	X	X	X	$2^1_a$					X	X	X
$4^1_z$	X		X	X		X	X	$2^1_B$					X	X	X
$4^3_z$	X		X	X		X	X	$2^1_E$					X	X	X
$3^1_z$	X	X	X	X	X	X	X	$2^1_H$					X	X	X
$3^2_z$	X	X	X	X	X	X	X	$2^1_\theta$					X	X	X
$2^1_z$	X	X	X	X	X	X	X	$2^1_\Lambda$					X	X	X
i			X				X	$s_x$				X	X		X
$\bar{12}^1_z$		X	X		X		X	$s_y$				X	X		X
$\bar{12}^5_z$		X	X		X		X	$s_A$				X	X		X
$\bar{12}^7_z$		X	X		X		X	$s_B$				X	X		X
$\bar{12}^{11}_z$		X	X		X		X	$s_\Gamma$				X	X		X
$\bar{6}^1_z$			X				X	$s_\Delta$				X	X		X
$\bar{6}^5_z$			X				X	$s_\theta$				X			X
$\bar{4}^1_z$		X	X		X		X	$s_\Lambda$				X			X
$\bar{4}^3_z$		X	X		X		X	$s_E$				X			X
$\bar{3}^1_z$			X				X	$s_H$				X			X
$\bar{3}^2_z$			X				X	$s_a$				X			X
$s_z$			X				X	$s_\beta$				X			X

**Figure A9.1**

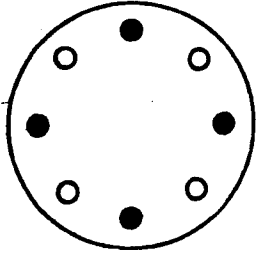
**Stereograms of the 8- and 12-fold point symmetry classes**



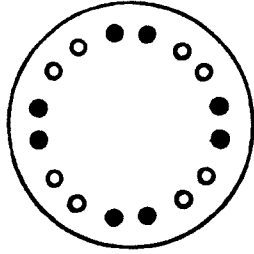
8/m



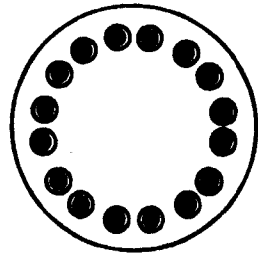
822



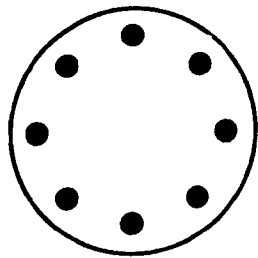
8



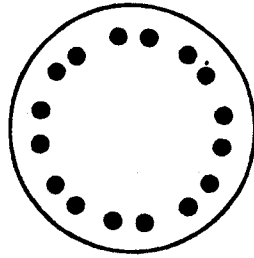
8m2



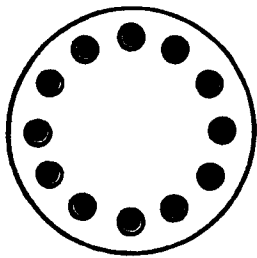
8/mmm



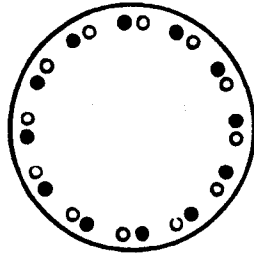
8



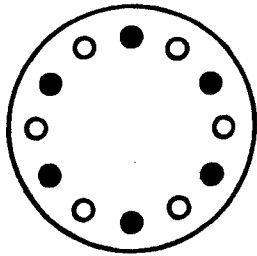
8mm



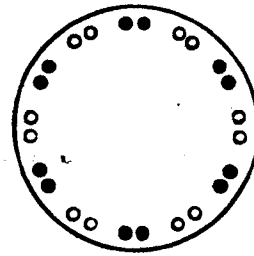
$\bar{12}/m$



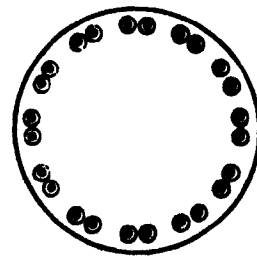
$\bar{12}22$



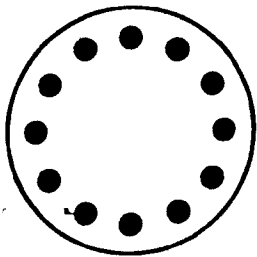
$\bar{12}$



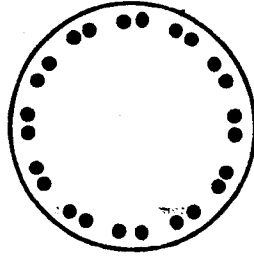
$\bar{12}m2$



$\bar{12}/m\bar{m}m$



$\bar{12}$



$\bar{12}m\bar{m}$

non-crystallographic antisymmetry groups requires the extension of these 'family trees' downwards or the establishing of new ordinary groups without halving subgroups.

In the particular case, the 8- and 12-fold classes belong to the  $C_1$  and  $C_3$  families respectively and therefore, the families are extended downwards. This is shown in figure A9.2. This figure is reproduced from the corresponding diagrams given by Boyle (1969) but the Hermann-Mauguin symbols are given instead of the Schönflies' notation and the 8- and 12-fold ordinary groups are included. The horizontal rows contain groups of the same order and adjacent rows differ in order by a factor of 2. The tie-lines relate a group  $G$  to its halving subgroups  $H$  above and the groups of which it is halving subgroup below.

As it has been mentioned in section 2.2 for any ordinary point group  $G$  there exists a grey group given by  $M = G + \underline{C}G$  (where  $\underline{C}$  is the colour-identity operation) and a number of black-white point groups. The latter are defined by  $M = H + \underline{C}(G-H)$  where  $H$  is a halving subgroup of  $G$ , and  $G-H$  means the set of elements of  $G$  that do not belong to  $H$ . It is immediately clear from the last relation that the black-white point groups corresponding to an ordinary point group are equal in number to the halving subgroups of the ordinary group.

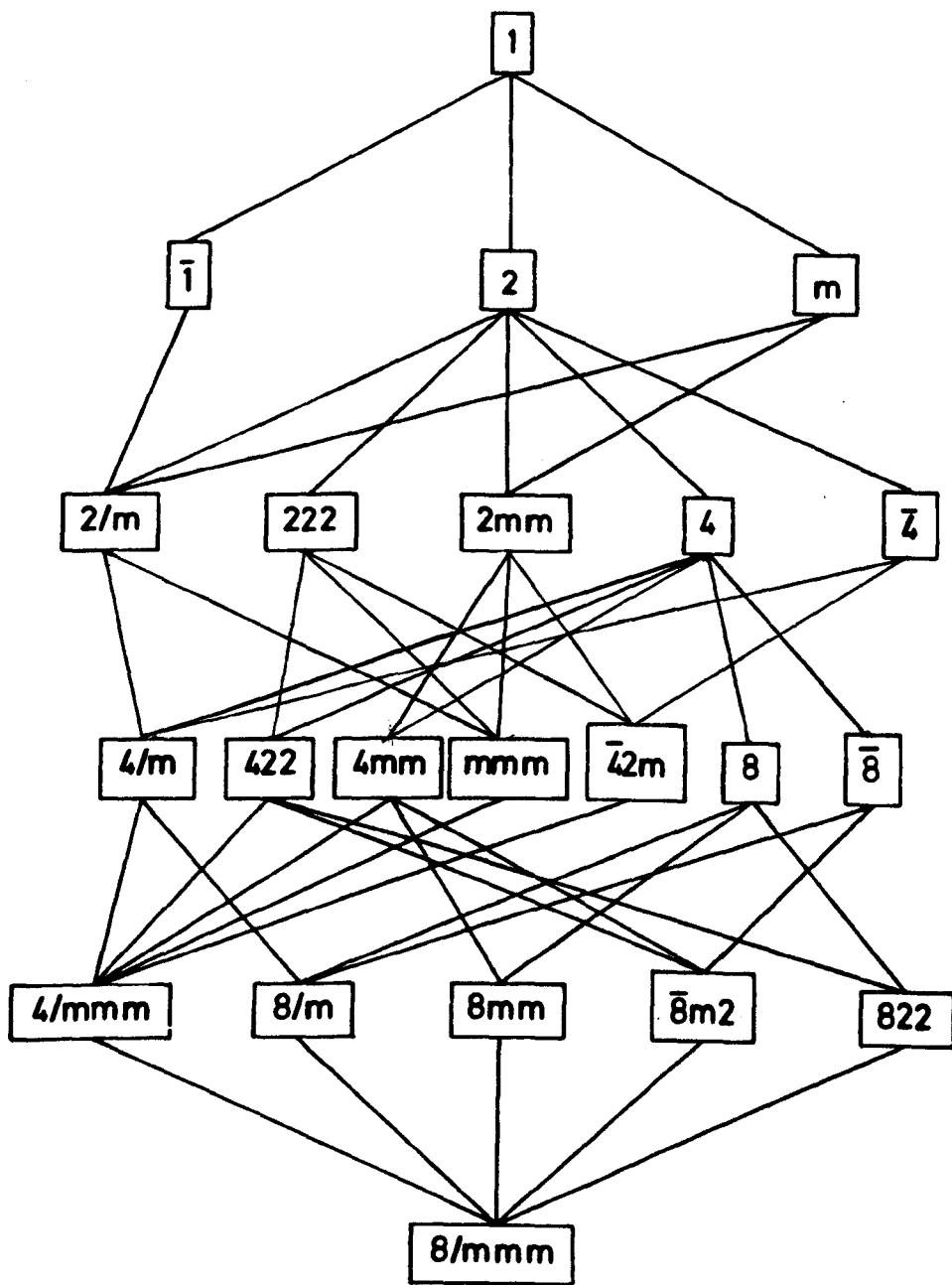
Therefore, each tie-line in figure A9.2 defines a black-white group. The lines connecting crystallographic point groups correspond to the 58 black-white groups found by Tavger & Zaitsev (1956). The rest of the tie-lines correspond to non-crystallographic black-white point groups of the 8- and 12-fold classes.

Applying this procedure the grey and black-white classes of the 8- and 12-fold axes are derived and the complete lists are given in

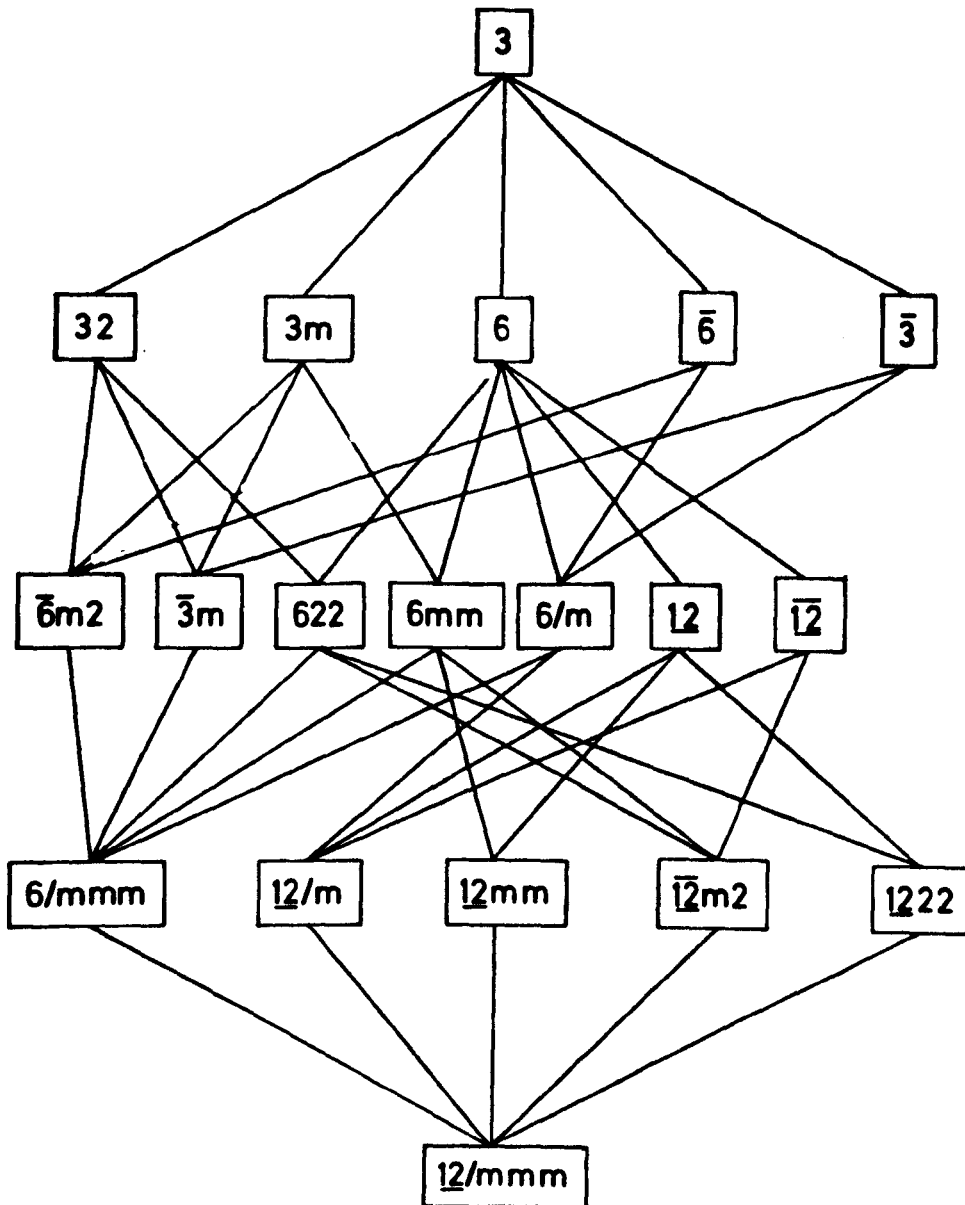
Figure A9.2

The 'family trees' of (one-coloured) point groups used for the construction of two-coloured point groups:

- (a) the  $C_1$  family
- (b) the  $C_3$  family
- (c) the T (or cubic) family

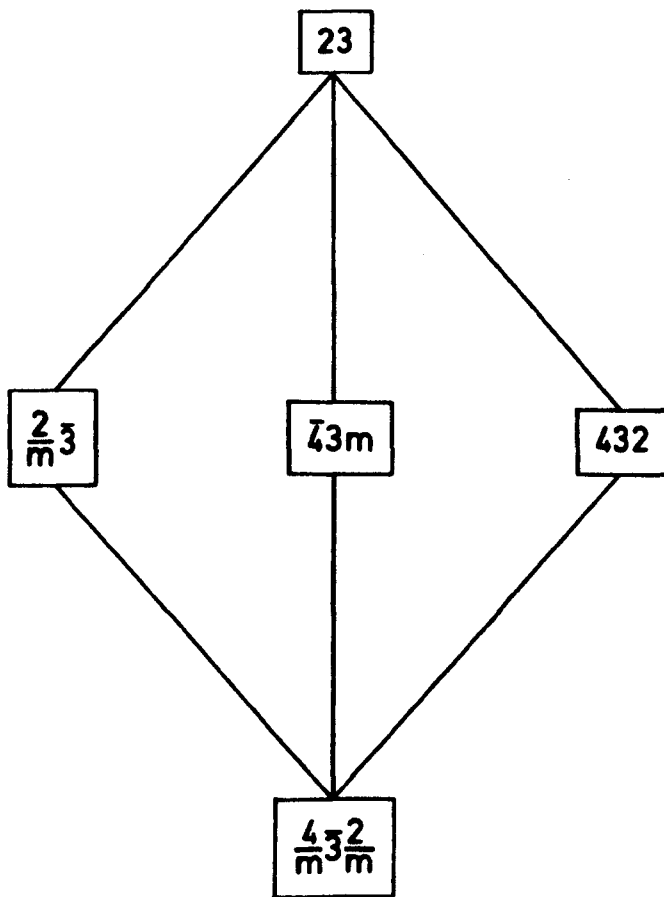


(a)



(b)





(c)

tables A9.2 and A9.3 respectively.

- - -

Footnotes 1: See also Tavger & Zaitsev (1956), Bertaut (1968), Krishnamurti & Gopalakrishnamurti (1969) and Schelkens (1970).

2: Halving subgroup is a subgroup of index 2, or alternatively stated, a subgroup which has half as many elements as the point group in question.

TABLE A9.2

Antisymmetry point groups containing an  
(ordinary or colour-reversing) 8-fold  
rotation axis

Ordinary groups	Grey groups	Black-white groups
8	81'	8'
$\bar{8}$	$\bar{8}1'$	$\bar{8}'$
8/m	8/m1'	8'/m, 8/m', 8'/m'
8mm	8mm1'	8'mm', 8m'm'
$\bar{8}m2$	$\bar{8}m21'$	$\bar{8}'m'2$ , $\bar{8}'m2'$ , $\bar{8}m'2'$
822	8221'	8'22', 82'2'
8/mmm	8/mmm1'	8/m'm'm', 8'/mmm', 8/mm'm', 8/m'mm, 8'/m'm'm

Altogether 31 two-coloured groups including the 7 ordinary and 7 grey groups.

TABLE A9.3

Antisymmetry point groups containing an  
(ordinary or colour-reversing) 12-fold  
rotation axis

Ordinary groups	Grey groups	Black-white groups
$\underline{12}$	$\underline{121}'$	$\underline{12}'$
$\overline{12}$	$\overline{121}'$	$\overline{12}'$
$\underline{12}/m$	$\underline{12}/m1'$	$\underline{12}/m', \underline{12}'/m, \underline{12}'/m'$
$\underline{12}mm$	$\underline{12}mm1'$	$\underline{12}m'm', \underline{12}'mm'$
$\overline{12}m2$	$\overline{12}m21'$	$\overline{12}m'2', \overline{12}'m2', \overline{12}'m'2$
$\underline{1222}$	$\underline{12221}'$	$\underline{122}'2', \underline{12}'22'$
$\underline{12}/mmm$	$\underline{12}/mmm1'$	$\underline{12}'/mmm', \underline{12}'/m'mm',$ $\underline{12}/m'm'm', \underline{12}/m'mm,$ $\underline{12}/mm'm'$

Altogether 31 two-coloured groups including the 7 ordinary  
and 7 grey groups

Appendix 10

ROD GROUPS CONTAINING 8- AND 12-FOLD ROTATION

(OR ROTOINVERSION) AXES

A figure without singular points and planes but with a singular axis is called a rod and the singular axis in it is called the axis of the rod. In addition to the translation axis, simple rotation, mirror-rotation and screw axes of any order may coincide with the axis of the rod.

The principles for the derivation of the (one-coloured) symmetry classes of rods is based on the fact that rods can not have inclined axes or symmetry planes, since these would give rise to several rod axes, whereas by hypothesis a rod can have only one singular or special axis. Hence, in order to derive all classes of rod symmetry, only the types of symmetry applicable to figures with a singular point can be used. Therefore, translation axis, screw axis, glide-reflection plane are located along the axis of the rod; additional derivative symmetry elements (centres of symmetry, planes and two-fold axes perpendicular to the rod axis, and mirror-rotation axes coinciding with the axis of the rod) can be arise. The Bravais lattice for a rod is the one-dimensional net, i.e. the primitive one-dimensional lattice ( $\rho$ ).

In this appendix the derivation of rod groups containing an 8- or 12-fold axis is given. It is evident from the considerations above that the 8- or 12-fold axis must coincide with the rod axis. It is, thus, necessary to add the 8- or 12-fold point symmetry elements to the translation to obtain the possible rod groups. Hence, it is required to consider the combination of the translation and the new rotation axes; in other words, the screw axes corresponding to 8- or 12-fold rotations must initially be determined.

These screw axes are characterized by the elementary angle  $\phi=360^\circ/8=45^\circ$  or  $360^\circ/12=30^\circ$  respectively, and also by the screw translation  $\tau=\frac{j}{n}t$ . In the latter relation  $t$  is the elementary translation along the axis of the rod,  $n$  is equal to 8 or 12 and  $j$  is the pitch component of the screw axis.

Consequently, the screw axes isogonal with the 8- and 12-fold rotation axes have translation components of  $\tau=\frac{j}{8}t$ s and  $\tau=\frac{j}{12}t$ s of the translation  $t$ ; or:

$$0t, \frac{1}{8}t, \frac{2}{8}t, \frac{3}{8}t, \frac{4}{8}t, \frac{5}{8}t, \frac{6}{8}t, \frac{7}{8}t,$$

$$\frac{8}{8}t, \frac{9}{8}t, \dots$$

$$\dots$$

and

$$0t, \frac{1}{12}t, \frac{2}{12}t, \frac{3}{12}t, \frac{4}{12}t, \frac{5}{12}t, \frac{6}{12}t, \frac{7}{12}t, \frac{8}{12}t, \frac{9}{12}t, \frac{10}{12}t, \frac{11}{12}t,$$

$$\frac{12}{12}t, \frac{13}{12}t, \dots$$

$$\dots$$

But note that only the first row of these sequences is really distinct. The second row, for example, can be taken from the first row by an elementary translation.

The results of this consideration for the 8- and 12-fold rotation axes are listed in table A10.1. The pairs of enantiomorphic axes are as follows:  $(8_1, 8_7)$ ,  $(8_2, 8_6)$ ,  $(8_3, 8_5)$ ,  $(\underline{12}_1, \underline{12}_{11})$ ,  $(\underline{12}_2, \underline{12}_{10})$ ,  $(\underline{12}_3, \underline{12}_9)$ ,  $(\underline{12}_4, \underline{12}_8)$ ,  $(\underline{12}_5, \underline{12}_7)$ .

Taking into account the operations of the 8- and 12-fold point symmetry (appendix 9) and translation (including screw axes and glide planes) the one-coloured rod groups are now derived (table A10.2). In table A10.2 the symbol  $\rho$  of the translation group is given first; the

TABLE A10.1

8- and 12-fold screw axes

n		permissible screws
8	$\phi$	$\pi/4 \ \pi/4 \ \pi/4 \ \pi/4 \ \pi/4 \ \pi/4 \ \pi/4 \ \pi/4$
	$\tau$	$0 \ \frac{1}{8}t \ \frac{2}{8}t \ \frac{3}{8}t \ \frac{4}{8}t \ \frac{5}{8}t \ \frac{6}{8}t \ \frac{7}{8}t$
	designation	8 8 <sub>1</sub> 8 <sub>2</sub> 8 <sub>3</sub> 8 <sub>4</sub> 8 <sub>5</sub> 8 <sub>6</sub> 8 <sub>7</sub>
12	$\phi$	$\pi/6 \ \pi/6 \ \pi/6 \ \pi/6 \ \pi/6 \ \pi/6 \ \pi/6 \ \pi/6 \ \pi/6 \ \pi/6 \ \pi/6 \ \pi/6$
	$\tau$	$0 \ \frac{1}{12}t \ \frac{2}{12}t \ \frac{3}{12}t \ \frac{4}{12}t \ \frac{5}{12}t \ \frac{6}{12}t \ \frac{7}{12}t \ \frac{8}{12}t \ \frac{9}{12}t \ \frac{10}{12}t \ \frac{11}{12}t$
	designation	12 12 <sub>1</sub> 12 <sub>2</sub> 12 <sub>3</sub> 12 <sub>4</sub> 12 <sub>5</sub> 12 <sub>6</sub> 12 <sub>7</sub> 12 <sub>8</sub> 12 <sub>9</sub> 12 <sub>10</sub> 12 <sub>11</sub>

TABLE A10.2

Rod groups containing an 8- or 12-fold rotation axis

8-fold	12-fold
$p_8, p_{8_1}, p_{8_2}, p_{8_3}, p_{8_4},$ $p_{8_5}, p_{8_6}, p_{8_7}$	$p_{12}, p_{12_1}, p_{12_2}, p_{12_3}, p_{12_4},$ $p_{12_5}, p_{12_6}, p_{12_7}, p_{12_8},$ $p_{12_9}, p_{12_{10}}, p_{12_{11}}$
$p_{\bar{8}}$	$p_{\bar{12}}$
$p_{8/m}, p_{8_4/m}$	$p_{12/m}, p_{12_6/m}$
$p_{8mm}, p_{8cc}, p_{8_4mm}$	$p_{12mm}, p_{12cc}, p_{12_6mm}$
$p_{822}, p_{8_122}, p_{8_222}, p_{8_322},$ $p_{8_422}, p_{8_522}, p_{8_622},$ $p_{8_722}$	$p_{1222}, p_{12_122}, p_{12_222}, p_{12_322},$ $p_{12_422}, p_{12_522}, p_{12_622},$ $p_{12_722}, p_{12_822}, p_{12_922},$ $p_{12_{10}22}, p_{12_{11}22}$
$p_{\bar{8}2m}, p_{\bar{8}2c}$	$p_{\bar{12}2m}, p_{\bar{12}2c}$
$p_{8/mmm}, p_{8_4/mmm},$ $p_{8/mcc}$	$p_{12/mmm}, p_{12_6/mmm},$ $p_{12/mcc}$



letter or number in the second, third and fourth positions of the symbol indicate that a particular symmetry element coincides with the coordinate axes  $a$ ,  $b$  and the bisector of the angle between the axes  $b$  and  $c$  (if no symmetry axes or normal to symmetry planes coincide with the coordinate axis the number 1 is placed in the corresponding position of the symbol, or the position is left vacant). The coordinate axis  $a$  is directed along the rod axis, and the axes  $b$  and  $c$  are orthogonal to the axis  $a$  and been topologically different make a right or oblique angle with each other, depending on the class of rod symmetry (8- or 12-fold).

The two-coloured rod groups containing 8- or 12-fold axes can be derived by considering the one-coloured rod groups (table A10.2) as the 'generating' groups and at the same time the possibility of coloured translation is taken into account, i.e. of a (second) black-white lattice (Belov, 1956). Then, according to Belov & Tarkhova (1956) starting from the monochromatic groups the grey groups are written down. Next come the two-coloured groups with uncoloured translation ( $\rho$ ). These are obtained by replacing in the monochromatic group symbol one (or more) symmetry elements by coloured ones. Finally the dichromatic groups with coloured translation ( $\rho'$ ) are considered. The complete list of the two-coloured rod groups containing the non-crystallographic 8- and 12-fold axes is given in table A10.3.

TABLE A10.3a

Antisymmetry rod groups containing a 8-fold symmetry axis

Number	Rod group symbol		
	One-coloured groups	Neutral (grey) groups	Two-coloured groups
1	$p_8$	$p_8 1'$	$p'_8, p_8'$
2	$p_8^1$	$p_8^1 1'$	$p'_8^1, p_8^1'$
3	$p_8^2$	$p_8^2 1'$	$p'_8^2, p_8^2'$
4	$p_8^3$	$p_8^3 1'$	$p'_8^3, p_8^3'$
5	$p_8^4$	$p_8^4 1'$	$p'_8^4, p_8^4'$
6	$p_8^5$	$p_8^5 1'$	$p'_8^5, p_8^5'$
7	$p_8^6$	$p_8^6 1'$	$p'_8^6, p_8^6'$
8	$p_8^7$	$p_8^7 1'$	$p'_8^7, p_8^7'$
9	$p_{\bar{8}}$	$p_{\bar{8}} 1'$	$p'_{\bar{8}}, p_{\bar{8}}'$
10	$p_8/m$	$p_8/m 1'$	$p'_8/m, p_8'/m, p_8/m', p_8'/m'$
11	$p_8^4/m$	$p_8^4/m 1'$	$p'_8^4/m, p_8^4'/m, p_8^4/m', p_8^4'/m'$
12	$p_8mm$	$p_8mm 1'$	$p'_8mm, p_8'mm', p_8m'm'$
13	$p_8cc$	$p_8cc 1'$	$p'_8cc, p_8'cc', p_8c'c'$
14	$p_8^4mm$	$p_8^4mm 1'$	$p'_8^4mm, p_8^4'mm', p_8^4m'm'$
15	$p_822$	$p_822 1'$	$p'_822, p_8'22', p_82'2'$
16	$p_8^122$	$p_8^122 1'$	$p'_8^122, p_8^1'22', p_8^12'2'$
17	$p_8^222$	$p_8^222 1'$	$p'_8^222, p_8^2'22', p_8^22'2'$

TABLE A10.3a-continued

Number	Rod group symbol		
	One-coloured groups	Neutral (grey) groups	Two-coloured groups
18	$\rho 8_3 22$	$\rho 8_3 221'$	$\rho' 8_3 22, \rho 8_3' 22', \rho 8_3 2' 2'$
19	$\rho 8_4 22$	$\rho 8_4 221'$	$\rho' 8_4 22, \rho 8_4' 22', \rho 8_4 2' 2'$
20	$\rho 8_5 22$	$\rho 8_5 221'$	$\rho' 8_5 22, \rho 8_5' 22', \rho 8_5 2' 2'$
21	$\rho 8_6 22$	$\rho 8_6 221'$	$\rho' 8_6 22, \rho 8_6' 22', \rho 8_6 2' 2'$
22	$\rho 8_7 22$	$\rho 8_7 221'$	$\rho' 8_7 22, \rho 8_7' 22', \rho 8_7 2' 2'$
23	$\rho \bar{8} 2m$	$\rho \bar{8} 2m1'$	$\rho' \bar{8} 2m, \rho \bar{8}' 2m', \rho \bar{8}' 2' m, \rho \bar{8} 2' m'$
24	$\rho \bar{8} 2c$	$\rho \bar{8} 2c1'$	$\rho' \bar{8} 2c, \rho \bar{8}' 2c', \rho \bar{8}' 2' c, \rho \bar{8} 2' c'$
25	$\rho 8/mmm$	$\rho 8/mmm1'$	$\rho' 8/mmm, \rho 8/m' m' m', \rho 8'/ mmm',$ $\rho 8/mm' m', \rho 8/m' mm, \rho 8/m' m' m$
26	$\rho 8_4/mmm$	$\rho 8_4/mmm1'$	$\rho' 8_4/mmm, \rho 8_4/m' m' m', \rho 8_4'/ mmm'$ $\rho 8_4/mm' m', \rho 8_4/m' mm, \rho 8_4/m' m' m$
27	$\rho 8/mcc$	$\rho 8/mcc1'$	$\rho' 8/mcc, \rho 8/m' c' c', \rho 8'/ mcc',$ $\rho 8/mc' c', \rho 8/m' cc, \rho 8/m' c' c$

TABLE A10.3b

Antisymmetry rod groups containing a 12-fold symmetry axis

Number	Rod group symbol		
	One-coloured groups	Neutral (grey) groups	Two-coloured groups
1	$\rho_{12}$	$\rho_{12}1'$	$\rho'_{12}, \rho_{12}'$
2	$\rho_{12_1}$	$\rho_{12_1}1'$	$\rho'_{12_1}, \rho_{12_1}'$
3	$\rho_{12_2}$	$\rho_{12_2}1'$	$\rho'_{12_2}, \rho_{12_2}'$
4	$\rho_{12_3}$	$\rho_{12_3}1'$	$\rho'_{12_3}, \rho_{12_3}'$
5	$\rho_{12_4}$	$\rho_{12_4}1'$	$\rho'_{12_4}, \rho_{12_4}'$
6	$\rho_{12_5}$	$\rho_{12_5}1'$	$\rho'_{12_5}, \rho_{12_5}'$
7	$\rho_{12_6}$	$\rho_{12_6}1'$	$\rho'_{12_6}, \rho_{12_6}'$
8	$\rho_{12_7}$	$\rho_{12_7}1'$	$\rho'_{12_7}, \rho_{12_7}'$
9	$\rho_{12_8}$	$\rho_{12_8}1'$	$\rho'_{12_8}, \rho_{12_8}'$
10	$\rho_{12_9}$	$\rho_{12_9}1'$	$\rho'_{12_9}, \rho_{12_9}'$
11	$\rho_{12_{10}}$	$\rho_{12_{10}}1'$	$\rho'_{12_{10}}, \rho_{12_{10}}'$
12	$\rho_{12_{11}}$	$\rho_{12_{11}}1'$	$\rho'_{12_{11}}, \rho_{12_{11}}'$
13	$\rho_{\overline{12}}$	$\rho_{\overline{12}}1'$	$\rho'_{\overline{12}}, \rho_{\overline{12}}'$
14	$\rho_{12}/m$	$\rho_{12}/m1'$	$\rho'_{12}/m, \rho_{12}'/m, \rho_{12}/m', \rho_{12}'/m'$
15	$\rho_{12_6}/m$	$\rho_{12_6}/m1'$	$\rho'_{12_6}/m, \rho_{12_6}'/m, \rho_{12_6}/m', \rho_{12_6}'/m'$
16	$\rho_{12}mm$	$\rho_{12}mm1'$	$\rho'_{12}mm, \rho_{12}'mm', \rho_{12}m'm'$
17	$\rho_{12}cc$	$\rho_{12}cc1'$	$\rho'_{12}cc, \rho_{12}'cc', \rho_{12}c'c'$

TABLE A10.3b-continued

Number	Rod group symbol		
	One-coloured groups	Neutral (grey) groups	Two-coloured groups
18	$\rho_{12_6}mm$	$\rho_{12_6}mm1'$	$\rho'_{12_6}mm, \rho_{12_6}'mm', \rho_{12_6}m'm'$
19	$\rho_{12}22$	$\rho_{12}221'$	$\rho'_{12}22, \rho_{12}'2', \rho_{12}2'2'$
20	$\rho_{12_1}22$	$\rho_{12_1}221'$	$\rho'_{12_1}22, \rho_{12_1}'22', \rho_{12_1}2'2'$
21	$\rho_{12_2}22$	$\rho_{12_2}221'$	$\rho'_{12_2}22, \rho_{12_2}'22', \rho_{12_2}2'2'$
22	$\rho_{12_3}22$	$\rho_{12_3}221'$	$\rho'_{12_3}22, \rho_{12_3}'22', \rho_{12_3}2'2'$
23	$\rho_{12_4}22$	$\rho_{12_4}221'$	$\rho'_{12_4}22, \rho_{12_4}'22', \rho_{12_4}2'2'$
24	$\rho_{12_5}22$	$\rho_{12_5}221'$	$\rho'_{12_5}22, \rho_{12_5}'22', \rho_{12_5}2'2'$
25	$\rho_{12_6}22$	$\rho_{12_6}221'$	$\rho'_{12_6}22, \rho_{12_6}'22', \rho_{12_6}2'2'$
26	$\rho_{12_7}22$	$\rho_{12_7}221'$	$\rho'_{12_7}22, \rho_{12_7}'22', \rho_{12_7}2'2'$
27	$\rho_{12_8}22$	$\rho_{12_8}221'$	$\rho'_{12_8}22, \rho_{12_8}'22', \rho_{12_8}2'2'$
28	$\rho_{12_9}22$	$\rho_{12_9}221'$	$\rho'_{12_9}22, \rho_{12_9}'22', \rho_{12_9}2'2'$
29	$\rho_{12_{10}}22$	$\rho_{12_{10}}221'$	$\rho'_{12_{10}}22, \rho_{12_{10}}'22', \rho_{12_{10}}2'2'$
30	$\rho_{12_{11}}22$	$\rho_{12_{11}}221'$	$\rho'_{12_{11}}22, \rho_{12_{11}}'22', \rho_{12_{11}}2'2'$
31	$\rho_{12}2m$	$\rho_{12}2m1'$	$\rho'_{12}2m, \rho_{12}'2'm, \rho_{12}'2m', \rho_{12}2'm'$
32	$\rho_{12}2c$	$\rho_{12}2c1'$	$\rho'_{12}2c, \rho_{12}'2'c, \rho_{12}'2c', \rho_{12}2'c'$
33	$\rho_{12}/mmm$	$\rho_{12}/mmm1'$	$\rho'_{12}/mmm, \rho_{12}/m'm'm', \rho_{12}'/mmm',$ $\rho_{12}/mm'm', \rho_{12}/m'mm, \rho_{12}/m'm'm$
34	$\rho_{12_6}/mmm$	$\rho_{12_6}/mmm1'$	$\rho'_{12_6}/mmm, \rho_{12_6}/m'm'm', \rho_{12_6}'/mmm',$ $\rho_{12_6}/mm'm', \rho_{12_6}/m'mm, \rho_{12_6}/m'm'm$
35	$\rho_{12}/mcc$	$\rho_{12}/mcc1'$	$\rho'_{12}/mcc, \rho_{12}/m'c'c', \rho_{12}'/mcc',$ $\rho_{12}/mc'c', \rho_{12}/m'cc, \rho_{12}/m'c'c$

Appendix 11

SUBGROUPS OF SPATIAL SYMMETRY GROUPS

A subgroup of a given spatial group is a group of lower symmetry obtained by the removal of certain operations from the given spatial group. The subgroup is composed of some, but not all, the symmetry operations of the basic group; the missing operations are suppressed. This definition is subject to possible misinterpretation. It does not follow from what has been said that the subgroups necessarily have the same cell dimensions as the cell of the basic group. The cell of the subgroup is bound to be different from that of the basic group if any operation of the lattice translation is among the suppressed set of operations.

A systematic method of deriving these subgroups was outlined by Hermann (1929b)<sup>1</sup>; later Buerger (1947) derived independently a method that is similar in most but not all respects. According to Hermann's approach the spatial subgroups are distinguished into:

(a) zellengleiche subgroups<sup>2</sup>, in which the descent in symmetry has only affected the rotations and reflections but not the accompanying translation in the unit cell. These subgroups can be subdivided as follows:

(a<sub>1</sub>) subgroups belonging to the same point group as the given group, and,

(a<sub>2</sub>) subgroups belonging to a different point group from that of the given group.

(b) klassengleiche subgroups<sup>2</sup>, in which only the translations and not the types of symmetry elements of the crystal class are affected. The crystal system of these subgroups is the same as that of the given group.

Hermann (1929b) has shown, however, that if a subgroup is neither zellengleich nor klassengleich then it is a klassengleich subgroup of a zellengleiche subgroup of the given group.

#### A11.1 Subgroups of one-coloured spatial groups

A list of the zellengleichen subgroups of the 230 (classical) space groups derived by Hermann has been published in the Internationale Tabellen zur Bestimmung von Kristallstrukturen (1935) and corrections to this table were given by Ascher, Gramlich & Wondratschek (1969). The notation in this first list follows, however, the lines laid down by the International Union of Crystallography in the 1935 edition and care must be given when these tables are used. More recently lists of zellengleichen and/or klassengleichen subgroups of the space groups were published by Ascher (1967, 1968), Neübuser & Wondratschek (1969, 1970) and Boyle & Lawrenson (1972a, b).

The zellengleichen and klassengleichen subgroups of the two-sided, one-coloured layer groups, on the other hand, have been listed by Holser (1958b).

#### A11.2 Subgroups of two-coloured spatial groups

No tables of the zellengleichen and klassengleichen subgroups of the two-coloured spatial groups are, in the best of the author's knowledge, available<sup>3</sup>. An enumeration of these subgroups is a very large task; alternatively, the method for the determination is outlined here. However, only the case of zellengleichen subgroups is treated here. The procedure for the determination of the klassengleichen subgroups is fairly complicated and the only available lists are those published by Boyle & Lawrenson (1972b) (for the classical space groups) and by Holser (1958b) (klassengleichen subgroups of the two-sided, one-coloured layer groups).

These tables as well as the list of sub- (and super-) operations of symmetry<sup>4</sup> are then used for determining the klassengleichen subgroups of the two-coloured spatial groups.

#### A11.2.1 Determination of the zellengleichen subgroups of two-coloured spatial groups

The deviation of the zellengleichen subgroups is based on the following theorem (Hermann, 1929b): 'there is only one zellengleiche subgroup for each subgroup of the point group which is isomorphic to the given spatial group'. Consequently, if the subgroups of the particular (two-coloured) point group are known then for each of them there will be one and only one isomorphous (spatial) zellengleiche subgroup. In the most of the cases the answer can be written immediately by inspecting either the symbol of the given spatial group or the diagrams of the two-coloured groups given by Koptsik (1966).

When the zellengleichen subgroups are determined regard must be given to the various possible orientations of the symmetry elements. If a point subgroup adopts more than one crystallographically non-equivalent orientation in the given point group then different zellengleiche subgroups might arise. Thus, it is advisable to use the point subgroup tables published by Ascher & Janner (1965) where all the subgroups of the two-coloured point groups are listed.

#### A11.2.2 The determination of the zellengleichen subgroups of the space group $I4/mm'm'$

As an example the two-coloured space group  $I4/mm'm'$  is now considered and its zellengleichen subgroups are determined.

The isomorphic point group is  $4/mm'm'$  and the list of its subgroups is given in table 6.2.1. As it can be seen in this table the



point group  $4/mm'm'$  contains a number of subgroups adopting different orientations. The two subgroups  $m'm'2=\{1, 2_y^1, s'_z, s'_x\}$  and  $m'm'2=\{1, 2_\beta^1, s'_\alpha, s'_z\}$ , for example, adopt two positions in  $4/mm'm'$  differing by a rotation by an angle of  $45^\circ$  about the 4-fold axis.

The question arising in such cases is: what could be the zellen-gleichen subgroups associated with each of these point groups? This can be found by inspecting the diagrammatic representation of the space group  $I4/mm'm'$ ; figure A11.1 shows the (001) projection of this space group. It is seen from this figure that if only the symmetry operations  $\{1, 2_y^1, s'_z, s'_x\}^5$  are retained the resulting space group is  $Im'm'2$ . On the other hand, if only the symmetry operations  $\{1, 2_\beta^1, s'_\alpha, s'_z\}$  are considered the zellengleiche subgroup is  $Fm'm'2$ . By similar considerations all the zellengleichen subgroups of the space group  $I4/mm'm'$  are uniquely determined in table A11.1.

- - -

Footnotes 1: A very short analysis can be found in the International Tables for X-ray Crystallography (1969); see also Senechal (1980).

2: Although the English terms cell-equivalent (=zellen-gleiche) and class-equivalent (=klassengleiche) express exactly the meaning of the German words they are rarely used in the literature.

3: With the exception of the list of halving klassengleiche and zellengleiche subgroups (of all indices) given by Koptsik (1966). This list contains, however, many errors and omissions.

4: See International Tables for X-ray Crystallography (1969).

5: The axes  $x, y, z$  of the coordinate system are considered along the directions  $[100]$ ,  $[010]$ ,  $[001]$  respectively.

Figure A11.1

(001) projection of the two-coloured space group  $I4/m'm'$   
(origin at centre  $4/m'm'$ )

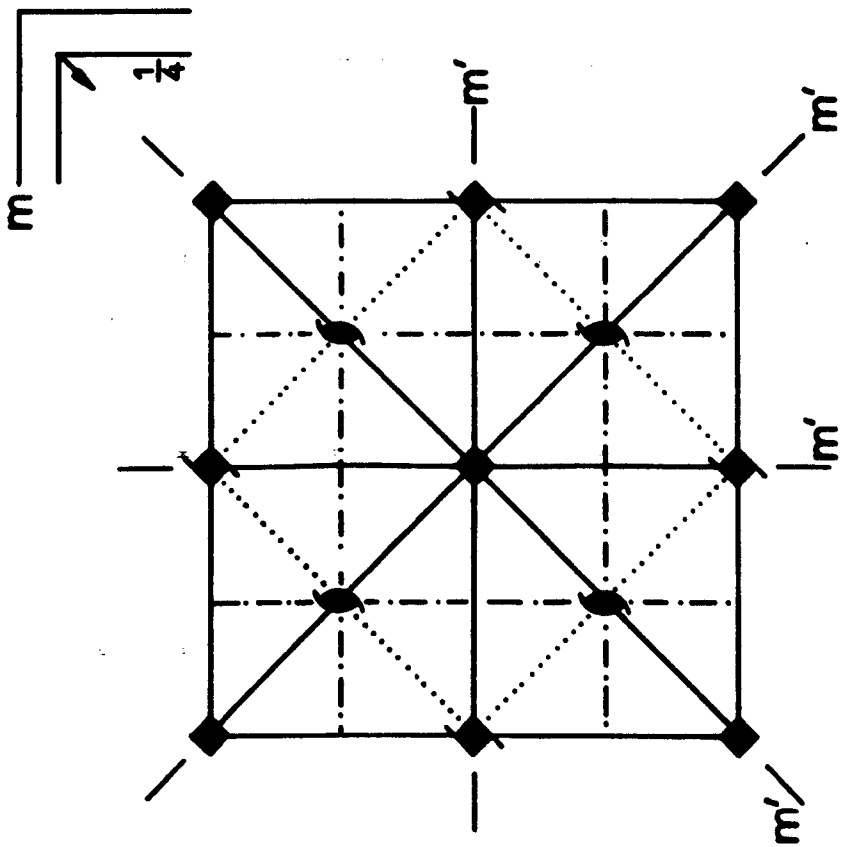


TABLE A11.1

Zellengleichen subgroups of the two-coloured space  
group  $I4/m\bar{m}'m'$

Number	Zellengleiche subgroup	Number	Zellengleiche subgroup
1	$I4/m\bar{m}'m'$	18	$C2'/m'$
2	$I\bar{4}2'm'$	19	$C2/m$
3	$I\bar{4}2'm'$	20	$Im'm'2$
4	$I4m'm'$	21	$Fm'm'2$
5	$I42'2'$	22	$I2'2'2$
6	$I4/m$	23	$F2'2'2$
7	$I\bar{4}$	24	$P\bar{1}$
8	$I4$	25	$Cm'$
9	$Im'm'm$	26	$Cm'$
10	$Fm'm'm$	27	$Cm'$
11	$Im'm2'$	28	$Cm'$
12	$Im'm2'$	29	$C2'$
13	$Fm'm2'$	30	$C2'$
14	$Fm'm2'$	31	$C2'$
15	$C2'/m'$	32	$C2'$
16	$C2'/m'$	33	$Cm$
17	$C2'/m'$	34	$C2$
		35	$P1$

Note: The serial numbers in the above table correspond to the ones in table 6.2.1.

.....  
Appendix 12

ACCURATE DETERMINATION OF THE BEAM DIRECTION  
IN ELECTRON DIFFRACTION PATTERNS

A method for the determination of the exact direction of the electron beam in the crystal is described in this appendix. The principle of the method is based on the main features of the geometry of Kikuchi patterns; these characteristics can be understood by making use of the simplified treatment first proposed by Kikuchi (1928a,b).

Kikuchi lines are the best means for an exact determination of the crystal orientation and several methods estimating the direction of the electron beam in a crystal have been proposed (Otte, Dash & Schaake, 1964; Heimendahl von, Bell & Thomas, 1964; Sheinin & Cann, 1965; Ryder & Pitsch, 1968; Pumphrey & Bowkett, 1970a,b; Heimendahl, 1971). The methods of Ryder & Pitsch and of Pumphrey & Bowkett, considered to be the most accurate, are based on the measurement of the relative position of Kikuchi lines and diffraction spots. In practice, however, it is often difficult to achieve the maximum accuracy of the above mentioned procedures, specially in thick foils where the reflections are diffused, and bright Kikuchi lines are broad when situated close to reflections. Moreover, in both methods the exact position of the centre of the diffraction pattern is required.

In table A12.1 the factors which influence the accuracy of the beam direction determination are summarized. It can be seen that no method is available for eliminating the errors due to the uncertainty in the position of the central spot. On the other hand, in the case of Kikuchi lines being intersected out of the plate the errors may be eliminated by employing the approach proposed by Kozumbowski (1977).

**TABLE A12.1**

**Factors influencing the accuracy with which the beam direction  
of a Kikuchi-line pattern can be obtained**

Error introduced by	Error causes	Error is eliminated by
Broad Kikuchi lines	Uncertainty in the determination of their position	i) SADP taken from an area reasonably thick ( 1/2 max usable penetration thickness) ii) using Kikuchi lines not situated close to reflection (*)
Kikuchi lines being intersected out of the plate	Uncertainty in the measurement of distances between Kikuchi poles and central spot	Using the method proposed by Kozumbowski (1977), i.e. by using the intersection of the dark Kikuchi lines surrounding the central spot
Diffuse central spot	Uncertainty in the measurement of distances between Kikuchi poles and central spot	
Use of the microscope itself (**)	The total inaccuracy by such effects is extremely small (Pumphrey & Bowkett, 1970b)	(negligible errors)

(\*) If the dark Kikuchi line is closer than  $\approx g/4$  to the central spot measurements may be safely made (Pumphrey, 1970)

(\*\*) Errors arise from lens aberrations, high-tension supply instabilities and the positioning of the plate in the microscope

However, it requires the use of reasonably large triangles of Kikuchi lines. This decreases the inherent accuracy of the method primarily because of ill-defined intersections of Kikuchi lines<sup>1</sup>.

Such errors are, however, eliminated by employing the method presented here. The procedure is based on the observation that the centre of the electron diffraction pattern as well as the intersections of the Kikuchi lines can be determined by means of analytical geometry.

#### A12.1 Description of the method

Suppose a selection is made of three Kikuchi lines which form a triangle enclosing the trace of the primary beam<sup>2</sup> (figure A12.1). If the analytical equations of the three lines and the coordinates of the diffraction spots relative to an (arbitrary) coordinate system are known then straightforward calculations yield the lengths and angles required for the indexing of the pattern and the determination of the beam direction (see e.g. Andrews et al. 1971).

Let that the equation of the line corresponding to the trace of the  $i$ -th reflecting planes is found to be  $y = \alpha_i x + \beta_i$  and that the coordinates of the  $j$ -th spot are  $(x_j, y_j)$ . Then, the coordinates of the Kikuchi poles  $P_{kl}$  are determined by the intersection of the  $k$ -th and  $l$ -th lines. Subsequently, the distances AB, BC, CA and the angles  $\alpha, \beta, \gamma$  (figure A12.1) are easily calculated from the usual formula of the distance between two points and the cosine law for the triangle ABC.

In order to determine the distances AO, BO, CO the coordinates of the central spot are required. This point lies in the intersection of the lines drawn perpendicular to the corresponding Kikuchi line and passing through the appropriate diffraction spot<sup>3</sup>. This is carried out as indicated in figure A12.2.

Figure A12.1

Sketch to illustrate indexing of any Kikuchi-line pattern



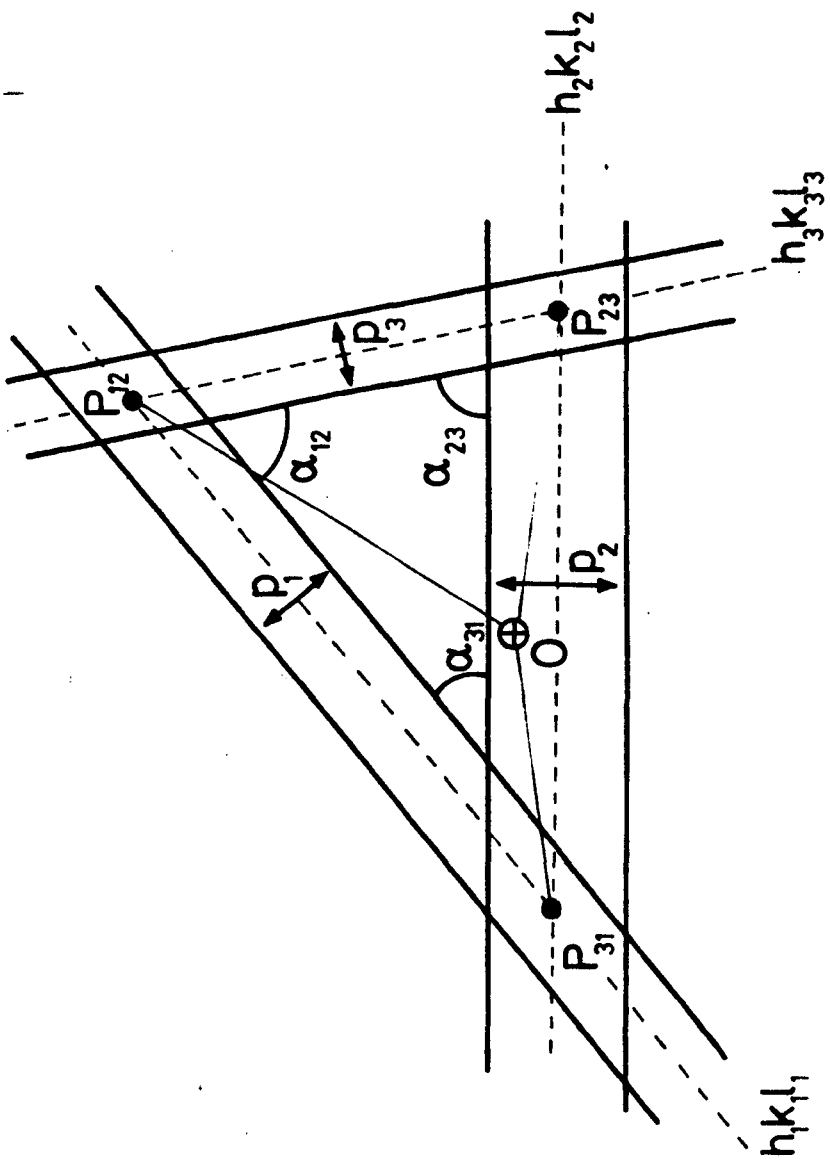
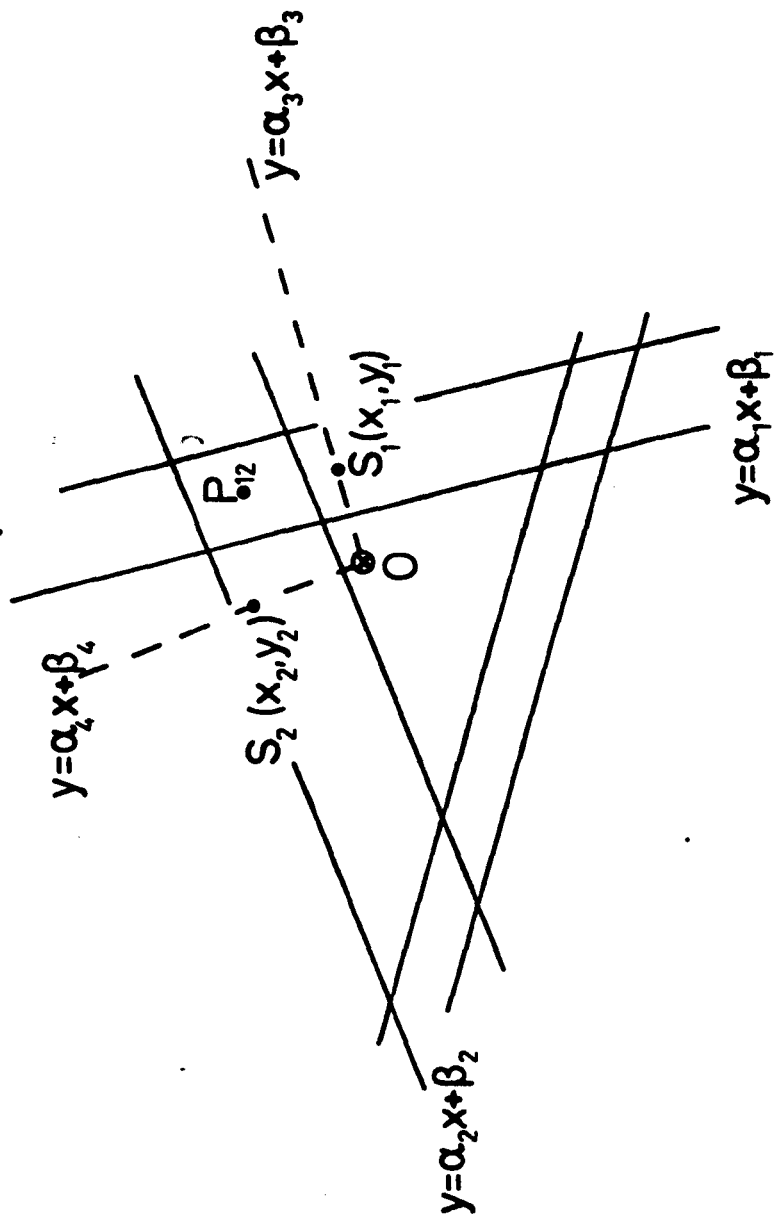


Figure A12.2

Sketch indicating the basic analytical calculations necessary for indexing a Kikuchi-line pattern and determining the beam direction. The pole  $P_{ij}$  lies in the intersection of the lines  $y = \alpha_i x + \beta_i$  and  $y = \alpha_j x + \beta_j$ . The central spot lies in the intersection of the lines drawn perpendicular to the corresponding Kikuchi lines and passing through the appropriate diffraction spot; thus, for example,  $y = \alpha_3 x + \beta_3$  with  $\alpha_3 = -1/\alpha_1$  and  $\beta_3 = y_1 - \alpha_3 x_1$ .



During the course of this thesis the determination of the coordinates of points lying on Kikuchi lines or diffraction spots were made by using a digitizer (see appendix 14 for details). This instrument provides the means of measuring coordinates directly from the plate (which is fixed firmly on the working table); the coordinates are expressed relative to an arbitrary origin.

The analytical equation of each of the Kikuchi lines is determined by measuring the coordinates of 20 points<sup>4</sup> lying on it. Then, the linear least-squares method is utilized for determining the 'best fitting' line. The inherent error in the determination of each line is estimated by calculating the correlation coefficient (see e.g. Chatfield, 1978). Similarly, the coordinates of the diffraction spots are determined as the averaged estimates  $(\bar{x}_i, \bar{y}_i)$  of the measured coordinates  $(x_{ij}, y_{ij})$  of the  $i$ -th spot.

#### A12.2 Application of the method

The application of the above method is illustrated by means of figure A12.3. In order to establish the inherent accuracy of the digitizer measurements as well as of the analytical geometry calculations the beam direction was determined by obtaining 10 estimates by using the triangle ABC of Kikuchi lines.

Measurements of the coordinates were made on the negative plate instead on a print in order to eliminate systematic errors which may be introduced by the printing process. The correlation coefficients for the lines A, B, C and the standard deviation of the coordinates of the diffraction spots  $S_1, S_2, S_3$  are given in table A12.2. These results indicate that the inherent accuracy of the digitizer is better than 0.015 cm (values of  $s_x$  and  $s_y$  remain within the range of 0.007 to 0.015 cm).

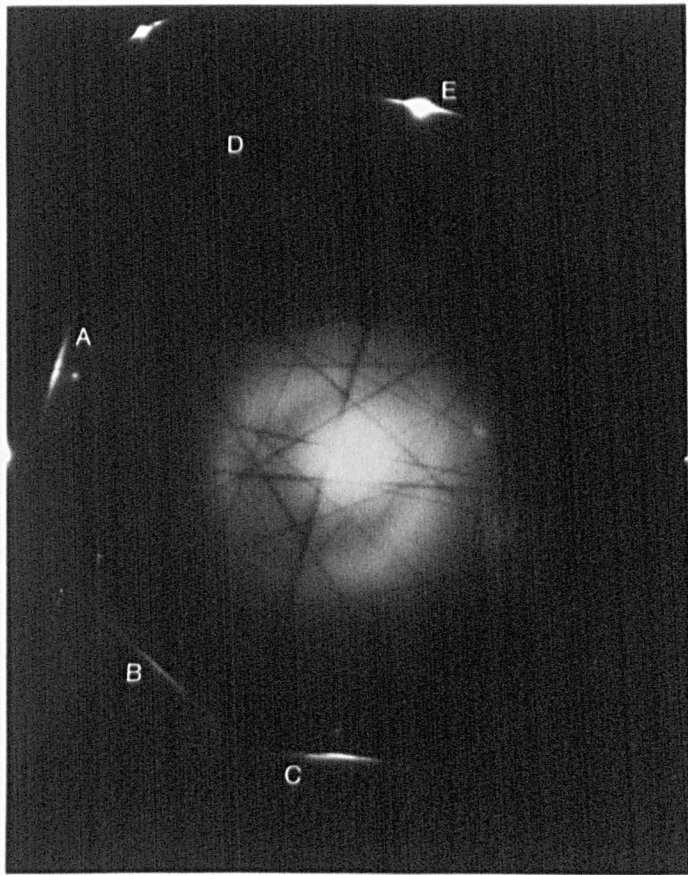


Figure A12.3

A Kikuchi-line pattern from silicon

TABLE A12.2a

Statistics indicating the inherent accuracy of the determination of the analytical equation of Kikuchi lines

Kikuchi-line pair	$\sigma$ *	$1-\sigma$	Standard deviation of a mean +
A	0.99970	$0.30 \times 10^{-3}$	$\pm 0.00019$
B	0.99850	$1.50 \times 10^{-3}$	$\pm 0.00024$
C	0.99976	$0.24 \times 10^{-3}$	$\pm 0.00015$

(\* ) Correlation coefficient of the least-squares method (mean value of 10 observations)

(+ ) Calculated from 10 estimates

TABLE A12.2b

Statistics indicating the inherent accuracy of the determination of the coordinates of diffraction spots

Diffraction spot	Standard deviation of a mean *	
	$s_x$	$s_y$
1	$\pm 0.015$	$\pm 0.014$
2	$\pm 0.009$	$\pm 0.008$
3	$\pm 0.009$	$\pm 0.007$

(\* ) Calculated from 10 estimates



When relatively strong diffraction spots are used the greater relative errors of determining the spot position reduce the final accuracy (spot no. 1). However, the use of excessively weak spots also increases the error, owing to a considerable reduce in contrast.

Relatively small differences between the correlation coefficients for the least-squares lines were obtained. In all cases the differences remain within the range  $0.15 \times 10^{-3}$  to  $0.24 \times 10^{-3}$ ; these results indicate a deviation from the ideal value ( $\sigma=1$ ) in the range of  $0.30 \times 10^{-3}$  to  $1.50 \times 10^{-3}$ . The relatively high deviation ( $1.5 \times 10^{-3}$ ) of  $\sigma$  for the line B probably originates from errors of measurements due to the relatively low contrast of the Kikuchi line B. On the other hand, the small deviation ( $0.30 \times 10^{-3}$ ) of  $\sigma$  for lines A and C seems at least partly to be due to the longest Kikuchi lines.

The inherent accuracy of the calculations can be found by an error propagation investigation. A means to establish this is by considering:

- (1) the standard deviation of the calculated estimates of the central point; the errors in the calculated x- and y-coordinates of the central spot were found to be  $\pm 0.030$  and  $\pm 0.026 \text{ cm}^5$  respectively, and,
- (2) the errors in the calculated distances  $P_1$ ,  $P_2$ ,  $P_3$  and angles  $\alpha$ ,  $\beta$ ,  $\gamma$  (figure A12.1); these are summarized in table A12.3. The unexpectedly low error in the estimation of angle  $\beta$  seems at least to be accidental.

These considerations lead to the conclusion that the distance between the Kikuchi poles  $P_{12}$ ,  $P_{23}$ ,  $P_{31}$  and between these poles and the centre of the pattern can be determined with an accuracy  $\pm 0.30 \text{ mm}$ . A Bragg angle for the 111 type reflection is typically  $0.5^\circ$ . If distances

**TABLE A12.3**

Comparison between measured and calculated values  
of the ratios  $p_i/p_j$  and angles  $\alpha, \beta, \gamma$

Ratios or angles	Measured value, M	Calculated value, C	Error  M-C
$p_2/p_1$	1.130	1.141	0.011
$p_1/p_3$	1.055	1.037	0.018
$p_2/p_3$	1.192	1.183	0.009
$\alpha$	-40.00°	-40.48°	0.48°
$\beta$	78.69°	78.88°	0.19°
$\gamma$	-61.03°	-60.72°	0.31°

on a plate are measured to  $\pm 0.30$  mm then deviation in the beam direction due to inaccuracy in length measurements is  $\Delta\theta = \frac{0.5^\circ \times 0.30}{10} \approx 54''$  of arc. Therefore, the overall error in the determination in the beam direction must be of the order of  $1'$  of arc.

- - -

- Footnotes
- 1: This is primarily due to the splitting of the lines caused by dynamical interactions between Kikuchi lines (Pfister, 1953; Gjønnes & Watanabe, 1966; Gjønnes & Høier, 1969).
  - 2: This requirement is not necessary since the centre of the diffraction pattern can equally well be outside the chosen triangle of Kikuchi lines.
  - 3: It is, therefore, obvious that the minimum information required is the presence of three Kikuchi lines and of the diffraction spots associated to two of these lines.
  - 4: It was found that the difference in the calculated analytical equations obtained by having 20 and 50 points was less than 1%, whereas the computer time required is directly proportional to the number of points.
  - 5: Standard deviation of a mean value (10 observations).

### Appendix 13

#### THE ACCURATE DETERMINATION OF THE MISORIENTATION MATRIX

It was mentioned in section 9.1 that the misorientation relationship of a bicrystal is expressed by a rotation  $\theta$  about a direction  $[hkl]$ , or, in matrix notation, by the rotation matrix  $\underline{R} = [r_{ij}]$  (Lange, 1967). This matrix expresses a rigid-body rotation and consequently it is a 3x3 orthogonal matrix (i.e.  $\underline{R}\underline{R}^{-1} = \underline{R}\underline{R}^T = \underline{I}$ , where  $\underline{R}^{-1}, \underline{R}^T$  are the inverse and transport matrices of  $\underline{R}$  and  $\underline{I}$  is the 3x3 unit matrix).

Experimentally  $\underline{R}$  is determined by establishing the indices of two pairs of parallel directions, with one of each pair in each crystal (a third pair of such directions follows automatically from the vector cross-product of the first two). It should be noticed, however, that this is the minimum information required to define an orientation relationship  $\underline{R}$  and that additional pairs of directions will overdetermine the relationship and allow an estimate of the error in the procedure to be obtained.

The experimental error introduced in the determination of  $\underline{R}$  arises from experimental errors in the determination of the beam directions (see appendix 12). The propagation of these errors through the calculations of  $\underline{R}$  causes to a systematic error among the components of  $\underline{R}$ . Therefore, it is important to prevent the propagation of systematic errors in  $\underline{R}$  and, at the same time, to find the best fitting  $\underline{R}$  to the available data.

The problem can be stated as follows. Given two sets (A and B) of N vectors  $\underline{a}_a, \underline{b}_a$  ( $a=1,2,\dots,N$ ) find an orthogonal rotation matrix  $\underline{R}$  with determinant +1 which converts the coordinates  $b_{ia}$  ( $i=1,2,3$ ) to

$b'_{ia} = \sum_{j=1}^n R_{ij} b_{ja}$  and minimizes the residual  $S = \sum_{ia} w_a (a_{ia} - b'_{ia})^2$ . Here  $w_a$  is a weight assigned to each of the vectors  $\underline{a}_a$ ,  $\underline{b}_a$  and in the present treatment it is assumed that  $w_a = 1$ .

Mackenzie (1957) considered the simpler case of the above mentioned problem where the best unconstrained transformation between the two sets of directions is to be determined. In other words, the transformation matrix  $\underline{R}$  calculated by the Mackenzie's method will not necessarily correspond to a rigid-body rotation (Diamond, 1976; see also below). The method presented here is in fact an extension of Mackenzie's method where the orthogonality constraints are also taken into account.

A similar problem occurs in various other crystallographic situations where the best rotation to fit a given atomic arrangement to approximately measured coordinates is to be found. Such situations are particularly common among biological macromolecules (Freer et al. 1970; Huber et al. 1971; Hendrickson, 1979); other crystallographic examples include related molecular structures from different crystals, multiple copies of the same molecule on a single asymmetric unit, and similar substructures within a single molecule. Several procedures have been described for finding the linear orthogonal transformation to superpose two structures (see e.g. Cox, 1967; MacLahlan, 1972; Rao & Rossmann, 1973; Nyburg, 1974; Diamond, 1976; Kabsch, 1976; Ferro & Hermans, 1977). In all these procedures, however, the only transformations considered are linear ones and in the first instance, although a non-orthogonal transformation is discovered, the information expressed by the non-orthogonality is suppressed.

Moreover, the just mentioned methods converge slowly unless the number of atomic positions to be superposed is high. Thus, these procedures are not appropriate for the determination of the misorientation matrix  $\underline{R}$ .

This matrix is usually deduced from five pairs of parallel directions plus their cross-products (see e.g. Clark, 1976). The method given here indicates, however, that a solution is also possible for a small number of data (only two experimentally determined pairs of parallel directions are required) despite the non-linear character of the problem. The solution is, in fact, an iterative process but sufficient convergence in the least-squares minimization is rapid and the process is quite free from false minima. But, the greatest advantage of the method is that the obtained matrix  $\underline{R}$  expresses in a very good approximation a linear orthogonal transformation.

### A13.1 The least-squares method for the calculation of the misorientation matrix

Suppose that the vectors  $\underline{a}_a$  and  $\underline{b}_a$  have already been referred to rectangular cartesian reference frames of uniform physical scale (e.g. Ångström units). Then the  $k$ -th vector  $\underline{b}_k$  in grain B can be related to the vector  $\underline{a}_k$  of the 'parallel' (ignoring experimental errors) direction in grain A by the linear transformation:

$$\underline{a}_k \cong \underline{b}'_k = \underline{R}\underline{b}_k \quad (\text{A13.1})$$

The optimal parameters for this general linear transformation will be these that minimize the weighted sum of squares of discrepancies between 'parallel' directions in the two crystals:

$$S = \sum_{k=1}^N (\underline{a}_k - \underline{b}'_k)^2 = \sum_{k=1}^N \left[ \sum_{i=1}^3 (a_{ik} - b'_{ik})^2 \right] \quad (\text{A13.2})$$

where the weighting factor  $w_k=1$  ( $k=1,2,\dots,N$ ) is omitted and  $a_{ik}$ ,  $b'_{ik}$  are the  $i$ -th components of the vectors  $\underline{a}_k$  and  $\underline{b}'_k$  respectively. This imposes a linear least-squares problem that can be solved directly and

and uniquely from the set of nine normal equations generated by minimization conditions that  $\partial S/\partial r_{ij}=0$  for all  $i$  and  $j$ .

The transformation matrix  $\underline{R}$  found in the minimization of (A13.2) will not necessarily correspond to a rigid-body rotation. Indeed, Diamond (1976) has shown how such a matrix can be factored into the product  $\underline{R}=\underline{A}\underline{S}$  of a pure rotation and a pure strain. The transformation  $\underline{S}$  is a symmetric matrix representing the strain, and the matrix  $\underline{A}$  expresses the rotation that brings into coincidence the principal axes of strain. Clearly, if the reference systems are to be 'moved as rigid bodies'  $\underline{R}$  itself must be an orthogonal transformation matrix (i.e.  $\underline{S}=\underline{I}$  and, hence,  $\underline{R}=\underline{A}$ ; see below). The elements of such a matrix are the direction cosines of the rectangular cartesian reference frame with respect to another. Consequently, the necessary and sufficient conditions that  $\underline{R}$  should represent an orthogonal transformation are:

$$\begin{aligned} g_1 &= r_{11}^2 + r_{12}^2 + r_{13}^2 - 1 = 0 \\ g_2 &= r_{21}^2 + r_{22}^2 + r_{23}^2 - 1 = 0 \\ g_3 &= r_{31}^2 + r_{32}^2 + r_{33}^2 - 1 = 0 \\ g_4 &= r_{21}r_{31} + r_{22}r_{32} + r_{23}r_{33} = 0 \\ g_5 &= r_{11}r_{31} + r_{12}r_{32} + r_{13}r_{33} = 0 \\ g_6 &= r_{11}r_{21} + r_{12}r_{22} + r_{13}r_{23} = 0 \end{aligned} \tag{A13.3}$$

The problem is then to find an orthogonal matrix  $\underline{R}$  which minimizes the function (A13.2) subject to the constraints (A13.3) (which can be written as  $\sum_k r_{ki}r_{kj} - \delta_{ij} = 0$  where the  $\delta_{ij}$  are the elements of the unit matrix). The desired linear transformation can be constrained to meet

the orthogonality conditions through the introduction of the Lagrange multipliers  $\lambda_{ij}$  (Wilson, 1952). Introducing a symmetrical matrix  $\underline{L}$  with elements  $\lambda_{ij}$  an auxiliary function  $F = \frac{1}{2} \sum_{i,j} \lambda_{ij} (\sum_k r_{ki} r_{kj} - \delta_{ij})$  is constructed and added to  $S$  to form the Lagrangian function  $G = S + F$ . Since for each different condition (A13.3) an independent number  $\lambda_{ij}$  is available, the constrained minimum of  $S$  is now included among the free minima of  $G$ . A free minimum of  $G$  can only occur where:

$$\frac{\partial G}{\partial r_{ij}} = \sum_{k=1}^3 r_{ik} \left( \sum_{n=1}^N a_{kn} a_{jn} + \lambda_{kj} \right) - \sum_{n=1}^N b_{in} b_{jn} = 0$$

and

$$\frac{\partial G}{\partial r_{mk} \partial r_{ij}} = \delta_{mi} \left( \sum_{n=1}^N a_{kn} a_{jn} + \lambda_{kj} \right)$$

are the elements of a positive definite matrix,  $a_{kn}$  and  $b_{kn}$  are the components of the vector  $\underline{a}_n$  and  $\underline{b}_n$  respectively.

Insomuch as the constraining conditions are quadratic, this minimization is not a straightforward linear least-squares problem. Kabsch (1976) has given an elegant eigenvalue solution of the above problem. Alternatively<sup>1</sup>, solution can be achieved if equations (A13.3) are linearized by a Taylor series expansion about approximate values for the matrix elements  $r_{ij}$ , and equation (A13.2) is also expressed as a first-order Taylor expansion. The initial parameters for these expansions derive from the unconstrained minimization of  $S$ . Parameters shifts tending to minimize  $S$ , and thereby, to impose the constraints are then found by solving the resultant set of fifteen normals equations  $\partial F / \partial \delta r_{ij} = 0$  and  $\partial F / \partial \lambda_l = 0$  for all allowed  $i, j, l$ . Note that the Lagrangian function  $F$  is now written in the form  $F = S + \sum_{l=1}^6 \lambda_l g_l$  in order to reduce the normal equations. The process is then iterated until sufficient convergence is reached.



### A13.2 The solution of the constrained least-squares minimization equations

In order that the Taylor expansions be carried out the following deviations are introduced:

$$p_{ij} = r_{ij} - t_{ij} \quad (\text{A13.4})$$

where  $p_{ij}$  and  $t_{ij}$  are the elements of the matrices  $\underline{P}$  and  $\underline{R}^0$  respectively.

Matrix  $\underline{R}^0$  contains the approximate values of the parameters  $r_{ij}$  obtained by some preliminary procedure (for example, by the unconstrained least-square method), and the elements of  $\underline{P}$  are the corrections for  $t_{ij}$ , that is, the corrections obtained from the least-squares calculation.

Now, if  $S$  is at its minimum value, and if any or all of the residuals then undergo small variations (expressed by  $\delta p_{ij}$ ) the variation in  $S$  will be zero to within higher powers of the variations in the residuals; in other terms:

$$\frac{1}{2} \delta S = \sum_{k=1}^N \left[ \sum_{i=1}^3 (a_{ik} - b'_{ik}) \delta p_{i1} + \sum_{i=1}^3 (a_{ik} - b'_{ik}) \delta p_{i2} + \sum_{i=1}^3 (a_{ik} - b'_{ik}) \delta p_{i3} \right] = 0 \quad (\text{A13.5})$$

Let, now,  $h_i$  be the small numbers by which the conditions  $g_i$  fail to be satisfied by the elements of the matrix  $\underline{R}^0$ , i.e.:

$$\begin{aligned} h_1 &= t_{11}^2 + t_{12}^2 + t_{13}^2 - 1 \\ h_2 &= t_{21}^2 + t_{22}^2 + t_{23}^2 - 1 \\ h_3 &= t_{31}^2 + t_{32}^2 + t_{33}^2 - 1 \\ h_4 &= t_{21} t_{31} + t_{22} t_{32} + t_{23} t_{33} \\ h_5 &= t_{11} t_{31} + t_{12} t_{32} + t_{13} t_{33} \\ h_6 &= t_{11} t_{21} + t_{12} t_{22} + t_{13} t_{23} \end{aligned} \quad (\text{A13.6})$$

Then, the constraints  $g_i$  can be expanded in a power series in the small quantities  $p_{ij}$  and only linear terms being retained:

$$h_1 = \left[ \frac{\partial g_1}{\partial r_{11}} \right]_{t_{11}} p_{11} + \left[ \frac{\partial g_1}{\partial r_{12}} \right]_{t_{12}} p_{12} + \left[ \frac{\partial g_1}{\partial r_{13}} \right]_{t_{13}} p_{13}$$

$$h_2 = \left[ \frac{\partial g_2}{\partial r_{21}} \right]_{t_{21}} p_{21} + \left[ \frac{\partial g_2}{\partial r_{22}} \right]_{t_{22}} p_{22} + \left[ \frac{\partial g_2}{\partial r_{23}} \right]_{t_{23}} p_{23}$$

$$h_3 = \left[ \frac{\partial g_3}{\partial r_{31}} \right]_{t_{31}} p_{31} + \left[ \frac{\partial g_3}{\partial r_{32}} \right]_{t_{32}} p_{32} + \left[ \frac{\partial g_3}{\partial r_{33}} \right]_{t_{33}} p_{33}$$

$$h_4 = \left[ \frac{\partial g_4}{\partial r_{21}} \right]_{t_{21}} p_{21} + \left[ \frac{\partial g_4}{\partial r_{22}} \right]_{t_{22}} p_{22} + \left[ \frac{\partial g_4}{\partial r_{23}} \right]_{t_{23}} p_{23} +$$

$$+ \left[ \frac{\partial g_4}{\partial r_{31}} \right]_{t_{31}} p_{31} + \left[ \frac{\partial g_4}{\partial r_{32}} \right]_{t_{32}} p_{32} + \left[ \frac{\partial g_4}{\partial r_{33}} \right]_{t_{33}} p_{33}$$

$$h_5 = \left[ \frac{\partial g_5}{\partial r_{11}} \right]_{t_{11}} p_{11} + \left[ \frac{\partial g_5}{\partial r_{12}} \right]_{t_{12}} p_{12} + \left[ \frac{\partial g_5}{\partial r_{13}} \right]_{t_{13}} p_{13} +$$

$$+ \left[ \frac{\partial g_5}{\partial r_{31}} \right]_{t_{31}} p_{31} + \left[ \frac{\partial g_5}{\partial r_{32}} \right]_{t_{32}} p_{32} + \left[ \frac{\partial g_5}{\partial r_{33}} \right]_{t_{33}} p_{33}$$

$$h_6 = \left[ \frac{\partial g_6}{\partial r_{11}} \right]_{t_{11}} p_{11} + \left[ \frac{\partial g_6}{\partial r_{12}} \right]_{t_{12}} p_{12} + \left[ \frac{\partial g_6}{\partial r_{13}} \right]_{t_{13}} p_{13} +$$

$$+ \left[ \frac{\partial g_6}{\partial r_{21}} \right]_{t_{21}} p_{21} + \left[ \frac{\partial g_6}{\partial r_{22}} \right]_{t_{22}} p_{22} + \left[ \frac{\partial g_6}{\partial r_{23}} \right]_{t_{23}} p_{23}$$

(A13.7)

The deviations in the above relations should be evaluated at the adjusted values of  $r_{ij}$  but they will actually be computed at  $t_{ij}$  which are assumed to be near enough. By differentiating the above relations:

$$\left[ \frac{\partial g_1}{\partial r_{11}} \right]_{t_{11}} \delta p_{11} + \left[ \frac{\partial g_1}{\partial r_{12}} \right]_{t_{12}} \delta p_{12} + \left[ \frac{\partial g_1}{\partial r_{13}} \right]_{t_{13}} \delta p_{13} = 0$$

$$\left[ \frac{\partial g_2}{\partial r_{21}} \right]_{t_{21}} \delta p_{21} + \left[ \frac{\partial g_2}{\partial r_{22}} \right]_{t_{22}} \delta p_{22} + \left[ \frac{\partial g_2}{\partial r_{23}} \right]_{t_{23}} \delta p_{23} = 0$$

$$\left[ \frac{\partial g_3}{\partial r_{31}} \right]_{t_{31}} \delta p_{31} + \left[ \frac{\partial g_3}{\partial r_{32}} \right]_{t_{32}} \delta p_{32} + \left[ \frac{\partial g_3}{\partial r_{33}} \right]_{t_{33}} \delta p_{33} = 0$$

$$\left[ \frac{\partial g_4}{\partial r_{21}} \right]_{t_{21}} \delta p_{21} + \left[ \frac{\partial g_4}{\partial r_{22}} \right]_{t_{22}} \delta p_{22} + \left[ \frac{\partial g_4}{\partial r_{23}} \right]_{t_{23}} \delta p_{23} +$$

(A13.8)

$$+ \left[ \frac{\partial g_4}{\partial r_{31}} \right]_{t_{31}} \delta p_{31} + \left[ \frac{\partial g_4}{\partial r_{32}} \right]_{t_{32}} \delta p_{32} + \left[ \frac{\partial g_4}{\partial r_{33}} \right]_{t_{33}} \delta p_{33} = 0$$

$$\left[ \frac{\partial g_5}{\partial r_{11}} \right]_{t_{11}} \delta p_{11} + \left[ \frac{\partial g_5}{\partial r_{12}} \right]_{t_{12}} \delta p_{12} + \left[ \frac{\partial g_5}{\partial r_{13}} \right]_{t_{13}} \delta p_{13} +$$

$$+ \left[ \frac{\partial g_5}{\partial r_{31}} \right]_{t_{31}} \delta p_{31} + \left[ \frac{\partial g_5}{\partial r_{32}} \right]_{t_{32}} \delta p_{32} + \left[ \frac{\partial g_5}{\partial r_{33}} \right]_{t_{33}} \delta p_{33} = 0$$

$$\left[ \frac{\partial g_6}{\partial r_{11}} \right]_{t_{11}} \delta p_{11} + \left[ \frac{\partial g_6}{\partial r_{12}} \right]_{t_{12}} \delta p_{12} + \left[ \frac{\partial g_6}{\partial r_{13}} \right]_{t_{13}} \delta p_{13} +$$

$$+ \left[ \frac{\partial g_6}{\partial r_{21}} \right]_{t_{21}} \delta p_{21} + \left[ \frac{\partial g_6}{\partial r_{22}} \right]_{t_{22}} \delta p_{22} + \left[ \frac{\partial g_6}{\partial r_{23}} \right]_{t_{23}} \delta p_{23} = 0$$

Now, by multiplying equations (A13.8) by  $-\lambda_1$ , 6 equations are obtained which are introduced in equation (A13.5). The nine equations are thus obtained which together with equations (A13.7) consist a

system of 15 equations with 15 unknown variables (the six  $\lambda_i$ 's and nine  $p_{ij}$ ). The solution of this system yields the values of  $p_{ij}$ .

### A13.3 Error propagation in the calculation of the misorientation matrix

The systematic errors in the components of  $\underline{R}$  introduced by the experimental errors in the determination of the beam directions can be expressed as follows.

Let  $\underline{R}_{=a}$  be the misorientation matrix calculated by the unconstrained least-squares method ('first approximation' matrix). Diamond (1976) has shown that if  $\underline{R}_{=a}$  is not an orthogonal matrix then it can be factorized according to

$$\underline{R}_{=a} = \underline{R}\underline{S} \quad (\text{A13.9})$$

The matrix  $\underline{R}$  is an orthogonal matrix expressing a pure rotation having three independent elements, and  $\underline{S}$  is symmetric having six independent elements, thus providing for nine independent elements in  $\underline{R}_{=a}$ . Equation (A13.9) states, therefore, that the transformation  $\underline{R}_{=a}$  is to be considered as a pure strain followed by the application of a pure rotation<sup>2</sup>. It is evident that if there are no experimental errors in the determination of the beam directions then  $\underline{S}=\underline{I}$ ; where  $\underline{I}$  is the 3x3 unit matrix. Thus, the deviation of  $\underline{S}$  from the 'ideal value'  $\underline{I}$  provides a means for the expression of the systematic errors introduced in the calculation of the misorientation matrix.

From (A13.9):

$$\underline{R}_{=a}^T \underline{R}_{=a} = \underline{S}^T \underline{R}^T \underline{R} \underline{S} = \underline{S}^T \underline{S}$$

(using the superscript to denote a transpose matrix), but since  $\underline{S}^T = \underline{S}$  by definition:

$$\underline{S} = (\underline{R}_{=a}^T \underline{R}_{=a})^{1/2}$$

and the factorization is complete by writing:

$$R = R (R^T R)^{\frac{1}{2}}$$

The matrix  $(R^T R)^{\frac{1}{2}}$  is real symmetric positive definite, and it has the same eigenvalues as  $R^T R$  and eigenvectors equal to the square roots of those of  $R^T R$  (Bellman, 1960). Only the positive square roots need to be considered; negative square roots correspond to an end-to-end reversal.

- - -

Footnotes 1: This solution is an application of three papers by Deming (1931, 1934, 1935).

2: It would, of course, be possible to write the factors in (A13.9) as  $\underline{SR}$  and to develop the subsequent formulation on that alternative basis.

## Appendix 14

### A PACKAGE OF COMPUTER PROGRAMS FOR THE FAST SOLUTION OF ELECTRON DIFFRACTION SPOT/KIKUCHI LINE PATTERNS

The determination of the misorientation across a grain boundary can be time consuming, particularly when large numbers of similar readings are required or repetitive calculations performed. This is especially true of the measurements required to determine the beam direction by using the method outlined in appendix 12. The employment of high speed digital electronics and fast computer programs reduces the required time as well as increases the accuracy of the determination.

#### A14.1 Description of the procedure

During the course of this project the determination of the coordinates of points lying on Kikuchi lines or diffraction spots were made using the Ferranti digitizer installed in the Liverpool University Computer Laboratory. This system has a point-to-point resolution of 0.025 mm over a wide range of temperature and humidity conditions (see 'ADE Modular Digitisers, User Handbook' published by Ferranti). This instrument provided the means of measuring coordinates directly from the plate (which is fixed on the working table); the coordinates are expressed relative to an arbitrary origin. The output, consisting of a list of point coordinates, is punched onto paper tape in ASCII code to allow the information to be fed directly in the George 3/4 filestore of the ICL 1900 series computer.

The use of the digitizer (together with the analytical method presented in appendix 12) provides a means for more accurate measurements of distances and angles. This immediately yields a higher accuracy in the determination of the beam direction. Also, it permits computer

assisted techniques to be successfully employed for the solution of the diffraction spot/Kikuchi line patterns. For this a package of computer programs has been written. Figure A14.1 shows the flow diagram summarizing the sequential operation of the package routines for a typical Kikuchi line pattern.

#### A14.2 Program INDEX for the indexing of electron diffraction spot/Kikuchi line patterns

Program INDEX, and its associated subroutines, calculates and prints out the indices of a diffraction spot or Kikuchi line pattern as seen in the electron microscope. The crystal giving rise to the pattern is of cubic symmetry and provision has been given to the following structures: simple cubic, face centred cubic, body centred cubic and diamond-type-structure. The indexing procedure is based on the approach of Thomas (1970).

The data specifying the pattern are on  $n-1$  data cards (where  $n$  is the number of spot/lines to be indexed). The program starts (figure A14.2) by reading the data of three spots/lines. It then generates the reciprocal lattice points allowed, as a consequence of space group restrictions, calculates the interplanar distances  $d_{hkl}$  (subroutine RECIPL) and sorts them in increasing order (subroutine SORTIN and NAG library subroutine MØ1AAF). This list is then searched (subroutine SOLVE) for determining the  $d_{hkl}$  which give values for the ratios  $P_i/P_j$  consistent (within a given error limit) to those measured. Thus, each spot/line is assigned a set of possible  $(hkl)$ .

The algorithm employed in subroutine SOLVE implies a significant reduction in the execution time (compared to other available programs). The computing time was further reduced by using optimizing techniques such as the binary technique for reaching an array (subroutine BINARY).

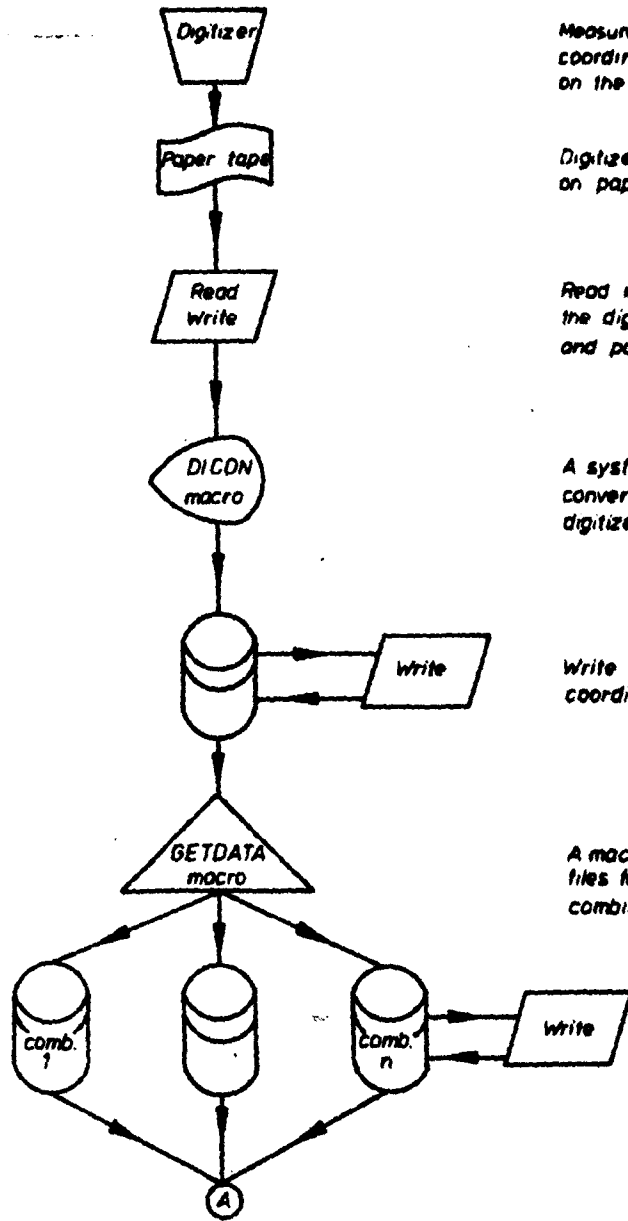
Figure A14.1

Flow diagram summarizing the sequential operation of the package routines for indexing a typical Kikuchi-line pattern and determination of the beam direction.



Store the converted coordinates on magnetic disc

Store and print out the various combinations



Measurement of the coordinates of points on the plate

Digitizer output punched on paper tape

Read in and print out the digitizer readings and parameters

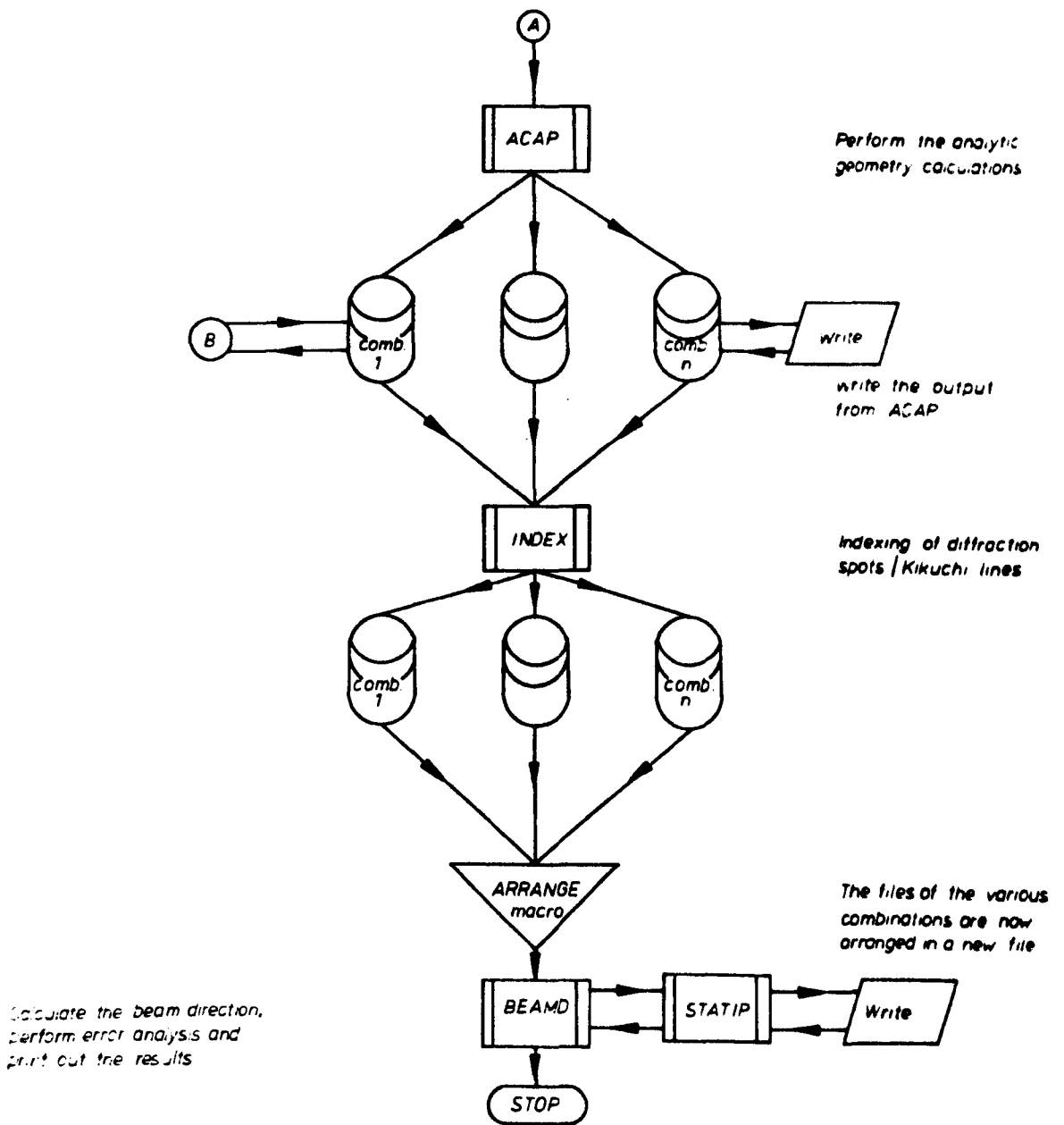
A system macro for converting the digitizer data

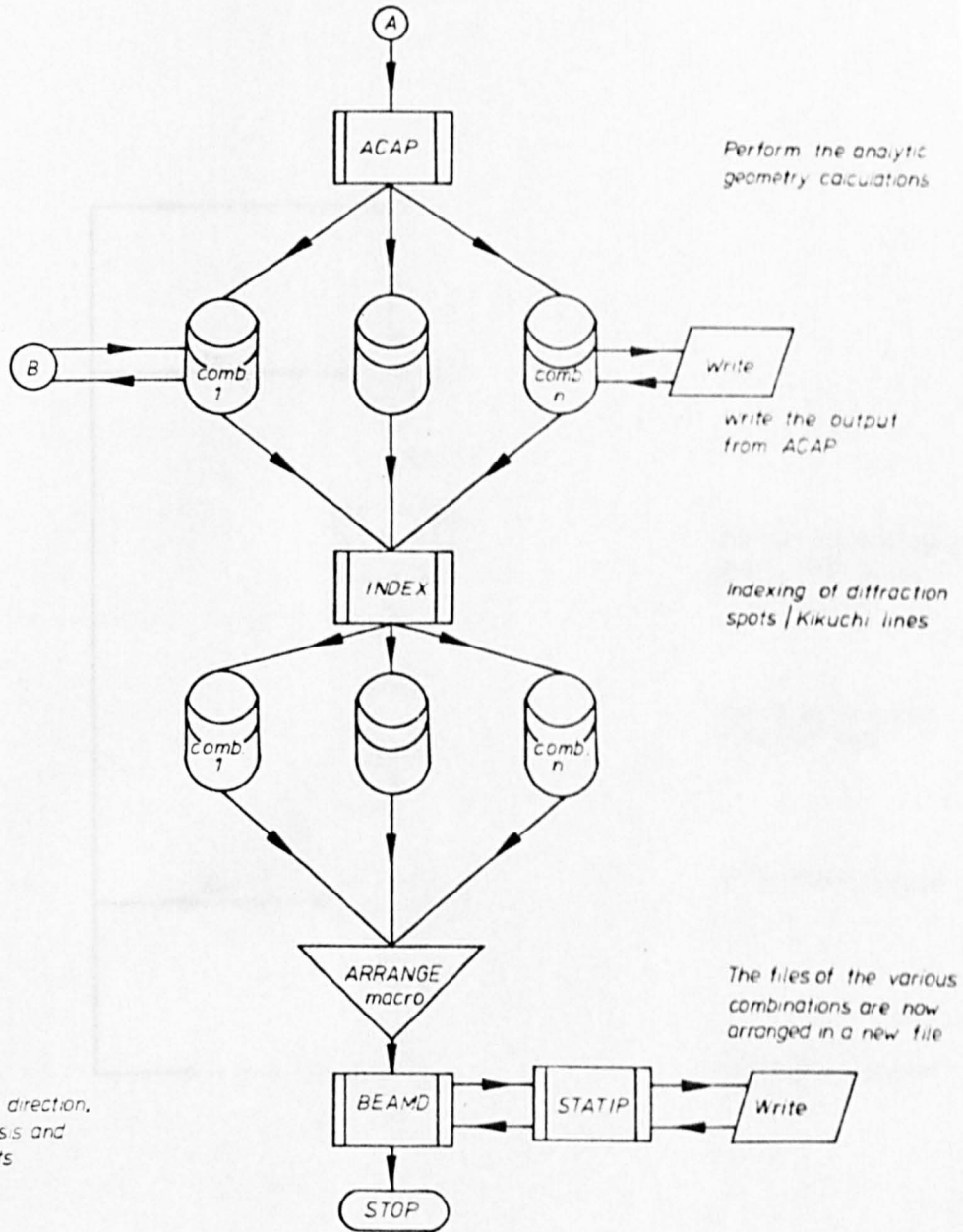
Write the converted coordinates

A macro written to create files for the various combinations

write

write





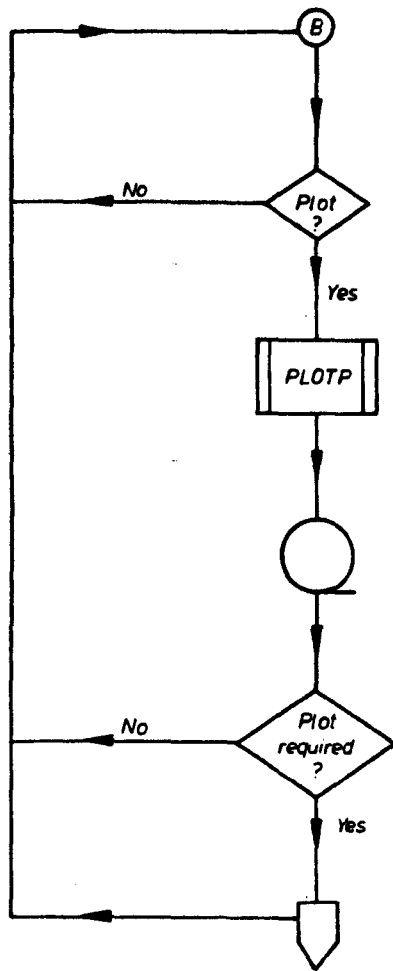
Perform the analytic geometry calculations

write the output from ACAP

indexing of diffraction spots / Kikuchi lines

The files of the various combinations are now arranged in a new file

Calculate the beam direction, perform error analysis and print out the results



*Plot the diffraction spots /  
Kikuchi lines using  
GHOST routines*

*Store graphical output  
on magnetic tape*

*Call for graphical output*

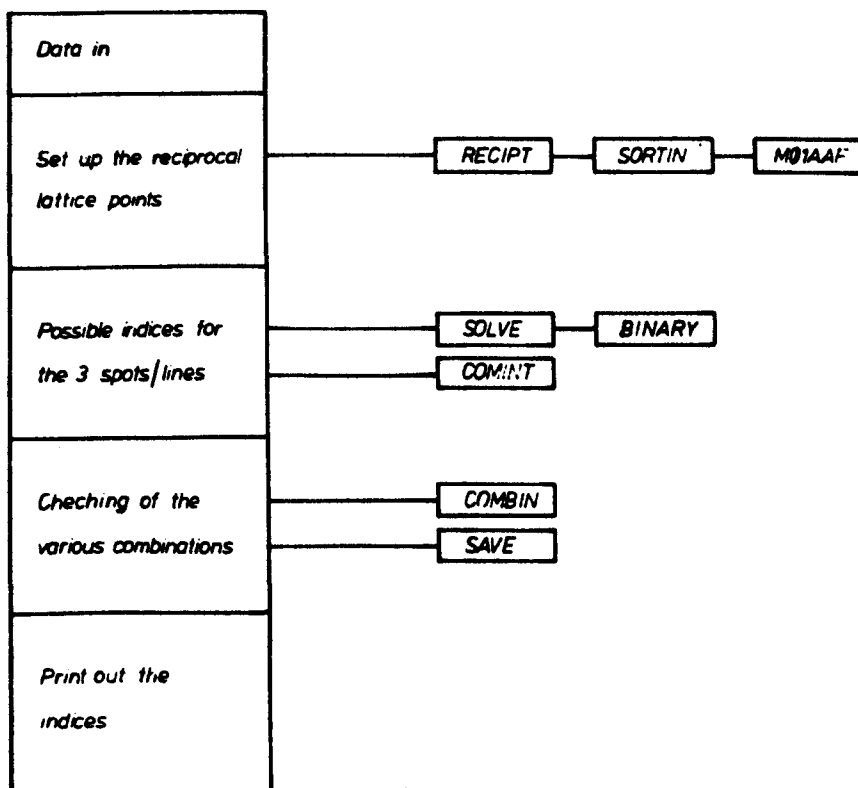
*Graph plotter activated*

Figure A14.2

Structure of the computer program INDEX

*Main program*

*Subroutines*



The program then chooses a pair of three 'indexed' diffraction spots/Kikuchi lines and determines all possible interplanar angles between them as dictated by the cubic lattice geometry. These calculated interplanar angles are then compared with the experimentally observed ones. Once a match is obtained, within the given angle error, another pair of diffraction spots/Kikuchi lines is chosen and the procedure is repeated for their possible (hkl) indices.

When consistences are obtained between calculated and observed interplanar angles for the three spots/lines the control passes to the subroutine SAVE. This subprogram assigns (hkl) indices to the rest of the spots/lines present in the particular pattern; this is achieved by using the already determined indices.

Finally, the program issues the print statement 'INDEXING OKEY' and prints out the indices of the diffraction spots/Kikuchi lines. If no fit can be obtained between the calculated reciprocal lattice points and observed spots/lines within the given linear and angular error limits, the program issues the print statement 'INDEXING FAILS'. The control returns then to the start to read in the next set of data specifying either another pattern or wider error limits.

## Appendix 15

### PREPARATION METHODS OF SILICON SAMPLES FOR TRANSMISSION ELECTRON MICROSCOPY

The material used throughout the course of the experimental work has been silicon. As it mentioned in section 1.3 this material has been primarily chosen for its great importance in technological applications.

In this appendix the specimen preparation methods employed during the course of this work are given. However, before carrying on to a detailed description of these methods it would be of interest to notice that there are two main difficulties associated with the preparation of semiconductor specimens:

- (1) a strictly non-preferential thinning process is required, and,
- (2) owing to the extreme brittleness of semiconducting materials the thinned specimens frequently break during handling before they can be examined in the electron microscope.

#### A15.1 Samples from bulk material

Generally the preparation of a TEM specimen involves two stages:

- (a) cutting of suitably shaped slides from the bulk and mechanical polishing up to 0.7-0.4 mm thickness (which is well above the limit, 0.1 mm, that the mechanical means safely permit; Irving, 1961), and,
- (b) thinning of the samples by non-mechanical means until an electron-transparent area is obtained.

Silicon discs 3 mm in diameter and 2 mm in thickness were cut out from the rod-shaped bulk<sup>1</sup> where profuse twinning occurred during crystal growth. These slides were then hand-thinned to 0.7 mm on wet grinding paper. For this a special designed jig (Irving, 1961) was used in order



to control the sample thickness as well as ensure that the two sides of the slide were parallel at the time during the polishing process.

In order to reduce further the thickness of the sample before the final thinning process as well as to remove any surface damage introduced by the grinding a fast chemical polishing technique was employed; the etchant used was a mixture of 100 cc  $\text{HNO}_3$  (69%), 60 cc HF (48%) and 60 cc  $\text{CH}_3\text{COOH}$  (100%). After the chemical polish the sample was about 200  $\mu\text{m}$  thick with a polished surface where a number of linear features were visible with naked eye. This enabled areas of particular interest to be selected and cut from the slide (see below).

Discs 3 mm in diameter were then cut off by a quick and simple technique described by Goodhew (1972). This involves the masking of 3 mm diameter areas of the sample with adhesive tape discs (3.05 mm in diameter) punched out from an acid-resistant tape supplied by Struers Chemiske Laboratorium<sup>2</sup>. The whole side of the slide sample was masked while several tape discs were stuck on the other side. The exposed areas were then dissolved by using the fast chemical solution mentioned above. The total time required for the unmasked areas to dissolve was about 5 mins (initial sample thickness approximately 200  $\mu\text{m}$ ) short enough to prevent chemical polishing of the edges of the masked discs.

By this method a total of 30 discs were cut off from a slide approximately 4 mm diameter. The main other advantage of the method is that it allows areas of particular interest to be selected and discs containing these areas to be cut. The discs so obtained were then used for preparing the TEM samples.

#### A15.2 Transmission electron microscopy sample preparation

It is well-known that in the transmission electron microscopy the transmitted intensity depends very strongly on the electron scattering

factor of the material, which increases with the atomic number. Thus, for silicon (atomic number 14) samples less than approximately 10,000 Å thick are required.

It is of interest to notice that both visible and 100 kV electrons are transmitted through silicon only in section 5,000 Å thick or less. Thus appearance of visible transmitted light through the sample during the preparation process can be used as index of area suitability for electron microscopy and for halting the thinning process.

#### A15.2.1 Chemical techniques

Two techniques can be used for the preparation of TEM silicon samples, mainly, the ion-beam thinning method and the chemical techniques. A number of chemical methods are available for the preparation of single-crystal silicon specimens<sup>3</sup>. The method by Booker & Sticker (1962) is simple and rapid, and allows the particular area of the specimen which is thinned to be previously selected. Moreover, the technique provides a rapid polishing rate and high quality non-preferential polish has been reported for the case of single silicon samples.

Kolbesen et al. (1975) described a method for preparing large (several millimeters in diameter) electron-transparent areas of single-crystal silicon. The method is based on employing rotation of both the etchant and sample, and produces TEM specimens with uniform thickness (the diameter of the transparent area is limited by the diameter of TEM sample holder).

On the grounds that no chemical method is available for TEM sample preparation of polycrystalline silicon, both the above techniques have been used during the course of this work. The method by Booker & Sticker (1962) was found by the author to be reasonably quick (as little as

10 mins per specimen of thickness 200  $\mu\text{m}$ ) and reproducible. Specimens prepared by this technique had, however, areas with rough surface. Furthermore, it was found very difficult to obtain a thin area containing a grain boundary, since a step across the boundary was always formed. This was explained by the fact that the thinning rate depends very sensitively on the surface orientation. The same effect was observed in specimens prepared by the technique of Kolbesen et al. (1975). This technique was developed for thinning silicon wafers and the authors had no experience in employing the method for polycrystalline silicon.

#### A15.2.2 Ion-beam thinning technique<sup>4</sup>

As an alternative the ion-beam thinning technique was used. Generally speaking, in semiconducting materials ion-beam thinning gives a smaller differential rate between differently orientated surfaces than does chemical attack (Booker, 1970). Conditions for ion-beam thinning of silicon films have been reported by Linington (1970) and Booker (1970) and the general conditions which must occur for all materials have been outlined by Abrahams et al. (1968) and Molcik (1970). It was found that the following conditions:

ion energy    6 kV  
 beam current 100  $\mu\text{A/gun}$   
 angle            10-15 $^{\circ}$

were the best compromise between thinning time and differential thinning rates between the two surfaces. In the later stage of thinning it is not thinning rate but depth of damage or differential thinning rates between two orientations which are important and hence the samples were finished at a glancing angle (5-10 $^{\circ}$ ).

The above operation conditions were found to give a sample with smooth, clear surface and no thinning-rate-dependence on the surface orientation was observed. Sometimes although large electron-transparent areas of the specimen were covered by various surface artefacts with the appearance of hills and valley or ripples; the scale of these artefacts is sub-micron. Such artefacts have already been reported by several workers (see e.g. Trillat, 1964) but no explanation has been proposed. It has been found during the course of this work that changes in the rotational speed of the specimen does not affect the size or the extent of such artefacts.

The overall time required for the ion-beam thinning process was appreciably long (typical times 24-36 hours). Moreover, it was found necessary to examine several specimens in order to find a boundary suitable for investigation. The reasons for this were that either the whole transparent area was covered by the above mentioned artefacts or the boundaries did not satisfy the requirements for the application of the method to determine the rigid-body displacements (see section 9.2).

- - -

- Footnotes 1: The bulk was kindly supplied by Dr. A.G. Cullis of the Royal Signal and Radar Establishment.
- 2: H. Struers Chemiske Laboratorium, 38 Skindergade, DK-1159 Copenhagen K, Denmark.
- 3: See Irving (1961), Riesz & Bjorling (1961), Aerts et al. (1962), Booker & Sticker (1962), Sticker & Booker (1963), Finch et al. (1963), Frankl (1964), Bickell (1973), Kolbesen et al. (1975).
- 4: The author wishes to express his thanks to Mr. R. Devenish for his willing help with the ion-beam thinning technique.

Appendix 16

## COVALENT BONDING IN DIAMOND-STRUCTURE-TYPE MATERIALS

The group IV elements, carbon, silicon, and germanium<sup>1</sup> crystallize with the diamond structure. This structure is the result of covalent bonding as is discussed immediately below.

The covalent bond is an electron pair (or homopolar) bond and is usually formed from two electrons, one from each atom participating in the bond. Thus, in the ideal model of the covalent bond these electrons (often called valency electrons) form a molecular orbital so as to be effectively localized between atoms. The strength of the resultant covalent bond will depend on the extent of overlap of the two atomic orbitals.

The number of covalent bonds that an atom form depends on its electronic configuration and the direction of the bonds is determined by which atomic orbitals are combined to form molecular orbitals. The covalent bonds that an atom form are thus limited in number and restricted in direction. In the case of silicon<sup>2</sup> maximum overlap of atomic orbitals is achieved when the four valency electrons are in  $sp^3$  hybrid orbitals, which have their directions of maximum electron density disposed towards the corners of a regular tetrahedron centred on the silicon nucleus. When molecular orbitals are formed from those  $sp^3$  atomic orbitals the silicon atom will be tetrahedrally coordinated; this leads to the well-known diamond-type crystal structure.

A crystal of silicon is effectively a macromolecule; all the bonds in the crystal are purely covalent bonds which are very strong. The requirement that the bonds from each silicon atom should be tetrahedrally disposed is imposed by the molecular orbital formation which otherwise

would not be energetically effective. Consequently, the conditions for minimum energy configuration in silicon can be expressed as follows:

- (1) all the  $sp^3$  atomic orbitals are combined to form molecular orbitals, or in other words, no dangling bonds exist, and,
- (2) the molecular orbitals give rise to tetrahedral coordination; the angles between any two intersecting bonds is equal to  $109^{\circ}28'$ .

However, the postulate of the tetrahedral atom requires that the atoms have a configuration that is tetrahedral but is not necessarily that of a regular tetrahedron. So long as the four bonds have a general tetrahedral orientation an increase in the bond energy is accounted for, since change from the tetrahedral angle is associated with loss in atomic orbital overlapping.

- - -

Footnotes 1: Also (grey) tin below  $13^{\circ}\text{C}$ .

2: The considerations, herein, apply to carbon, germanium and grey tin as well.

## Appendix 17

### ADDITIONAL ELECTRON DIFFRACTION INFORMATION FOR SILICON

As may be seen from the Howie-Whelan (1960, 1961) equations there are a number of parameters required before these equations may be evaluated for the calculation of the intensity profiles. These parameters must be determined with the highest possible accuracy so an accurate determination of the rigid-body displacement is feasible (section 9.2). This brief appendix presents values for the most important of these parameters.

#### A17.1 Silicon structure data

Silicon is in the fourth column of the periodic table, possessing the diamond structure with symmetry type  $Fd\bar{3}m$  of atomic number 14. The space lattice of silicon is face centred cubic. A primitive basis of two identical atoms at  $(0,0,0)$  and  $(\frac{1}{4},\frac{1}{4},\frac{1}{4})$  is associated with each lattice point<sup>1</sup>. There are eight atoms in a unit cube; each atom has four nearest neighbors and twelve next-nearest neighbors. The tetrahedral bonding of the silicon structure is the result of covalent bonding (appendix 16). The lattice parameter of pure silicon (corrected for refraction) at 25°C is  $a=5.5307 \text{ \AA}$  (Pearson 1956, 1967)<sup>2</sup>.

#### A17.2 Extinction distances of silicon

Values of the extinction distances,  $\xi_g$ , may be calculated from the atomic scattering amplitudes for electrons given by Ibers (1957), Smith & Burge (1962) and Doyle & Turner (1968) or from the crystal potential calculations of Radi (1970). Table A17.1 gives the values of  $\xi_g$  for silicon calculated from the results of Doyle & Turner (1968) as well as the values obtained from Hirsch et al. (1965). It may be seen that the calculated values are from 5% to 15% larger than those of Hirsch et al.

TABLE A17.1

Relativistically corrected extinction distances  $\Xi_g$  and  $\Xi'_g$  (Å) for silicon  
(100kV electrons) and anomalous absorption coefficient ( $\Xi_g/\Xi'_g$ )

$h^2+k^2+l^2$	Reflection hkl	$\Xi_g$ (Å)		$\Xi'_g$ (Å)	$\Xi_g/\Xi'_g$	
		Calculated	Hirsch et al. (1965)		Humphreys & Hirsch (1968)	Radi (1970)
0	000	283		5821*	0.0481*	0.061
3	111	634	602	45286	0.014	0.019
8	220	768	757	36571	0.021	0.025
11	311	1323	1349	49000	0.027	0.028
16	400	1236	1268	35314	0.035	0.033
19	331	1971	2046	49275	0.040	0.035
24	422	1672		37155	0.045	0.039
27	511/333	2578	2645	54851	0.047	0.045
32	440	2091	2093	41000	0.051	0.048
35	531	3093		57278	0.054	
40	620	2410		41552	0.058	0.049
43	533	3590		60847	0.059	0.052
51	711/551	4103		63123	0.065	
56	642	3025		45833	0.066	
59	731/553	4468		65706	0.068	
64	800	3306		42935	0.077	

(\*) value quoted by Sutton (1977)

Note: No correction has been made to the atomic scattering amplitude to allow for thermal vibrations.



The calculated values have been used where  $\xi_g$  was required.

The values of  $\xi_g$  in table A17.1 are deduced for crystalline silicon at 0°K. In order to correct these values for the effect of temperature the values of  $\xi_g$  should be multiplied by the Debye-Waller factor. This factor may be written  $\exp(-M_g)$  where  $M_g = B(\sin\theta_B)^2 \lambda^{-2}$ . The thermal Debye parameter B for silicon is 0.24 Å<sup>2</sup> (International Tables for X-ray Crystallography, 1969).

### A17.3 Anomalous absorption coefficients for silicon

The anomalous absorption coefficient is defined as the ratio of the two-beam extinction distance  $\xi_g$  to the two-beam anomalous extinction distance  $\xi'_g$ . An equivalent definition obtained from the wave-mechanical formulation may be given using the notion of a complex crystal potential. If the g-th order Fourier coefficient of the complex crystal potential is written as  $V_g + iV'_g$  where  $V_g$  is the Fourier coefficient of the real crystal potential, then the anomalous absorption coefficient may be written as  $V'_g/V_g$  (Humphreys & Hirsch, 1968).

Estimates of the anomalous absorption coefficient for silicon and various diffracting vectors can be made from the theoretical values of Humphreys & Hirsch (1968) or, alternatively, from the values of  $V_g$  and  $V'_g$  given by Radi (1970). It should, however, be noticed that the values shown in Humphreys & Hirsch's plots and those obtained from Radi's results are for the theoretical case of 'zero aperture' and in practice, when objective apertures with angular diameters of the order of the order of the Bragg angle are used, these values generally need to be increased (Metherell & Whelan, 1967; Titchmarch, 1971).

The values of the anomalous absorption coefficient obtained by the two methods mentioned above are shown in table A17.1. The values taken

from Humphreys & Hirsch (1968) were subsequently used for calculating the (two-beam) anomalous extinction distances given also in table A17.1.

#### A17.4 Determination of the crystal deviation from the Bragg reflecting position

The deviation from the Bragg condition, represented by  $w = s\epsilon_g$ , where  $s$  is the distance in reciprocal space from the reciprocal lattice point corresponding to the operating diffraction vector to the Ewald sphere, is required not only for the integration of the Howie-Whelan equations, but also for the determination of the effective extinction distance when  $w \neq 0$ .

Following Head et al. (1973) the value of  $w$  is expressed as a linear function of  $\Delta x_2/x$ , where  $\Delta x_2$  is the distance between the second order diffraction spot and its associated excess Kikuchi line, and  $x$  is the measured distance between neighbouring spots in the systematic row on the diffraction pattern. The full expression for  $w$  is:

$$w = \epsilon_g |\underline{g}| \theta_B (1 - 2\Delta x_2/x)$$

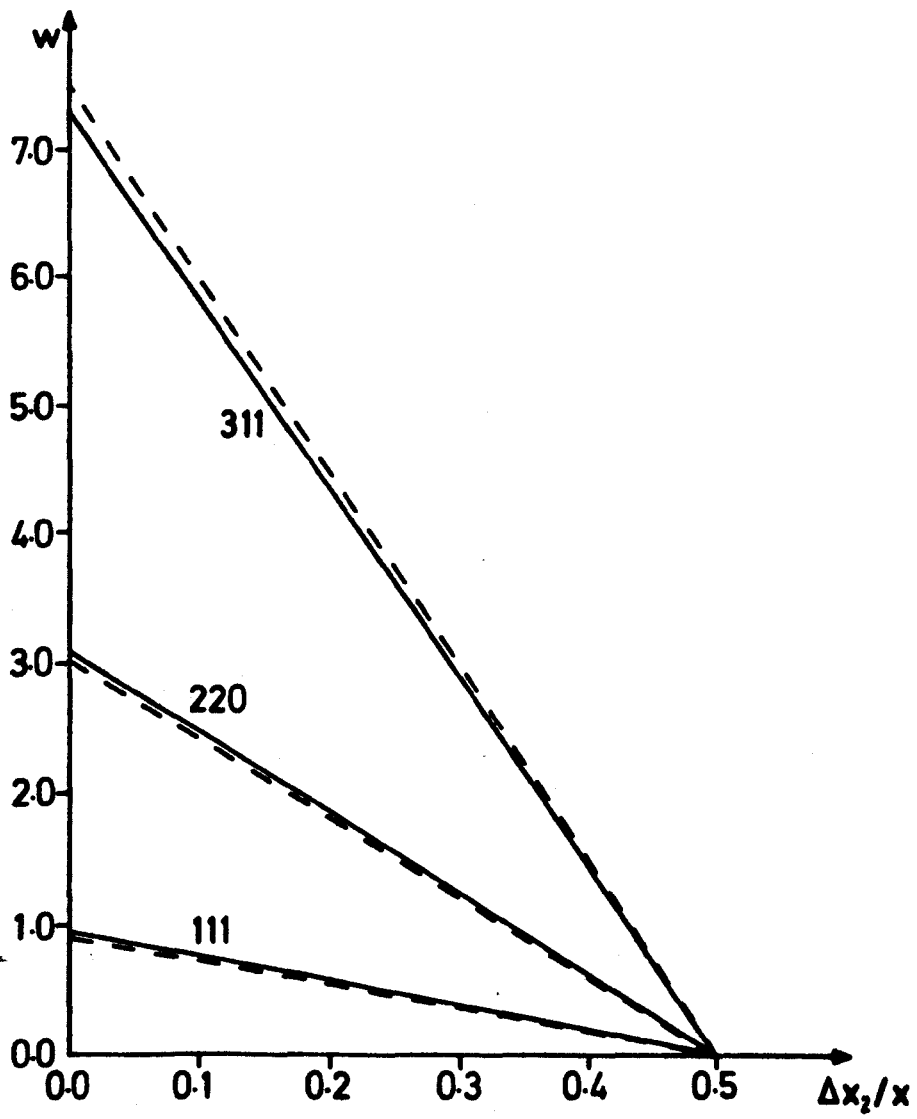
For rapid determination of  $w$  is useful to plot  $w$  as a function of  $\Delta x_2/x$ . The plot for silicon is shown in figure A17.1; the dashed lines are the values of  $w$  plotted using the  $\epsilon_g$  of Hirsch et al. (1965). Note that the error introduced is relatively small (less than 10%) and decreases with increasing  $|\underline{g}|$ .

- - -

- Footnotes 1: There is no way of choosing a primitive cell such that the basis contains only one atom.
- 2: See also Jette & Foote (1935), Lipson & Rogers (1944), Straumanis & Aka (1952), Stramanis et al. (1961), Beu et al. (1962).

Figure A17.1

Plot of  $w$  vs.  $\Delta x_2/x$  for silicon and 150 keV energy electrons.  
Solid lines are from values of  $\xi_g$  calculated in this thesis,  
dashed lines use  $\xi_g$  values of Hirsch et al. (1965).



## REFERENCES

- Abdalla, M.I. (1973) Ph.D. thesis, Univ. of London
- Abdalla, M.I. & Holt, D.B. (1973) Phys. Stat. Sol. (a), 17, 267
- Abdalla, M.I., Holt, D.B. & Wilcox, D.M. (1973) J. Mater. Sci., 8, 590
- Abrahams, M.S., Buiocchi, C.J. & Coutts, M.D. (1968) Rev. Sci. Instrum., 39, 1944
- Acton, A.F. & Bevis, M. (1971) Acta Cryst., A27, 175
- Adams, G.W. & Day, R.E. (1877) Proc. Roy. Soc., A25, 113
- Aerts, E., Delavignett, P., Siems, R. & Amelinckx, S. (1962) J. Appl. Phys., 33, 3078
- Aizu, K. (1970) Phys. Rev. B, 2, 754
- Alexander, E. & Herrmann, K. (1929) 'Die 80 zweidimensionalen Raumgruppen', Z. Kristall., 70, 328 (in German)
- Andrews, K.W., Dyson, D.J. & Keown, S.R. (1971) Interpretation of electron diffraction patterns, 2nd edition, A. Hilger Ltd
- Ascher, E. & Janner, A. (1965) Acta Cryst., 18, 325
- Ascher, E. (1967) Chem. Phys. Letters, 1, 69
- Ascher, E. (1968) Lattices of equi-translation subgroups of the space groups, 2nd edition, Geneva: Internal report of the Battelle Institute of Advanced Studies Centre
- Ascher, E., Gramlich, V. & Wondratschek, H. (1969) Acta Cryst., B25, 2154
- Aust, K.T. & Rutter, J.W. (1959) A.I.M.E., 215, 119
- Aust, K.T., Ferran, G. & Cizeron, G. (1963) C. R. Acad. Sci. Paris, 257, 3595
- Bellman, R.E. (1960) Introduction to matrix analysis, 2nd edition, New York: McGraw-Hill
- Belov, N.V., Neronova, N.N. & Smirnova, T.S. (1955) 'The 1651 Shubnikov groups (dichromatic space groups)' Trudy Inst. Kristallogr. Akad. Nauk. SSSR, 11, 33 (in Russian). English translation in: A.V. Shubnikov & N.V. Belov Colored Symmetry (1964) pp. 175-210, New York: Pergamon Press where the table published by Belov, Neronova & Smirnova (1957) was substituted for the table originally published in the Russian paper; corrections to the original (1954) table pointed out by Donnay, Belov, Neronova & Smirnova (1958)
- Belov, N.V. (1956) 'One-dimensional infinite crystallographic groups', Kristallografiya, 1, 474 (in Russian). English translation in: Sov. Phys.-Cryst., 1, 372 (1956); also in: A.V. Shubnikov & N.V. Belov Colored Symmetry (1964) pp. 222-227, New York: Pergamon Press

- Belov, N.V. & Tarkhova, T.N. (1956) 'Color symmetry groups', Kristallografiya, 1, 4 and 1, 619 (in Russian). English translation in: Sov. Phys.-Cryst., 1, 5 and 1, 487 (1956); also partial translation of the first paper in: A.V. Shubnikov & N.V. Belov Colored Symmetry (1964) pp. 211-219, New York: Pergamon Press
- Belov, N.V., Neronova, N.N. & Smirnova, T.S. (1957) 'Shubnikov groups', Kristallografiya, 2, 315 (in Russian). English translation in: Sov. Phys.-Cryst., 2, 311 (1957). This paper gives the corrected list of Shubnikov groups- published initially by Belov, Neronova & Smirnova (1955)- according to corrections by Donnay, Belov, Neronova & Smirnova (1958)
- Bertaut, E.F. (1968) Acta Cryst., A24, 455
- Beu, K.E., Musil, F.J. & Whitney, D.R. (1962) Acta Cryst., 15, 1292
- Bickell, R.W. (1973) J. Phys. D: Appl. Phys., 6, 1991
- Billings, A.R. (1969) Tensor properties of materials: generalized compliance and conductivity, Wiley-Interscience
- Bloch, F. (1928) Z. Phys., 52, 555
- Bohm, J. (1963) Neus Jahrbuch für Mineralogie Abhandlungen (Neus Jb. Miner. Abh.) 100, 113 (in German)
- Bohm, J. & Domberger-Schiff, K. (1966) Acta Cryst., 21, 1004
- Bollmann, W. (1970) Crystal defects and crystalline interfaces, Berlin: Springer-Verlag
- Booker, G.R. & Sticker, R. (1962) Brit. J. Appl. Phys., 13, 446
- Booker, G.R. (1970) 'Preliminary experiences with semi-conductors', Ion-beam thinning symposium, London
- Boyle, L.L. (1969) Acta Cryst., A25, 455
- Boyle, L.L. & Lawrenson, J.E. (1972a) Acta Cryst., A28, 485
- Boyle, L.L. & Lawrenson, J.E. (1972b) Acta Cryst., A28, 489
- Bragg, W.L. (1924) Proc. Roy. Soc., A105, 16
- Bragg, W.L. (1937) Atomic structure of minerals, Ithaca: Cornell
- Bragg, W.L. (1940) Proc. Phys. Soc., 52, 54
- Bragg, W.L. & Claringbull, G.F. (1965) Crystal structure of minerals, London: Bell
- Brandon, D.G., Ralph, B., Ranganathan, S. & Wald, M.S. (1964) Acta Metall., 12, 813
- Brandon, D.G. (1966) Acta Metall., 14, 1479
- Bravais, M.A. (1866) Études cristallographiques, Paris (in French). English translation: Deviation of the Bravais lattices, American Cryst. Association (1953)
- Bristowe, P.O. & Crocker, A.G. (1975) Phil. Mag., 31, 503
- Brown, R.A. (1977a) J. Phys. F: Metal Phys., 7, 1269
- Brown, R.A. (1977b) J. Phys. F: Metal Phys., 7, 1283
- Brown, R.A. (1977c) J. Phys. F: Metal Phys., 7, L95

- Brown, R.A. (1977d) J. Phys. F: Metal Phys., 7, 1477
- Brown, R.A. (1977e) J. Phys. F: Metal Phys., 7, 1977
- Bucksch, R. (1971) J. Appl. Cryst., 4, 156
- Bucksch, R. (1972) J. Appl. Cryst., 5, 96
- Burger, M.J. (1940) Proc. Phys. Soc., 52, 23
- Burger, M.J. (1945) Am. Miner., 30, 469
- Burger, M.J. (1947) J. Chem. Physics, 15, 1
- Burger, M.J. (1950a) Acta Cryst., 3, 87; see also Acta Cryst., 3, 243
- Burger, M.J. (1950b) Acta Cryst., 3, 243
- Burger, M.J. (1963) Elementary Crystallography, New York: Wiley
- 
- Cahn, R.W. (1953) Acta Metall., 1, 49
- Cahn, R.W. (1954) Advances in Physics, 3, 363
- Cassels, J.W.S. (1959) An introduction to the geometry of numbers, New York: Springer Verlag
- Chadwick, G.A. & Smith, D.A. (1976) Grain boundary structure and properties, London: Academic Press
- Chalmers, B. (1953) Proc. Phys. Soc., 47, 733
- Chapin, D.M., Fuller, C.S. & Pearson, G.L. (1954) Journ. Appl. Phys., 25, 676
- Chatfield, C. (1978) Statistics for technology: a course in applied statistics, London: Chapman & Hall
- Chen, S.H. (1967) Phys. Rev., 163, 532
- Chopra, K.L. & Khan, I.H. (1967) Surface Sci., 6, 33
- Christian, J.W. (1975) The theory of transformations in metals and alloys, part I: equilibrium and general kinetic theory, Pergamon Press
- Clark, R., Craing, G.B. & Chalmers, B. (1950) Acta Cryst., 3, 479
- Clark, R. & Craing, G.B. (1953) Progress in metal physics, 3, chapter 4
- Clark, W.A.T. (1976) Ph.D. thesis, University of Oxford
- Cochran, W. (1952) Acta Cryst., 5, 630
- Cole, W.F., Sörum, H. & Kennard, O. (1949) Acta Cryst., 2, 280
- Corbett, J.M. & Sheinin, S.S. (1976) Phys. Stat. Sol. (a), 38, 151
- Cornwell, J.F. (1969) Group theory and electronic energy band in solids, Amsterdam: North-Holland
- Cowher, M.E. & Sedgwick, T.O. (1972) J. Electrochem. Soc., 119, 1565
- Cox, J.M. (1967) J. Mol. Biol., 28, 151
- Coxeter, H.S.M. (1969) Introduction to geometry, John Wiley & Sons
- Cracknell, A.P. (1968) Applied group theory, Pergamon Press
- Curie, P. (1894) 'Sur la symétrie dans les phénomènes physiques, symétrie d'un champ électrique et d'un champ magnétique' J. de Phys., 3, 3 (in French)

- Curie, P. (1908) Oeuvres de Pierre Curie, Paris: Société française de Physique (in French)
- Curien, H. & LeCorrè, Y. (1958) 'Notations des macles à l' aide du symbolisme des groupes de couleurs de Choubnikov', Bulletin de la Société française de minéralogie et de cristallographie (Bull. Soc. fr. Minér. Cristallogr.) 81, 126 (in French)
- Curien, H. & Donnay, J.D.H. (1959) Am. Miner., 44, 1067
- Dahl, R.E. (1970) Ph.D. thesis, North Carolina State University
- Dahl, R.E., Beeler, Jr., J.R. & Bourquin, R.D. (1971) Computer Phys. Comm., 2, 301
- Dahl, R.E., Beeler, Jr., J.R. & Bourquin, R.D. (1972a) in: P.C. Gehlen, Beeler, Jr., J.R. & Jaffee, R.I. (edis.) Interatomic potentials and simulation of lattice defects, pp. 673-692, New York: Plenum
- Dahl, R.E., Beeler, Jr., J.R. & Bourquin, R.D. (1972b) in: H. Hu (ed.) The nature and behaviour of grain boundaries, pp. 123-151, New York: Plenum
- Daud, T., Koliwad, K.M. & Allen, F.G. (1978) Appl. Phys., 33, 1009
- Deming, W.E. (1931) Phil. Mag., 11, 146
- Deming, W.E. (1934) Phil. Mag., 17, 804
- Deming, W.E. (1935) Phil. Mag., 19, 389
- Desch, C.H. (1912) J. Inst. Metals, 8, 149
- Diamond, R. (1976) Acta Cryst., A32, 1
- Donnay, G. (1954) quoted by R.W. Cahn in 'Twinned crystals' Advances in Physics, 3, 363
- Donnay, G. & Donnay, J.D.H. (1954) article on crystal geometry in International Tables for X-ray Crystallography, vol. 2, Birmingham: Kynock Press
- Donnay, G., Belov, N.V., Neronova, N.N. & Smirnova, T.S. (1958) 'The Shubnikov groups', Kristallografiya, 3, 635 (in Russian). English translation in: Sov. Phys.-Cryst., 3, 642 (1958)
- Donnay, J.D.H. & Donnay, G. (1972) 'Symbols for symmetry operations' paper presented in the 9th International Congress of the International Union of Crystallography; abstract in supplement to Acta Cryst., A28, S110
- Doyle, P.A. & Turner, P.S. (1968) Acta Cryst., A24, 390
- Dunn, C.G., Daniels, F.W. & Bolton, M.J. (1950) J. Metals, 2, 1245
- Edington, J.W. (1974) Practical electron microscopy in materials science, Philips technical library, Philips Gloeilampenfabrieken, Eindhoven
- Eisenhart, L.P. (1933) Continuous groups of transformations, Princeton
- Ellis, W.C. & Treuting, R.G. (1951) Trans. Amer. Inst. Min. Metall. Engrs., 181, 53
- Ewing, J.A. & Rosenhain, W. (1901) Phil. Trans. Roy. Soc., A195, 279



- Faraone, D., Sabelli, C. & Zanazzi, P.F. (1967) Rend. Acc. Naz. Lincei, 43, 369
- Fedorov, E.S. (1949) Symmetry and the structure of crystals: principal works (originals 1888-1896) Izd. Akad. Nauk. SSSR (in Russian). English translation: Symmetry of crystals, American Cryst. Association (1971)
- Ferro, D.R. & Hermans, J. (1977) Acta Cryst., A33, 345
- Finch, R.F., Queisser, H.J., Thomas, G. & Washburn, J. (1963) J. Appl. Phys., 31, 406
- Fontaine, C. & Rocher, A. (1979) 'Characterization of grain boundaries observed in polycrystalline silicon for solar applications' in: Microscopy of Semiconducting Materials Conference, Univ. of Oxford, 9-11 April 1979; abstract in Proceedings RMS, supplement in volume 14
- Forwood, C.T. & Humble, P. (1975) Phil. Mag., 31, 1025
- Frank, F.C. (1950) Symposium on the plastic deformation of crystalline solids, p. 150, sponsored by Carnegie Inst. of Technology and O.N.R.
- Frankl, R.F. (1964) J. Appl. Phys., 35, 217
- Fraser, H.L. (1977) Scr. Metall., 11, 47
- Freer, S.T., Kraut, J., Robertus, J.D., Wright, H.T. & Xuong, Ng. H. (1970) Biochem. Wash., 9, 1997
- Friedel, G. (1926) Leçons de cristallographie, Paris: Bergers Levrault (in French)
- Friedel, J., Cullity, B.D. & Crussard, C. (1953) Acta Metall., 1, 79 (in French)
- Galois, E. (1897) Oeuvres mathématiques d'Évariste Galois, 1st ed.; 2nd rev. and corrected ed. 1951, Paris: Gauthier-Villars (in French)
- Galyarskii, E.I. & Zamorzaev, A.M. (1965) 'A complete deviation of crystallographic STEM groups of symmetry and different types of antisymmetry', Kristallografiya, 10, 147 (in Russian). English translation in: Sov. Phys.-Cryst., 10, 109 (1965)
- Geary, N.A. & Bacon, D.J. (1976) Nucl. Metall., 20, 479
- Gejji, H.F. & Holt, D.B. (1975) J. Electrochem. Soc., 122, 535
- Genthe, J.E. & Aldrich, R.E. (1971) Thin Solid Films, 8, 149
- Gjónnes, J. & Watanabe, D. (1966) Acta Cryst., 21, 297
- Gjónnes, J. & Høier, R. (1969) Acta Cryst., A25, 595
- Goodhew, P.J. (1972) Specimen preparation in materials science, in: A.M. Glauert (ed.) Practical methods in electron microscopy, Amsterdam: North-Holland
- Gough, H.J. (1928) Trans. Faraday Soc., 24, 137
- Goux, C. (1961) Mém. Sci. Rev. Mét., 58, 769

- Goux, C. (1974) Can. Met. Quat., 13, 9
- Graef, M.W.M., Bloem, J., Giling, L.J., Monkowski, J.R. & Maes, J.W.C. (1979) 'The influence of grain size and dopant concentration on the electrical properties of polycrystalline silicon films' contribution in the 2nd E.C. Photovoltaic Solar Energy Conference held at Berlin (West) 23-26 April 1979, Dordrecht: D. Reidel
- Gratias, D. & Portier, R. (1979) 'Contrast simulations of planar coincidence-site lattice interfaces' contribution in the Microscopy of Amorphous, Disordered and Partially Ordered Solids Conference, University of Cambridge, 26-28 March 1979; abstract in Proceedings RMS, supplement in volume 14
- Grimmer, H., Bollmann, W. & Warrington, D.H. (1974) Acta Cryst., A30, 197
- Guan, D.Y. & Sass, S.L. (1973a) Phil. Mag., 27, 1211
- Guan, D.Y. & Sass, S.L. (1973b) Phil. Mag., 27, 1225
- Hargreaves, F. & Hills, R.J. (1929) J. Inst. Met., 41, 257
- Hasson, G.C., Guillot, J.B., Baroux, B. & Goux, C. (1970) Phys. Stat. Sol. (a), 2, 551
- Hasson, G.C. & Goux, C. (1971a) Scr. Metall., 5, 889
- Hasson, G.C. & Goux, C. (1971b) Scr. Metall., 5, 965
- Hasson, G.C., Lecoze, J. & Lesbats, P. (1971c) C.R. Acad. Sci. Paris, 273, 1314
- Hasson, G.C. (1972a) thesis, l' universite de Paris VI
- Hasson, G.C., Boos, J., Herbeuval, I., Biscondi, M. & Goux, C. (1972b) Surface Sci., 31, 115
- Hasson, G.C., Biscondi, M., Lagarde, P., Levy, J. & Goux, C. (1972c) in: H. Hu (ed.) The nature and behaviour of grain boundaries, pp. 3-40, New York: Plenum
- Head, A.K., Humble, P., Clarbrough, L.M., Morton, A.J. & Forwood, C.T. (1973) Computed electron micrographs and defect identification, Amsterdam: North-Holland
- Heesch, H. (1929) 'Zur Strukturtheorie der Ebenen Symmetriegruppen', Z. Kristall., 71, 95 (in German)
- Heesch, H. (1930) 'Zur systematischen Strukturtheorie, III: Über die vierdimensionalen Gruppen des dreidimensionalen Raumes', Z. Kristall., 73, 325
- Heimendal, M.M. (von), Bell, W. & Thomas, G. (1964) J. Appl. Phys., 35, 3614
- Heimendal, M.M. (von) (1971) Phys. Stat. Sol. (a), 5, 137
- Helmreich, D. & Seiter, H. (1979) 'Polycrystalline silicon and its characterization' contribution in the 2nd E.C. Photovoltaic Solar Energy Conference held at Berlin (West) 23-26 April 1979, Dordrecht: D. Reidel
- Hendrickson, W.A. (1979) Acta Cryst., A35, 158

- Hermann, C. (1929a) 'Zur systematischen Strukturtheorie, III: Ketten- und Netzgruppen', Z. Kristall., 69, 250
- Hermann, C. (1929b) 'Zur systematischen Strukturtheorie, IV: Untergruppen', Z. Kristall., 69, 533
- Higman, B. (1955) Applied group-theoretical and matrix methods, Oxford: Clarendon Press
- Hirsch, P.B., Howie, A., Nicholson, R.B., Whelan, M.J. & Pashley, D.W. (1965) Electron microscopy of thin crystals, London: Butterworths
- Holser, W.T. (1958a) Z. Kristall., 110, 249
- Holser, W.T. (1958b) Z. Kristall., 110, 266
- Holser, W.T. (1960) Spain: Consejo Superior de Investigaciones Cientificas, Instituto de Investigaciones Geologicas Lucas Mallada, Cursos y Conferencias, 7, 19
- Holser, W.T. (1961) Acta Cryst., 14, 1236
- Holt, D.B. & Wilcox, D.M. (1971) J. Cryst. Growth, 9, 193
- Holt, D.B. (1974) Thin Solid Films, 24, 1
- Hovel, H.J. (1975) Semiconductors and semimetals, vol. 11: Solar cells, Academic Press
- Howie, A. & Whelan, M.J. (1960) Proc. Eur. Conf. on Electron Microscopy, p. 181, Delft
- Howie, A. & Whelan, M.J. (1961) Proc. Roy. Soc., A263, 217
- Huber, R., Epp, O., Steigemann, W. & Formanek, H. (1971) Europ. J. Biochem., 19, 42
- Humble, P. & Forwood, C.T. (1975) Phil. Mag., 31, 1011
- Humphreys, C.J., Howie, A. & Booker, G.R. (1967) Phil. Mag., 15, 507
- Humphreys, C.J. & Hirsch, P.B. (1968) Phil. Mag., 18, 115
- Ibers, J.A. (1957) Acta Cryst., 10, 86
- Indenbone, V.L. (1960) 'Phase transitions without change in the number of atoms in the unit cell', Kristallografiya, 5, 115 (in Russian). English translation in: Sov. Phys.-Cryst., 5, 106 (1960)
- International Tables for X-ray Crystallography (1969) published for the International Union of Crystallography by Kynock Press, Birmingham
- Internationale Tabellen zur Bestimmung von Kristallstrukturen, Bd. 1: Gruppentheoretische Tafeln (1935) Berlin: Gebrüder Borntraeger (in German, French, English)
- Irving, B.A. (1961) Brit. J. Appl. Phys., 12, 92
- Janseen, T. (1973) Crystallographic groups, Amsterdam: North-Holland
- Jette, E.R. & Foote, F. (1935) J. Chem. Phys., 3, 605

- Johan, A., Ayerza, J., Bielle-Daspert, D., Rocher, A. & Fortaine, C. (1979) 'Transport properties and TEM observation of R.A.D. polycrystalline films' contribution in the 2nd E.C. Photovoltaic Solar Energy Conference held at Berlin (West) 23-26 April 1979, Dordrecht: D. Reidel
- Jones, B. & Taylor, W.H. (1961) Acta Cryst., 14, 443
- Joshua, S.J. (1974) Acta Cryst., A30, 353
- Kabsch, W. (1976) Acta Cryst., A32, 922
- Kê, T.S. (1947) Phys. Rev., 71, 533
- Kê, T.S. (1949) J. Appl. Phys., 22, 274
- Kikuchi, S. (1928a) Japan J. Phys., 5, 83
- Kikuchi, S. (1928b) Proc. Imp. Acad. Japan, 4, 271
- King, R. & Chalmers, B. (1949) Progress in metal physics, pp. 127-162, London: Butterworths
- Klassen-Neklyodova, M.V. (1964) Mechanical twinning of crystals, translated from Russian by J.E.S. Bradley, New York: Consultants Bureau
- Köhn, J.A. (1958) Am. Miner., 43, 263
- Kolbesen, B.O., Mayer, K.R. & Schuh, G.E. (1975) J. Phys. E: Scien. Instr., 8, 197
- Koliwan, K.M., Daud, T. & Liu, J.K. (1979) 'Some characteristics of low-cost silicon sheet' contribution in the 2nd E.C. Photovoltaic Solar Energy Conference held at Berlin (West) 23-26 April 1979, Dordrecht: D. Reider
- Koptsik, V.A. (1966) Shubnikov groups, handbook on the symmetry and physical properties of crystal structures, Izd. Mgk., Moscow (in Russian). Authorized English translation: Shubnikov groups: reference monograph on symmetry and physical properties of crystal structures, ed. N.F.M. Henry, to be published by the International Union of Crystallography (announced 1975; not seen)
- Koptsik, V.A. (1967) 'A general sketch of the development of the theory of symmetry and its applications in physical crystallography over the last 50 years', Kristallografiya, 12, 755 (in Russian). English translation in: Sov. Phys.-Cryst., 12, 667 (1968)
- Kozubowski, J.A. (1977) Phys. Stat. Sol. (a), 43, 535
- Krishnamurti, T.S.G. & Gopalakrishnamurti, P. (1969) Acta Cryst., A25, 329
- Krivanek, O.L., Isoda, S. & Kobayashi, K. (1977) Phil. Mag., 36, 931
- Kronberg, M.L. & Wilson, F.H. (1949) Trans. A.I.M.E., 185, 501
- Kurosh, A. (1955) Group theory, 2nd edition, New York: Chelsea
- Lange, F.F. (1967) Acta Metall., 15, 311
- Linington, P.F. (1970) 7th Int. Congr. Electron Microscopy, Grenoble, vol. 2, p. 447

- Lipson, H. & Rogers, L.E.R. (1944) Phil. Mag., 35, 544
- Loeb, A.L. (1971) Color and symmetry, New York: John Wiley
- Lomer, W.M. & Nye, J.F. (1952) Proc. Roy. Soc., 212, 576
- Maradudin, A.A. & Vosko, S.H. (1968) Rev. Mod. Phys., 40, 1
- Mataré, M. (1956) 'Zum elektrischen Verhalten von Bikristallzweischichten', Z. Physik., 145, 206
- Metherell, A.J.F. & Whelan, M.J. (1967) Phil. Mag., 15, 755
- Mokievskii, V.A. & Shafranovskii, I.I. (1957) 'The symmetry, antisymmetry and pseudosymmetry of induction surfaces', Kristallografiya, 2, 23 (in Russian). English translation in: Sov. Phys.-Cryst., 1, 19 (1957)
- Mokievskii, V.A., Shafranovskii, I.I. & Afanas'ev, I.I. (1965) 'Complete deduction of twinning laws and a very simple method of representing them', Mineralog. sb. L'vov. geol. obshch. Pri. Univ., 19, 10
- Mokievskii, V.A., Shafranovskii, I.I., Vovk, P.K. & Afanas'ev, I.I. (1966) 'A geometrical derivation of the twinning laws for crystals' Kristallografiya, 11, 539 (in Russian). English translation in: Sov. Phys.-Cryst., 11, 477
- Mokievskii, V.A. (1968) 'Generalization of the symmetry groups of twins', Kristallografiya, 13, 379 (in Russian). English translation in: Sov. Phys.-Cryst., 13, 311 (1968)
- Molcik, M. (1970) Prakt. Metallog., 7, 361
- Mott, N.F. (1948) Proc. Roy. Soc., 60, 391
- Mugge, O. (1917) Zbl. Miner. Geol. Palaont., 8, 233
- Mugge, O. (1927) Z. Kristall., 65, 603
- Multi, A.R. & Holt, D.B. (1972) J. Mater. Sci., 7, 694
- Murr, L.E., Horyler, R.J. & Lin, W.N. (1970) Phil. Mag., 22, 515
- Mackay, A.L. (1957) Acta Cryst., 10, 543
- Mackenzie, J.K. (1957) Acta Cryst., 10, 61
- McLachlan, A.D. (1972) Acta Cryst., A28, 656
- McLean, D. (1957) Grain boundaries in metals, Oxford: Oxford University Press
- McLean, D. (1973) J. Mat. Sci., 8, 571
- McWeeny, R. (1963) Symmetry, an introduction to group theory and its chemistry and chemical physics, edited by H. Jones, Pergamon Press
- Neronova, N.N. & Belov, N.V. (1961) 'A single scheme for the classical and black-and-white crystallographic space groups', Kristallografiya, 6, 3 (in Russian). English translation in: Sov. Phys.-Cryst., 6, 1 (1961)
- Neubüser, J. & Wondratschek, H. (1969) Maximal subgroups of the space-groups, Internal report of the International Union of Crystallography, 2nd typing (original edition 1965). The whole work was prepared for publication in the next edition of vol. I of the International Tables of X-ray Crystallography

- Neubüser, J. & Wondratschek, H. (1970) Minimal supergroups of the space-groups, Internal report of the International Union of X-ray Crystallography. The whole work was prepared for publication in the next edition of the International Tables of X-ray Crystallography
- Neuman, J.R. (1956) The world of mathematics, vol. 1, p.671, Simon & Schuster
- Neumann, F.E. (1885) Vorlesungen über die Theorie Elastizität der festen Körper und des Lichtäthers, Leipzig: Teubner (in German)
- Niggli, A. (1959) Z. Kristall., 111, 4
- Niggli, P. (1919) Geometrische Kristallographie des Diskontinuums, Leipzig: Verlag von Gebrüder, Bontraeger (in German)
- Niggli, P. (1924) Lehrbuch der Mineralogie, I: Allgemeine Mineralogie, 2nd edition, Berlin: Verlag von Gebrüder, Bontraeger (in German)
- Niggli, P. (1926) 'Die regelmässige Punktverteilung längs einer Geraden in einer Ebene (Symmetrie von Bordürenmuster)', Z. Kristall., 63, 255 (in German)
- Nowacki, W. (1960) Fortschr. Min., 38, 96
- Nyburg, S.C. (1974) Acta Cryst., B30, 257
- Nye, J.F. (1957) Physical properties of crystals, Oxford: Oxford University Press
- Otte, H.M., Dash, J. & Schaake, H.F. (1964) Phys. Stat. Sol., 5, 527
- Overstraeten, R. van & Palz, W. (1979) Proceedings of the 2nd E.C. Photovoltaic Solar Energy Conference, held at Berlin (West) 23-26 April 1979, Dordrecht: D. Reidel
- Palistrant, A.F. & Zamorzaev, A.M. (1963) 'The symmetry and antisymmetry groups of layers', Kristallografiya, 8, 166 (in Russian). English translation in: Sov. Phys.-Cryst., 8, 120 (1963)
- Palistrant, A.F. (1965) 'Planar point groups of symmetry and different types of antisymmetry', Kristallografiya, 10, 3 (in Russian). English translation in: Sov. Phys.-Cryst., 10, 1 (1965)
- Palz, W. (1979) 'Photovoltaics for development', contribution in the 2nd E.C. Photovoltaic Solar Energy Conference held at Berlin (West) 23-26 April 1979, Dordrecht: D. Reidel
- Pashley, D.W. (1956) Advan. Phys., 5, 173
- Pashley, D.W. (1965) Advan. Phys., 14, 327
- Pauling, P. (1967) The chemical bond: a brief introduction to modern structural chemistry, Ithaca: Cornell University Press
- Pearson, W.H. (1956) Handbook of lattice spacing and structures of metals, vol. 1 in: G.V. Raynor (ed.) International series of monographs on metal physics and physical metallurgy, London: Pergamon Press

- Pearson, W.H. (1967) Handbook of lattice spacing and structures of metals Vol. 2, in G.V. Raynor (ed.) International series of monographs on metal physics and physical metallurgy, London: Pergamon Press
- Pfister, S.L. (1953) Ann. Phys., 11, 239
- Polya, G. (1924) 'Über die Analogie der Kristallsymmetrie in der Ebene' Z. Kristall., 60, 278
- Pond, R.C. & Smith, D.A. (1974) Can. Met. Quat., 13, 39
- Pond, R.C., Smith, D.A. & Clark, W.A.T. (1974) J. Microscopy, 102, 309
- Pond, R.C. (1975) J. de Phys., Coll. C4, 36, C4-315
- Pond, R.C. (1976) unpublished work
- Pond, R.C., Smith, D.A. & Vitek, V. (1976) Inst. of Metall., Conf. on grain boundaries, A19
- Pond, R.C. & Smith, D.A. (1976) Inst. of Metall., Conf. on grain boundaries, A1
- Pond, R.C. (1977) Proc. Roy. Soc., A357, 471
- Pond, R.C. & Vitek, V. (1977) Proc. Roy. Soc., A357, 453
- Pond, R.C. (1979) J. Microsc., 116, 105
- Pond, R.C., Smith, D.A. & Vitek, V. (1979) Acta Metall., 27, 235
- Pond, R.C., Vitek, V. & Smith, V. (1979) Acta Cryst., A35, 689
- Pond, R.C. & Bollmann, W. (1979) Phil. Trans. Roy. Soc., 292, 449
- Pond, R.C. (1980) Structure and kinetics of grain boundaries, ASM conference, Milwaukee, Sept. 1979
- Pond, R.C. (1980a) submitted for publication in Acta/scr. Metall.-conference series
- Pumphrey, P.H. (1970) Ph.D. thesis, University of Cambridge
- Pumphrey, P.H. & Bowkett, K.M. (1970a) Phys. Stat. Sol. (a), 2, 339
- Pumphrey, P.H. & Bowkett, K.M. (1970b) Phys. Stat. Sol. (a), 3, 375
- Radi, G. (1970) Acta Cryst., A26, 41
- Rao, S.T. & Rossmann, M.G. (1973) J. Mol. Biol., 76, 241
- Rapperport, E.J. & Hartley, C.S. (1950) Deformation modes of zirconium at 77°K, 300°K, 575°K, and 1075°K, USAEC report NM1-1243
- Read, W.T. & Shockley, W. (1950) Phys. Rev., 78, 275
- Reynolds, D.C., Leies, G., Antes, L.L. & Marburge, R.E. (1954) Phys. Rev., 96, 533
- Riesz, R.P. & Bjorling, C.G. (1961) Rev. Sci. Instrum., 32, 889
- Rosenhain, W. (1925) Metall. Suplt. Engineer, 1, 2
- Ryder, P.L. & Pitsch, W. (1968) Phil. Mag., 18, 807
- Sabelli, C. & Zanazzi, P.F. (1968) Acta Cryst., B24, 1214
- Santoro, A. & Mighell, A.D. (1972) Acta Cryst., A28, 284

- Santoro, A. & Mighell, A.D. (1973) Acta Cryst., A29, 171
- Sass, S.L. (1980) J. Appl. Cryst., 13, 109
- Schacke, I. (1938) 'Zwillingsbildung als Gittergeometrisch-Zahlentheoretisches Problem mit Anwendung auf einige reale Falle', Z. Kristall., 98, 143; 98, 211; 98, 281 (in German)
- Schelkens, R. (1970) Phys. Stat. Sol., 37, 739
- Schönflies, A. (1891) Kristallsysteme und Kristallstrukture, Leipzig (in German)
- Schwutke, G.H. (1977) Phys. Stat. Sol. (a), 43, 43
- Seitz, F. (1936) 'On the reduction of space groups' (in German). English translation in: A.P. Cracknell: Applied group theory, Pergamon Press (1968)
- Senechal, M. (1980) Acta Cryst., A36, 845
- Shafranovskii, I.I. (1960) 'An extended theory of crystal forms and the morphology of twins', Fifth International Congress and Symposia, Cambridge, p. 108
- Shafranovskii, I.I. & Pis'mennyi, V.A. (1961) 'Generalized shapes of twinned crystals', Kristallografiya, 6, 31 (in Russian). English translation in: Sov. Phys.-Cryst., 6, 27 (1961)
- Sheinin, S.S. & Cahn, C.D. (1965) Phys. Stat. Sol., 11, K1
- Sheinin, S.S. & Corbett, J.M. (1976) Phys. Stat. Sol. (a), 38, 675
- Shubnikov (Schubnikov) A.V. (1930) 'Über die Symmetrie des Semikontinuums', Z. Kristall., 73, 430 (in German)
- Shubnikov, A.V. (1945) 'New ideas in the theory of symmetry and its applications' in Report of the General Assembly of the Academy of Sciences of USSR, October 14-17, 1944 (in Russian) Izd. Akad. Nauk. SSSR, Moscow, pp. 212-227 (not examined)
- Shubnikov, A.V. (1951) 'Simmetriia i antisimetriia konechnikh figur' (Symmetry and antisymmetry of finite figures) Izd. Akad. Nauk. SSSR, Moscow (in Russian). English translation in: A.V. Shubnikov & N.N. Belov: Colored Symmetry (1964) pp. xv-xxv and pp. 1-172, New York: Pergamon Press
- Shubnikov, A.V. (1959) 'Symmetry and antisymmetry of rods and semicontinua with a principal axis of infinite order and finite translations along it', Kristallografiya, 4, 279 (in Russian). English translation in: Sov. Phys.-Cryst., 4, 261 (1960)
- Shubnikov, A.V. (1962a) 'Symmetry and antisymmetry groups (classes) of finite strips', Kristallografiya, 7, 3 (in Russian). English translation in: Sov. Phys.-Cryst., 7, 1 (1962)
- Shubnikov, A.V. (1962b) 'Black-white groups of infinite strips', Kristallografiya, 7, 186 (in Russian). English translation in: Sov. Phys.-Cryst., 7, 145 (1962)
- Shubnikov, A.V. (1962c) 'Black-white groups of strips', Kristallografiya, 7, 805 (in Russian). English translation in: Sov. Phys.-Cryst., 7, 651 (1963)



- Shubnikov, A.V. & Koptsik, V.A. (1974) Symmetry in Science and Art, New York: Plenum Press
- Slawson, C.B. (1950) Am. Miner., 35, 193
- Smith, G.H. & Burge, R.E. (1962) Acta Cryst., 15, 182
- Smith, D.A. & Pond, R.C. (1976) International Metals Reviews, 205, 61
- Smith, D.A., Vitek, V. & Pond, R.C. (1977) Acta Metall., 25, 475
- Smoluchowski, R. (1953) Phys. Rev., 87, 482
- Speiser, A. (1924) Theorie der Gruppen von endlicher Ordnung, Berlin: Springer; 4th enlarged and rev. ed., Basel: Birkhäuser (1956)
- Sticker, R. & Booker, G.R. (1963) Phil. Mag., 8, 859
- Straumanis, M.E. & Aka, E.Z. (1952) J. Appl. Phys., 23, 330
- Straumanis, M.E., Boregeand, P. & James, W.J. (1961) J. Appl. Phys., 32, 1382
- Sumberg, D.A., Dayanidhi, K.K., Parker, P.M. & Spence, R.D. (1972) Acta Cryst., A28, 338
- Sutton, A.P. (1977) A theoretical and experimental investigation of some aspects of grain boundary structure using electron diffraction techniques, St. Catherine's College, Univ. of Oxford
- Sutton, A.P. & Pond, R.C. (1978) Phys. Stat. Sol. (a), 45, 149
- Takeda, H., Donnay, J.D.H. & Appleman, D.E. (1967) Z. Kristall., 125, 414
- Tanaka, K. & Kamion, K. (1931) Mem. Coll. Sci. Engng., 14, 79
- Tavger, B.A. & Zaitsev, V.M. (1956) 'Magnetic symmetry of crystals', Zh. Eksp. teor. Fiz., 30, 564 (in Russian). English translation in: Sov. Phys.-JETP, 3, 430 (1956)
- Tendeloo, G. van & Amelinckx, S. (1974a) Acta Cryst., A30, 431
- Tendeloo, G. van & Amelinckx, S. (1974b) Group-theoretical considerations concerning domain formation in ordered alloys, Supplementary publication No. SUP30347, British Library Lending Division
- Titchmarch, J.M. (1971) Ph.D. thesis, University of Oxford
- Thomas, G. (1970) Kikuchi-electron diffraction and applications, in: S. Amelinckx, R. Gevers, G. Remaut & J. van Landuyt (eds.) Modern Diffraction and Imaging Techniques in Materials Science, 1st ed., North-Holland
- Trillat, J.J. (ed.) (1964) Ionic bombardment, theory and application, New York: Gordon & Breach
- Tucker, M.O. (1969) Phil. Mag., 19, 1141
- Vogel, F.L., Pfann, W.G., Corey, H.E. & Thomas, E.E. (1953) Phys. Rev., 90, 489
- Warrington, D.H. & Bufalini, P. (1971) Scr. Metall., 5, 771
- Warrington, D.H. & Bollmann, W. (1972) Phil. Mag., 25, 771

- Warrington, D.H. (1975) J. de Phys., Coll. C4, 36, C4-87
- Weber, L. (1929) 'Die Symmetrie homogener Ebener Punktsysteme', Z. Kristall., 70, 309
- Weins, M.J., Chalmers, B., Gleiter, H. & Ashby, M. (1969) Scr. Metal., 3, 601
- Weins, M.J. (1970a) Ph.D. thesis, Harvard University
- Weins, M.J., Gleiter, H. & Chalmers, B. (1970b) Scr. Metal., 4, 235
- Weins, M.J., Gleiter, H. & Chalmers, B. (1971a) J. Appl. Phys., 42, 2639
- Weins, M.J. (1971b) Scr. Metal., 5, 969
- Weins, M.J. (1972a) in: P.C. Gehlen, J.R. Jr. Beeler & R.I. Jaffee (eds.) Interatomic Potentials and Simulation of Lattice Defects, New York: Plenum
- Weins, M.J. (1972b) Surface Sci., 31, 138
- Westlake, D.G. (1961) Acta Cryst., 9, 327
- Weyl, H. (1952) Symmetry, Princeton: Princeton University Press; this is the modern classic on symmetry, part of the book is reprinted in J.R. Neuman: The world of mathematics (Simon & Schuster) vol. 1, p. 671
- Whitwhan, D., Mouflard, M. & Lacombe, P. (1951) Trans. Amer. Inst. Min. Metall. Engrs., 191, 1070
- Wigner, E.P. (1930) Nachr. Kgl. Ges. Wiss. Göttingen Math.-Physik, K1, pp. 133-146 (in German). English translation in: R.S. Knox & A. Gold Symmetry in the Solid State (1967) pp. 173-189, New York: W.A. Benjamin
- Wilcox, D.M. & Holt, D.B. (1969) J. Mater. Sci., 4, 672
- Wilcox, D.M. (1970) Ph.D. thesis, University of London
- Wilson, E.B. (1952) An introduction to scientific research, New York: McGraw-Hill
- Yamaguchi, M., Vitek, V. & Pope, D.P. (1980) 'Planar faults in the  $\text{Li}_2$  lattice: Stability and structure' in press
- Young, C.T., Steele, J.H. & Lytton, J.L. (1973) Met. Trans., 4, 2081
- Zamorzaev, A.M. (1953) 'Generalization of the space groups' Dissertation, Leningrad State University (in Russian) (not examined; see Zamorzaev, 1962)
- Zamorzaev, A.M. (1957) 'Generalization of Fedorov groups', Kristallografiya, 2, 15 (in Russian). English translation in: Sov. Phys.-Cryst., 2, 10 (1957)
- Zamorzaev, A.M. (1962) 'On the 1651 Shubnikov groups', Kristallografiya, 7, 813 (in Russian); first published as a dissertation in Leningrad State University. English translation in: Sov. Phys.-Cryst., 7, 661 (1963)